University of Reading

The James Hutton Institute

Measuring peatland carbon uptake by remote sensing

PhD

Department of Geography and Environmental Science

Kirsten Lees

January 2019

Abstract

Peatlands are an important ecosystem for carbon storage, due to their semi-permanent water saturated condition which inhibits decomposition. Many peatlands in the UK have been degraded through human land use to the point where they are releasing carbon, and restoration is now a priority to protect these landscapes and the carbon held within them. Most methods of monitoring peatland restoration are small-scale and expensive. Remote sensing methods, however, are large-scale and often freely available to the end user.

This project considers the potential benefits of using remote sensing to estimate peatland carbon uptake, and describes experiments which answer research questions in this area. Much of the work was done within the Forsinard Flows RSPB reserve, which has a chronosequence of blanket bog sites at different stages of restoration.

A laboratory experiment on the effects of drought stress on the carbon flux and spectral reflectance of *Sphagnum* moss was first completed. This was followed by a field experiment to assess factors affecting peatland GPP and whether these could be detected by remote sensing data. The final part of this project involved the development of a Temperature and Greenness (TG) model using remote sensing to estimate GPP across blanket bog ecosystems.

The project used both flux chamber and eddy covariance techniques to measure carbon uptake and compared the results to spectral reflectance at small-scale using a hand-held spectrometer, and large-scale using satellite data from MODIS.

The results from these experiments suggest that spectral indices, and models using them, can give information about *Sphagnum* drought stress, seasonal change in peatland vegetation, and restoration progress, and are functional at scales from a few centimetres up to one kilometre. Next steps could include calibrating the developed model for a range of sites to broaden its applicability, and further work into monitoring water table depth using remote sensing.

Declaration: I confirm that this is my own work and the use of all material from other sources has been properly and fully acknowledged.

Kirsten Lees

Acknowledgements

Firstly, thanks are due to all my supervisors, Jo, Tristan, Rebekka, and Myroslava, who have been consistently supportive and encouraging. I am grateful to Jo for encouraging me to present at conferences and to publish, thereby preparing me for an academic career. Thanks to Tristan for bringing his expertise in remote sensing to the project, and for his many sensible suggestions to improve my writing. Thanks to Rebekka for being so dedicated to supporting me and my studies, even at a distance of 500 miles! And thanks to Myroslava, for her encouragement both in the field and at conferences. I am also grateful to Kevin White for being my panel chair throughout the PhD, and also for teaching me how to use the spectrometers. Thanks also to my two PhD examiners, Angela Harris and Shovonlal Roy, for their insightful comments.

Thanks to everyone who has helped with my fieldwork in any way. That includes especially Ainoa Pravia and Jose van Paassen, who were with me on the March field trip and helped with site set up, and Valeria Mazzola, whose cheerfulness on the most miserable of days is inspiring. Many thanks also to Pete Gilbert, Paul Gaffney, Wouter Konings, Jonathon Ritson, Elias Costa, Zsofi Csillag, David and Parissa Lumsden, and Joe Croft. Special thanks are due to Myroslava who was with me on 6 out of 7 field trips in 2017 and helped keep me sane by supervising the cooking as well as my PhD! Thanks to Alison Wilkinson who made the fieldwork collars, and to my Dad who made the lab collars!

Thanks to the RSPB who let me use their reserve as my field site. I would particularly like to mention Neil Cowie, Danni Klein and Mark Hancock, whose dedication to peatland restoration is inspirational. Thanks to Roxane Anderson for all the work she does in bringing the Flow Country researchers together. I am also very grateful to the whole peatlands research community who have consistently made me feel welcome.

Thanks to all my colleagues in Room 20 who have made doing this PhD so much more enjoyable. Particularly Rob, Heather, Harriet, and Charlotte, whose regular chats during tea breaks have kept me going.

Finally, I would like to thank my family. Thanks to Grandma Stears for initiating my love of peatlands. Thanks to Grandma and Grandad Lees for their support throughout my PhD. Thanks to Mum, Dad and Suzanne for their ongoing encouragement. I could not have done it without you all.

Contents

List of tables and figures

Glossary of terms

µm - micrometer (10^{-6})

APAR – Absorbed Photosynthetically Active Radiation

AVHRR – Advanced Very High Resolution Radiometer

CAI – Cloud and Aerosol Imager

CH_4 – Methane

CIm – modified Chlorophyll Index

CO_2 – Carbon dioxide

DIC – Dissolved Inorganic Carbon

DOC – Dissolved Organic Carbon

DoD – Department of Defence

EC- Eddy Covariance

EF – Evaporative Fraction

EO – Earth Observation

EOM – Ecosystem Organic Matter

ESA – European Space Agency

ETM+ - Enhanced Thematic Mapper Plus

EUMETSAT – European Organization for the Exploration of Meteorological Satellites

EVI – Enhanced Vegetation Index

fBWI – floating Water Band Index

FIR – Far-Infrared

FTS – Fourier Transform Spectrometer

GHG – Greenhouse Gas

GLO-PEM - Global Production Efficiency Model

GMAO - Global Modelling and Assimilation Office

GOSAT - The Greenhouse Gases Observing Satellite

GPP – Gross Primary Productivity

H_2O – water

InSAR – Interferometric Synthetic Aperture Radar

IR – Infra-Red

IRGA – Infra-Red Gas Analyser

JAXA – Japan's Aerospace Exploration Agency

LAI-Leaf Area Index

LiDAR – Light Detection and Ranging

LST – Land Surface Temperature

LSWI – Land Surface Water Index

LUE –Light Use Efficiency

MERIS – Medium Resolution Imaging Spectrometer

MIR – Mid-Infrared

MODIS – Moderate Resolution Imaging Spectrometer

MSI – Multi-Spectral Imager

MTCI - MERIS Terrestrial Chlorophyll Index

NASA – National Aeronautics and Space Administration

NDVI –Normalised Difference Vegetation Index

NDWI – Normalised Difference Water Index

NEE – Net Ecosystem Exchange

nm - nanometer (10^{-9})

O_2 - Oxygen

OCO – Orbiting Carbon Observatory

OLI – Operational Land Imager

PAR –Photosynthetically Active Radiation

POC – Particulate Organic Carbon

PRI – Photosynthetic Reflectance Index

Ra – autotrophic Respiration

R_{eco} – ecosystem Respiration

REP – Red Edge Position

Rg – growth Respiration

Rh – heterotrophic Respiration

Rm – maintenance Respiration

RS – Remote Sensing

RSPB – Royal Society for the Protection of Birds

SAR – Synthetic Aperture Radar

SIF – Solar Induced Fluorescence

SIPI – Strucure Insensitive Pigment Index

SLSTR - Sea and Land Surface Temperature Radiometer

SMD – Soil Moisture Deficit

SOM – Soil Organic Matter

SPOT – Satellite Pour l'Observation de la Terre

Suomi-NPP – Suomi National Polar Orbiting Partnership

SWIR – Short-Wave Infrared

TANSO – Thermal and Near-infrared Sensor for carbon Observation

TG – Temperature and Greenness

TGWa – annual Temperature, Greenness and Wetness

TIR – Thermal Infra-Red

USGS – United States Geological Survey

VI – Vegetation Index

VIIRS - Visible Infrared Imaging Radiometer Suite

VPM – Vegetation Photosynthesis Model

VPD – Vapour Pressure Deficit

WI – Water Index

WTD – Water Table Depth

1.Introduction

1.1. Research context

Peatlands are a valuable ecosystem both for their carbon storage potential, and for their diversity of rare flora and fauna. These areas make up only 3% of global surface area, but store approximately a third of the world's soil carbon (Gorham, 1991;Limpens et al., 2008). Peatland areas are water saturated, creating conditions which limit aerobic decomposition and lead to the build up and storage of organic carbon (Chapman et al., 2009; Yu, 2012). This thesis focuses on blanket bogs, a type of acidic peatland supported by rainwater (Lindsay, 2010). Blanket bogs require wet and cool climates to thrive (Clark et al., 2010). They are a key ecosystem in the UK, covering large areas of land particularly in Scotland where they make up approximately 14% of land cover (Chapman et al., 2009).

Unfortunately, many peatlands in Great Britain have been degraded through historical management decisions (Holden et al., 2007; Worrall et al., 2011). This has included drainage ditches being dug in an attempt to improve the land for grazing, planting for commercial forestry, and historical peat-cuttings (JNCC, 2011). This degradation of peatland ecosystems leads to a loss of function as a carbon sink and store, and increases the risk of peat oxidisation resulting in increased carbon dioxide emissions to the atmosphere (Holden et al., 2007; Silvola et al., 1996; Worrall et al., 2011). Nearly half of all blanket bog in the UK has experienced degradation, some of which is still severely damaged, but some of which is now undergoing restoration (JNCC, 2011).

Policy makers are now recognising the value of peatlands as carbon stores, and peatland restoration is becoming accepted as a way of reducing national carbon emissions (European Commission, 2018; Hiraishi et al., 2014; IUCN, 2016). Restoration includes methods such as drainage ditch blocking to raise the water table, restructuring the peatland surface, and encouraging regrowth of natural vegetation communities (Andersen et al., 2017; Parry et al., 2014). These measures aim to limit erosion and carbon loss, and ultimately restore as much of the peatland areas as possible to functioning carbon sinks (Minayeva et al., 2017; Soini et al., 2009; Strack and Zuback, 2013).

Long-term, reliable monitoring is a crucial part of any restoration scheme. In order to determine the success of restoration progress, monitoring needs to be continued over several years or even decades to assess the full implications of the management scheme (Hancock et al., 2018; Soini et al., 2009; Strack and Zuback, 2013; Waddington et al., 2010). Any carbon flux monitoring methodology needs to reliably match measurements on the ground under different conditions, with strong intra- and inter-annual relationships. Where the aim of the restoration process is increased carbon storage, traditional monitoring

methods include flux chambers and eddy covariance towers. These methods, however, are small-scale, expensive, and require high time inputs for instrument maintenance, data collection and processing (Andersen et al., 2017; Hill et al., 2017; Humphreys et al., 2006; Marushchak et al., 2013). More recent methodologies have included using vegetation communities as a proxy for carbon fluxes (eg. Couwenberg et al., 2011), but this also requires a detailed knowledge of the vegetation coverage of a site, which can be heterogenous and hard to determine across peatland areas. Many peatland ecosystems are remote and difficult to access, as well as being sensitive to disturbance, and therefore detailed vegetation surveys are not always practical. Satellite data has the potential to provide low-cost, large-scale monitoring which does not require frequent site visits (Chasmer et al., 2018).

Remote sensing has previously been used to estimate water content, vegetation extent and photosynthesis over peatland landscapes with some success (Harris and Dash, 2011; Kross et al., 2013; Letendre et al., 2008; Schubert et al., 2010). There are several models which can be used to estimate photosynthesis from remote sensing data, but these were developed over ecosystems other than peatlands (Sims et al., 2008; Wu, 2012; Xiao et al., 2004; Yuan et al., 2010). The best methods to use in estimating photosynthesis over peatland are still uncertain, therefore, and very little work has yet been done using remote sensing over peatlands undergoing restoration (Chasmer et al., 2018). This thesis presents laboratory and field-based studies which aim to reduce that uncertainty and fill the study gaps.

1.2. Aims and objectives

Aim: To use remote sensing data to estimate the photosynthesis of blanket bog vegetation under different conditions, and to upscale these techniques in order to assess peatland restoration progress and success.

Objective 1: To analyse the current state of remote sensing for peatland carbon flux estimation, and to determine the gaps in our knowledge.

> Remote sensing is starting to be used to gather information about the carbon fluxes of peatland landscapes, but much of the work done is at single sites and there is as yet no consistently determined best methodology. There are also concerns raised in the literature around the challenges of using remote sensing models over peatlands, such as the mix of vegetation, small-scale heterogeneity, and water saturation. These were used to define research questions to determine the direction of this research project.

Objective 2: To assess how peatland vegetation carbon fluxes change under stress, and whether this change is detectable using remote sensing.

For a model of photosynthesis to be viable as an alternative to traditional methods of measuring carbon flux, it must be shown to be reliable even under extreme conditions. One extreme we expect to occur more regularly under climatic change is hot, dry summers, and this was the case in 2018. Drought can make the carbon stores in peatland vulnerable to decomposition and loss to the atmosphere, as water saturation is needed for peat accumulation. Therefore, it is important to assess how well remote sensing derived data represents the observed changes to peatland carbon fluxes as a result of prolonged drought stress.

Objective 3: To compare different spectral indices under a range of conditions and determine which give the most accurate information about peatland environments.

Vegetation indices are a key component of photosynthesis models using remote sensing data, and can give information about plant health and carbon function. To determine the most accurate model of peatland photosynthesis, these indices need to be tested under a range of conditions, in the field and in the laboratory, in order to measure which has the best match to measured conditions and carbon function. Of particular interest is the difference between broad-band indices which can be calculated from freely available satellite data, compared to hyperspectral indices which require more spectrally sensitive sensors.

Objective 4: To develop a model using remote sensing data that can give reliable and accurate estimates of peatland GPP.

The work done to assess the usefulness of remote sensing techniques and especially vegetation indices under different conditions now needs to be combined into a model of peatland photosynthesis. Reviewing the literature gave suggestions as to what elements are required to create a reliable model of peatland photosynthesis, and suggests models which may give good results over peatland landscapes.

Objective 5: To use the developed model to measure restoration progress at a landscape scale.

Restoration of damaged peatland landscapes is an underdeveloped area of research in remote sensing, yet it could provide useful monitoring technology. The RSPB has invested in forestry removal and peatland restoration across much of the Forsinard Flows reserve, but information about the success of these measures is incomplete

and covers only some sites. Remote sensing has the potential to give a clearer picture of restoration progress and success for enhancing carbon uptake across the area of the reserve.

Objective 6: To assess whether the developed model is accurate at both small and large scale, particularly taking into account the small-scale heterogeneity of many peatland landscapes.

Upscaling is a key focus in ecology, as many field studies are completed at small-scale, but the information needed by stakeholders and decision-makers is often ecosystem or landscape scale. Remote sensing can make measurements at both small and large scale, and so has the potential to be a link between scales, and a useful monitoring methodology over large areas.

1.3. Field site

The field site for the majority of this work is the Forsinard Flows RSPB reserve, in the Flow Country of Northern Scotland. This site includes some areas of near-natural blanket bog which have had no human management in recent history. Much of the reserve, however, was planted for commercial forestry by previous land owners, and these areas are now being felled and undergoing restoration. The reserve provides an ideal field site for this work as it has a chronosequence of sites undergoing restoration from those which were felled in 1998 to the present, and also near-natural control sites (Hancock et al., 2018). For more information on the field sites see chapters 4, 5 and 6.

1.4. Thesis structure

This thesis is written as a ‘collection of papers’ as described by University of Reading graduate school guidelines, and each chapter (2 to 6) is written in the style of the journal by which it has been published, or to which it will be submitted. All chapters within this thesis were developed by me with the input of my four academic supervisors. Their contribution included advice on experimental design, literature search, help with data collection in the field, data analysis and presentation, and guidance on writing the manuscripts. Some chapters also include data from other co-authors, and these are detailed below. Jonathon Ritson is listed as a co-author on several of the chapters (Chapters 4,5,6) for completing the vegetation survey at the Forsinard Flows sites. The RSPB are represented by a co-author on chapters which use their field sites (Chapters 4,5,6); the RSPB representatives include Neil Cowie, Mark Hancock, and Daniela Klein.

Chapter 2 is a review of the current literature in this topic, and is intended as a guide for peatland researchers to the current state of remote sensing for carbon flux estimation in this

field, and the potential it has for future work. It fulfils objective 1 by identifying the gaps in the literature, some of which this thesis aims to address. This chapter has been published as a paper in Science of the Total Environment (Lees et al., 2018).

Chapter 3 is a laboratory study which answers objective 2 by subjecting *Sphagnum* moss to different levels of drought stress. *Sphagnum* moss is a peat-forming genus which is adapted to the water saturated environment of blanket bogs, and which loses carbon function during periods of drought stress (Harris, 2008; Laine et al., 2009). This chapter is under review in the Journal of Ecohydrology (Lees et al., in review).

Chapter 4 combines field and laboratory data to achieve objective 3. Water indices are compared to water content measurements, and vegetation indices are compared to GPP. This chapter will be submitted as a paper to the IEEE Transactions on Geoscience and Remote Sensing (Lees et al., in prep).

Chapter 5 fulfils objective 4 by developing a temperature and greenness model for peatland environments and adding an annual water component to create the annual Temperature, Greenness and Wetness (TGWa) model. Two sites at the Forsinard Flows reserve, and the Glencar blanket bog site in Ireland, were used to develop and calibrate this model. This chapter also accomplishes objective 5 by applying the TGWa to six sites undergoing restoration across the Forsinard Flows RSPB reserve. This chapter has been accepted as a paper by the Journal of Environmental Management (Lees et al., in press). This chapter was completed with several co-authors: Matteo Sottocornola and Ger Kiely provided the eddy covariance data from Glencar, whilst Graham Campbell, Matthew Saunders, Tim Hill, and Neil Cowie contributed the eddy covariance data from the Forsinard Flows RSPB reserve.

Chapter 6 is an upscaling study which compares GPP results from flux chambers, eddy covariance towers, handheld spectrometry, and satellite. It answers objective 6 by analysing the factors affecting peatland GPP at small scales, and assessing whether the model will give reliable results at both small and large scale. The EC data for this study was processed by Myroslava Khomik and Tim Hill.

Finally, the Discussion and Conclusions chapter draws together the key findings of the thesis and conceptualises the relationships between factors measured throughout. It also suggests future avenues of research which could be developed from this work.

2. Potential for using Remote Sensing to estimate carbon fluxes across Northern peatlands – A Review.

Lees KJ, Quaife T, Artz RRE, Khomik M & Clark JM

Abstract

Peatlands store large amounts of terrestrial carbon and any changes to their carbon balance could cause large changes in the greenhouse gas (GHG) balance of the Earth's atmosphere. There is still much uncertainty about how the GHG dynamics of peatlands are affected by climate and land use change. Current field-based methods of estimating annual carbon exchange between peatlands and the atmosphere include flux chambers and eddy covariance towers. However, remote sensing has several advantages over these traditional approaches in terms of cost, spatial coverage and accessibility to remote locations. In this paper, we outline the basic principles of using remote sensing to estimate ecosystem carbon fluxes and explain the range of satellite data available for such estimations, considering the indices and models developed to make use of the data. Past studies, which have used remote sensing data in comparison with ground-based calculations of carbon fluxes over Northern peatland landscapes, are discussed, as well as the challenges of working with remote sensing on peatlands. Finally, we suggest areas in need of future work on this topic. We conclude that the application of remote sensing to models of carbon fluxes is a viable research method over Northern peatlands but further work is needed to develop more comprehensive carbon cycle models and to improve the long-term reliability of models, particularly on peatland sites undergoing restoration.

2.1. Introduction

Peatlands are a large store of terrestrial carbon and any change in their carbon balance could therefore cause large changes in the atmospheric greenhouse gases (GHGs) of the planet. The atmospheric store of carbon is estimated to be about 750 GtC, compared to an estimated 500 ± 100 Gt C stored in Northern peatlands (Yu, 2012). Although peatlands are an important part of the terrestrial carbon cycle and store approximately a third of the world's soil carbon (Gorham, 1991; Limpens et al., 2008), there is still much uncertainty about how these areas are affected by climate and land use change. There is also much variation between peatland types, with the greatest difference between acidic rain-fed bogs and more nutrient rich minerotrophic fens. Peat bogs in pristine condition are considered to be net carbon sinks (Yu, 2012), yet many areas of peatland have experienced degradation through human activity (such as draining, grazing and burning and conversion to plantation forestry), which decreases the net carbon uptake from the atmosphere (Fleischer et al., 2016). Peatland restoration is recognised as one of the ways to reach carbon emission reduction

targets under the Kyoto Protocol (Hiraishi et al., 2014), and it is therefore essential to develop ways of verifying and quantifying the effect of such restoration procedures. Field measurement techniques are limited by scale and cost, whereas Remote Sensing (RS) presents an opportunity to provide data to carbon flux models over large areas quickly and cheaply.

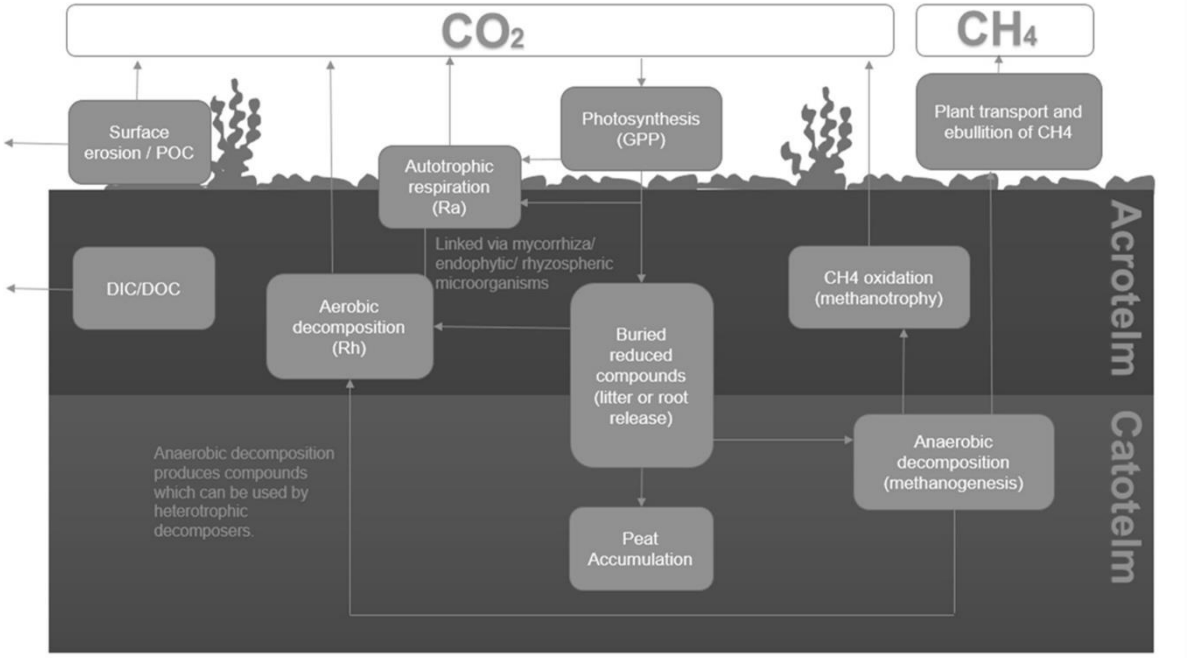

Figure 2.1 – Simplified carbon cycle in peat bogs. The catotelm is deep peat which remains saturated, whilst the acrotelm is where the water table varies. Net Ecosystem Exchange (NEE) is the combination of Gross Primary Productivity (GPP) and all ecosystem Respiration (R_{eco}). R_{eco} is the combination of autotrophic respiration (Ra) and aerobic decomposition/ heterotrophic respiration (Rh). Net Primary Productivity (NPP) is the combination of GPP and Ra.

Peatland ecosystems differ from other areas due to their high water table and very distinctive vegetation composition. Fluctuations in the water table influence the amount and distribution of oxygen available in the soil profile, which in turn influences carbon emissions. The carbon cycle of peatland ecosystems is complex and includes many components (a conceptual diagram of key components of the cycle in peat bogs is shown in Figure 2.1). CO_2 enters the peatland system though photosynthesis of the vegetation (Gross Primary Productivity or GPP), and leaves it through autotrophic (plant) respiration (Ra), and heterotrophic respiration (Rh) (microbial decomposition). The sum of Ra and Rh gives ecosystem respiration (R_{eco}), whilst the difference between R_{eco} and GPP equals Net Ecosystem Exchange (NEE).

Models using RS data focus on estimating GPP, R_{eco} and also NPP – Net Primary Productivity, which is the difference between GPP and Ra. The various flux processes in the peatland carbon cycle are typically considered at timescales from hours to a few years, largely due to the short monitoring records currently available. Over the course of a peatland's lifetime which often spans several millennia, however, natural (e.g. natural fires) and human (e.g. afforestation) disturbances should also be considered to capture the full breadth of a peatland's carbon cycle, as should shifts in climatic conditions. Methane (CH_4) is not considered in this review, as methane and carbon dioxide are often studied separately and require different methodologies. At this time, RS methods for estimating CH_4 emissions are still in their infancy compared to those of CO_2 estimates (see Tagesson et al., 2013). In peatland, carbon can also leave the system as dissolved organic/inorganic carbon (DOC/DIC) in streams and pipe outflow, or as particulate organic carbon (POC) due to surface erosion through wind and washout; these are not included in RS estimations of NEE. For more information about the peatland carbon cycle see Limpens et al. (2008). The current review focuses on biogenic CO_2 fluxes, which are the largest and most variable component at annual timescales (Helfter et al., 2015).

Field based studies show that several factors affect the spatial and temporal variance of carbon fluxes across peatlands, particularly water table depth (WTD) and temperature (Bubier et al., 2003; Dinsmore et al., 2009a; Lafleur et al., 2003; Lund et al., 2012; Strachan et al., 2016). Temperature and WTD help to determine plant species composition in the long term, while, in the shorter term, changes in these climatic variables affect plant photosynthesis and soil respiration (Bubier et al., 2003). Unusually dry or drained peatlands produce more CO_2 but less CH_4, whilst in wet peatlands this is reversed (Waddington and Price, 2000).

Peatland NEE is also strongly linked to vegetation composition, as different plant species have differing responses to climatic variables, and provide differing quantities of available organic matter for microbial decomposition. Different vegetation species dominate on different peatland types, with the most commonly considered distinction being between bog and fen. Bogs are generally acidic and support *Sphagnum* moss cover, whilst fens are more variable and support a greater proportion of sedges. The composition of vegetation communities is also affected by the site's microtopography, which often consists of areas of low waterlogged land (hollows), lawns, and higher, dryer areas (hummocks) (Lindsay et al., 1985; Nilsson et al., 2008) (see Figure 2.2). This paper considers variations in peatland topography at the microscale (hummocks and hollows, 0.2 to 2 m), mesoscale (pools and intrusions of forest etc. 2 to 50 m), and macroscale (landscape level).

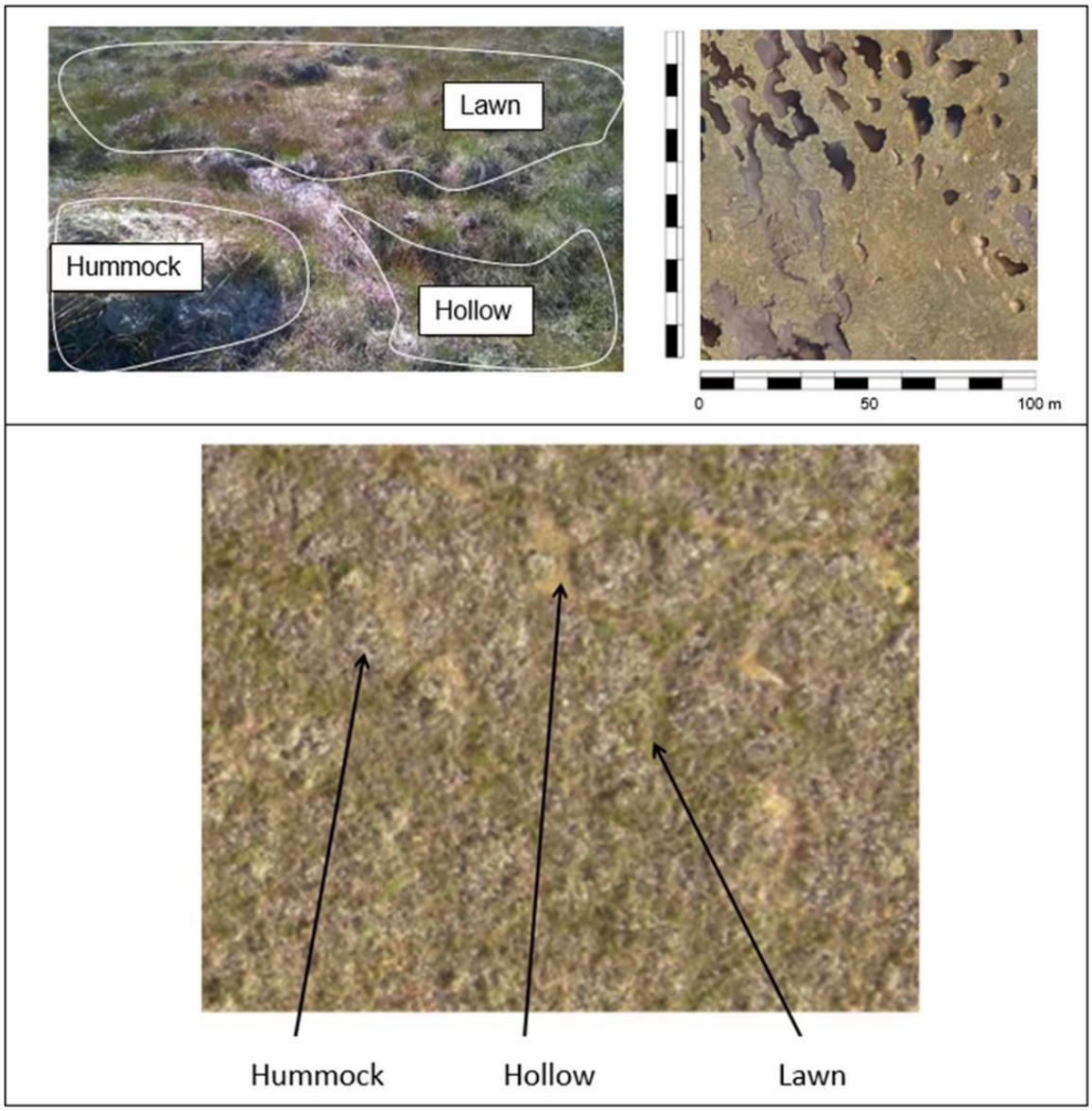

Figure 2.2 - Photos showing peatland microtopography at Forsinard Flows RSPB reserve, Scotland. Hummocks are raised features, hollows are depressed, and lawns are relatively flat surfaces. Each of these features is also characterised by a different vegetation complement. Top left: View as seen by the human eye. Top right: a 100 m^2area as the satellite would see it (5 cm resolution aerial photography). Lower image: The microtopographical features across an area of 10 m by 8 m using 5 cm resolution aerial photography.

Current field-based methods of estimating NEE on peatlands include flux chambers and eddy covariance (EC) towers (see Figure 2.3). Chamber studies measure NEE on a cm^2 scale, and so are useful for gaining information about microscale spatial heterogeneity of fluxes within peatland sites, such as contributions of different species and microtopographic

variations. However, due to logistical constraints, chamber measurements are often taken infrequently and over relatively brief timescales, so temporal variation is poorly explored (Marushchak et al., 2013). Furthermore, the small spatial scale does not allow for easy upscaling due to the difficulty of averaging or interpolating across such a varied landscape (Humphreys et al., 2006). EC towers estimate NEE over a larger area (m^2 to km^2), known as a footprint, from measurements of CO_2 concentration and air turbulence. Flux tower measurements are recorded at high frequency and over relatively extended periods of time (i.e. able to record half-hourly averages of CO_2 measurements taken at frequencies of around 10 Hz all year round), allowing good analysis of temporal variation over the site. However, EC towers have high equipment and maintenance costs, often suffer down-time due to equipment failure, and there are not many in place on peatland sites. The data from EC towers are also often noisy and prone to gaps. The spatial heterogeneity of peatlands means that a single flux tower cannot necessarily be assumed to be a good proxy for an entire landscape or region.

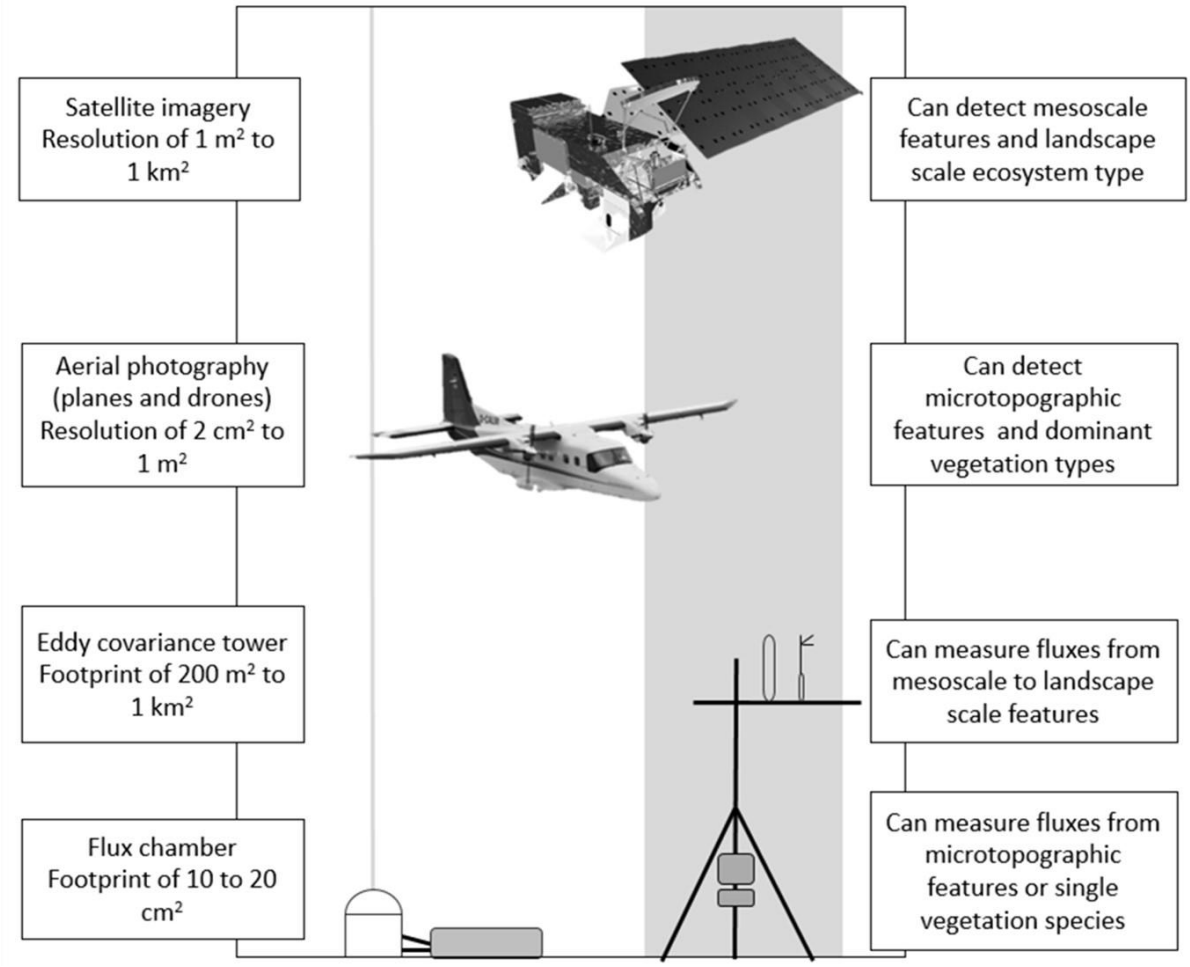

Figure 2.3 – Spatial scales at which carbon flux estimation tools can operate. The shading indicates a rough guide to the footprint of a flux chamber and an EC tower, compared to the

footprint of a satellite such as MODIS (whole box). Aerial remote sensing is included here but not discussed in the text. Microscale is considered to be changes in topography and vegetation up to 2 m, whilst mesoscale concerns larger areas of variation, such as bog pools or small areas of forestry. (Aeroplane image from NERC, 2016; satellite image from NASA, 2010).

Remote sensing has several advantages over traditional field studies, in particular, cost, scale, and viewing of remote locations. While RS also includes measurements by aeroplanes, unmanned aerial vehicles and kites, here we focus exclusively on satellite remote sensing. Satellites such as Terra, Aqua and Landsat have been used in many studies of terrestrial carbon fluxes over various ecosystems (Prince and Goward, 1995; Sims et al., 2008; Wu, 2012; Xiao et al., 2004; Yuan et al., 2010). Many satellite datasets are freely available, have a regular resampling interval (between one and sixteen days for the most widely used satellites) and cover large areas of land (Crichton et al., 2015; Harris et al., 2005). Some also have a relatively long time series archive (e.g. Landsat, dating from the 1970s). Remote sensing also has the advantage of allowing researchers to be able to study an environment whilst minimising exposure to the risks of field work, and disruption to the environment in question, as well as maximising the usefulness of available resources (Malenovský et al., 2015). It has the potential to be particularly useful for peatland studies, which often cover large isolated areas and can be difficult to access for continuous field studies (Connolly et al., 2009). However, data from many satellites have a coarse spatial resolution which makes it difficult to accurately distinguish the small scale heterogeneity of peatlands (Crichton et al., 2015). Remote sensing in general is limited by the fact that it only measures energy incident at the sensor, the distribution of which (e.g. as a function of wavelength) then has to be used to infer the characteristics of interest. Such techniques cannot measure gas fluxes directly and rely on models to estimate properties such as GPP and NEE. The extreme remoteness of satellite data also means that the radiation is affected by absorption by gases in the atmosphere, and atmospheric scattering from aerosols and other molecules, which can reduce its accuracy (Vermote et al., 1997). Peat bog areas are particularly prone to heavy rainfall and therefore cloud cover due to their prevalence in, and indeed reliance upon, humid environments.

Despite recent advances in the use of remote sensing to monitor carbon fluxes across ecosystems such as forests and cropland (e.g. Sims et al., 2008; Xiao et al., 2004; Yuan et al., 2010), less attention has been given to the application of RS in peatland areas even though they are a critical component of the carbon cycle (Yu, 2012). In this review paper we evaluate the current state of knowledge concerning the estimation of CO_2 fluxes in peatland using remote sensing and identify priority areas in need of future research. This review

paper consists of five sections including this introduction. Section 2 reviews current methodologies, summarizing key satellites used and various methods of estimation of peatland carbon dynamics from RS data. Several of the most commonly used models and their strengths and weaknesses are discussed. Section 3 reflects on previous studies where remote sensing was used to estimate carbon and water dynamics over peatlands. The insights gained in this section generate an assessment of those model parameters likely to produce the best results in a peatland landscape, and offer an understanding of current research gaps. Section 4 considers the challenges which the researcher must be aware of when using remote sensing to study peatlands, and suggests ways in which these difficulties may be overcome. The final discussion section (Section 5) summarises the areas of research in this topic which are at the forefront of current study and are only just beginning to be explored, as well as the main areas in need of further work concerning the estimation of CO_2 fluxes in peatlands using remote sensing.

2.2. Methods of measuring carbon fluxes remotely

2.2.1. Satellite sensors: what do they measure?

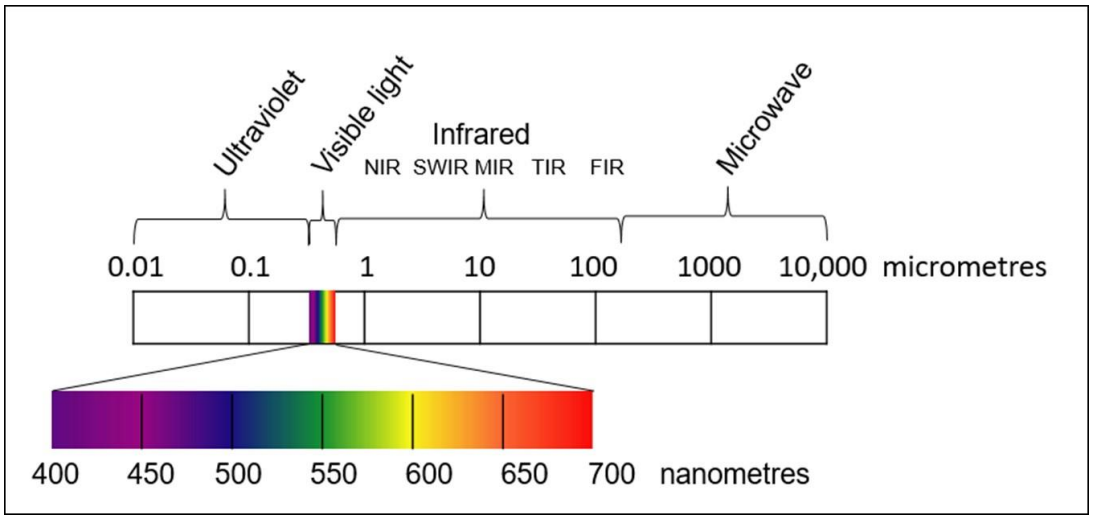

Figure 2.4 – diagram of the relevant section of the electromagnetic spectrum.

Some of the most commonly used remote sensing instruments are passive sensors detecting reflectance within the electromagnetic spectrum (see Figure 2.4). This includes visible and near-infrared (NIR), and also thermal infrared (TIR) and microwave sensing spectroscopy. Visible and NIR sensors detect changes in the absorbance/reflectance ratio over landscapes. Where there is a large cover of green plants, for instance, green light will be reflected and red light absorbed, causing a peak in the green wavelengths detected by the sensor. Vegetation indices make use of this effect (see Section 2.2.2.2.). Similarly, TIR spectroscopy can be used to measure surface temperatures and also to infer soil water content by detecting thermal infrared radiation emitted by a surface (Harris et al., 2006).

Active remote sensing involves equipment which interacts with the landscape by emitting energy towards the surface and measuring how much is reflected back to the sensor. Microwave imaging can be used to detect land cover and vegetation structure, and also soil water content, through the amount of backscatter detected (Kasischke et al., 2009). Light Detection and Ranging (LiDAR) uses a laser to measure structural changes at the earth's surface, and can therefore be useful in assessing the structure of vegetation. Synthetic Aperture Radar (SAR) can detect ground motion through very precise measurements of Earth surface height, allowing short term elevation changes due to subsidence or oxidisation, seasonal elevation changes due to the gas content of the peat (peat breathing), and other changes in surface texture and vegetation height to be observed (Cigna and Sowter, 2017).

This review focuses mainly on the visible and NIR data, as these are the most useful for estimating carbon fluxes due to their association with plant photosynthesis.

There are many satellites now in orbit which are specifically designed for Earth Observation (EO) uses. A selection showing the range of satellite data available to researchers for carbon flux estimation are detailed below and in Table 2.1.

- Terra and Aqua are satellites run by NASA. Both carry an instrument known as **MODIS** (Moderate Resolution Imaging Spectroradiometer). They cover the majority of the Earth's surface every 1-2 days, and can acquire data in 36 spectral bands (from 0.4 to 14.4 micrometres) with a spatial resolution of 250 m to 1 km (NASA, 2016a). MODIS is particularly useful in that is has a processing system which creates several data products, including vegetation indices and an estimate of GPP (see Section 2.2.3.1) using models designed to convert measurements of energy into secondary derived parameters. For most other satellites this processing must be done by the user.
- The **Landsat** program is a series of satellites (Landsat 7 and 8 are currently operating) run by the US Geological Survey (USGS). Each satellite covers the Earth every 16 days, collecting data in several bands within the visible/NIR and TIR wavelengths at a spatial resolution of 30 m for the visible/NIR and 100 m for the thermal bands (USGS, 2016). The first Landsat was launched in 1972. The availability of over forty years of data means that Landsat is especially useful for researchers studying change over time. However, the completeness of the data archive is limited, especially during the 1970s and 1980s.
- **Sentinel-2** is a mission run by the European Space Agency (ESA), consisting of two satellites: Sentinel-2A and Sentinel-2B. Each satellite carries a multispectral imager

with image resolution on certain sensors down to 10 m, and when both satellites are operational the return interval is every five days (ESA, 2016). This mission is a continuation of the SPOT and Landsat missions, and similar orbits should allow data from Sentinel-2 to be used as an addition to existing datasets (ESA, 2016). The finer resolution and frequent return interval of this mission should make the data it produces invaluable for a number of land-monitoring applications, including peatland carbon fluxes. Sentinel-1 (SAR) does not currently have a known application in modelling GHG exchange, although it is being used by some researchers to estimate peatland condition.

- **Sentinel-3** also consists of two satellites; Sentinel-3A is already in orbit, and Sentinel-3B is scheduled to be launched in 2018. Sentinel-3 will collect spectral data over land (**Ocean and Land Colour Instrument (OLCI)**), and temperature data (**Sea and Land Surface Temperature Radiometer (SLSTR)**) every two days (ESA, 2016). Although it has a faster revisit time than Sentinel-2, the spatial resolution is much coarser, being 300 m at best.
- **Hyperion** was an imaging spectrometer on board EO-1 designed to be compatible with Landsat data (and flew in formation with Landsat 7), but had a much higher spectral resolution and could detect 220 bands (0.4 to 2.5 micrometres) at 30 m spatial resolution (USGS, 2011). This means the data are useful for calculating indices such as the Photochemical Reflectance Index (PRI) and red-edge (see Section 2.2.2.2), which require a high spectral resolution (Gitelson et al., 2012; Harris et al., 2014; Yu et al., 2014). Hyperion's fine resolution also made it especially useful in heterogeneous environments (Christian et al., 2015). Unfortunately EO-1 has now been decommissioned and only ever captured data on request, but all data which were collected are now freely available.
- **Worldview** is a series of 3 satellites owned by DigitalGlobe, which provide commercial earth observation data. The spatial resolution can be as high as 30 cm, with daily coverage and both multi- and super-spectral bands available (DigitalGlobe, 2016).
- **GOSAT** is a Japanese satellite which carries out column gas abundance measurements using the **Thermal And Near-infrared Sensor for carbon Observation (TANSO)** instrument (composed of the Fourier transform spectrometer (FTS) and the cloud and aerosol imager (CAI) (NIES, 2016). Column gas abundances are calculated by analysing the IR light reflected from the surface compared to the IR light emitted from the atmosphere, allowing the amounts of CO_2, CH_4, H_2O and O_2 to be estimated (NIES, 2016). Column gas abundance satellite

missions can be used to estimate CO_2 fluxes by inverting atmospheric transport models. Unfortunately the outputs tend to be very coarse resolution (0.5 to 1.5 km), which makes them less useful for studies of specific land cover types.

- **Orbiting Carbon Observatory 2 (OCO-2)** is also a column gas abundance mission run by NASA. It has a longer return interval than GOSAT (16 days), and a footprint of 1.29 x 2.25 km. It carries three high resolution spectrometers, with two focused on CO_2 channels, and one on O_2 (NASA, 2016b).

Planned future sensors include: **FLEX (Fluorescence Explorer)** which is specifically designed to detect energy at the vegetation fluorescence peaks (see Section 2.2.2.2.1. for the uses of fluorescence data) (ESA, 2015; Kraft et al., 2014); **EnMAP**, which will carry a hyperspectral sensor and is due to launch in 2018 (EnMAP, 2016); and **HyspIRI** which will focus on the infrared region (NASA, 2016c).

One sensor which is no longer running, but which is mentioned in the following sections of this paper, and for which the data are still available, is the **Medium Resolution Imaging Sensor (MERIS)** (ESA, 2017).

Table 2.1 – Comparison of satellite sensors used for carbon flux estimation which are mentioned in this review. For key to acronyms please see text and the table of acronyms given at the start of this manuscript

Satellite (Instrument)	Spectral resolution	Spatial resolution	Temporal resolution	Operated by	In operation since	Other Notes
Terra and Aqua (MODIS)	0.4 to 14.4 µm (36 bands)	250 m, 500 m, 1 km	1-2 days	NASA	Terra: Dec., 1999, Aqua: May, 2002	
Landsat 7 (ETM+)	0.45 to 12.50 µm (8 bands)	30 m	16 days	USGS/NASA	Apr., 1999	Band 8 panchromatic and at 15 m spatial resolution
Landsat 8 OLI and TIRS	0.43 to 12.51 µm (11 bands)	30 m	16 days	NASA/USGS	Feb., 2013	Band 8 at15 m resolution
Sentinel-2 (MSI)	0.44 to 2.19 µm (13 bands)	10m, 20m, 60 m	5 days	ESA	Mar., 2017	Vis and IR bands at 10m spatial resolution; IR and NIR at 20 m.
Sentinel-3A OCLI	400 to 1020 nm (21 bands)	300 m to 1 km	1-4 days	EUMETSAT	Feb., 2016	
Sentinel-3A SLSTR	550 to 12000 nm (9 bands)	300 m to 1 km	2 days	EUMETSAT	Feb., 2016	
Hyperion	0.4 to 2.5 µm (220 bands)	30 m	16 days	NASA	Nov., 2000 to Jan., 2017	Only source of spaceborne hyperspectral imaging till 2005
WorldView-1	400 to 900 nm (1band)	0.5 m	2 days	DigitalGlobe	Sep., 2007	Commercial
WorldView-2	0.4 to 1.4 µm (8 bands)	0.3 to 2 m	1 day	DigitalGlobe	Oct., 2009	Commercial

WorldView-3	400 to 2245 nm (28 bands)	0.3 to 3.7 m	1 day	DigitalGlobe	Aug., 2014	Commercial
GOSAT (TANSO-FTS)	0.758 to 14.3 µm (4 bands)	10.5 km diameter footprint	3 days	JAXA	Jan., 2009	Only 2-5% of data usable, detects CH_4, CO_2 in air column
GOSAT (TANSO-CAI)	0.380 to 1.62 µm (4 bands)	0.5 to 1.5km	3days	JAXA	Jan., 2009	Only 2-5% of data usable, due to cloud cover.
OCO-2	3 high resolution channels (0.76µm, 1.61 µm, 2.06 µm)	1.29 km × 2.25 km	16 days	NASA	Jul., 2014	Data impacted by cloud cover; detects CO_2 in air column
SUOMI-NPP (VIIRS)	0.41 to 12.5 µm (22 bands)	357m, 750m	2 to 4 days	NASA/NOAA/DoD	Oct., 2011	To succeed MODIS
SPOT 6 & 7	450 to 890nm (5 bands)	1.5 to 6m	When commissioned	Spot Image	SPOT 6: Sept 2012, SPOT 7: June, 2014	Commercial
MERIS	0.39 to 1.04µm (15 bands)	260 x 300 m (land)	3 days	ESA	March, 2002 to May, 2012	No longer in use
FLEX	500 to 780nm	300m	1 month	ESA	Not yet launched	
EnMAP	hyperspectral	30m	unknown	German Research Centre for Geosciences (GFZ)	Not yet launched	
HyspIRI	Infrared region	unknown	unknown	NASA	Not yet launched	Study phase

2.2.2. Estimating GPP

There are several techniques using RS data which have been developed to estimate carbon fluxes, and many of the most well-known are explained in this section. It is also important to mention the ground validation techniques which are commonly used to assess the accuracy of these models. The two ways of measuring carbon fluxes directly are flux chambers and EC towers (see Figure 2.3). Flux chambers are not often used as a validation method for models using satellite data due to their small coverage. EC towers are more commonly used, and rely on the principle that gas movement in the atmosphere is through turbulent motion. See Section 2.1 for discussion of the coverage of these two methods, and Section 2.4 for discussion of some of the problems arising from their use as ground-validation methods.

2.2.2.1. The LUE model

The most widely used model for estimating GPP from remotely sensed data is currently the **Light Use Efficiency (LUE)** model developed by Monteith (1977) (Hilker et al., 2008). The equation for this model is:

$$GPP = fPAR * PAR * \varepsilon$$

Where PAR is the total photosynthetically active radiation incident on the vegetation, *f*PAR is the fraction of photosynthetically active radiation absorbed by vegetation, and ε is the conversion efficiency of absorbed energy which is then fixed as carbon within an ecosystem. The product of *f*PAR and PAR is sometimes given as APAR (Absorbed Photosynthetically Active Radiation). PAR is measured as the amount of light within the wavelengths that plants are able to absorb and use for photosynthesis (400 to 700 nm), and can be calculated using weather and climate data (Pfeifer et al., 2012). PAR is affected by cloud cover (Min, 2005), and when considering ground plant species such as mosses, also by the presence of a higher vegetation canopy (Chong et al., 2012). In many LUE models *f*PAR is modelled as a function of a vegetation index, and is often assumed to have a linear relationship with the NDVI (Normalised Differentiation Vegetation Index) (Huemmrich et al., 2010). *f*PAR is also related to Leaf Area Index (LAI) as this partially determines how much energy is absorbed by the canopy (Pfeifer et al., 2012; Yuan et al., 2007). An issue with the relationship between *f*PAR and LAI for *Sphagnum* is in defining an appropriate light extinction coefficient, which is often set to unrealistic values (Weston et al., 2015). ε is often calculated from a constant of εmax for a specific biome (e.g. grassland, forest, cropland) adjusted for limiting factors such as temperature and moisture availability (Garbulsky et al., 2011; Tan et al., 2012). It is also possible to calculate ε directly from the Photochemical Reflectance Index (PRI – see Section 2.2.2.2).

LUE-based models are very useful because they require few species-dependent parameters, and can be fairly easily calculated from remotely sensed data (Anderson et al., 2008). However, the calculation of ε in many models is considered to be overly simplistic. LUE varies with plant species, ecosystem types, and seasons, and so is unlikely to be accurately represented by a modified constant (Penuelas et al., 1995).

2.2.2.2. Vegetation Indices

Many EO implementations of the LUE model use a vegetation index (VI) to estimate *f*PAR, and in some cases to infer other ecosystem properties. VIs can be useful proxies for environmental variables such as water content of vegetation (see Section 2.3.3), for identifying land cover categories, and in some cases (such as PRI) as a proxy for ε in the LUE model. Below we review some key VIs useful in GPP estimation studies.

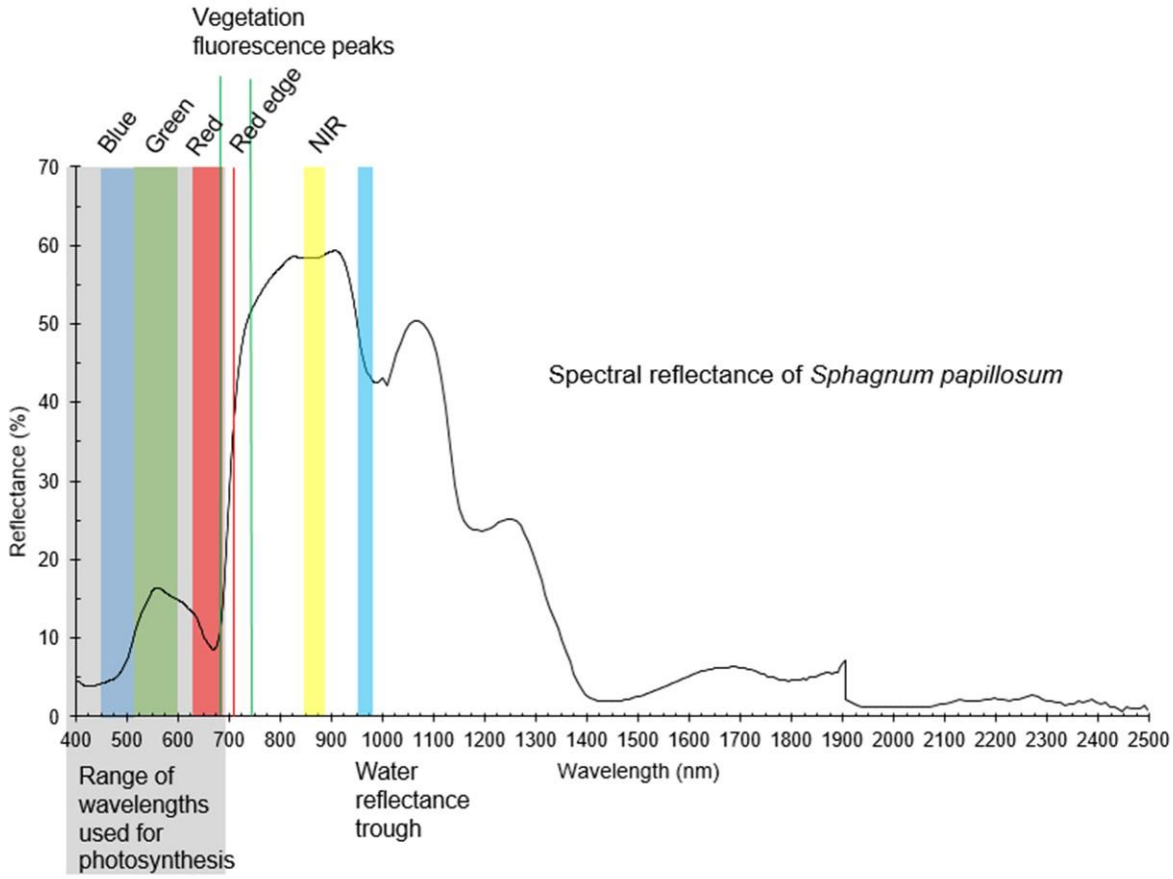

Figure 2.5 – An example of a spectral reflectance graph of Sphagnum moss. The visible and NIR bands follow the wavelengths used by Landsat (blue 450-515 nm; green 525-600 nm; red 630-680 nm; NIR 845-885 nm). Vegetation fluorescence peaks (690 and 740 nm) and the water reflectance trough (950-970 nm, used by the WI) are added. The sample was taken from the Forsinard Flows RSPB reserve and the reflectance was taken in the laboratory using a Ger3700 spectrometer (unpublished data). It is worth noting that the

reflectance of Sphagnum is greatly impacted by water content, bleaching and increasing reflectance in all wavelengths as it dries.

One of the oldest and most widely used VIs is the **NDVI (Normalised Difference Vegetation Index)**, which is calculated from the difference in reflection between the red band and the near-infrared (NIR) band (see Figure 2.5).The equation is:

NDVI = (NIR – red) / (NIR + red)

As healthy green plants absorb light in the red band and reflect it in the NIR band, where there is an abundance of green vegetation the NDVI values will be high. However, the NDVI tends to saturate at high LAI values and is sensitive to the scattering effect of atmospheric aerosols (Walker et al., 2014). The saturation effect can cause a summer plateau in NDVI values in some ecosystems but may not be particularly noticeable in northern peatlands due to the low LAI values of these environments (see Section 2.3.2).

The **Enhanced Vegetation Index (EVI)** is designed to overcome some of the limitations of NDVI. In particular, it includes reflectance in the blue light band to counteract the effect of aerosols, as the light which interacts with these is mostly in the blue portion of the spectrum (Balzarolo et al., 2016) and has generally lower values to compensate for the saturation effect of the NDVI (Huete et al., 2002; Rahman et al., 2005). In general it is agreed that the EVI is a more structural measure, linked to LAI and vegetation canopy structure, as it is more sensitive to NIR (Rossini et al., 2012), whilst the NDVI correlates better with plant chlorophyll content by being more sensitive to the red bands (Huete et al., 2002; Walker et al., 2014). Verma et al. (2015) found that EVI alone, validated against the Fluxnet dataset which included several different ecosystems, gave as much information about seasonal GPP change as the more complex PAR-based models, and as the MOD17 model (see Section 2.2.2.3). The MODIS product MOD13 contains both NDVI and EVI products.

The **Red Edge Position (REP)** index monitors the position of the point of steepest slope between the red and NIR wavelengths in a spectral image (see Figure 2.5) (Baranoski and Rokne, 2005). As chlorophyll increases, more red light can be absorbed by the plant and so the red edge moves to increasingly longer wavelengths (Dash and Curran, 2004). Stresses such as low water availability reduce the chlorophyll content and so the red edge shifts to lower wavelengths (Harris et al., 2005). REP is best calculated with narrow-band sensors (e.g. Hyperion – see Section 2.2.1) which can more accurately determine the position of the red-edge (Yu et al., 2014), although Dash and Curran (2004) created a successful index known as the MTCI (MERIS Terrestrial Chlorophyll Index), which used this principle on MERIS data (Rossini et al., 2012).

The **Photochemical Reflectance Index (PRI)** is a more recent VI development, and measures LUE through a different mechanism than plant greenness. The NDVI and EVI are considered useful proxies for the *f*PAR because they indicate leaf area and chlorophyll amount. The PRI is considered to be a proxy for ε because it measures light-use efficiency directly (Garbulsky et al., 2011; Peñuelas et al., 2011). PRI, and also fluorescence (see Section 2.2.2.2.1), are based on our understanding of the photoprotective mechanisms within plants. In some circumstances plants will absorb more light energy than can be used by chlorophyll to make glucose. When this is the case, light energy is either transferred to xanthophyll molecules inside the photosynthetic organelles and emitted as heat energy, or emitted as fluorescence (Gamon et al., 1992; Penuelas et al., 1995). The shift in reflectance associated with increased xanthophyll concentration can be detected at a wavelength of 531nm by comparison with a reference wavelength. The reference wavelength is often given as 570nm, although there is some debate (Gamon et al., 1992; Grace et al., 2007; Van Gaalen et al., 2007) about what specific wavelength works best at leaf or canopy scale.

PRI is better than alternative ways of estimating LUE from look-up tables based on vegetation type, as done in many satellite-based LUE models of GPP, because a single measurement already includes environmental constraints and can vary freely across different biomes without the use of categorisation (Peñuelas et al., 2011; Tan et al., 2012). However, PRI requires narrowband sensors with a spectral resolution of 3 to10 nm. One of the biggest issues with the PRI is that the ratio has not yet been standardised across studies, with different wavelengths being used at different sites and scales, which makes cross-comparison difficult (Garbulsky et al., 2011). PRI was originally developed at the leaf level (Gamon et al., 1992) and it is uncertain how well the same wavelengths can be transferred to canopy measurements where scattering affects the signature (Gamon et al., 1992; Garbulsky et al., 2011; Penuelas et al., 1995).

The high spectral resolution required to accurately calculate PRI means that broad band sensors such as those used on most satellites are not well suited to calculating this index. Hyperspectral sensors cover the spectrum close to continuously, and so have a band centred at 531 nm, whereas most broad-band sensors do not have such a band. MODIS is an exception, however, because Band 11 happens to be centred at around 531 nm (actually 526-536 nm) (Drolet et al., 2005; Goerner et al., 2011). This band has only recently been made routinely available from the Terra satellite (previously it was only processed over the ocean), but it is expected that it will be used in many carbon flux studies over the next few years. There is no band at 570 nm, which means that alternative bands must be used as the reference wavelength. Bands 1 (620-670nm), 4 (545-565nm), 12 (546-556nm) and 13 (662-

672nm) have been found to give reasonable results as reference bands (Drolet et al., 2005; Goerner et al., 2011).

Finally, there are two key points to keep in mind when considering VIs as a proxy for GPP. First, most VIs measure plant greenness rather than actual photosynthesis. Greenness often reaches its maximum before maximum photosynthesis and stressed leaves often reduce photosynthesis without changing colour (Gamon et al., 1992; Grace et al., 2007). Balzarolo et al. (2016) found that the MODIS VIs predict an earlier growing season start date than in-situ EC data suggests, over a range of different ecosystem types, as a result of this effect. Kross et al. (2013) found that this phenological disparity between carbon dynamics and biomass dynamics was evident in four peatland sites of different types, although they suggested that this may be overcome by using an index such as PRI which is more closely related to photosynthetic activity. Second, as well as the problems with the calculation of specific vegetation indices, all VIs are affected by disturbance from other factors such as topography, observance angle, soil background effects, moisture and atmospheric conditions (see Section 2.4 for more discussion of these issues) (Garbulsky et al., 2011; Peñuelas et al., 2011; Pfeifer et al., 2012; Walker et al., 2014).

2.2.2.2.1. Fluorescence

Solar Induced Fluorescence (SIF) is a photo-protective mechanism by which excess light not used during photosynthesis is emitted at longer wavelengths. Although fluorescence can provide useful information about plant stress, the relationship between photosynthetic carbon flux and fluorescence is not simple due to the interaction with the xanthophyll cycle (Harris, 2008). Once plant stress occurs, fluorescence decreases with photosynthesis as the xanthophyll mechanism (measured by PRI) is activated (Meroni et al., 2009). Fluorescence is, however, a good way of detecting photosynthesis changes over short timescales, and responds before chlorophyll abundance or LAI show any change (Meroni et al., 2009).

The two fluorescence peaks in vegetation are at approximately 690 nm in the red bands and 740 nm (see Figure 2.5) in the NIR (Meroni et al., 2009; Van Wittenberghe et al., 2015). However, measuring fluorescence requires sensors even finer than those used for PRI, with a resolution of <1 nm (Grace et al., 2007). The precise centre wavelength of the band used also varies slightly with resolution; Meroni et al. (2009) found that a spectral resolution of 0.005 nm was optimal, and anything larger caused a degradation of the signal. As with PRI, fluorescence has been suggested to be more easily measured at leaf level to avoid the canopy scattering and re-absorbance effects (Penuelas et al., 1995; Van Wittenberghe et al., 2015). Because of the technical challenges associated with measuring fluorescence, almost all previous studies have used ground-based or airborne sensors (Meroni et al., 2009).

However, Guanter et al. (2007) showed that space-based fluorescence detection was possible using MERIS. It has also been demonstrated from OCO and GOSAT, as the high spectral resolution used in these sensors is able to pick out the fluorescence signal (Frankenberg et al., 2014). The launch of the ESA FLEX mission will make fluorescence detection over large areas from space much more accessible.

2.2.2.3. LUE model development

Several models have been developed to estimate GPP, working from the basis of the LUE model and often incorporating vegetation indices as proxies for *f*PAR and/or ε. This section details some of the most well-known models which have been developed over the last two decades, and compares their model formulations and variables in Table 2.2.

Early GPP models such as CASA (Potter et al., 1993) and 3-PG (Landsberg and Waring, 1997) combined satellite data with field data such as meteorological inputs and soil/vegetation types**.** The first model to rely solely on remotely sensed data was the **Global Production Efficiency model (GLO-PEM)** (Prince and Goward, 1995). GLO-PEM uses data from the AVHRR (Advanced Very High Resolution Radiometer) to calculate a basic LUE model with a developed ε parameter. ε_{max} is given a different value for C3 and C4 plants, and modified by air temperature, Vapour Pressure Deficit (VPD) and soil moisture (Prince and Goward, 1995). VPD is calculated as the difference between the saturation point of air and the current water vapour in the air, and is linked to carbon fluxes through the relationship between photosynthesis and evapotranspiration (Shurpali et al., 1995). GLO-PEM was an important step forward, but as the first fully RS-reliant model it should be considered as method development, and many further improvements have been made in later models. In particular, Tan et al. (2012) found that GLO-PEM's generalisations of plant categories only poorly account for ecosystem variation.

The **terrestrial Vegetation Photosynthesis Model (VPM)** is a modified LUE model which uses the Land Surface Water Index (LSWI) as a modifier of ε. The *f*PAR is calculated as a linear function of the Enhanced Vegetation Index (EVI), and attempts to solve problems created by non-photosynthetic vegetation registering as photosynthetically active in remote sensing data (Xiao et al., 2004). Dong et al. (2015) found that the VPM was the best model for explaining variance in cropland and prairie under drought conditions, and attributed this to the combination of EVI and a water content index. Dong et al. (2015) also pointed out, however, that the VPM requires more data inputs than simpler models and so cannot be used in places where there is no meteorological data. The VPM has been validated over a number of different ecosystems and has been shown to give good results using data from several satellite sensors, including both MODIS and Hyperion (Christian et al., 2015; Xiao et

al., 2004). The VPM was used over peatlands by Kross et al. (2016), as is discussed in more detail in Section 2.3.2.

The **EC-LUE (Eddy Covariance LUE model)** is so named because it is a modified LUE model which was developed using the latent heat flux measured by EC towers in its calculation (Yuan et al., 2007). The model relies on air temperature and evaporative fraction (EF) to modify LUE. Interestingly, the model constrains GPP by either temperature or water deficiency, depending on which is most limiting (Yuan et al., 2007). In the original 2007 model the EF was calculated using latent heat flux and the Bowen ratio (Yuan et al., 2007), but later versions of the model use net radiation from climate observation networks, modified by evapotranspiration parameters (Yuan et al., 2010). This means that the model can now be applied to large areas without tower data, and has also been shown to be more accurate than the 2007 EC-LUE model (Yuan et al., 2010). The EC-LUE model was validated against fifty-four sites with EC towers, but these sites only covered six major biomes, and did not specifically include peatland or wetland sites. Yuan et al. (2010) found that the model overestimated GPP at high latitude sites, and suggested that this may be caused by a high proportion of mosses which have a lower LUE than vascular plants.

Temperature and greenness (TG) models are a general class of satellite based GPP models which use land surface temperature (LST) as a proxy for other environmental variables in the LUE equation. A recent example is that of Sims et al. (2008) which only includes LST and EVI, and is therefore easily calculated from MODIS products. Sims et al. (2008) found that the LST dataset from MODIS correlates well with both PAR and VPD, and can therefore be used as a remotely sensed proxy. Their results showed that the TG model performed better than MOD17 across a range of North American biomes, but noted that it performs significantly less well at sites where vegetation is sparse (Sims et al., 2008). Verma et al. (2015) found that the TG model performed as well as more complex models when compared to EC data from the Fluxnet dataset across several different biomes. However, Dong et al. (2015) point out that it does not include any water stress modifier and so estimates variance in drought years rather poorly.

NASA uses MODIS data to produce an estimate of GPP. This product, which has been assigned a data code of **MOD17**, uses a modified version of the LUE algorithm to produce an 8-day total GPP at 1 km resolution across the globe (Running et al., 2015). The difference between the MOD17 product and other LUE models is that it uses modelled processes rather than vegetation indices to calculate *f*PAR. This MOD17 *f*PAR is taken from the MODIS LAI product (MOD15), which is generated by inversion of a physical model of light scattering in the plant canopy against observed MODIS reflectance data. Daily

meteorological data from the NASA Global Modelling and Assimilation Office (GMAO), including Vapour Pressure Deficit (VPD) and minimum temperature, are used to calculate PAR, and also to limit ε_{max} (Running et al., 2015, 2004; Tan et al., 2012).

Several studies have attempted to analyse the accuracy of the MOD17 product for different biomes and have concluded that there are inherent errors associated with the meteorology, radiometry and biophysical inputs. Heinsch et al. (2006) found that the largest source of error across fifteen sites in different biomes across North America was the VPD, which is calculated from NASA/GMAO data and used as a drought proxy to limit ε. In MOD17 VPD was found to often be underestimated, leading to a GPP overestimation compared to EC tower data (Heinsch et al., 2006). Another source of error in ecosystem studies is that the MOD17 εmax and the limits of VPD and temperature are estimated from the MODIS land cover classification product, MOD12Q (Tan et al., 2012). MOD12Q has a limited number of land cover classifications (see Table 2.3). This can cause errors in GPP estimation. It can be seen (Table 2.3) that there is no specific class for peatlands. This means that peatlands as a whole are classified as other land cover types. Such land-cover types almost certainly do not possess the high percentage of organic matter and waterlogged conditions so characteristic of peatland ecosystems. Kross et al. (2013) found that northern peatlands were often misclassified as evergreen needleleaf forest, mixed forest, or closed shrubland. Finally, Tan et al. (2012) point out that the MOD17 product does not include any estimate of surface moisture, which may particularly limit its usefulness when used on peatland sites. Some peatland species rely on high surface moisture for their water inputs, and including this factor in models can help to assess desiccation effects on photosynthesis (see Section 2.3.3).

Table 2.2 – Simplified description of well-known RS GPP models, and their major strengths and weaknesses for use over peatlands.

Model	Equation	Source of fPAR	Source of other variables	Strengths and weaknesses	Reference
MOD17	GPP = fPAR x PAR x E_{max} x f(T_{min}) x f(VPD)	from LAI (MOD15)	VPD (Vapour Pressure Defecit - determined from land cover MOD12)	Strength: No site optimisation needed Weakness: No peatland classification	Running and Zhao, 2015
			Tmin (minimum temperature from GMAO)		
GLO-PEM	GPP = fPAR x PAR x Ta x VPD x soil moisture	NDVI	Ta (air temperature from NDVI and LST relationship)	Strength: First fully RS-based model Weakness: Broad plant category generalisations	Prince and Goward, 1995
			soil moisture (from NDVI and LST relationship)		
			VPD (vapour pressure deficit from thermal infra-red)		
VPM	GPP = fPAR x PAR x Emax x Ts x Ws x Ps	EVI	Ts (air temperature scalar from ground data)	Strength: Validated under drought conditions Weakness: Requires meteorological data	Xiao et al., 2004
			Ws (water scalar from LSWI)		
			Ps (leaf phenology scalar based on deciduous/evergreen and LSWI relationship)		

EC-LUE	GPP = fPAR x PAR x Emax x min(Ts, Ws)	NDVI	Ts (air temperature scalar from ground data)	Strength: Validated across a wide range of ecosystems Weakness: May overestimate GPP at moss-dominated sites	Yuan et al., 2007; 2010
			Ws (water scalar, from evaporative fraction)		
TG	GPP = EVIs x LSTs x m	-	LSTs (land surface temperature scalar)	Strength: Only requires two inputs Weakness: No water stress component	Sims et al., 2008
			EVIs (enhanced vegetation index scalar)		
			m (unit scalar)		

1

Table 2.3 – MOD17 land cover types, from Running and Zhao (2015) p11. Note there is no peatland/wetland category.

Class value	**Class description**
0	Water
1	Evergreen Needleleaf Forest
2	Evergreen Broadleaf Forest
3	Deciduous Needleleaf Forest
4	Deciduous Broadleaf Forest
5	Mixed Forest
6	Closed Shrubland
7	Open Shrubland
8	Woody Savanna
9	Savanna
10	Grassland
12	Cropland
13	Urban or Built-Up
16	Barren or Sparsely Vegetated
254	Unclassified
255	Missing Data

2.2.3. Estimating ecosystem respiration

To obtain a full picture of ecosystem carbon exchange (i.e. to estimate NEE), we need both an estimate of GPP and an estimate of ecosystem respiration (R_{eco}). Ecosystem respiration is a combination of two sources of respiration: autotrophic respiration (Ra) from the plants themselves, and heterotrophic respiration (Rh) from microbiota within the soil (Figure 2.1). Ra consists of maintenance respiration and growth respiration, whilst Rh consists of rhizomicrobial respiration, and microbial decomposition of plant residues and other soil organic matter (SOM) (Gao et al., 2015). There are far fewer successful models of ecosystem respiration (R_{eco}) compared to GPP because it is much harder to account for the variation found between ecosystems, particularly using RS (Jägermeyr et al., 2014; Olofsson et al., 2008).

Many models produce an estimate of NPP, which is the difference between GPP and Ra. In LUE-based models maintenance and growth respiration can be accounted for as part of the ε parameter (Running et al., 2004) but there are fewer models which seek to estimate respiration directly, and particularly soil (heterotrophic) respiration. Despite this, several studies have suggested that the relationships between R_{eco} and GPP (Vourlitis et al., 2003) and R_{eco} and temperature (Olofsson et al., 2008; Rahman et al., 2005) are strong enough to estimate R_{eco} from RS data. Some models use a Q_{10} function, which gives a change in

sensitivity of respiration to temperature with every ten degrees (Reichstein et al., 2003) Some studies and models which include soil respiration are discussed below, and listed in Table 2.4.

Reichstein et al. (2003) found that soil water and temperature were good predictors for soil respiration. They also found that adding LAI as a proxy for productivity to the model improved the result. Their study was based on closed-chamber data from forest and shrubland sites across Europe and North America, but it was suggested that the variables could easily be estimated from RS data. This was proved to be the case by Anderson et al. (2008) who used a model which calculated soil moisture from microwave sensing, soil temperature from thermal imaging, and LAI from a vegetation index. Their model results showed good agreement with tower flux data over pasture land in Oklahoma (Anderson et al., 2008). Model development over such a small area, however, is unlikely to create a model which is reliable over other ecosystems or climates, and more validation work is needed.

Turner et al. (2006) created a model which estimates both Ra and Rh. The Ra portion of the model calculates maintenance respiration using a base rate and a Q_{10} function, while the growth respiration equation is based on the fraction of carbon available for growth (given as 0.33) used in respiration. Rh is calculated using a base rate modified by in-situ measurements of soil temperature, soil moisture and stand age. Both maintenance respiration and heterotrophic respiration are scaled by *f*PAR as a proxy for live biomass (Turner et al., 2006). Turner et al.'s (2006) model shows potential for a fully remote sensing based model, but also relies on data from a process-based model and in-situ data.

Wu et al. (2014) used NDVI and LST from MODIS to calculate soil respiration, along with two further parameters determined from site LAI. They found that night-time LST is more useful as it is a less noisy signal than daytime LST. Their model explained 78% of variance in eight years of flux data from a Canadian forest, but was limited by the lack of a soil water variable.

Jägermeyr et al. (2014) designed the **RECO** model to estimate global respiration. They assigned the world's ecosystems to one of three climate zones, each zone then being divided into further sub-categories of forested and non-forested biomes. Different model parameters were then created for each category. The model equation has two components: R_{ref} which is the reference respiration (calculated from yearly means of EVI and LST), and R_{std} which is the seasonal variation in the ratio of R_{ref} to R_{eco} (calculated using night-time LST, EVI and the difference between day and night LST as a soil water proxy). The model results were compared with several different sites across the Fluxnet network to give an R^2 value of 0.62. The limited classification of biomes in the model, however, means that

parameterisation may not take into account the wide variety of ecosystems that were not specified. This may be acceptable for a global model, but could cause large errors if applied to a specific ecosystem without additional parameterisation.

Gao et al. (2015) created the model **ReRSM**, which separates R_{eco} into GPP derived components (growth and rhizomicrobial respiration) and ecosystem organic matter (EOM) derived components (maintenance respiration, respiration from decomposition of plant residue and other SOM). The GPP component is calculated using EVI and LSWI (Land Surface Water Index). The EOM contribution to total respiration is calculated using the Lloyd-Taylor model which is another exponential function which relates temperature and respiration (Lloyd and Taylor, 1994) calculated from MODIS LST (Gao et al., 2015). They found that this model could explain 90% of the variation in respiration from EC data over five different ecosystem types in Northern China and the Tibetan plateau, with a root mean squared error (RMSE) of 0.05. These numbers suggest an excellent model performance, but cannot necessarily be transferred well to other ecosystem types, and may particularly be less accurate in areas affected by drought as there is no soil water component affecting the EOM derived respiration (Gao et al., 2015).

These GPP and R_{eco} models were all developed on ecosystems other than peatland, and future application of these models to peatland areas will require an assessment of the effect of parameters such as temperature and soil moisture on respiration in different peatland types (see Hilker et al. (2008) and Tan et al. (2012) for reviews of GPP models over other ecosystems).

Table 2.4 – Respiration models and their major strengths and weaknesses for use over peatlands.

Model	Equation	Variables	Strengths and weaknesses	Reference
Anderson et al, 2008	$Rh=(0.135+0.054 \times LAI)\theta_{10}\exp[0.069(T_{S,10}-25.0)]$	LAI (from vegetation index)	Strength: Fully RS based Weakness: Only developed over pasture land	Anderson et al., 2008
		θ_{10} (the 0 to 10cm average volumetric water content, derived from microwave data)		
		$T_{S,10}$ (the 10-cm soil temperature, derived from thermal band imagery)		
Turner et al., 2006	Rm = Rm_b* Q10^((Tair - 20)/10) * (1/ - k)(log(l - FPAR)	R m_b (base rate of maintenance respiration, from model)	Strength: Calculates Rh and Ra separately Weakness: Relies on in-situ data	Turner et al., 2006
		Q10 (change in rate for a 10°C increase in temperature, 2.0 used by Turner et al., 2006)		
		Tair (daily (24 hr) mean air temperature from database)		
		k (radiation extinction coefficient, 0.5 used)		
	Rg = (GPP - Rm) * Rg_frac,	Rg_frac (fraction of carbon available for growth that is used for growth respiration (0.33, Waring and Running, 1998))		

	Rh = Rh_base * SsT * SSW * SSA * FPAR	Rh_base (base rate of heterotrophic respiration, from model)		
		SST (scalar for soil temperature from database)		
		SSWh (scalar for soil water content from database)		
		SSA (stand age factor from Landsat data)		
Wu et al., 2014	Rh=a(NDVI×LSTn)+b	LSTn (night time LST)	Strength: Simple to use Weakness: No soil water parameter	Wu et al., 2014
		a=slope (related to annual LAI max)		
		b=intercept (related to annual LAI average)		
RECO	Re_{ref} = p1 + p2 x EVImean + p3 x LSTmean	EVImean (mean annual springtime EVI)	Strength: Good results across the Fluxnet network Weakness: Limited biome classification	Jägermeyr et al., 2014
		LSTmean (mean annual daytime LST)		

	Re_{std} = (p4/(p5 + p6 – ((LSTn – 10)/10)) +p7 x EVI + p8	LSTn (night-time LST)		
		EVI (8-day EVI/EVImean)		
ReRSM	Re = a x GPP + Rref x e^(E_0 x ((1/61.02) – (1/T + 46.02)))	Rref (derived from $R_{EOM)}$	Strength: Excellent model performance over Tibet and Northern China Weakness: Only validated over limited ecosystems	Gao et al., 2015
		T (average of daytime and night-time LST)		

2.3. Previous studies on peatlands

Remote sensing studies of peatland carbon fluxes can be placed into two broad categories: classification studies, which divide the landscape into types with similar conditions, and carbon flux estimation studies using models such as those explored in Section 2.2 (Whiting, 1994).

2.3.1. Classification studies

Classification studies can be used both to identify peatland as a distinct land use (in comparison with areas of forest or agricultural land for example) and also to identify vegetation communities and topographic features within a peatland environment. These classification studies can then be used to define key parameters (e.g. εmax) in order to adjust a general model to specific conditions.

Peatlands are often classified in RS studies on the basis of vegetation types. Different plant species dominate under different conditions, and can affect the carbon fluxes of the peatland. A higher proportion of vascular plants to mosses increases both photosynthesis and autotrophic respiration and is also likely to be associated with an increase in heterotrophic respiration because a larger amount of available substrate is present (Dinsmore et al., 2009a; Limpens et al., 2008; Walker et al., 2016). It is important to note that different vegetation compositions on peatland differ not only in their overall NEE, but also in the response of their carbon fluxes to environmental change (Bubier et al., 2003). Bubier et al. (2003), for example, showed that sedge-dominated communities within a bog experienced a greater decrease in photosynthesis under drought conditions than communities dominated by ericaceous shrubs in the same ecosystem. It is therefore important to have an understanding of vegetation communities and differential responses when creating a carbon flux model. Some carbon flux estimations can be achieved simply by applying knowledge of differential responses to land cover and climatic data, as can be seen at a large scale in MOD17.

Several studies have considered the heterogeneity of peatland vegetation at different scales, and have developed ways of classifying areas of differing vegetation composition based on spectral reflectance and structural data – these are not specifically discussed here but can be found in papers such as Anderson et al. (2010) Bubier et al. (1997) Crichton et al. (2015) Forbrich et al. (2011) Frolking et al. (1998), Parry et al. (2015) and Thomas et al. (2003).

2.3.2. Carbon flux estimation studies

Relating remote sensing directly to peatland carbon fluxes is an area of research which is growing rapidly, although as yet there are still only a few published studies from this

increased research activity and therefore any conclusions must necessarily be of a tentative nature. Some studies have used the MOD17 GPP product compared with data from flux towers, but have found that this product has poor accuracy over peatland environments (Kross et al., 2013; Schubert et al., 2010). Kross et al. (2013) found that the MOD17 product underestimated Eddy Covariance GPP at three of their four sites across Canada and Finland (one bog and two fen). They suggest this is due to the unsuitability of the εmax downscaling algorithm in peatland ecosystems. Connolly et al. (2009), however, showed that the MODIS *f*PAR product had a good relationship with *f*PAR derived from field-based LAI measurements. This suggests that although the MOD17 product may provide a good structural analysis and estimate of potential photosynthesis, it is held back by the algorithms for establishing LUE, which are not calibrated well within peatland environments. Kross et al. (2013) suggest that the VPD modifier of LUE in the MOD17 product may be particularly unnecessary over peatlands, as it appears to have had little effect during their study period, and does not have much of a relationship to soil moisture (Harris and Dash, 2011).

Other studies have used vegetation index models as an estimate for field flux data (see Table 2.5). Harris and Dash (2011) compared MTCI, which uses the red-edge principle, to GPP observations at a raised bog and a moderately rich treed fen and found that there was a good relationship in the active growing seasons of 2004 and 2005 for both sites. Unfortunately, they did not compare this to the performance of other vegetation indices, although the MTCI principle is similar to the NDVI. Kross et al. (2013) considered MODIS NDVI at one raised bog site and three different fen sites, and found that the relationship between NDVI and GPP observations was good at capturing interannual variation at individual sites, and that moreover the same regression coefficient (for NDVI and GPP observations) could be used at several sites with similar characteristics. This suggests that NDVI would be a useful vegetation index in developing a peatland RS model which could be used without site-specific calibration. Harris and Dash (2011) give the R^2 value for a 1:1 relationship between MTCI and GPP values as 0.71 (0.46-0.87), whilst Kross et al. (2013) give the R^2 value for NDVI and GPP as 0.43 (0.39-0.71). These are not directly comparable, however, as the studies were over different sites and time spans, and because the MTCI uses MERIS data whilst Kross et al. (2013) used MODIS NDVI.

Whiting (1994) give a positive correlation value between NDVI (measured in the field using a handheld spectroradiometer) and NEE of 0.43 (using chamber data) over a combination of bog and fen sites, but observed unexpectedly high NDVI values at a site which had a large proportion of brown-green *Sphagnum* species present, and suggest that the differing combinations of moss and vascular plants may complicate the NDVI:NEE relationship. Levy and Gray (2015) studied a peat bog site in Northern Scotland and found only a low

correlation coefficient of 0.23 between EC GPP and MODIS NDVI. These studies suggest that NDVI can give us some information about peatland carbon flux, but more factors are needed to create an accurate model on a large scale.

Schubert et al. (2010) compared MODIS NDVI and EVI as predictors of GPP across a raised bog and a minerotrophic fen in Sweden and found that EVI gave better results (R^2 values of 0.37 and 0.45 compared to 0.26 and 0.36). In particular, they noted that the NDVI curve levelled off in summer, indicating saturation. (Letendre et al., 2008) completed a study using a handheld spectroradiometer which found that the R^2 value for NDVI and NEE at their *Sphagnum*-dominated open raised bog site in Canada was as low as 0.12, but that combining NDVI with PRI gave a better result (R^2 of 0.26). Letendre et al. (2008) discovered that the Chlorophyll Index (CI, based on red-edge position) gave the best correlation with NEE, with an R^2 of 0.37. Van Gaalen et al.'s (2007) and Harris' (2008) laboratory studies found that PRI was a good indicator of short term (minutes to hours) changes in photosynthetic efficiency within individual *Sphagnum* species, but required *a priori* knowledge of the species present. This means it may provide good results under laboratory conditions, but may not translate well to larger scale field studies with the intermixture of *Sphagnum* species present in field conditions. *Sphagnum* patches of a single species rarely exceed 20 cm^2, and it is common to find species entirely intermingled to the extent that even a fine resolution spectrometer would pick up reflectance signals from more than one species.

Kross et al. (2016) considered the variation of the LUE parameter ε over different peatland types in Canada and Finland (same sites as Kross et al., 2013). They found that monthly variations in ε correlated with variations in air temperature and MODIS NDVI, and that annual variations correlated with wetness as measured using LSWI. They also applied the VPM to their study sites, and found good agreement between ε calculated using MODIS data to drive the VPM, and ε calculated using ground-measured data. Unfortunately they did not publish the carbon flux estimates from the VPM.

Table 2.5 – Simple vegetation indices using NIR and red bands (NDVI and MTCI) compared to ground measurements of carbon flux. This table highlights the difficulty of comparing across studies due to different methods of carbon flux and spectral measurement.

Study	**Site type**	**Comparison**	**R2**	**CO_2 data**	**Spectral data**
Whiting, 1994	Coastal fen, interior fen and bog	NEE:NDVI	0.18	Chamber	Field spectroradiometer
Letendre et al., 2008	Open raised bog	NEE:NDVI	0.12	Chamber	Field spectroradiometer
Schubert et al., 2010	Raised temperate ombrotrophic bog	GPP:NDVI	0.26	Eddy Covariance	MODIS 250 m
Schubert et al., 2010	Boreal oligotrophic minerotrophic fen	GPP:NDVI	0.36	Eddy Covariance	MODIS 250 m
Harris & Dash, 2011	Raised bog	GPP:MTCI	0.74	Eddy Covariance	MERIS 1 km
Harris & Dash, 2011	Moderately rich treed fen	GPP:MTCI	0.77	Eddy Covariance	MERIS 1 km
Kross et al., 2013	Raised ombrotrophic bog	GPP:NDVI	0.71	Eddy Covariance	MODIS 250 m
Kross et al., 2013	Moderately rich treed fen	GPP:NDVI	0.66	Eddy Covariance	MODIS 250 m
Kross et al., 2013	Open minerotrophic moderately rich fen	GPP:NDVI	0.64	Eddy Covariance	MODIS 250 m
Kross et al., 2013	Mesotrophic sub-arctic poor fen	GPP:NDVI	0.39	Eddy Covariance	MODIS 250 m
Levy and Gray, 2015	Blanket bog	GPP:NDVI	0.09	Eddy Covariance	MODIS 250 m

2.3.3. Temperature and water content

The two variables most widely considered to affect peatland GPP are soil moisture/Water Table Depth (WTD) and temperature (Harris and Dash, 2011). However, there are issues with including these in RS-driven models as there is debate over whether RS indices can adequately represent these variables, and therefore to what extent including them improves a model (Connolly et al., 2009; Harris and Dash, 2011; Schubert et al., 2010).

Harris and Dash (2011) found that adding LST to their MTCI-based model did not greatly improve results. They suggest that this may be due to the poor performance of LST as a proxy for more stable soil temperatures, but allow that it may be a useful VPD proxy, and therefore more valuable under drought conditions. In contrast, Schubert et al. (2010) found that adding LST to their EVI-based model did improve results, and also gave a good correlation with R_{eco}. Harris and Dash (2011) based their work on a raised bog and a moderately rich treed fen in Canada, whereas Schubert et al. (2010) were working on a raised ombrotrophic bog and an oligotrophic minerotrophic fen in Sweden – both used EC data as a ground validation method.

Soil water content is likely to be a particularly important model variable in peatland environments as these ecosystems rely on exceptionally high water tables to function. In a natural bog the catotelm will remain saturated all year round, whilst the acrotelm experiences fluctuations (see Figure 2.1). Even a small drop in the water table can impact productivity, because *Sphagnum* moss is particularly sensitive to moisture availability. It is also important to note that damaged peatlands and those undergoing restoration may experience much greater fluctuations than natural bog.

Zhang et al. (2015) make the point that the effect of water content on LUE is complex, and different indices may provide additional information within one model. Several studies (Bryant and Baird, 2003; Harris et al., 2006; Harris et al., 2005; Van Gaalen et al., 2007; Vogelmann and Moss, 1993) have shown that the spectral reflectance of several *Sphagnum* species changes as the mosses respond to different moisture conditions – in particular, reflectance increases as the *Sphagnum* dries and becomes paler. *Sphagnum* has very pronounced water absorption features at 990 and 1200 nm (Harris et al., 2005; 2006). The subject of measuring peatland water content from remote sensing data could provide enough material for an entire paper in itself, so a brief summary is all that is given here (see Harris and Bryant, 2009, for more information).

Water indices, as with vegetation indices, can be calculated using visible and infra-red data from satellites. The Water Index (WI) studies the changes in the reflectance trough at 950-970 nm (see Figure 2.5), which is caused by the light absorbance of water in plants,

compared to a reference wavelength at 900nm (Penuelas et al., 1997). The Land Surface Water Index (LSWI), also known as the Normalised Difference Water Index (NDWI) uses the principle that the SWIR band at 1.24 μm measures both water content and other plant factors, whereas the NIR band at 0.86 μm only responds to factors other than water content – the difference is therefore an index of vegetation water content (Gao, 1996). The floating Water Band Index (fWBI) considers the minima between 930 and 980 nm to be the water absorption band. This minimum is compared to the reference wavelength at around 900 nm (Harris, 2008; Strachan et al., 2002).

Mcmorrow et al. (2004) and Meingast et al. (2014) used specific bands (1400 and 1940 nm; 970, 1200, 1450, 1950 and 2250 nm) to indicate water content and estimate WTD. Meingast et al. (2014) found that the bands in the NIR range gave the best results over vegetated peat. This corroborates Harris et al.'s (2005) work which found that water indices using the NIR range gave the best results in their laboratory work on *Sphagnum* drought stress. Letendre et al. (2008) found that both the LSWI and the WI had strong correlations with volumetric water content in peat (Pearson's coefficients of 0.77 and 0.75 respectively). They also found that using a ratio of NDVI/WI improved the relationship between the vegetation index alone and NEE values at their study site in Canada (Letendre et al., 2008). Harris (2008) found that the fWBI correlated very well with the pooled data for photosynthetic efficiency from five different *Sphagnum* species under drought stress (correlation coefficients of 0.58-0.90). Overall, studies show that water indices using the visible and NIR wavelengths are adequate proxies for water content in the vegetation and acrotelm of bog environments, although passive RS is unlikely to give much information about water contents deeper in the soil. There is no consensus as yet on which is the best, and it may be the case that different indices are better suited to different peatland landscapes and vegetation communities.

2.4. Challenges of working with RS on peatlands

Remote sensing of peatland vegetation can be a challenge when there are both vascular plants and mosses present at a site, due to the different heights of the species. It can be difficult to accurately measure LAI when there is vertical heterogeneity in the vegetation (Garrigues et al., 2008), and if there is a thick vascular canopy the presence and spectral signal of *Sphagnum* can sometimes be missed altogether (Parry et al., 2015). This height differentiation can also cause a difference in the PAR received by different plants (Chong et al., 2012). Huemmrich et al. (2010) suggest that at some sites it is necessary to treat peatlands as a two-level environment, with a moss understory and a vascular canopy, and to include this distinction in remote sensing models.

The response of *Sphagnum* mosses to environmental conditions is spectrally very different to that of vascular plants. Reflectance in the SWIR regions of the spectrum is lower than for vascular plants due to the higher water content of *Sphagnum* (Bryant and Baird, 2003; Bubier et al., 1997). Calculating NDVI over peatlands has shown unusually high values compared to vascular plant communities, and this can affect GPP estimates in peatlands where *Sphagnum* is prevalent (Letendre et al., 2008; Whiting, 1994). Different plant types also have differing spectral responses to drought (Bryant and Baird, 2003; Lund et al., 2009; Urbanova et al., 2013). Yuan et al. (2014) adjusted the EC-LUE model over boreal forests to take into account the presence of mosses and their effect on GPP estimations. They found that a model with separate εmax values for vascular plants and mosses, and an estimation of proportional contribution to the satellite signal from each, gave a more accurate result (Yuan et al., 2014). Letendre et al. (2008) suggest that the *Sphagnum* challenge may be at least partly overcome by including a water index in any given model.

The prevalence of different vegetation species is strongly related to the type of peatland being studied. There is some evidence that the difference between types of peatland is great enough to affect the relationship with spectral data (see Section 2.3.2), but as yet there are not enough studies available to quantify this difference. Correctly identifying peatland type and relating this to spectral data is important for generating accurate estimates of carbon flux.

Many peatlands are water-saturated for a large proportion of the year, which can cause problems for remote sensing. High water content may cause an increase in light scattering, or a change in absorption features, which will affect the satellite signal. Also, many of the models discussed (e.g. MOD17, GLO-PEM, EC-LUE, VPM, Anderson et al., 2008, Turner et al., 2006) in this paper assume that a lack of water is a limiting factor on GPP and R_{eco}. However, healthy peatland environments almost always have a very high water table so the water factors in many of these models developed in other ecosystems may need to be re-evaluated for peatlands. Another aspect these models do not consider is that complete saturation is a limiting factor on soil respiration in peatland environments.

Peatland environments are often very cloudy, which can limit the data available from remote sensing. This is an issue with all remote sensing in the visible and infrared wavelengths, but is a particular problem in some ecosystems such as high latitude wetlands. One of the ways to deal with this issue is to use data from a satellite which has a frequent pass interval (e.g. MODIS, Sentinel-3), as there is then a higher chance of collecting a reasonable amount of useful data which can be gap-filled sensibly. The trade-off here is in terms of spatial resolution. Other options include using active sensors which can penetrate cloud cover, or

utilising aerial imaging which can be obtained by flying below the cloud layer – though shadows and low light may then become major factors. One issue associated with cloud cover is that the GPP estimated from RS data may be overestimated if only clear day estimates are used. The range of LUE values is generally much smaller on clear days than on cloudy days – and peatlands occur most widely in areas of high cloud cover (Drolet et al., 2005).

The microtopography of peatlands (see Figure 2.2) can also affect carbon fluxes (Bubier et al., 2003; Forbrich et al., 2011), but is difficult to detect directly with RS, particularly when spatial resolution is coarse (Crichton et al., 2015). Waddington and Roulet (1996) found that the scale from which extrapolation is attempted can affect whether the overall estimate is a sink or a source – variation in fluxes is greatest at the microtopography level, although there are also carbon flux variations at the mesoscale due to features such as pools and sections of different land cover. Pools in particular are an important component of the carbon cycle on peatlands, and ignoring their presence may lead to an inaccurate estimate of NEE (Lindsay, 2010; Turner et al., 2016; Waddington and Roulet, 1996).

There are several ways to solve the heterogeneity issue; the first is to use very fine resolution imagery which can detect different vegetation communities, and use this data to analyse the proportion of land which is hummocks and hollows in order to estimate variations in carbon flux within the cells of coarser resolution data (Forbrich et al., 2011). The second is to assume that although peatland is heterogeneous at a small scale, peatland sites are fairly homogenous at a larger scale (this is known as a repeat mosaic). In other words, the assumption is that the grid square size covered by satellites such as MODIS will be a reasonably representative sample of the entire peatland area. A third option is to downscale data from a coarse resolution satellite. There are several methods for downscaling (e.g. Hill et al., 2011; Stoy and Quaife, 2015), one of which is the model STARFM (Spatial and Temporal Adaptive Reflectance Fusion Model) which combines Landsat data (which has fine spatial resolution but a long pass interval, with data from MODIS (which has a coarse spatial scale but short pass interval), to create a product with fine resolution and a short repeat interval (Feng Gao et al., 2006; Walker et al., 2014).

Validation of remote sensing carbon flux models is usually performed using data from EC towers, but there can be issues with scale and geolocation (see Figure 2.3). Both EC footprints and satellite pixel sizes can vary. EC footprints change size and shape with wind direction and speed, whilst satellites typically collect data from a slightly different area on each pass, and require geo-correction (Harris and Dash, 2011; Schubert et al., 2010). Clearly, the larger the area covered by the EC footprint, the more chance there is of being

able to match it to a satellite pixel (see Figure 2.3). The assumption that peatlands are fairly homogenous at large scales and that one satellite point or EC footprint is representative of the whole landscape is necessary for this validation to be meaningful. More work is needed to determine whether or not this assumption can be considered reasonable.

Every method of calculating carbon flux is subject to its own errors, including RS, EC and chamber techniques. For optical sensors in satellites, corrections for atmospheric effects must be made before the data are used. The translation of raw RS data into products and models also introduces error. Data from EC towers, in the form which is often used for validation of RS models, are the result of a series of processing steps which include calculating the flux from the raw turbulence and gas concentration data; averaging the flux over time periods; removing periods of very low turbulence; gap-filling; and partitioning into GPP and Reco (typically using a temperature dependant model of Reco fitted to night time data when GPP is zero). This means that eddy covariance data are not a truly accurate measure of carbon flux, yet they are often treated as though they are a direct measurement. Chamber fluxes are usually considered to be on too small a scale to be a useful validation method for remotely sensed flux estimates, and there are concerns that collar insertion methodology may cause inaccurate results (Heinemeyer et al., 2011). In particular, the short timescale and small area of chamber measurements means that extrapolating to a whole satellite pixel over several months is likely to give results so inaccurate as to be meaningless.

One advantage of satellites with long time series, such as Landsat and MODIS, is that between instrument errors are avoided. Infra-Red Gas Analysers (IRGAs) used in chamber studies and Eddy Covariance towers have advanced greatly in precision over the last decade, meaning that comparison between early and modern chamber or EC studies is difficult. Satellites with long time series do not have this problem because the instrument is the same. Satellites also avoid the operator error which can occur between researchers using different protocols for their chamber or EC studies. The frequency of measurements can increase precision in satellite data compared to chamber studies, particularly for satellites with a frequent return interval.

Future studies intending to use RS data should consider the resolution and coverage of available RS data when designing their ground-validation methodology. In particular, footprint size and coverage in relation to EC towers, and sampling locations and frequency in relation to chamber studies, should be decided with regard to the RS data. One potential solution to the different coverage of chamber, EC and RS data is to scale fluxes using proportional cover (Forbrich et al., 2011; Marushchak et al., 2013). This can be done in

terms of microtopography by considering the proportion of the measured area comprising of hummocks, hollows and lawns (see Figure 2.2) or in terms of variation in vegetation species. Issues to consider when attempting proportional cover corrections include the time and access needed to identify features or vegetation over the entire area of the EC footprint or satellite pixel. Enough measurements should be taken to allow a reliable average for each identified feature type or vegetation species. The proportional cover can be determined by surveying the entire footprint area, possibly using aerial photography. It is also important to have ground validation data for all seasons, as different vegetation species can have a proportionally very different contribution to fluxes at different times of the year.

2.5. Potential future work

The previous section (Section 2.4) has highlighted a number of challenging issues which must be addressed when RS methods are applied to peatland environments. More work is clearly needed in overcoming these challenges, particularly in separating the signal of vascular plants from mosses, and in considering the problems of heterogeneous microtopography and peatland types (see Section 2.4). This section, however, discusses some of the largest gaps this review has identified in the literature which need to be addressed in future in order to improve remotely sensed estimates of carbon fluxes over peatlands.

The area of remote sensing carbon flux estimation over all ecosystems is dynamic and wide ranging, with many different models and methodologies being developed. The problem with many of these studies, however, is that they are too narrow for comparison. They consider one particular site in one particular ecosystem, and develop a remote sensing model which gives good results compared to the flux measuring method on the ground (most often EC). Even studies which look at multiple sites and attempt to create a global model often focus on a narrow range of only four or five ecosystem types. Peatlands and their huge variety of types are almost never included as a separate category in remote sensing models of carbon flux, and as such are certain to be over or under-estimated. More cohesive studies are therefore needed, which not only look at peatland carbon fluxes across sites and countries, but also which link peatland flux models to those developed in other ecosystems.

Roulet et al. (2007) point out that the peatland carbon cycle is complex and includes many components, some of which are under-studied. Peatland studies using remote sensing have so far focused almost entirely on estimating GPP, and there is a need for more work on the potential of remote sensing for estimating respiration fluxes. One major challenge when using current models of R_{eco} over peatland environments is that they are designed for use on well-drained soils, and so do not include the concept that water saturation may decrease soil

respiration. In carbon peatland studies using field measurements, NEE calculations dominate. There are few studies that combine NEE with CH_4 and DOC, and there is very little work combining these using remote sensing (Sturtevant and Oechel, 2013; Watts et al., 2014).

Considering the range of GPP models discussed in Section 2.2.2.3, it is evident that LUE-based models are still the dominant method for using RS to assess the carbon uptake of ecosystems. Most studies agree that the MOD17 product is a poor estimate for peatland GPP, most likely because the LUE modifiers are based on a look-up table with no specific peatland category. NDVI and EVI are both widely used as proxies for *f*PAR, and studies over peatland have given good results using one or the other of these indices. More work is needed, however, to determine which is the most effective proxy, particularly when combined with other model factors. Narrow-band indices such as PRI should also be considered in future studies, particularly with the operation of new narrow-band satellite sensors such as EnMAP.

In both peatland and other ecosystem studies, temperature and water stress have been shown to be useful modifiers of LUE and to improve the model results. There is still much debate about the best indices to use, however, particularly for water stress which is an essential consideration in peatlands, given their semi-permanent saturation. Future studies should seek to determine which water indices are best able to capture the entire range of water contents experienced within peatland landscapes.

An interesting avenue of future work would be to consider combining visible and NIR data with RS data from other sources such as InSAR. The combination of texture, elevation and colour changes has the potential to inform a future generation of peatland models.

There is a need for more long-term studies on peatland in order to inform the temporal variability that should be expected of model outputs, and the inputs that are most influential in longer-term peatland carbon flux variations (Helfter et al., 2015; Marushchak et al., 2013; Strachan et al., 2016). Some satellites (e.g. Landsat) have long data archives, which could be extremely useful in historical studies of peatland carbon flux, but only if the models used are validated under appropriate conditions. Carbon fluxes are known to vary greatly between years at the same site, and it is possible for a peatland to be a carbon source one year and a sink the next (Lafleur et al., 2003; Roulet et al., 2007; Silvola et al., 1996; Yu, 2012). For example, Roulet et al. (2007) monitored a bog in Canada for six years, with the lowest annual NEE (greatest sink) during the period of -112 gCO_2/m^2 and the highest (smallest sink) of -2 gCO_2/m^2. Many field studies only report on one growing season and exclude winter fluxes altogether, therefore potentially underestimating annual R_{eco} (Roulet et al.,

2007; Sturtevant and Oechel, 2013). It is also important to repeat studies across several different types of peatland, as it cannot be assumed that areas with different characteristics will respond in a similar manner to environmental changes (Kross et al., 2016; Lund et al., 2009). Remote sensing has the potential to easily estimate carbon fluxes over large areas and long periods of time and could therefore fill a gap in the literature of long-term carbon flux studies over peatlands - but it is important to have reliable models first, and to continue to validate models appropriately.

As restoration of peatland offers the potential to increase carbon sequestration (Beetz et al., 2013; Silvola et al., 1996; Urbanova et al., 2013), it is important to increase understanding of how rewetting affects peatland carbon fluxes in the long term (Bussel et al., 2010). Modelling driven by remote sensing data could be a useful approach for large-scale monitoring of peatland restoration schemes, but more work is needed on whether RS data can adequately detect changes in peatland carbon fluxes that are due to restoration processes. We are currently unaware of any published studies utilising remotely sensed data to examine the effects of restoration on carbon fluxes from peatlands. Restoration is generally accepted to improve carbon uptake in comparison to drained and degraded sites, even if the resulting carbon balance is still net emitting or near neutral (Beetz et al., 2013). However, several studies have shown that rewetting is more effective on some peatland sites than others, and there may be some areas which can be improved but never fully restored to a near-natural condition (Basiliko et al., 2007; Clark et al., 2010; Worrall et al., 2011). It is therefore important to have more long term (5 years plus) studies on restoration of different peatland types, in an attempt to characterise what makes a peatland more or less likely to be producing reduced carbon emissions through restoration, and to analyse which restoration methods are the most successful (Bain et al., 2011). Many restoration programmes on Northern peatlands are still in their early stages, and it will be important to continue monitoring on longer timescales of several decades. This is an area of future work into which RS could be usefully integrated.

2.6. Conclusions

This critical review provides clear evidence for the potential of using RS methods in Northern peat bog carbon flux estimations as well as in other peatlands around the world. The review also highlights a number of cautionary issues which must be accommodated when using RS methods in a peatland habitat, and it identifies a number of challenges which have yet to be adequately tackled.

Some researchers have already applied GPP models to peatland ecosystems, and some have focused on the effectiveness of specific aspects, such as the correlation of vegetation

indices with peatland dynamics. The studies considered in this review suggest that the best RS GPP model for peatlands is likely to include either NDVI or EVI, and to have both temperature and water modifiers of LUE. There are many ways of measuring water stress using RS data, and the studies in this review suggest that visible and NIR wavelengths produce potentially usable estimates of peatland water through indices such as the LSWI, WI and fWBI. The best model is therefore likely to be based on visible and NIR wavelengths which are readily available from several satellite sensors already in operation, although spatial resolution will be improved by newer satellites with finer sensor capabilities.

Respiration is a harder problem to solve in RS models of peatland carbon fluxes. Different studies have modelled respiration in very different ways, and there is as yet no commonly used model structure as there is with the LUE model for GPP. The studies considered in this review suggest that respiration (both Ra and Rh) is sensitive to temperature and to productivity/biomass. In addition, soil respiration is concluded to be sensitive to soil water content. Water is especially important in peatlands, which may have the opposite response to most ecosystems – increasing soil respiration with lower than normal water levels.

Many of the problems encountered when applying RS models of carbon fluxes to peatlands are the same as for any other ecosystem: satellite issues such as atmospheric scattering and geocorrection and ground validation issues with the estimation of fluxes from methods such as EC. However, other concerns are unique to peatland environments, such as the spectral and height differences between vascular and non-vascular vegetation types, and the microscale heterogeneity of many peatlands. More work is therefore needed into the upscaling of fluxes from a repeat mosaic environment, and into the potential of having a model which splits its parameterisation between vascular and non-vascular vegetation.

This review suggests that there is a need for multi-disciplinary studies across several peatland sites over several years using RS. Remote sensing models, particularly those for GPP, are now attaining levels of confidence where they could be considered plausible additions to the suite of methods used to measure carbon exchange in peat bog sites. Of particular interest would be studies that explore the potential use of RS in the construction of total carbon budgets, including GPP, Reco, CH_4 and DOC. There is, however, so far little published information in the peer-reviewed literature from sites which have been subject to restoration management. This dearth of information is surprising, given the high profile now afforded peatland ecosystems within decision-making circles around the world and the scale of resources devoted to such restoration in order to stem carbon losses and restore long-term carbon storage.

Acknowledgements

Thanks to RSPB Forsinard for site access and sampling permission. Thanks to Kevin White for help with the Ger3700 spectrometer. Thanks to Matt Aitkenhead for proof reading and comments and to the two anonymous reviewers for their helpful critiques.

Funding

This work was supported by the Natural Environment Research Council (NERC) SCENARIO DTP (Grant number: NE/L002566/1). Tristan Quaife is funded by the NERC National Centre for Earth Observation (NCEO). Myroslava Khomik and Rebekka Artz are funded by The Scottish Government Strategic Research Programme.

3. Changes in carbon flux and spectral reflectance of *Sphagnum* mosses as a result of simulated drought

Lees KJ, Clark JM, Quaife T, Khomik M & Artz RRE

Abstract

1. Different rainfall simulations were applied to two species of *Sphagnum* from blanket bog to assess the impact of drought on carbon function. After eighty days all samples were rewetted to assess recovery. The rainfall simulations included inputs analogous to actual precipitation at the field site, potential future changes in rainfall, and extended total drought.

2. During the experiment Gross Primary Productivity (GPP) and respiration were measured. Photosynthesis decreased after approximately 30 days of continuous drought (ie. days without rain). This is somewhat comparable to the drought seen at the sampling site (Northern Scotland) in the summer of 1995, where only 1 mm of rain fell over 21 days.

3. Spectral reflectance was measured to assess *Sphagnum* bleaching. The spectral absorption feature of *Sphagnum* associated with red light (around 650 nm) was affected by drought, and did not recover after rewetting during the experimental period.

4. No significant difference was found between the two *Sphagnum* species studied with respect to their photosynthesis or respiration, but there was a significant difference in optimum water content and spectral reflectance between the two.

5. Synthesis: The results from this study suggest that *Sphagnum* carbon function is resilient to quite long drought periods, but once damage has occurred recovery is likely to be difficult. The spectral reflectance of *Sphagnum* can give useful information in assessing whether significant desiccation damage has occurred.

3.1.Introduction

Sphagnum moss is an important peat-forming genus, and is instrumental in the sequestration of carbon in Northern ombrotrophic peatlands. The function of peatlands as a carbon sink is of interest to policy makers, as peatland restoration can now be claimed as a carbon abatement in national accounting under the Kyoto Protocol (Hiraishi et al., 2014).

Drought has been shown in previous studies to affect *Sphagnum* function (Bragazza, 2008; Clymo, 1973; Harris, 2008; Strack & Price, 2009; Van Gaalen, Flanagan, & Peddle, 2007), and this could become important as climate change increases the frequency of occurrence of hotter, dryer summers (Jenkins et al., 2010; Hoegh-Guldberg, Jacob, & Taylor, 2018). It is uncertain, however, how long and how extreme drought needs to be before it affects

Sphagnum function (Bragazza, 2008). It is also unclear whether, and to what extent, *Sphagnum* can recover its functionality after desiccation. Some studies suggest that desiccated *Sphagnum* can recover its carbon function after a period of rewetting (McNeil & Waddington, 2003; Robroek et al., 2009), whilst others suggest that extreme desiccation may be irreversible (Bragazza, 2008; Schipperges & Rydin, 1998).

Frequent small precipitation events can relieve the effects of drought on carbon function by rewetting the moss capitula (Nijp et al., 2014; Robroek et al., 2009). There is also some evidence that frequency of rainfall events is more important than overall water input due to the inability of *Sphagnum* to draw water up from a deep water table (Adkinson & Humphreys, 2011; Nijp et al., 2014; Robroek et al., 2009; Strack & Price, 2009). Raindays are considered particularly important, and the temporal distribution of precipitation has been shown to be more important than total amounts in terms of maintaining carbon function (Backeus, 1988; Lindsay et al., 1988).

Spectral reflectance can provide information about *Sphagnum* health, including carbon functioning under water limitation (Harris, 2008; Letendre et al., 2008; Van Gaalen et al., 2007). Certain areas of the reflectance spectrum of *Sphagnum* moss indicate water content, chlorophyll, and plant health. This could be a useful way to detect the impact of drought on *Sphagnum's* carbon functioning when direct measurements are unavailable. It is particularly important to develop understanding of the spectral reflectance of *Sphagnum*, as this is a key genus considered an indicator for healthy blanket bog. It has also been found to have a different spectral response compared to other peatland vegetation (Whiting, 1994).

The Normalised Vegetation Index (NDVI) which we consider in this study is a widely used spectral index which can be easily calculated from satellite or UAV (Unmanned Aerial Vehicle) data. Validation of this in the laboratory will be particularly useful for researchers using remote sensing over peatlands at large scales (Lees et al., 2018).

In this study five experimental water input regimes were set up in the laboratory to test the relative impacts of different rainfall amounts and frequencies on *Sphagnum* carbon dioxide gas exchange. Different *Sphagnum* species may react differently to low water contents, with hummock-growing species being more tolerant to drought conditions than species which grow closer to the water table (Harris, 2008; Robroek *et al.*, 2009; Strack and Price, 2009). Two *Sphagnum* species*, S. capillifolium* and *S. papillosum*, are compared to assess whether different *Sphagnum* species have differing responses to drought stress. In this work we are particularly seeking to address how drought stress affects the carbon function (photosynthesis and respiration) of *Sphagnum* samples, and whether this functioning recovers after a rewetting event. Finally, we also consider the changes in spectral

reflectance in *Sphagnum* during drought stress, as this may be a useful way to assess *Sphagnum* health using remote sensing.

This study aims to contribute to research by combining measurements of several variables in a single experiment. Previous studies have considered the optimum water content (eg. Adkinson and Humphreys, 2011; Titus et al., 1983), drought recovery (eg. Nijp et al., 2014; Robroek et al., 2009; Schipperges and Rydin, 1998), or spectral reflectance (eg. Harris, 2008; Van Gaalen et al., 2007) of *Sphagnum* mosses, and this research aims to bring all these together to study their interactions in detail. We hypothesise that (1) *S. papillosum* will be more sensitive to drought than *S. capillifolium*, with a higher optimum water content and less resilience to water reduction as it prefers slightly wetter microhabitats (Robroek et al., 2009). (2) water content reduction will lead to a decrease in photosynthesis and respiration, but that this may be ameliorated by more frequent water input, and that the carbon function will recover after rewetting; and (3) that changes in spectral reflectance will correlate well with changes in *Sphagnum* carbon function during the experiment.

3.2.Method

3.2.1.*Sphagnum* species

Figure 3.1- Clockwise from top left: S. papillosum in the field at sampling time, S. papillosum texture, S. papillosum samples in the lab, S. capillifolium samples in the lab, S. capillifolium texture, S. capillifolium in the field at sampling time.

Our study sites were located at the Royal Society for the Protection of Birds (RSPB) Forsinard Flows reserve in Northern Scotland (58.3552, -3.9993 to 58.4458, -3.6972 WGS84). Parts of the reserve were undergoing restoration from forest to bog and were at

different stages of restoration. The samples collected for our lab study were collected from three areas of the reserve, known as Talaheel (58.4116, -3.7992 WGS84), Catanach (58.4020, -3.7130 WGS84), and Raphan (58.4109 -3.7318).

S. capillifolium and *S. papillosum* were selected as two contrasting *Sphagnum* species (see Figure 3.1). *S. capillifolium* is red to green and grows in tightly packed clusters with a 'pom-pom' appearance due to its hemi-spherical capitulum (Laine et al., 2009). *S. papillosum* is green to yellow-brown and grows in carpets and low hummocks often interspersed with other species. *S. capillifolium* is a hummock-forming species, whilst *S. papillosum* prefers slightly wetter conditions and is often found in lawns and occasionally in ditches (Hayward and Clymo, 1983, 1982). *S. capillifolium* is found throughout the Forsinard Flows reserve, whilst *S. papillosum* is more common on undisturbed sites. Both species are present at peatland sites across the UK (NBN Atlas Partnership, 2017), and other boreal Sphagnum-dominated peatlands (Gunnarsson, 2005).

3.2.2.Experimental set-up

Samples of *Sphagnum* moss (6 cm deep and 10 cm diameter, n=20 of each species) were collected by cutting around and below white plastic tubing of these dimensions. The samples were kept moist in a coolbox whilst being transported between the field sites and the laboratory. When the samples first arrived in the laboratory they were inundated with deionised water and the excess drained off to bring them to saturation. Once in the lab the samples were placed in 1 litre, straight-sided, clear polycarbonate jars and stored in a growth cabinet (Panasonic MLR-352H-PE) on a 12-hour day and night cycle.

The average climate of the Forsinard Flows reserve was used to set growth cabinet conditions. Climate averages were estimated from records of four surrounding weather stations from 1981-2010: Wick John O Groats Airport, Kinbrace, Altnaharra SAWS, and Strathy East (Met Office, 2018). Conditions from April to September were considered (see Figure 3.2). The average daily maximum temperature for the four sites over those 6 months ranged from 10.4 to 17.1 degrees C, and the average daily minimum ranged from 2.7 to 9.8 degrees C. The average relative humidity was approximately 80% (Met Office, 2018). During the day the growth cabinet was kept at maximum light levels (20,000 lx) 15˚C, and 70% relative humidity (slightly lower than the average at the site to aid drying of samples). At night the cabinet was dark, at 5˚C, and the humidity was unregulated.

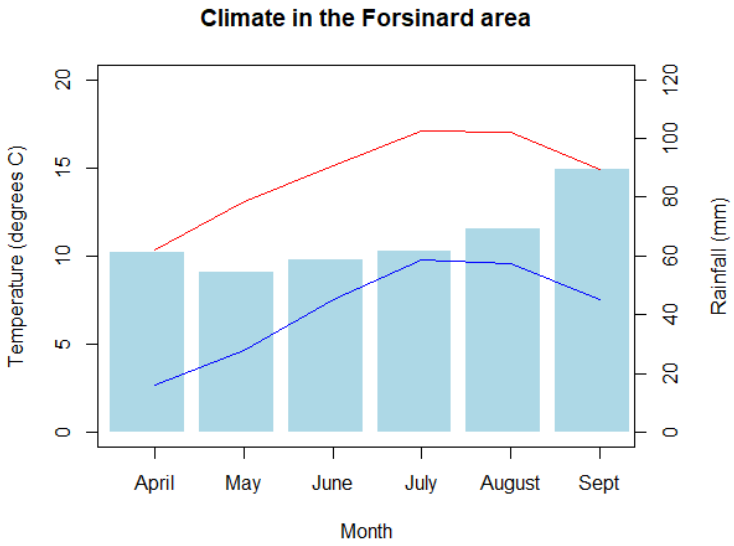

Figure 3.2– Climate in the Forsinard area, taken from 1981-2010 averages of the four nearest weather stations: Wick, John O Groats Airport, Kinbrace, Altnaharra SAWS, and Strathy East. Top line (red) gives daily maximum temperatures, lower line (blue) gives daily minimums. Bars give monthly rainfall.

The samples were left in the growth cabinet and watered regularly with de-ionised water (40 ml, equating to 5 mm, every 2 days to maintain saturation) for a week prior to beginning the experiment to allow them to acclimatise. During the experiment, the samples were moved around within the cabinet in order to minimise edge effects. Within the cabinet there were three shelves; all samples within each group (A to E, see Section 3.2.3.1.) were kept together on the same shelf, but the groups were moved to different shelves every measurement day, and the samples within each group were moved around randomly in relation to each other every watering day.

3.2.3.Experimental procedure

3.2.3.1.Rainfall simulations

The conditions in the growth cabinet were kept the same as described above. Five different rainfall simulations were designed to represent a range of rainfall conditions at the site, including a control set with steady-state water content corresponding to field conditions. Four replicates of each species were exposed to each regime.

The average rainfall (April-September, 1981-2010) was 66 mm per month, with 13 raindays per month (Met Office, 2018). 13 raindays a month is approximately the same as watering three times per week, and this was set as the steady-state watering schedule. 66 mm divided by 13 raindays gives an approximate input of 5 mm per rainday. However, when this

was trialled during the acclimatisation period it caused an increase in water levels rather than a steady-state (shown by an increase in weight), and so the input was halved to approximately 2.5 mm (20 ml) per sample per rainday. This lower steady-state input was needed to account for missing water fluxes that would be observed in the field, including vertical and lateral drainage into the peat, vascular plant competition, and run-off. Under experimental simulations, all water input into the samples in the laboratory was kept within the jars and could only be used by the *Sphagnum*. Deionised water was used for rainfall simulations to maintain consistency with previous studies (Clark et al., 2012, 2006) administered by drips using a laboratory wash bottle.

Rainfall simulation treatment followed a factorial design. There were five treatment groups, each comprising four samples of each *Sphagnum* species. The precipitation treatments used were: two different precipitation amounts, two different frequencies. In addition, we included continuous drought (see Table 3.1). Group A was designated as the control group, as the samples were given 20 ml of water three times per week, the amount required to maintain steady-state water content. These treatment regimes were maintained until drought effects were observed in the carbon flux and spectral reflectance results (see Section 3.2.3.2.). This process took twelve weeks.

Table 3.1 – The five rainfall simulations treatment groups A to E, with precipitation frequency and amount over the 12 week experiment shown. Each group included four samples of S. capillifolium and four of S. papillosum.

Group	**Precipitation amount (ml per fortnight)**	**Precipitation frequency (per fortnight)**
A (control)	120	6
B	120	3
C	60	3
D	60	6
E (total drought)	0	N/A

After the first three weeks (a time period of total drought which we would expect to show visible change in the field, Bragazza, 2008) little effect was observed in carbon flux. Therefore, to increase the intensity of the experimental simulation, the humidity in the growth cabinet was reduced to 55% (the minimum the cabinet was able to regulate), in order to dry the samples as much as possible. This is lower than would be found under normal conditions at the field sites (approx. 80%), but was used to encourage faster drying of the samples. In field conditions there would be higher evapotranspiration due to wind, even at

higher humidities, so this drop in experimental humidity compensated for the lack of air movement.

After the rainfall simulations had been run for 12 weeks total, all the samples were flooded to within 2 cm of the top of the clear plastic jars to simulate total rewetting. Complete inundation was used to simulate rewetting following a period of drought or limited rainfall. The *Sphagnum* samples in their plastic collars floated at the surface of the water, meaning that although they were inundated they still had contact with the air. They were kept in the cabinet (70% humidity) for one month whilst inundated, in order to assess recovery following full rewetting. Rochefort, Campeau and Bugnon (2002) found that a month of inundation will not harm *Sphagnum*, and may even encourage growth. After one month all excess water was drained, and the carbon flux measurements were repeated three times over a week to compare dynamics with drought and pre-drought conditions.

3.2.3.2. Measurements

Three times per fortnight (after watering of sets A-D) the net carbon fluxes of all the samples (groups A-E) were measured. The flux measurements were taken using a LICOR-8100 infrared gas analyser (LICOR Inc., Lincoln, Nebraska, USA), connected to a custom-built clear plastic chamber. Each sample was brought out of the growth cabinet and placed under a high pressure sodium growth lamp (Philips Belgium 9M SON-T-AGROO 400) in a laboratory in order to keep light levels as constant as possible (at 55,500 lm) The clear chamber was placed over the sample using a foam seal in between the sample container and chamber, and a measurement taken of the net carbon flux for 90 seconds. A blackout cloth cover was then placed over the chamber, and another measurement taken to get the respiration flux. Gross Primary Productivity (GPP) was calculated as the difference between the light and dark chamber measurement values. The time the samples spent out of the growth cabinet was minimised as much as possible in order to reduce the effects of variable air temperature and relative humidity (the longest any sample spent outside the cabinet was ten minutes maximum). The order in which samples were measured was randomised to minimise background effects.

To reduce the effect of varying background light levels (due to working in a laboratory with access to natural light) a PAR sensor was added to the experimental set-up four weeks in to the experiment, and calculations were applied to remove the effect of background light levels on GPP. This adaptation was made after viewing preliminary data. Measurements taken in the first four weeks were corrected based on time of measurement. Given that the measurements were taken at regular intervals over the course of the mornings, time was used as a proxy from PAR in the correction calculations for the data from the first four

weeks. Variations in background light levels due to cloud cover are not accounted for in the first four weeks of results (See Appendix A for fuller explanation).

Samples were weighed three times a week before and after watering throughout the experiment. At the end of the experiment samples were dried in a laboratory oven at 70˚C for 72 hours and the dry weights collected in order to retrospectively calculate moisture contents. All water contents are given in g fresh weight/g dry weight (g/g).

The spectral reflectance was measured using a Ger3700 spectrometer (Geophysical and Environmental Research corp., 1999) mounted in a dark room with a single constant light source (1000 W high-intensity halogen lamp at an angle of 45° and a distance of 0.5 m). Each sample was placed under the spectrometer and a measurement taken; the sample was then rotated and another measurement taken, and rotated again for a third measurement. The average of these three spectra was taken to compensate for potential structural effects. A spectralon reference panel was used to take reference spectra between samples. The sample and reference panel were viewed at nadir (90°).

The red absorption feature in the reflectance spectra was found to be a good indicator of drought stress (see Section 3.3.2.), and the Normalised Difference Vegetation Index (NDVI) was used to measure this effect across the experiment. The NDVI is one of the most widely used vegetation indices, and has previously been shown to give agreement with changes in *Sphagnum* photosynthesis (Harris, 2008; Lees et al., 2018). The NDVI is calculated as:

$$NDVI = (R_{NIR} - R_{red})/ (R_{NIR} + R_{red})$$

The red and NIR bands were calculated by averaging the reflectance values for 630-680 nm and 845-885 nm respectively.

3.2.3.3. Statistical analysis

All statistical analysis was done using RStudio (R Core Team, 2017). In order to create a robust statistical analysis of this experiment, the first three measurement days (day 1 to 10) were averaged into a result category ‘start’, the last three days of the water input regimes (day 71 to 80) were averaged into ‘end’, and the three measurements after rewetting (day 113 to 120) were averaged into ‘rewetted’. The effect of Group and Species on each of the four measured variables (Water content, GPP, R, and NDVI) was analysed for each of the three time period results.

In each case the Fligner-Killeen test for equal variance was performed, as this test is robust when using non-normally distributed data. A two-way ANOVA was performed for Species

and Group effects in order to assess interactions. The normality of the ANOVA residuals was assessed visually and using the Shapiro-Wilks test.

Two Kruskal-Wallis tests, one with Species as the independent variable and one with Group, were used. Post-hoc testing using Dunn's test was done with the PMCMRplus package (Pohlert, 2018). Kruskal-Wallis is a non-parametric equivalent to a one-way ANOVA, and as such should account for the non-normal distribution and unequal variances which were found to be a feature of some of the data.

In order to consider the relationships between measured variables without including autocorrelation from repeated measures we subtracted all results for each sample from the first measurement made of that sample. To determine the optimum water content for *Sphagnum* carbon function a quadratic model was fitted to the data and solved for the vertex. Linear models were fitted to analyse the relationship between water content and GPP, and between GPP and NDVI.

3.3.Results

3.3.1. Carbon function and water content

Overall patterns in the experiment were as follows. We found that water, GPP and respiration decreased across the water input regimes period for the water-limited groups C, D and E (see Table 3.2, Figures 3.3 & 3.4). After rewetting the water content of all groups recovered, but the GPP of drought group E did not recover (Table 3.2 and Figure 3.3). The results show that there was no significant species effect at any point during the experiment on water content, GPP, or respiration (Table 3.2).

Table 3.2 – Results from the statistical tests, Kruskal-Wallis results shown as highly sig. if p<0.05, moderately sig. if <0.1. N=4 for each species in each group. The measured variables are water in g/g, GPP and Respiration in umol/m^2/s.

Measured variable	**Fligner-Killeen**	**Two-way ANOVA**	**Kruskal-Wallis test with Dunn's test**
Water – Start	Equal	No sig diff	
Water – End	Equal	Residuals non-normal Group effect No species effect No interaction effect	A to E highly sig B to C,D,E highly sig
Water – Rewetted	Equal	No sig diff	
GPP-Start	Non-equal	No sig diff	
GPP – End	Equal	Residuals normal Group effect No species effect No interaction effect	D to E highly sig E to A, C moderately sig
GPP – Rewetted	Equal	Residuals normal	E to A,B,C,D highly sig

		Group effect No species effect No interaction effect	
R – Start	Equal	Residuals normal Group effect Moderately sig species effect No interaction effect	A to E highly sig C to E highly sig
R – End	Equal	Residuals normal Group effect No species effect No interaction effect	B to C highly sig E to A, C, D highly sig A to B hoderately sig
R - Rewetted	Equal	Residuals normal Group effect No species effect No interaction effect	B to C,E highly sig D to E highly sig

Water content of the *Sphagnum* ranged from 12.8 to 38.4 g/g in all samples pre-treatment, and from 1.2 to 3.3 g/g in the total drought group E at the end of the treatment period. Figure 3.3 shows the changes in water content for the five groups. The water content was relatively constant for A and B, as expected because of the rainfall input, although the average water contents for group B (averaging 29.2 g/g) appeared higher than group A (averaging 22.4 g/g) across the whole experiment. C, D, and E showed decreases by the end of the watering regimes period, with the decrease greatest in group E (drought group). Rewetting increased the water content of all groups (by up to approx. 44 g/g).

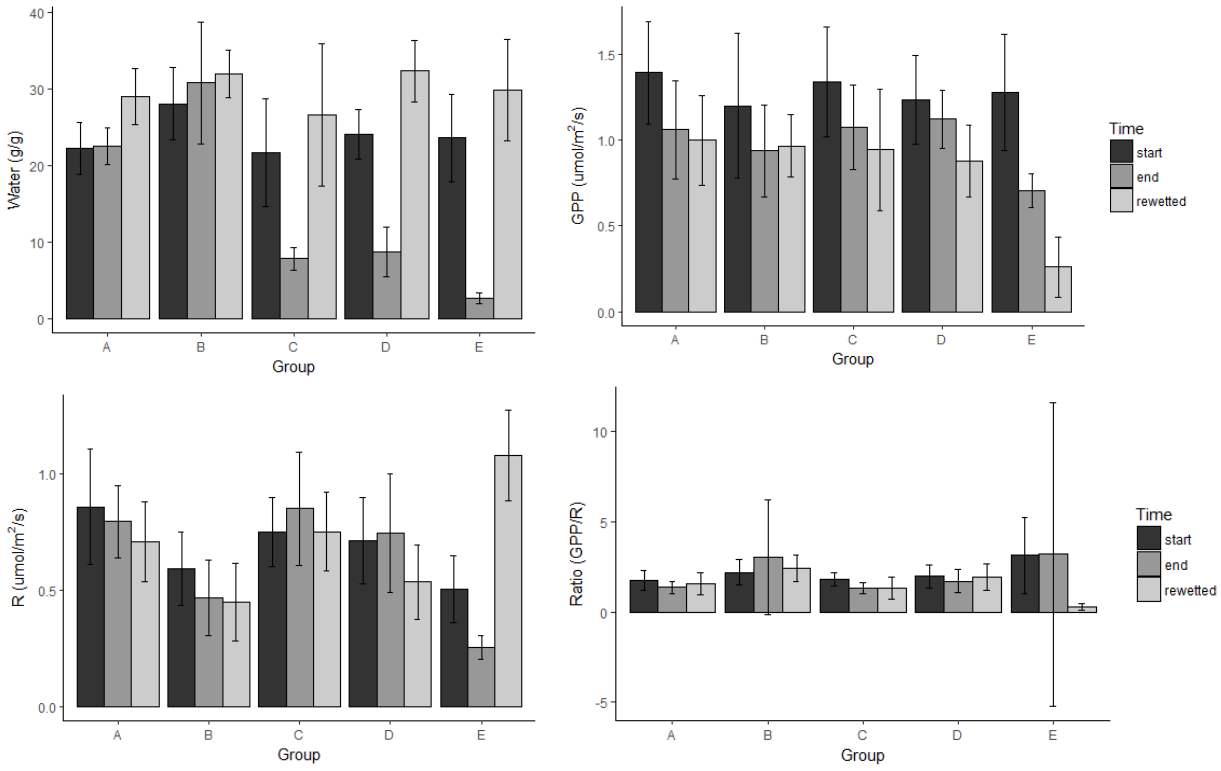

Figure 3.3 – Clockwise from top left: Water content (g fresh weight/g dry weight); PAR corrected GPP; Respiration; Ratio of GPP/Respiration. Each graph shows the five groups at the start of the period, end of the watering regimes, and after rewetting. Error bars show the standard deviation of the group.

GPP ranged from 0.39 to 2.10 umol/m^2/s in all samples pre-treatment, and from 0.39 to 1.07 umol/m^2/s in group E at the end of the treatment period. Figure 3.3 shows the changes in GPP for each of the five treatment groups. The GPP of all samples decreased over the watering regimes period. The decrease of the control samples (group A) is a statistically significant ($p<0.05$), although very small (a slope of -0.0039), trend across the 80-day period. This decrease may be due to a lack of nutrients, as de-ionised water was all that they received and blanket bogs receive their nutrient inputs from precipitation.

At the end of the water input regimes period the GPP of group E (0.70 umol/m^2/s) was highly significantly different to the GPP of group D (1.12 umol/m^2/s, $p<0.05$), and moderately significantly different to the GPP of groups A and C (1.06, 1.07 umol/m^2/s, $p<0.1$). After rewetting the GPP of group E was significantly different to all other groups (0.26 umol/m^2/s, compared to 0.88 to 1.00 umol/m^2/s, $p<0.05$, see Table 3.2 and Figure 3.3).

Respiration varied from 0 to 1.44 umol/m^2/s in all samples pre-treatment, and from 0 to 0.45 umol/m^2/s in group E at the end of the treatment period. Figure 3.3 shows the respiration results for the five groups. Respiration for groups A-D stayed constant, whilst E showed a

slight decrease towards the end of the 80 day experimental period, and then after rewetting a sharp increase. At the end of the water input period group E (0.25 umol/m^2/s) was significantly different to groups A, C and D (0.80, 0.85, 0.75 umol/m^2/s, $p<0.05$).

The ratio of GPP:R was similar throughout the first 80 days, with Group A ranging from 0.40 to 2.84 and averaging 1.56 (see Figure 3.3). Group B shows slightly higher ratios generally due to slightly lower respiration values. Group E shows a large range in ratios at the end of the water input period, partly due to the small values of both GPP and R, and a decrease after rewetting due to the higher respiration values.

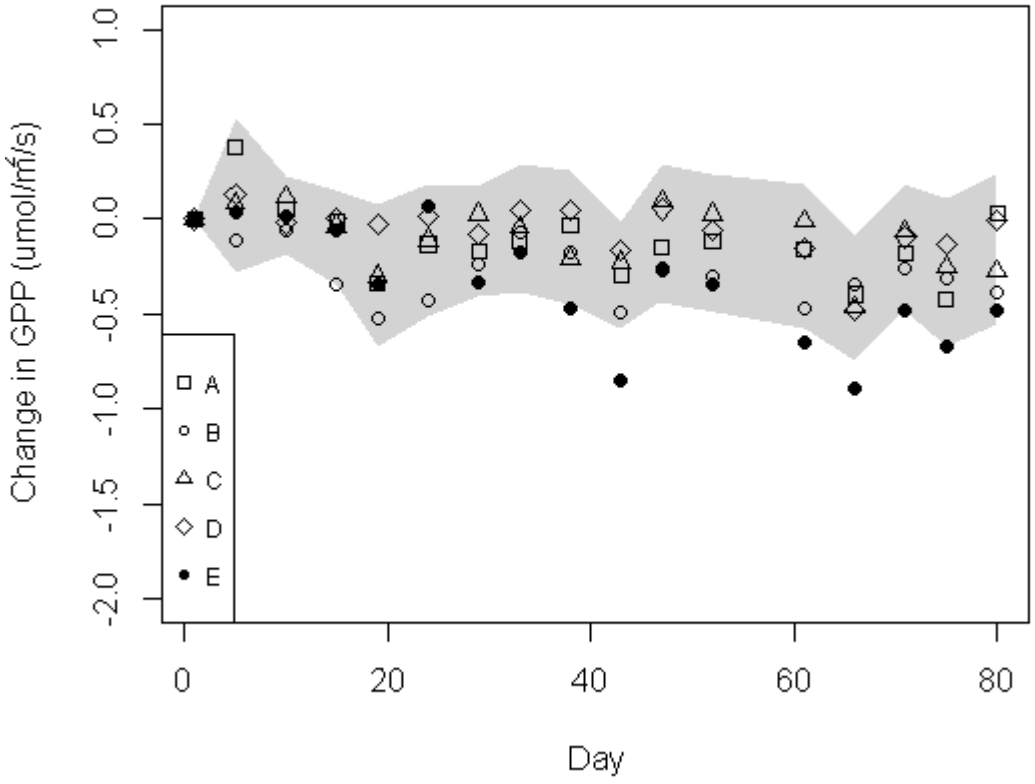

Figure 3.4 – The mean of each group change in GPP across the 80 days experimental period. Both species are included in the group means as there were no significant species differences in GPP. Grey area shows the standard deviation for groups A to D.

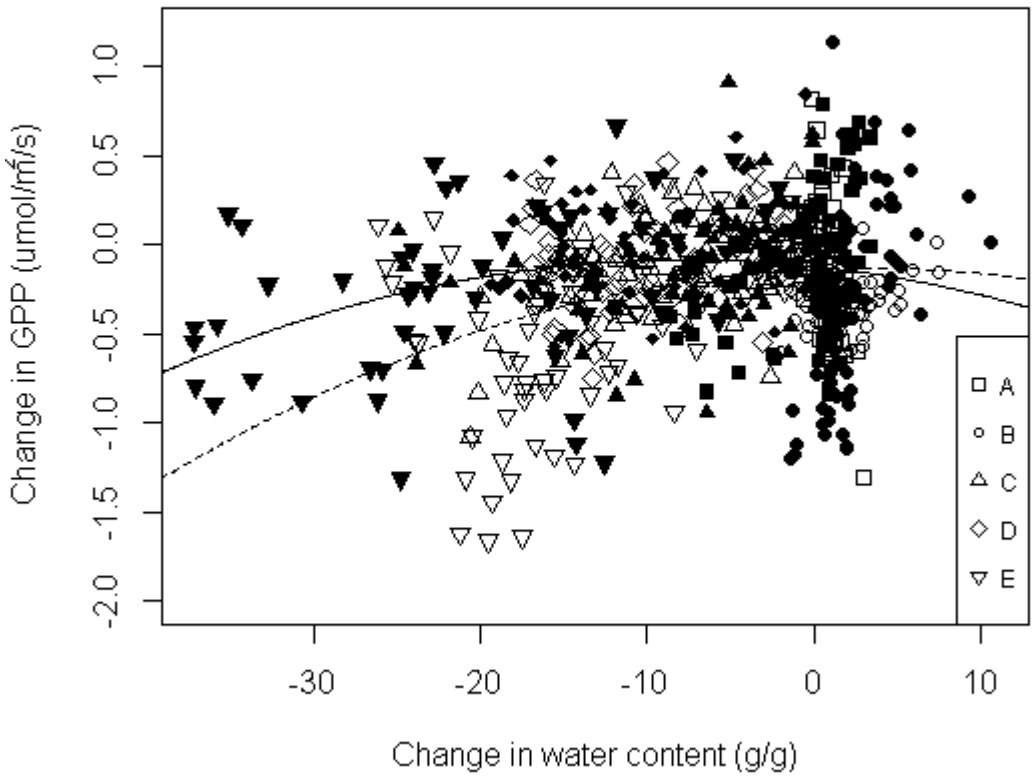

Figure 3.5 – Change in water content plotted against change in GPP for the 80 days of watering regimes. Empty symbols show S. capilifollium, filled show S. papillosum. Quadratic functions are fitted to each species, both significant at the p<0.05 level, solid shows S. capillifolium, dotted shows S. papillosum.

Figure 3.4 shows the change in GPP in each group across the water input period. It can be seen that the mean of group E GPP is below the means of all other groups from day 29 onwards (with the exception of day 47 when the mean is similar to group B). Due to the large range relative to absolute values in GPP for all groups across the period, Group E is not consistently significantly different from the other groups, but the days when the difference is significant are more frequent in the second half of the period.

Figure 3.5 shows that the relationship between water content and GPP corresponds to a quadratic model. The optimum of *S. capillifolium* is -7.6 g/g change, whilst for *S. papillosum* it is 3.1 g/g change. By taking all values less than 1 g/g different to the starting water content, we can calculate the starting water content for GPP for *S. capillifolium* as 23.4 g/g (16.5 to 29.5), and for *S. papillosum* as 24.4 g/g (12.6 to 38.4). Therefore, the optimum water

content for *S. capillifolium* is 15.8 g/g (8.9 to 21.9 g/g) and for *S. papillosum* it is 27.5 g/g (15.7 to 41.5 g/g).

Figure 3.6 shows the significant linear relationship (R^2 = 0.13, p<0.05) between respiration and GPP in our *Sphagnum* moss samples across the water input period.

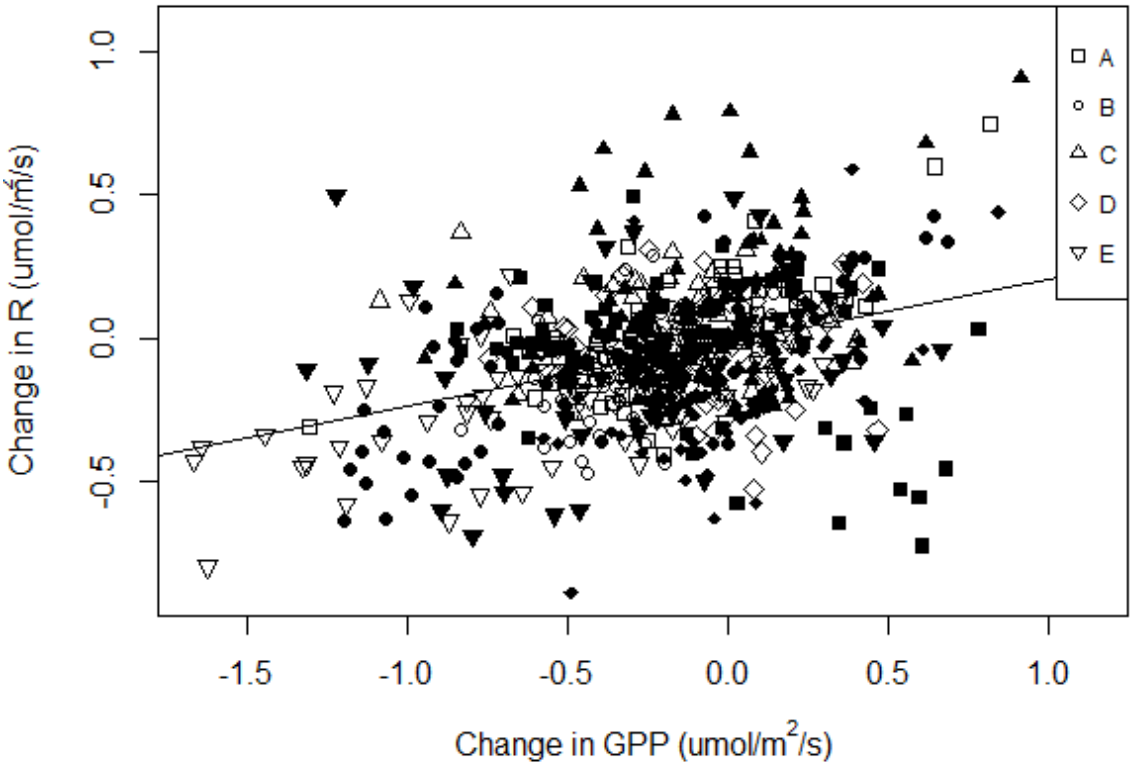

Figure 3.6 – Change in respiration plotted against change in GPP throughout the 80 days watering regimes. The linear model shows a significant relationship (p<0.05) between GPP and R for all samples, with the equation y= 0.22x - 0.015 and adjusted R^2 value of 0.13. Empty symbols represent S. capillifolium, filled S. papillosum.

3.3.2. Spectral reflectance

The drying effect on *Sphagnum* reflectance was visible to the naked eye. Both species showed bleaching as the experiment progressed (see Figure 3.7), due to an increase in reflectance in all optical wavelengths (see Figure 3.8), although the effect was more pronounced in *S. capillifolium*.

Figure 3.7 – photos showing S. capillifolium of groups A to E (left to right) at the end of the 80 day drying period. The photos illustrate the bleaching effect of reduced water content.

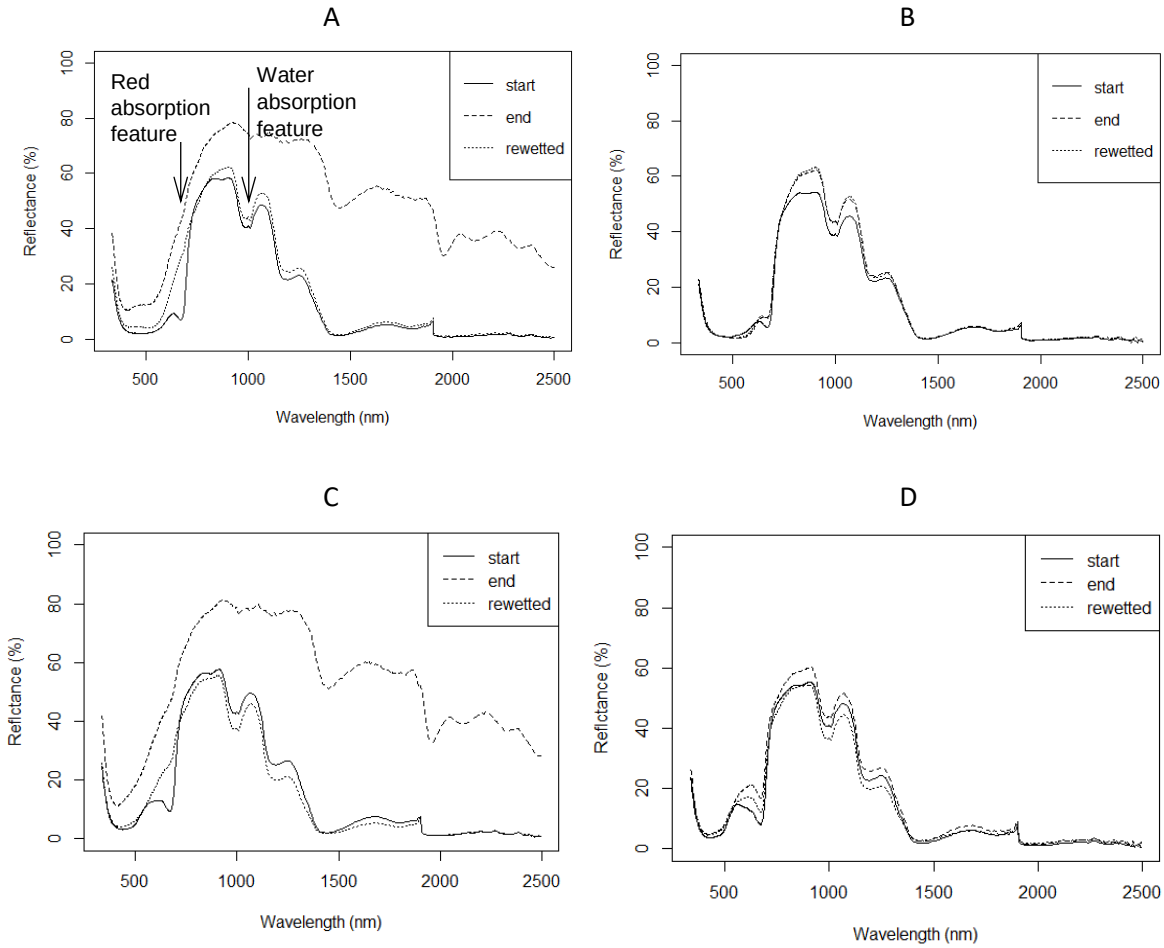

Figure 3.8 – A: change in spectral reflectance in an S. capillifolium sample from total drought group E from the beginning of the 80 day experimental period (wet) to the end (dry), and also after rewetting (rewetted). The increase in reflectance at all wavelengths in the dry sample is clearly obvious. Also note the lack of a red absorption feature (at approx. 650nm) and the water absorption trough (at approx. 1000nm) in the dry spectrum. The red absorption feature is still absent in the rewetted spectrum. B: spectra of an S. capillifolium

sample from control group A, showing very little change. C and D show spectra of S. papillosum from groups E and A respectively.

Spectral data from the two *Sphagnum* species were significantly different throughout the experiment ($p<0.05$), as shown in Figure 3.9 and Table 3.3, with *S. capillifolium* having higher NDVI results than *S. papillosum*. Water-limited groups C, D and E all showed a decrease in NDVI across the water input period (Figure 3.10), but only group E (0.32) showed a significant difference to control group A (0.64) at the end of the period (Table 3.3, $p<0.05$). After rewetting the NDVI of these three groups recovered slightly, but the NDVI of group E (0.41) was still significantly different to all other groups ($p<0.05$).

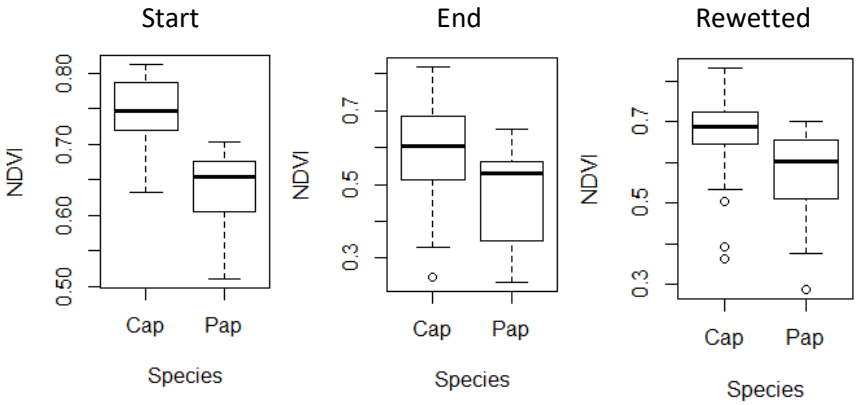

Figure 3.9 - S. capillifolium had higher NDVI values than S. papillosum throughout the experiment.

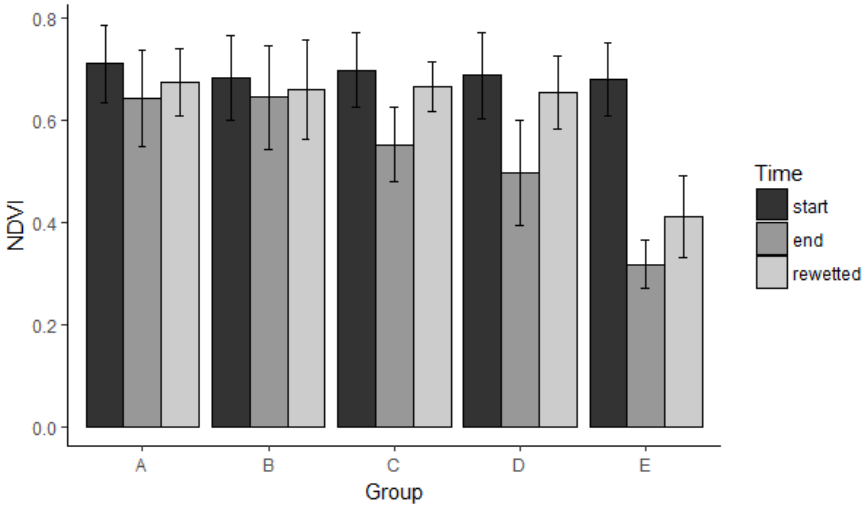

Figure 3.10 – NDVI values for each of the five groups at start and end of watering regimes, and after rewetting.

Figure 3.11 considers the relationship between change in GPP and change in NDVI, and shows that the relationship is significant for group E in both species, and for groups C and D in *S. capillifolium* only. We also tested the relationship between GPP and NDVI for each species at the start and end of the water input regimes to test whether the NDVI can detect differences in photosynthetic capacity between samples, but none of the relationships were significant at the p<0.05 level.

Table 3.3 – Results from the statistical tests, Kruskal-Wallis results shown if p<0.05.

Measured variable	**Fligner-Killeen**	**ANOVA**	**Kruskal-Wallis test with Dunn's test**
NDVI – Start	Equal	Residuals non-normal No group effect Species effect No interaction effect	Cap to Pap
NDVI – End	Equal	Residuals normal Group effect Species effect No interaction effect	Cap to Pap E to A, B, C
NDVI – Rewetted	Equal	Residuals normal Group effect Species effect No interaction effect	Cap to Pap E to A, B, C, D

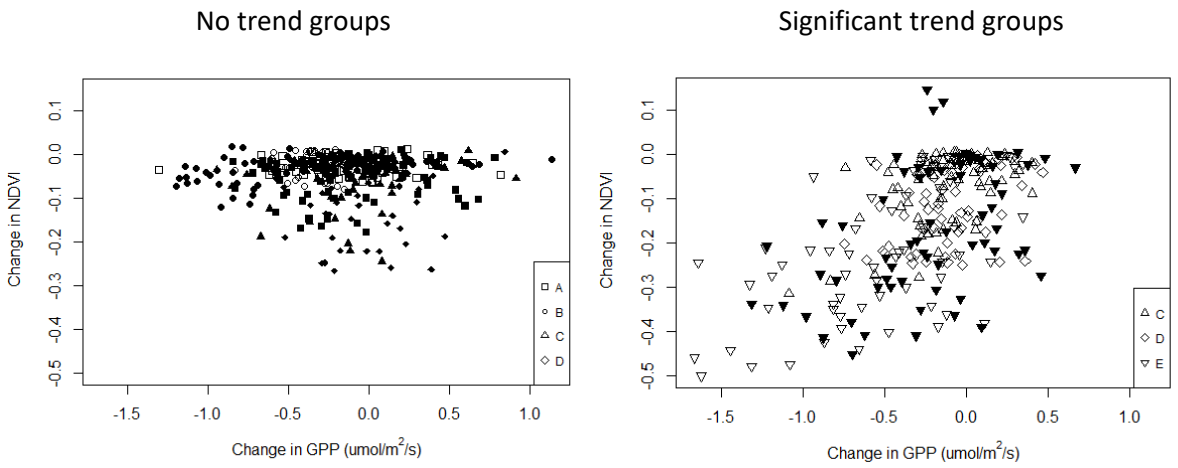

Figure 3.11 – Change in NDVI plotted against change in GPP throughout the 80 days experimental regimes. Unfilled symbols show S. capillifolium, filled show S. papillosum. Groups A and B show no trend in either species (actually group B in S. papillosum does give a significant linear model, but the slope is so small that it is almost non-existent), groups C and D show a trend in S. capillifolium but not S. papillosum, group E shows a trend in both. The groups which show no trend are plotted in the left-hand graph, whilst those with a significant trend are shown in the right-hand graph.

3.4.Discussion

The NDVI paralleled differences in GPP, and also showed a species effect. GPP and NDVI of group E did not recover after rewetting. The greatest effect of water stress on *Sphagnum spp.* studied here was in colour changes that could be seen by eye in terms of bleaching and quantified using spectral data and indices. Spectral data shows that the red absorption zone (630-680 nm) detected drought stress effects in *Sphagnum* moss. At the end of the watering regime period the NDVI could detect a difference between group E and the control group A. This suggests that NDVI is a useful tool for monitoring *Sphagnum* drought stress. Bubier, Rock and Crill (1997) recognised that their samples which had been dried and rehydrated had shallower chlorophyll absorption features (at 660 nm) than fresh samples, but did not consider the significance of this in terms of plant function indexes. Van Gaalen, Flanagan and Peddle's (2007) laboratory study, however, did not show significant changes in the red absorption feature when their samples were dried to approx. 5 g/g, suggesting either that water content needs to be below this to show change in this region of the spectrum, or that their experiments were on too short a timescale (hours rather than weeks) to cause measurable damage to *Sphagnum* chlorophyll function.

In terms of the relationship between optical measures of *Sphagnum* health by NDVI and its photosynthetic performance measured by GPP, the range of change in GPP associated with little change in NDVI (see Figure 3.10) in groups A and B for both species suggests that NDVI was only sensitive to change in GPP due to drought stress in this experiment and not due to other causes. As the other factors influencing GPP were kept as constant as possible in this experiment, it is likely that the large range in GPP in groups A and B is primarily due to natural fluctuation in photosynthesis. Harris (2008) completed a laboratory study comparing photosynthetic efficiency (measured using chlorophyll fluorescence, Φ_{PSII}) of water limited *Sphagnum* mosses to spectral indexes. In agreement with the current work, Harris' (2008) study found that the NDVI gave a strong positive correlation with the photosynthetic efficiency of all samples pooled (0.68 correlation). This study found a correlation of 0.58 between NDVI and GPP for all samples in drought group E.

Our results suggest that a period of at least 29 days is required to affect *Sphagnum* carbon function (photosynthesis and respiration). This result might, however, be different in field conditions as there are several factors which we did not replicate in the lab, for example wind increasing evapotranspiration, peat presence affecting water availability and drainage, and the composition of rainwater. In August 1995 there was a period of 21 days when only 1 mm of rainfall fell at Altnaharra meteorological station, suggesting that this length of drought is possible but very rare (Met Office, 2012). However, the UKCP09 report (Jenkins et al.,

2010) suggests a 50% chance of 20% lower summer rainfall in their higher emissions scenario for the Forsinard Flows area by 2080. This increases the possibility of a long drought period occurring in the future, which could have a negative impact on *Sphagnum* function, and ultimately the presence of blanket bog in this area (Clark et al., 2010).

Table 3.4 – Previous studies determining optimum water content for carbon function in different Sphagnum species.

Study	**Species**	**Optimum water content**	**Notes**
Current study	*S. capillifolium* *S. papillosum*	15.8 g/g (8.9-21.9) 27.5 g/g (15.7-41.5)	*Sphagnum* cores, lab
Robroek et al., 2009	*S. rubellum* *S. magellanicum* *S. cuspidatum*	Approx. 20 g/g Approx. 28 Approx. 30	Intact *Sphagnum* cores, lab
Van Gaalen et al., 2007	*S. teres*	8-9 g/g	Thin samples from moss lawn, lab
Adkinson and Humphreys, 2011	Mixed hummock species	5-13 g/g	Capitula water content, mat flux, field
Schipperges and Rydin, 1998	*S. fuscum* *S. papillosum* *S. magellanicum* *S. balticum* *S. cuspidatum*	370-1300 % dry wt. 620-2550 % 700-1550 % 600-1500 % 400-1450 %	Capitula, lab
McNeil and Waddington, 2003	*S. capillifolium*	11.3-26.7 g/g	Moss cushion, lab
Titus, Wagner, & Stephens, 1983	*S. fallax* *S. nemoreum*	Approx. 6-11 g/g Approx 9 g/g	Capitula, lab

Our study found that the water effect on GPP corresponded to a quadratic curve, with different parameters for the two species tested. Optimum water content for *S. capilifollium* and *S. papillosum* was found to be 15.8 g/g and 27.5 g/g respectively. Optimum water contents for photosynthesis reported in the literature vary (see Table 3.4); Adkinson and Humphreys (2011) suggested an optimum water content of 5-13 g/g at their Canadian peat bog site in hummock species, whilst Schipperges and Rydin (1998) suggested an optimum range of water contents 400-2500 % of dry weight within the capitula (approx. equal to 6-27 g/g using values from our study for comparison), and McNeil and Waddington (2003) gave an optimum of 11.3 to 26.7 g/g in the moss cushion. Robroek et al. (2009) noted the point at which water content causes a decrease in GPP to be between approx. 15-25 g/g, whilst Van Gaalen et al. (2007) found that GPP decreased above 9 and below 8 g/g dry weight using shallow *Sphagnum teres* mats. Adkinson and Humphreys (2011) found that GPP decreased

below capitula water content of 5 g/g in a field experiment at their Canadian peat bog site. The optimum water contents found in the current study are within the range given by previous studies, and show a lower optimum water content for *S. capillifolium*, the hummock-forming species. Studies considering larger *Sphagnum* samples generally seem to give higher optimum water contents than those studying individual capitula, likely due to pockets of water held within the *Sphagnum* cushion.

We did not find that water input frequency had an effect on carbon function. Group B (full water, half days) showed higher than average water contents and lower than average GPP and respiration at points throughout the experiment. It may be the case that, as measurements were taken within 12 hours of all samples being watered, the samples in group B were often above optimum water content on measurement days. However, as there are almost no significant differences in measured variables between groups C and D we cannot say that the different rainfall frequencies tested in this experiment have a lasting impact.

The decrease and increase in respiration of extreme drought group E suggests two different effects. Firstly, the significant decrease during the watering regimes period of the experiment concurs with the GPP results suggesting a loss of plant function during this period. The literature agrees that *Sphagnum* respiration also decreases under drought, but apparently at a slower pace than GPP (Schipperges and Rydin, 1998; Adkinson and Humphreys, 2011). The ratio of GPP:R in the current work is similar at the start and end of the period (although the range is greater at the end due to generally smaller values and large variation in both GPP and respiration), suggesting that the change in respiration is strongly linked to the change in GPP.

Secondly, we suggest that the sudden increase in group E respiration after rewetting may be due to the presence of slime mould and other microorganisms which were decomposing the dead *Sphagnum* matter; slime mould was observed on several of the samples in group E after rewetting. An increase in these microorganisms could cause an increase in respiration such as was measured (Schipperges and Rydin, 1998; Robroek et al., 2009). Adkinson and Humphreys (2011) found the compensation point (GPP=R, NEE=0) to be 5 g/g, whilst Schipperges and Rydin (1998) found it to be 100-225% (approx. equal to 3.4-3.8 g/g). In contrast, we found that respiration in group E decreased at roughly the same rate as GPP and the ratio GPP:R remained similar (see Figure 3.3), which means that compensation point was only reached after rewetting when there was a spike in R and very low GPP.

Several previous studies have assessed the effects of rewetting desiccated *Sphagnum* (see Table 3.5). In this study we rewetted the desiccated *Sphagnum* for 30 days, but there was

little sign of recovery in the GPP of group E. Group E NDVI values were also significantly different to all other groups, despite the values of C and D recovering to the level of A and B. Schipperges and Rydin (1998) found that totally desiccated *Sphagnum* did not recover after rewetting, although their study did not allow much time (12 hours) for rewetting and recovery. In contrast, Robroek et al. (2009) found that their *Sphagnum* samples were assimilating carbon after 16 days of high water table following 23 days of drought treatment, but not to the extent of pre-drought treatment assimilation. The lowest water content reached in their experiment was approximately 6 g/g, however, compared to this study which reached an average of 2.2 g/g in group E by the end of the 80 days drying. McNeil and Waddington (2003) found that in *Sphagnum* which had been dried to 6% Volumetric Moisture Content (VMC) (approximately the same as our samples reached) photosynthesis recovered after 20 days of saturation. Nijp et al. (2014) found that *S. fuscum* (hummock species) recovered after 11 days rewetting following 17 days drought, but hollow-preferring species did not recover to pre-desiccation levels after rewetting. Van Gaalen et al. (2007) found that *Sphagnum* respiration increased after rewetting but GPP remained lower than initial values, in agreement with this work. Wagner & Titus (1984) found that *S. fallax* was more tolerant of drought periods than *S. nemoreum*, despite preferring wetter microhabitats. Both species showed slow and limited recovery after more than five days of total drought.

Table 3.5 – Previous studies measuring whether Sphagnum GPP recovered after desiccation and rewetting.

Study	**Species**	**Minimum water content**	**Rewetting period**	**Recovery of GPP?**
Current study	*S. capillifolium* *S. papillosum*	80 days drought, 2.2 g/g	30 days	No
Schipperges and Rydin, 1998 (Experiment 3)	*S. fuscum* *S. papillosum* *S. magellanicum* *S. balticum* *S. cuspidatum*	Capitula below 100 %, 12 days	12 hrs	No
Robroek et al., 2009	*S. cuspidatum* *S. magellanicum* *S. rubellum*	23 days drought, water table 10 cm below *Sphagnum* surface (6 g/g)	16 days	Yes, but not to pre-drought levels
McNeil and Waddington, 2003	*S. capillifolium*	6% VMC, 7 days	20 days	Yes
Nijp et al., 2014	*S. fuscum*	17 days drought	11 days	Yes
Nijp et al., 2014	Hollow species	17 days drought	11 days	Not to pre-desiccation levels
Van Gaalen et al., 2007	*S. teres*	2-3 hrs, approx. 5 g/g	10 mins	No

Wagner & Titus, 1984	*S. fallax* *S. nemoreum*	5 days, 1.2 g/g	30 hours	Not to pre-desiccation levels

Figure 3.10 shows that although the NDVI values did increase somewhat after rewetting, it was not enough to restore them to pre-experimental levels. This agrees with the GPP of Group E showing little recovery after rewetting. The loss of the red light absorption feature in group E samples, both before and after rewetting, indicates a significant loss of plant function. It is likely that a breakdown of plant cells during extreme desiccation leads to a decrease in carbon function which is either entirely irreversible, or certainly slow to recover. Future studies should consider monitoring desiccated *Sphagnum* for longer time periods after rewetting to monitor if recovery occurs, and how long it takes.

In this study, although a majority of the *Sphagnum* cushion depth was kept in the samples, the removal of the upper parts of the plant from the basal stem held in the peat may have affected desiccation progress and recovery. Water table movements within the peat can have an effect on *Sphagnum* desiccation (Ketcheson & Price, 2014; Moore & Waddington, 2015; Weber et al., 2017), and it is possible that *Sphagnum* left in situ would have greater resilience. Removal of part of the moss cushion could also have increased desiccation from the edges by removing contact with surrounding moss (Robroek et al., 2007). Future work on intact *Sphagnum* in a peatland environment would be very useful in furthering this research.

The lack of difference in GPP, respiration or water content between the two species, *S. capillifolium* and *S. papillosum*, was somewhat surprising. The different environments of the two species would suggest that *S. papillosum*, a lawn-preferring species, would be less tolerant to drought than *S. capillifolium*, a hummock-forming species. This difference between hummock and hollow species was suggested by Harris (2008) and Strack and Price (2009), although as both these studies only used one sample of each species it may be that this was a sample-specific difference rather than a species-specific response. Titus et al. (1983) found the opposite effect between two *Sphagnum* species which preferred different microhabitats; they showed that *S. fallax*, although growing closer to the water table than *S. nemoreum*, actually functions better at low water contents. *S. nemoreum* was shown to have a higher water-holding capacity and more effective capillary transport (Titus and Wagner, 1984).

It may be the case that the habitats of the two species used in this study, *S. capillifolium* and *S. papillosum*, are too similar to show differential responses to moisture content, although the difference in optimum water contents was clear. Robroek et al. (2009) found a species-

specific difference in carbon assimilation response to water table in a large study using *S. magellanicum (S. medium), S. cuspidatum* and *S. rubellum*. Schipperges and Rydin (1998) tested the response of individual *Sphagnum* capitula of various species to desiccation, and found that those species with a compact growing structure survived drought better than those with a loose growing structure. *S. capillifolium* would be in the former category and *S. papillosum* in the latter, but this had no effect in our experiment. There was however, a significant difference between species NDVI values, possibly due to the naturally red colouring of *S. capillifolium*. This difference suggests that the usefulness of the NDVI as a tool for monitoring peatland vegetation drought stress may be limited by knowledge of the species present. Under natural conditions *Sphagnum* is often found growing in communities of different species, and also mixed with vascular vegetation. Future work should therefore consider how variation in plant presence can affect the NDVI signal and its changes under drought conditions.

We found that there was no difference in water content or carbon function between species, and that water input frequency did not have a clear impact on carbon function. Water input amount did have a clear effect, and drought group E was significantly different to control group A in all measured factors at the end of the 80 days. Nijp *et al.* (2014) and Robroek et al. (2009) found that rainfall frequency affected carbon fluxes during dry conditions (defined as water table more than 15cm below surface, and 10 cm below surface, respectively), but not during wet conditions (defined as optimum for each species, and 1 cm below surface, respectively), and it may be the case that the conditions which groups A to D were subjected to were never extreme enough for precipitation frequency to have an impact. Future work in this area should measure carbon fluxes both before and after experimental watering, and also explore small water input impacts on *Sphagnum* which has been subjected to prolonged drought.

3.5. Conclusions

We conclude that *Sphagnum capillifolium* and *Sphagnum papillosum* from blanket bogs are resilient to long (approx. 30 days) drought periods, but once prolonged drought affects carbon function significantly, recovery is difficult. The effect of long drought periods can be seen in the red zone of the reflectance spectra of *Sphagnum*, meaning that the NDVI has the potential to provide useful information about *Sphagnum* carbon function. The GPP and NDVI of severely desiccated *Sphagnum* did not recover with rewetting, indicating that such spectral indices are not only useful for detecting contemporary water limitation damage, but also the longer term effects of such periods even after water tables have risen. The success of the NDVI in matching the GPP results from group E is encouraging for researchers who

use spectral indices to gain information about peat bogs from remote sensing. The NDVI is widely used as a method of estimating plant health from remote sensing (Lees et al., 2018), and our work with *Sphagnum* proves that this index can be a useful tool in peat bog ecosystems, particularly in hot and dry seasons when drought damage is predicted. Future work should consider how successful the NDVI is in matching changes in carbon fluxes in mixed *Sphagnum* patches, and other peatland vegetation species. We envisage that this index will be most informative when used alongside measures of species composition and environmental parameters such as temperature.

Acknowledgements

Thanks are due to the Forsinard Flows RSPB reserve for allowing us to collect *Sphagnum* samples for this work, and also to Stephen Fry and Vicky Russell at the Chobham Common NNR for allowing us to collect a few *Sphagnum* samples for sampling and storage methods testing. Thanks to Mike Lees for making the 40 *Sphagnum* sample collars.

Funding

Kirsten Lees was part funded by a studentship from The James Hutton Institute, and part funded by the Natural Environment Research Council (NERC) SCENARIO DTP (Grant number: NE/L002566/1). Tristan Quaife was funded by the NERC National Centre for Earth Observation (NCEO). Myroslava Khomik and Rebekka Artz were funded by The Scottish Government Strategic Research Programme 2016-2021.

4. Broad-band indices perform as well as hyperspectral indices in estimating peatland vegetation photosynthesis and water content

Lees KJ, Artz RRE, Khomik M, Clark JM, Ritson J, Hancock MH, Cowie NR, & Quaife T

Abstract

Peatlands provide important ecosystem services including carbon storage and sequestration, and biodiversity conservation. It is therefore important to monitor peatland condition, for which remote sensing shows much potential. Moisture content is a crucial factor in peatland condition, and carbon storage within these ecosystems relies on maintaining a high water table. Most remote sensing products are developed in unsaturated environments and it is unclear how well they can perform in peatland ecosystems. This study combines results from both laboratory and field experiments to assess the relationship between spectral indices and the moisture content and photosynthesis of peatland (blanket bog) vegetation. The aim was to consider how well the selected indices perform under a range of conditions, and whether more costly hyperspectral indices offer an improvement over broad-band indices which can be calculated from freely available satellite data. Two *Sphagnum* moss species with different niches were subjected to 80 days of drought in a laboratory experiment in order to judge how well spectral indices can measure changes in moisture content in this critical wetland plant genus, and also how well spectral indices compare to the resulting changes in photosynthesis. A field study was conducted across three sites in Northern Scotland, UK, and considered changes across the main growing season March-September. Our results showed that both water indices had similar relationships with moisture content in the laboratory, although the correlation was less conclusive in the field. All vegetation indices tested were shown to have some relationship with Gross Primary Productivity (GPP), but the three best performing vegetation indices were the EVI, NDVI and CIm. Overall our results show that broad-band indices such as those calculated from freely available MODIS, VIIRS, Sentinel-2, and Landsat satellite data, show little disadvantage compared to hyperspectral indices for estimating photosynthesis or water content of blanket bog peatland vegetation.

4.1.Introduction

Peatlands are an important ecosystem for the sequestration and storage of carbon, and also for supporting biological diversity (Minayeva et al., 2017). Peatlands around the world store approximately a third of the world's soil carbon (Gorham, 1991; Turunen et al., 2002), as within the waterlogged environment of peat substrates decomposition is limited and so organic matter is retained. Many peatlands have, however, been subject to deleterious management schemes, including drainage, commercial harvesting, overgrazing, planting for

commercial forestry, and burning (Bonn et al., 2016; JNCC, 2011). These processes can lower the water table and increase bare peat surfaces, leaving them vulnerable to drought and its subsequent effects on photosynthesis of peatland vegetation, and consequently carbon sequestration.

Policy makers are now beginning to see peatland carbon storage as a useful part of efforts to mitigate climate change, and peatland restoration is being encouraged (Irving and Zhou, 2013). It is therefore important to develop cost-effective methods of assessing peatland condition and carbon sequestration. Spectral information from peatland vegetation can be used for remotely estimating the condition and carbon fluxes of peatlands (Lees et al., 2018). Certain spectral indices, including those used in this study, have been shown to correlate with both moisture content and carbon fluxes of peatland vegetation (Harris, 2008; Harris et al., 2006; Harris et al., 2005; Letendre et al., 2008; Meingast et al., 2014; Van Gaalen et al., 2007). Vegetation indices can be used to estimate plant health and photosynthesis, whilst water indices are useful proxies for moisture. These indices can be used alone to detect changes in either GPP or water content, or in combination for more complex analysis of peatland condition.

Hyperspectral data can be used to calculate vegetation indices which precisely align with specific plant functions, such as the Photochemical Reflectance Index (PRI) which corresponds to the xanthophyll photochemical protective mechanism. These newer indices require data which is more expensive and harder to obtain than the data needed by older indices such as the Normalised Difference Vegetation Index (NDVI). This study tests the accuracy and reliability of both hyperspectral and broad-band indices as proxies for water content and photosynthesis under a range of field and laboratory conditions.

Sphagnum moss is a key genus in peatland formation, and its presence is an indication of good blanket bog condition (Bonnet et al., 2009). Peat-forming plants such as *Sphagnum* are well adapted to the wet environment of blanket bogs, and grow less well when water tables are low (Harris, 2008; Strack and Price, 2009; Van Gaalen et al., 2007). Many *Sphagnum* species have an optimum water content of approximately twenty times their dry weight, and have been shown to decrease photosynthesis as moisture content is reduced (Lees et al., in review; McNeil and Waddington, 2003; Robroek et al., 2009). As *Sphagnum* dries beyond a certain threshold it experiences bleaching, which affects the spectral reflectance and can be detected by vegetation indices (Bortoluzzi et al., 2006; Bragazza, 2008; Lees et al., in review.)

Here we used both laboratory and field experiments to compare spectral indices and peatland vegetation under a range of conditions. The laboratory experiments compared two

different species of *Sphagnum* moss (*S. capillifolium* and *S. papillosum*) and subjected them to drought, in order to measure the effect of water limitation on both carbon fluxes and spectral reflectance. The field experiment included carbon flux and spectral reflectance measurements over three different peatland areas within the Forsinard Flows reserve (northern Scotland) in different conditions (one near-natural site and two at different stages of restoration), and measurements were taken across the main growing season. These field measurements included a range of typical peatland vegetation, including mosses, sedges and dwarf shrubs (see Section 2.3).

The aim was to assess the usefulness of a mixture of indices which can be calculated from the bands of freely available satellite data, in this study referred to as broad-band indices, and mono-spectral indices which are calculated using costly data from hyperspectral instruments. We chose two indices that estimate moisture content and five that estimate plant function for this study. The first water index was the hyperspectral floating Water Band Index (fWBI) which considers the water absorption feature between 930 and 980nm. The second, broad-band, water index used was the Normalised Difference Water Index (NDWI) which uses the difference between NIR (near infrared) and SWIR (short-wave infrared) to assess water content. The broad-band plant function indices were the Normalised Difference Vegetation Index (NDVI) and the Enhanced Vegetation Index (EVI). These both focus on the difference between the red and NIR zones of the reflectance spectrum, and the EVI also includes the blue band to correct for atmospheric aerosols. The hyperspectral plant function indices included the Photochemical Reflectance Index (PRI) which is sensitive to the xanthophyll photoprotective mechanism; the Structure Insensitive Pigment Index (SIPI) which considers the chlorophyll/carotenoid ratio; and the modified Chlorophyll Index (CIm) which focuses on the red-edge (see Tables 4.1 and 4.2).

All the vegetation indices selected for this study have been shown to correlate with peatland vegetation Gross Primary Productivity (GPP), some during drought studies in the laboratory, and some in the field (Harris, 2008; Letendre et al., 2008; Van Gaalen et al., 2007). Our work here aims to make a thorough examination of the selected indices to determine which give the best results in peatland environments. To do this we include both a laboratory study of replicate samples of *Sphagnum* moss cushions which were subjected to a long (80 days) period of drought, and a field study carried out over three different sites during the growing season. Our objectives were to determine (1) whether the selected indices correlate with water content and GPP, (2) which indices show the clearest and most consistent relationships across a range of peatland species and conditions, and (3) whether the hyperspectral indices perform better than the broad-band indices.

Table 4.1 –The averaged bands used in this study for broad-band indices compared to the bands of commonly used satellites MODIS, Landsat, VIIRS and Sentinel-2.

Band	**Wavelengths averaged in this study**	**MODIS**	**Landsat 8**	**VIIRS**	**Sentinel-2A (central wavelength/band width)**
Blue	450 to 515 nm	Band 3 (459 to 479 nm)	Band 2 (450 to 512 nm)	M3 (478 to 498 nm)	Band 2 (447.6 to 545.6 nm)
Red	630 to 680 nm	Band 1 (620 to 670 nm)	Band 4 (636 to 673 nm)	M6 (662 to 682 nm)	Band 4 (645.5 to 683.5)
NIR	841 to 876 nm (NDWI)/845 to 885 nm (NDVI & EVI)	Band 2 (841 to 876 nm)	Band 5 (851 to 879 nm)	I2 (846 to 885 nm)	Band 8A (848.3 to 881.3)
SWIR	1628 to 1652 nm	Band 6 (1628 to 1652 nm)	Band 6 (1566 to 1651 nm)	I3 (1580 to 1640 nm)	Band 11 (1542.2 to 1685.2)

Table 4.2 – The water indices and vegetation indices used in this study, their equations and relevant references (for the development of the equations in the form used in this study). In the equations given in this section 'R' subscripted by a number is a single wavelength in a mono-spectral index. 'R' subscripted by a band name (Table 4.1) indicates a band. Colour band equivalents are given in Table 4.1 and shown in Figure 4.2.

Index	**Equation**	**Relevant references**	**Broad-band or hyperspectral**
Floating Water Band Index (fWBI)	$fWBI = R_{920} / \min (R_{930-980})$	Strachan et al., 2002; Harris, 2008	Hyperspectral
Normalised Water Difference Index (NDWI)	$NDWI = (R_{NIR} - R_{SWIR})/(R_{NIR} + R_{SWIR})$	(Gao, 1996)	Broad-band
Normalised Difference Vegetation Index (NDVI)	$NDVI = (R_{NIR} – R_{red})/ (R_{NIR} + R_{red})$	Rouse et al., 1974	Broad-band
Enhanced Vegetation Index (EVI)	$EVI = 2.5 \times ((R_{NIR} – R_{red})/(R_{NIR} + 6 \times R_{red} + 7.5 \times R_{blue} + 1))$	Didan et al., 2015	Broad-band
Photochemical Reflectance Index (PRI)	$PRI = (R_{531} - R_{570})/ (R_{531} + R_{570})$	Gamon et al. 1992; Penuelas et al., 1995; Van Gaalen et al., 2007	Hyperspectral

Structurally Insensitive Pigment Index (SIPI)	SIPI = (R_{800} – R_{445})/(R_{800} – R_{680})	Penuelas et al., 1995; Harris, 2008	Hyperspectral
Modified Chlorophyll Index	CIm = (R_{750} - R_{705})/(R_{750} + R_{705} – 2 x R_{445})	Sims and Gamon, 2002	Hyperspectral

4.2.Method

4.2.1. Field site

The field site for this study was the Forsinard Flows RSPB reserve (https://www.rspb.org.uk/reserves-and-events/reserves-a-z/forsinard-flows/) in North Scotland (approx. 58.3552, -3.9993 to 58.4458, -3.6972 WGS84, see Figure 4.1). This site is part of the 4,000 km^2 Flow Country blanket bog; Europe's largest blanket bog (Lindsay et al., 1988), of which approximately 1,300 km^2 is protected under EU Habitats and Birds Directives. The area includes extensive blanket bogs with only minor human impacts (Littlewood et al., 2010) and lightly grazed by deer. These areas are referred to here as 'near-natural'. Other areas of the Flow Country were planted with non-native conifers for commercial forestry, and in many areas, including in Forsinard Flows, the trees have been felled and the sites are now undergoing restoration. In many of the restoration sites the landscape still shows distinctive furrows and ridges from the drainage ditches created for forestry. More information about the specific areas of the site used in this study is given in Section 2.3.

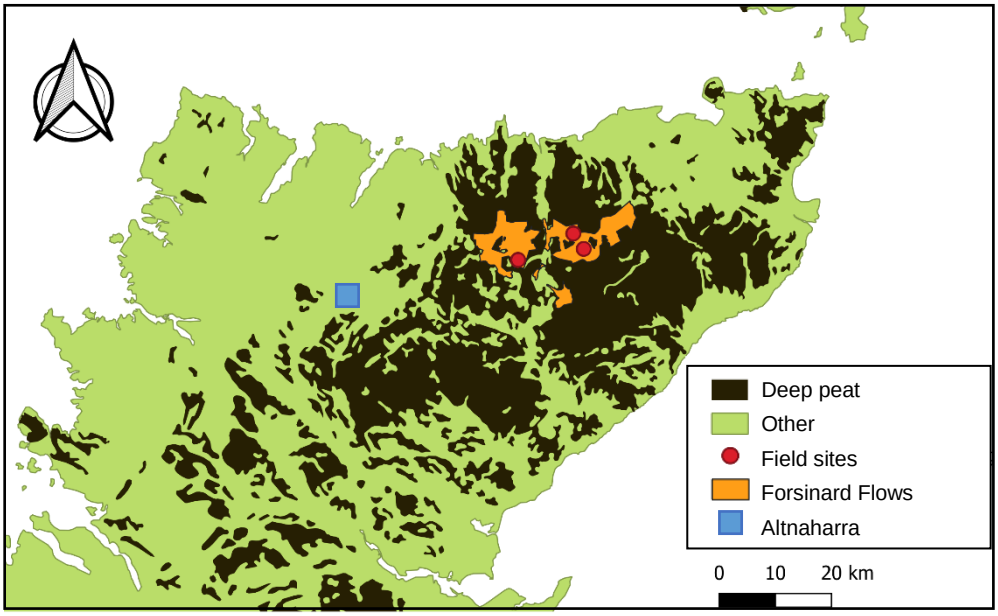

Figure 4.1 - Map of the northern Scottish mainland showing peatland areas in dark brown (British Geological Survey, 2007), the Forsinard Flows RSPB reserve in orange (European

Environment Agency, 2017), the three field sites as red circles, and the meteorological station at Altnaharra as a blue square. The peatland dominated landscapes in this area are referred to as the 'Flow Country'.

The nearest meteorological station with daily data available was Altnaharra, approximately 35 km south-west of the Forsinard Flows reserve (see Figure 4.1). This has been used for weather data in Section 3.2.1.

4.2.2. Laboratory experiment

This experiment was designed to assess whether the relationship between the selected vegetation indices and GPP, and between the selected water indices and water content, remains constant under extreme water limitation conditions in key peat-forming *Sphagnum* species.

Two *Sphagnum* species, *S. capillifolium* and *S. papillosum*, were selected. Both species are commonly found at our study sites but prefer different microhabitats. *S. capillifolium* is hummock-forming, red to green in appearance, with hemi-spherical capitula (Laine et al., 2009). *S. papillosum* is green to yellow-brown, prefers wetter conditions and grows in carpets (Laine et al., 2009). *S. capillifolium* is also more tolerant to disturbance than *S. papillosum*, and is one of the first species to re-colonise areas of peatland undergoing restoration (RSPB, unpublished data).

Samples of each species were collected from the Forsinard Flows RSPB reserve in PVC tubing 6 cm deep and 10 cm diameter during September 2016. The samples were kept moist and transported from the field to the laboratory in a coolbox over a period of 3 days. Once in the laboratory the samples were placed in 1 litre, straight-sided, clear polycarbonate jars and maintained in a growth cabinet (Panasonic MLR-352H-PE) on a 12-hour day and 12-hour night cycle (similar to conditions in the field during the collection period in September). During the day the growth cabinet was kept at maximum light levels (20,000 lx), 15˚C, and 70% relative humidity (slightly lower than the average at the site to aid drying of samples). At night the cabinet was dark, at 5˚C, and the humidity was unregulated.

When the samples first arrived in the laboratory they were inundated with deionised water (for consistency with previous studies eg. Clark et al., 2012, 2006) and the excess drained off manually to bring them to saturation. After a week-long acclimatisation period, during which the samples were regularly watered (also with deionised water) to maintain saturation, four samples of each species were subjected to total drought for 80 days. This length of drought would be very unlikely in the field but was used to analyse complete desiccation. Three times per fortnight (every 4-5 days) the CO_2 fluxes of all the samples were measured.

The flux measurements were taken using a LICOR-8100 (LICOR Inc., Lincoln, Nebraska, USA) and a clear polycarbonate custom-built chamber (13 cm tall, 11 cm diameter). Each sample was brought out of the growth cabinet and placed under a high-pressure sodium growth lamp (Philips Belgium 9M SON-T-AGROO 400) in a laboratory in order to keep light levels as constant as possible. The clear chamber was placed over the sample using a foam seal and a 90 second measurement taken of Net Ecosystem Exchange (NEE). A blackout cloth cover was then placed over the chamber, and the measurement taken again to gather net respiration data (Rtot). The Gross Primary Productivity (GPP) was calculated as the difference between the light and dark chamber results. Four weeks into the study, we observed that variation in ambient lighting affected our results. Therefore, from that point onwards we measured photosynthetically active radiation (PAR) during each experiment. This allowed us to correct later results. Earlier results were corrected by estimating PAR from measurement time (see Appendix A).

Samples were weighed three times a week before and after watering throughout the experiment. At the end of the experiment the samples were dried in a laboratory oven at 70˚C for 72 hours, and the dry weights measured to retrospectively calculate moisture content. This method assumes there was no significant growth in the *Sphagnum* samples during the experimental period. All moisture contents are given in grams fresh weight/grams dry weight (g/g).

Spectral reflectance was measured using a Ger3700 spectrometer (Geophysical and Environmental Research Corp., 1999) mounted in a dark room with a single constant light source (1000 W high-intensity halogen lamp at an angle of 45° and a distance of 0.5 m). Each sample was placed under the spectrometer and a measurement taken of the central area of the sample (approximately 4 cm diameter); the sample was then rotated by approximately 120˚ for a second measurement and rotated again for a third measurement. The average of these three spectra was taken to compensate for potential structural effects. Reference spectra, using a spectralon panel, were taken between samples and used to convert the measured radiances to reflectances (Salisbury, 1998).

4.2.3. Field experiment

This experiment was designed to assess how the selected vegetation indices and GPP vary spatially and temporally across the growing season of a typical peatland with a mix of vegetation species. This experiment also considers the use of the selected water indices to estimate moisture content in the field, and whether these indices are aligned with Water Table Depth (WTD) and soil moisture measurements.

This study used three sites within the Forsinard Flows RSPB reserve. Two of these were ex-forestry sites on deep peat, being restored towards blanket bog (Hancock et al., 2018): Lonielist, which was felled in 2003-04, and Talaheel, which was felled in 1998 and was subject to further hydrological management in 2015/16 whereby plough furrows were dammed. The third site was at Cross Lochs (Levy and Gray, 2015); this area of intact bog was considered to be a near-natural control. All three sites had an Eddy Covariance (EC) tower installed. At each of the sites eight plots were located along two perpendicular transects. The transects were arranged within the footprint of the EC towers according to the size of the tower footprint and the dominant wind directions (Hambley, 2016). At Lonielist the main transect was 80 m and the secondary transect was 60 m, with all plots 20 m apart. At Talaheel the transects were 100 m and 75 m with the plots 25 m apart, and at Cross Lochs the transects were 120 m and 90 m with plots 30 m apart.

At each plot two PVC collars (24 cm in diameter) were located one on higher ground (ridges in the restored sites, hummocks at Cross Lochs) and one on lower ground (in the furrows at the restored sites, lawns at Cross Lochs). The vegetation within the collars included various species of typical blanket bog vegetation, including the *Sphagnum* mosses used in the laboratory experiment, but also other mosses, sedges Cyperaceae, and dwarf shrubs Ericaceae (see Appendix B for tables of vegetation species, and example photos). The percentage cover of each species within the collars was estimated and used to assess which collars were *Sphagnum*-dominated (over 50% cover). The Lonielist site set-up included manually monitored dipwells used to record WTD (Rydin and Jeglum, 2013) paired with each of the collars. Measurements, including CO_2 fluxes, spectral reflectance, and environmental conditions, were taken once a month during the 2017 growing season March to September.

CO_2 flux measurements were taken using a LICOR-8100 (LICOR Inc., Lincoln, Nebraska, USA) and clear Perspex custom-built chambers (24 cm diameter, 30 cm height). Small battery-operated fans were installed within the chambers to circulate the air. Light (NEE) and dark (Rtot) measurements were taken as consecutive measurements, sealing to the chamber with rubber mastic (Terostat). Each measurement was taken for five minutes, with a 20 second pre-measurement period for stabilisation.

Spectral measurements in the field were taken using a handheld SVC HR-1024 spectroradiometer mounted on a monopod and held approximately 1m from the surface. Three measurements were taken of the vegetation within each collar, rotated between each measurement by approx. 90˚ whilst avoiding shadow creation, to minimise structural effects.

A spectralon reference panel was used before each measurement to correct for changing light conditions.

Photosynthetically Active Radiation (PAR) was measured using a sensor planted in the peat outside the chamber and connected to the Licor-8100. Soil moisture was measured using a moisture probe (ThetaKit moisture meter, 6 cm, Dynamax) and the dipwells at Lonielist were manually monitored. Soil temperature was measured at 5 cm and 15 cm from the moss surface (lollipop thermometer, Fisherbrand, accurate to ±1˚C) and surface temperature inside the chamber at the start and end of each measurement.

4.2.4. Indices

The indices used in this study were all calculated using reflectance values averaged over a range of wavelengths which can be compared to those used by different satellites (see Table 4.1 and Figure 4.2).

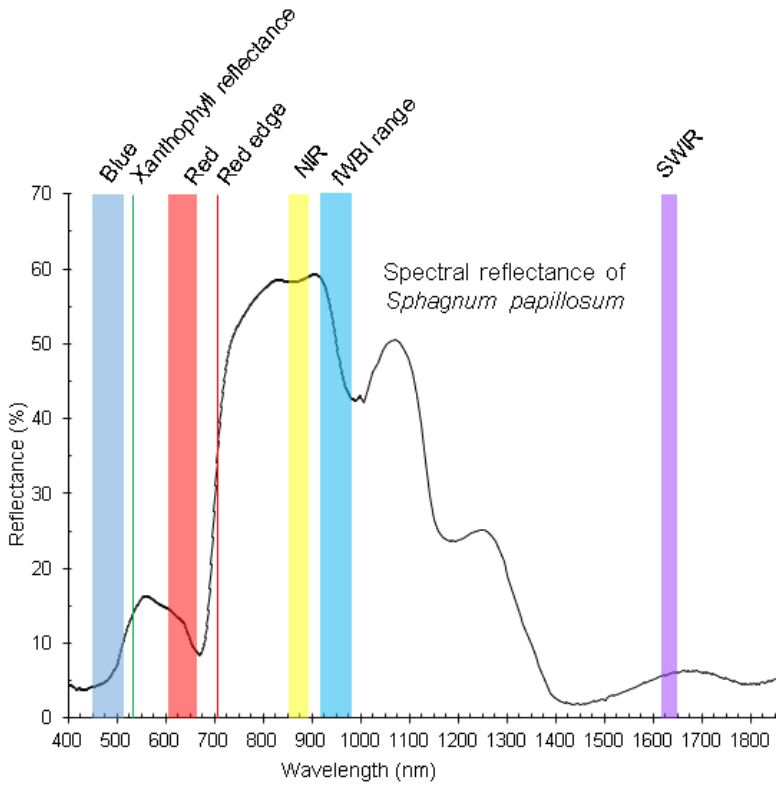

Figure 4.2 – Spectral reflectance graph of a healthy sample of S. papillosum, showing the ranges and wavelengths used by the indices in this study.

4.2.4.1. Water indices

The water indices used in this study are shown in Table 4.2. The fWBI was calculated following Strachan et al. (2002) on the rationale that the water absorption feature is not static but shifts between 930 and 980nm. This is compared to a reference wavelength at 920nm as used by Harris (2008). The NDWI was calculated using the NIR and SWIR ranges. The SWIR is affected by both the vegetation chlorophyll and the water content, whilst the NIR is not affected by water content.

4.2.4.2. Plant function indices

The vegetation indices used in this study are shown in Table 4.2. The NDVI is a broad-band index which focuses on the difference between the red light absorbed by healthy vegetation and the NIR reflected. The equation for EVI follows the calculation of the MOD13 product (Didan et al., 2015), and is less sensitive to atmospheric aerosols and saturation over dense canopies than the NDVI (Huete et al., 2002).

The PRI calculation follows Gamon et al. (1992) and Penuelas et al. (1995).The PRI works on the principle that 531 nm is the wavelength at which the xanthophyll photoprotective mechanism can be detected, and is therefore a direct measure of light use efficiency in plants (Gamon et al., 1992). 570 nm was used as the reference wavelength following Van Gaalen et al. (2007).

The SIPI developed by Penuelas et al. (1995) considers the chlorophyll/carotenoid ratio, which Harris (2008) found to increase as photosynthesis decreases.

The CIm makes use of the red-edge principle, which considers the movement of the boundary between the red absorption zone and the NIR reflectance region. Adding R_{445} to the equation is a measure of surface reflectance not affected by chlorophyll or carotenoids, to compensate for generally high leaf reflectance (Sims and Gamon, 2002).

4.2.5. Statistical analysis

4.2.5.1. Laboratory analysis

In order to create composite models and to perform comparative statistics, the laboratory data for all samples were binned into twelve groups of equal size using the water content for water indices analysis and the GPP for vegetation indices analysis (using R package ggplot2, Wickham, 2016). For the water indices analysis the two species were binned separately, as the relationship to the water indices was found to be species dependent in a mixed effects model. A value of 1 was subtracted from the fWBI values to create an index with a starting value of 0, and for NDWI a value of 0.1 was subtracted for the same reason.

The relationship between both water indices and water content (binned data for each species) was fitted to a linear model and an alternative Gompertz function model, and Akaike information criterion (AIC) was used to compare the fit of the two models. Gompertz functions are similar to logistic growth functions, but do not have the assumption of centrality and symmetry in the point of inflection (Vieira and Hoffmann, 1977).

To assess the relationships between each vegetation index and GPP in the laboratory study, both linear and polynomial regression models of 2nd order were first assessed using the data averaged within 12 GPP bins of equal count. AIC was used to assess the relative quality of each model. For all five vegetation indices tested, a linear model was found to be better than a polynomial model. A linear mixed model including species and sample was therefore fitted to the data for each index. The Breusch-Pagan test for heteroscedasticity (package lmtest, Zeileis and Hothorn, 2002) was applied to the models, and if heteroscedasticity was present a Box-Cox transformation (package EnvStats, Millard, 2013) was applied to the index data series.

4.2.5.2. Field analysis

In order to consider the relationship with soil moisture deficit (SMD), rainfall amounts, sunshine hours, temperatures, relative humidities and wind speeds were downloaded for the Altnaharra meteorological station (Met Office, 2012). Reference evapotranspiration was calculated using the Penman-Monteith equation following Zotarelli et al. (2010), and gaps were filled by averaging the evapotranspiration of the two days on either side of the gap. Soil moisture deficit was calculated using the previous day's SMD, rainfall data, and the reference evapotranspiration. Field capacity was assumed to be -10 mm, and if SMD was ever less than -10 mm and rainfall was also less than 10 mm during the following 24 hour period, then a drainage term equalling half the excessive water was introduced.

A fitted logarithmic model (calculated using all field data combined) was used to correct for the effects of PAR on GPP in the field:

$$GPP_{corrected} = GPP - 0.9 \times \ln(PAR) + 2.51$$

Heinemeyer et al. (2013) found that the relationship between PAR outside and inside a similar Perspex chamber was linear, with a 34% decrease due to the chamber. We have assumed that a linear relationship between internal and external PAR is true in this study, and so the logarithmic correction applied to the GPP is the same in both cases.

For the field measurements of GPP, a linear model incorporating GPP and month as independent variables, and assessing the interaction between them, was used.

All statistical work was done in R (R Core Team, 2017).

4.3.Results

4.3.1. Laboratory results

4.3.1.1. Moisture content

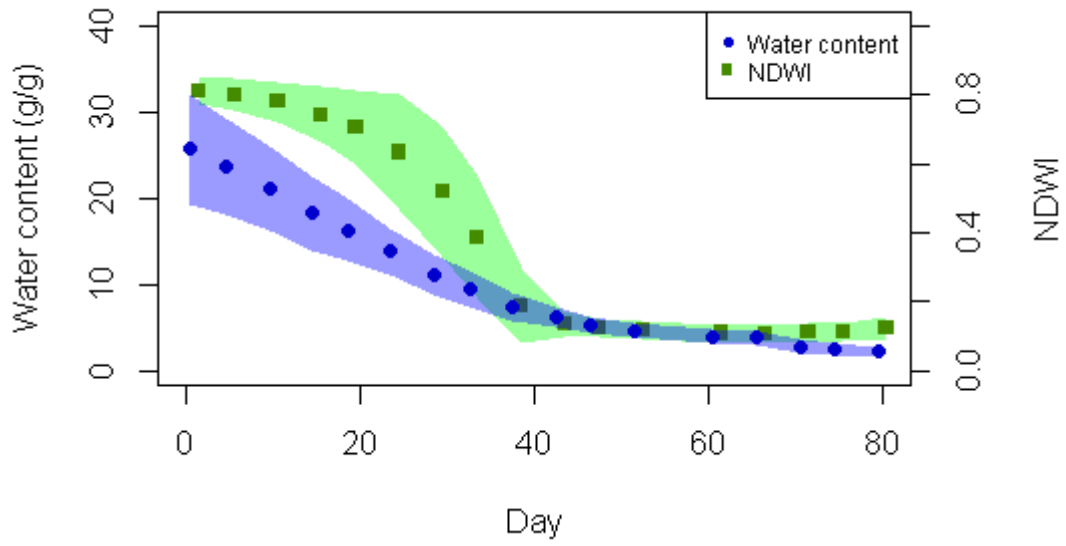

Figure 4.3 – The change in average water content and NDWI of all 8 microcosms over the 80 day experimental drought period, with standard deviation of values shown as coloured areas. The two datasets are offset by half a day in this plot (actually taken within 10 hours of each other) so both are visible.

The changes in water content and the NDWI across the experimental period are shown in Figure 4.3. The water content decreased steadily across the experimental period until about day 40, when the decrease slowed. Meanwhile the NDWI had the most rapid period of decrease between approximately day 20 and day 40. The relationships between *Sphagnum* moisture content and the two water indices (fWBI and NDWI) therefore showed a non-linear increase for both species (Figure 4.4). For both indices, the relationship with moisture content for the *S. capillifolium* samples fitted well to Gompertz functions, with little variation of the indices at high and low moisture contents and a rapid change between (see Figure 4.4A and 4.4C). *S. papillosum*, however, did not conform as consistently to this pattern for both indices. The NDWI and fWBI of *S. papillosum* samples continued to increase, albeit at a slower rate, whereas the fitted Gompertz functions predict an upper limit. In general, the relationship between indices and moisture content showed more scatter for *S. papillosum*.

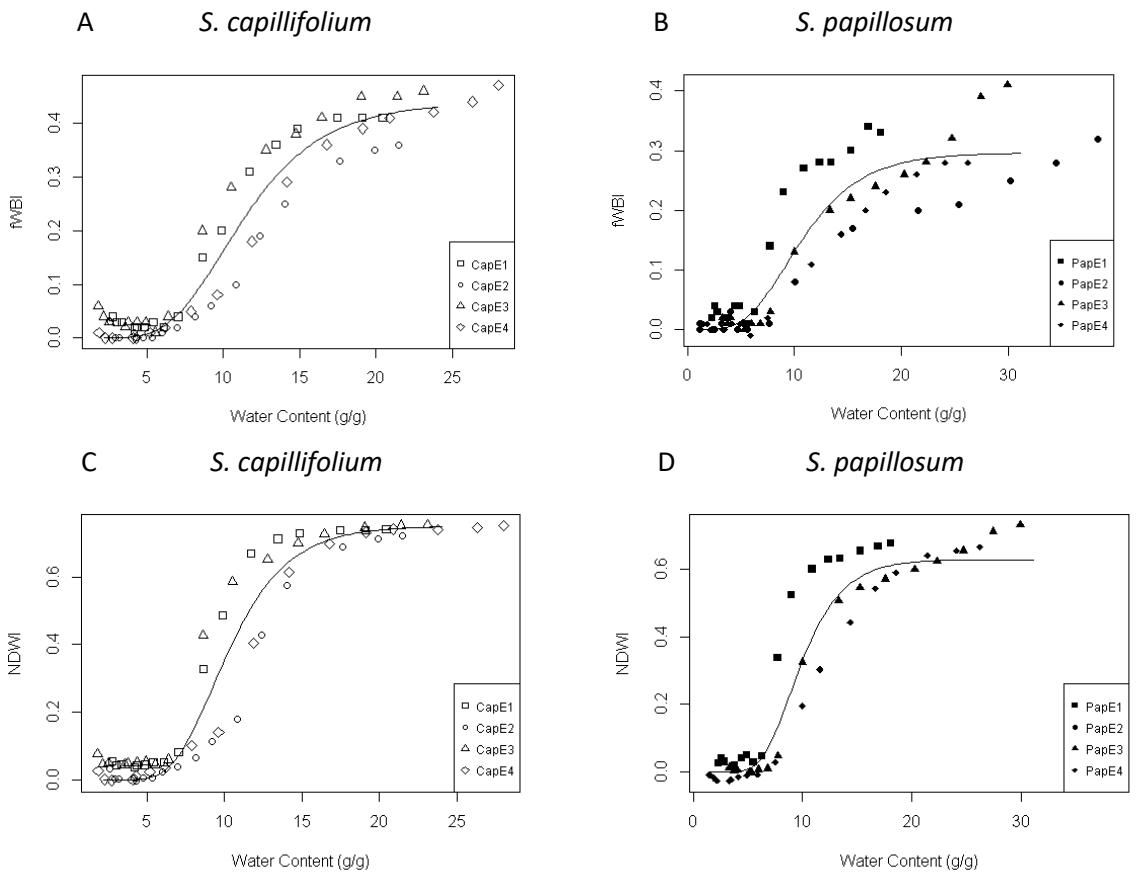

Figure 4.4 –A: Relationship between water content and fWBI for S. capillifolium samples. B: Relationship between water content and fWBI for S. papillosum. C: Relationship between water content and NDWI for S. capillifolium samples. D: Relationship between water content and NDWI for S. papillosum samples. Gompertz functions fitted using the binned water content data for each species are shown as lines to illustrate the relationships.

4.3.1.2. GPP

The linear mixed model for the NDVI relationship with GPP was highly significant ($p<0.001$, $R^2 = 0.38$) and showed no significant effects or interactions of species or sample (see Figure 4.5A). The same was true for the EVI ($p<0.001$, $R^2 = 0.44$, see Figure 4.5B).

The model for the CIm showed heteroscedasticity, and so a Box-Cox transformation was applied to the dataset. The model using transformed data was highly significant ($p<0.001$, $R^2=0.43$, see Figure 4.5C) and showed no significant effects or interactions apart from an effect of sample 'CapE3' ($p<0.05$). The SIPI model also required transformation, and the resulting model was also highly significant ($p<0.001$, $R^2 = 0.32$, see Figure 4.5D) with no effects or interactions other than an effect of 'CapE3' ($p<0.05$).

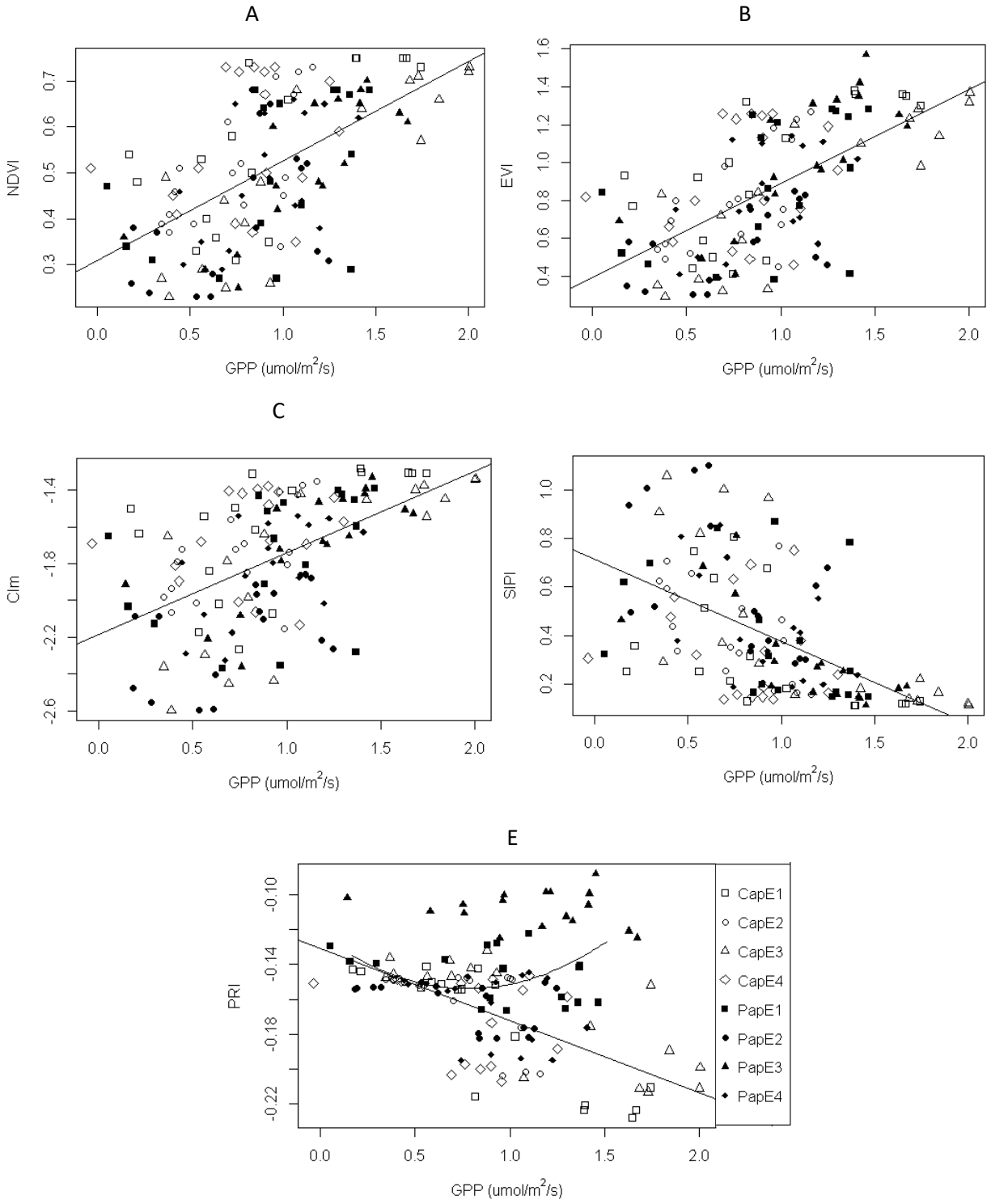

Figure 4.5 – Relationships between GPP and vegetation indices for the eight laboratory samples. The graphs showing SIPI (D) and CIm (E) use the transformed data. Black lines show the models fitted to averaged binned data. The graph showing PRI (C) includes the linear model for S. capillifolium, and the polynomial for S. papillosum. Black symbols are for S. papillosum, white symbols for S. capillifolium. Numbers in the legends refer to the individual microcosms.

The PRI model also showed heteroscedasticity, and this was not improved by applying a Box-Cox transformation. The model showed a significant species effect, so we decided to fit the two *Sphagnum* species separately. A linear model was found to be the best option for the binned data of *S. capillifolium* alone. The linear mixed model, including GPP and sample, for *S. capillifolium* was highly significant ($p<0.001$, $R^2 = 0.50$), and did not show heteroscedasticity. It did show a significant effect for sample 'CapE4', and also a significant interaction of 'CapE4' with GPP. *S. papillosum*, however, did not conform well to a linear model. The binned data showed a significant ($p<0.05$) polynomial relationship (see Figure 4.5E).

4.3.2. Field results

4.3.2.1. Moisture content

Figure 4.6 shows the seasonal changes in SMD over the growing season compared to the measurements of moisture content and WTD. The SMD values were negative throughout most of the growing season, indicating high water levels. Likewise, the soil moisture results were mostly close to the maximum for saturation and did not show much variation. The results were somewhat difficult to interpret due to the low temporal frequency of measurements and generally wet conditions, but the linear relationships between soil moisture and SMD at Talaheel and Cross Lochs were significant at the 90% level (p-values of 0.066 and 0.063). WTD at Lonielist had a highly significant linear relationship with SMD (R2 = 0.18, p-value = 0.0001).

Neither the soil moisture nor the WTD had a clear relationship with either of the two water indices. Figure 4.6 compares the NDWI and fWBI to the SMD. Again, the results of the measured variables had large ranges and therefore it was difficult to interpret relationships with SMD, but some agreement can be seen. There was a significant linear relationship between SMD and the NDWI at Lonielist ($R^2 = 0.26$, p-value = 0), and at Talaheel ($R^2 = 0.057$, p-value = 0.017). There was also a significant linear relationship between SMD and the fWBI at Lonielist (0.17, 0.00045).

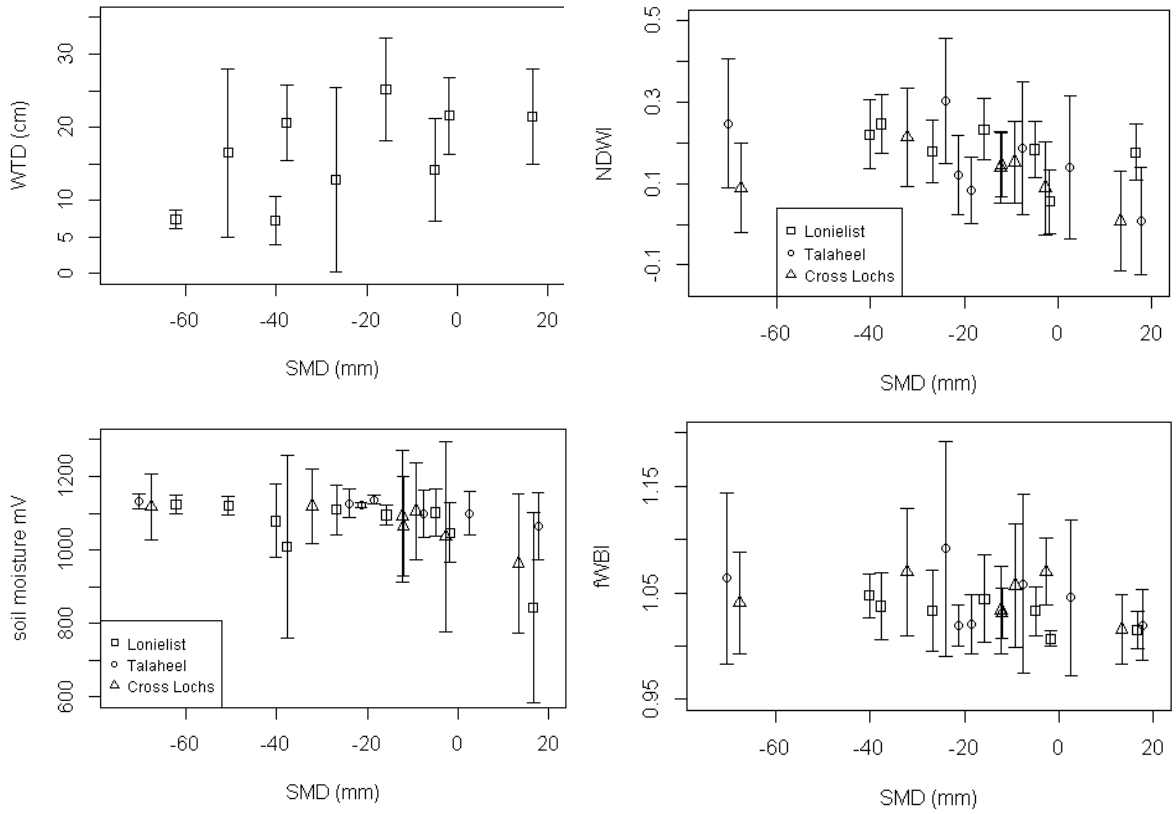

Figure 4.6 – SMD data from Altnaharra compared to average Water Table Depth (WTD) at Lonielist (top left) and soil moisture measured in the field (bottom left), compared to average NDWI (top right) and fWBI (bottom right) (n=9 to 16).

4.3.2.2. GPP

The mixed effects linear regression model for NDVI showed a significant relationship with GPP, and also a significant interaction between GPP and month in every month. This indicates that the slope of the relationship between GPP and NDVI varies across the seasons (see Figure 4.7). The adjusted R^2 of the model was 0.49 ($p<0.001$). The same model interactions were true of the EVI (R^2 0.54, $p<0.001$), and the SIPI (R^2 0.48, $p<0.001$).

The CIm regression model showed a strongly significant relationship with GPP, but fewer significant interactions with months. This suggests that the slope of the relationship between GPP and CIm is less affected by seasonality (month) than it is for the NDVI or EVI. The adjusted R^2 of this model was 0.60 ($p<0.001$).

The regression model for PRI is significant ($p<0.01$), but shows no significant effects or interactions, and has a very small R^2 value of 0.068.

When each month was considered individually, the NDVI showed significant relationships with GPP for every month apart from April and June (see Figure 4.7); these two months had poor weather conditions which prevented full dataset collection. The linear model for March had a much steeper slope than the other months (0.073 compared to a range of 0.020 to 0.022). This pattern was also true of the EVI, CIm and SIPI.

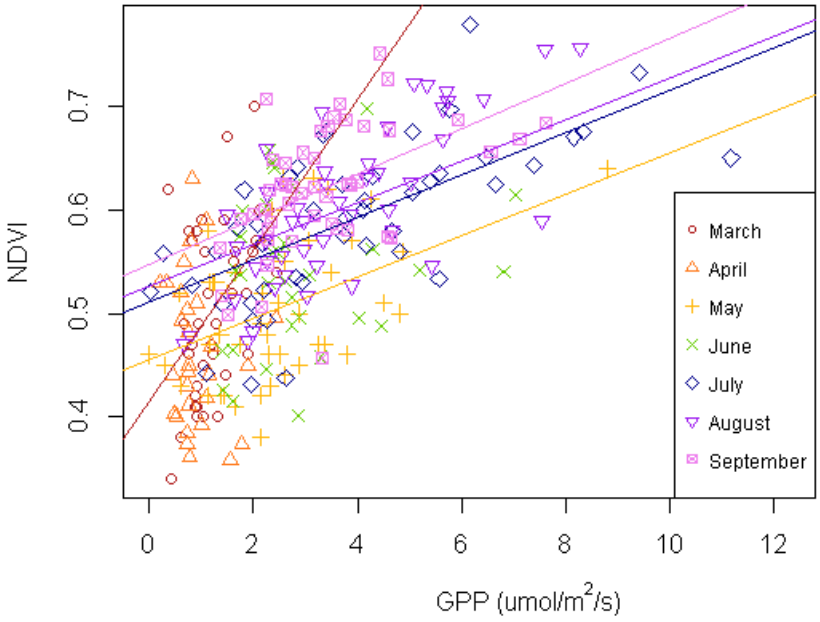

Figure 4.7 – Relationships between GPP and NDVI for each month in the field. Lines show the significant ($p<0.05$) linear models for each month in different colours.

4.3.3 Field and laboratory comparison

The range of values seen in the field for the two water indices was towards the lower end of the range seen in the lab (monthly averages of 0.062 to 0.25 compared to measurement day averages of 0.12 to 0.81 for the NDWI). The field collars which were *Sphagnum*-dominated (*Sphagnum* coverage of over 50%), however, had higher average NDWI values than the non-*Sphagnum*-dominated collars in every month.

Figure 4.8 shows the relationship of NDVI with both laboratory and field values. The slope of the laboratory results was much steeper than that obtained for the field results, and the slope of the field results for March was closer to the laboratory results than the July relationship. The slope of the collars which were *Sphagnum* dominated was also closer to the slope of

laboratory results than the model for all field collars. Similar variations in slope between laboratory results, field results, months, and *Sphagnum*, were seen in EVI, CIm, and SIPI.

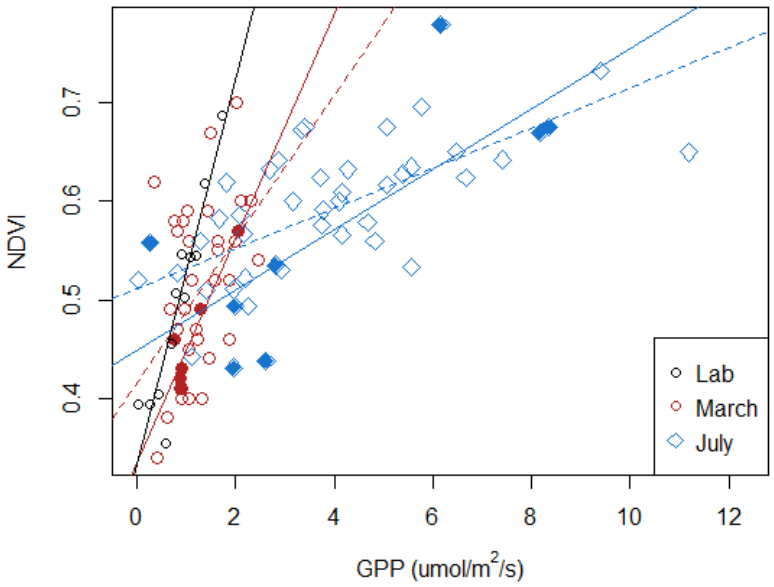

Figure 4.8 – Comparison of lab results with March and July field results. The black circles and line show the laboratory data binned by GPP. The filled symbols and solid lines show only the field collars with a proportion of Sphagnum over 50%, the unfilled symbols and dashed lines show all the field collars.

4.4.Discussion

4.4.1. Moisture content

The results from these experiments showed that both water indices tested, the fWBI and NDWI, had positive correlations with moisture content in the laboratory study on single *Sphagnum* species, and a link with SMD in the field on mixed, *Sphagnum*-rich peatland vegetation. This agrees with previous studies (Harris, 2008; Letendre et al., 2008; Van Gaalen et al., 2007) that have also found good correlations between moisture content and water indices in *Sphagnum* species (*S. teres; S. rubellum, S. fuscum, S. magellanicum, and S. fallax; S. pulchrum, S. tenellum, S. capillifolium, S. subnitens, and S. papillosum*). Letendre et al. (2008) calculated a Pearson's correlation coefficient of 0.77 for water content and the NDWI of four replicates of three different *Sphagnum* species, and higher correlations for each species considered separately. Within their study only *S. fuscum* showed a pattern similar to the Gompertz function (they did not use *S. capillifolium* or *S. papillosum*).

Van Gaalen et al. (2007) found strong linear relationships between water content and the Water Band Index (a precursor of the fWBI) for three samples of different *Sphagnum* species. Their water content results were in the range of 5 to 20 g/g, however, and it was mainly beyond this range that our results showed saturation of the water index signals; a wider range of water contents might have shown a non-linear pattern.

In agreement with the current work, Letendre et al. (2008) and Harris et al. (2005) found that relationships between water indices (NDWI, Water Index (WI), Relative Depth Index (RDI), and two different formulations of fWBI, Moisture Stress Index (MSI), respectively) and water content were species specific. In this study we found that *S. papillosum* showed less clear saturation of the water indices signals at higher water contents, possibly because it prefers wetter microhabitats compared to *S. capillifolium*.

Although statistical testing of the field data did not show any significant relationships between soil moisture or WTD and either of the two indices, it appears that soil moisture, WTD and the water indices may all be linked to SMD. Harris et al. (2006) did find significant relationships between the fWBI and the moisture content in the top 6 cm (measured using a ThetaProbe), and between the fWBI and water table depth, at their study site at Cors Fochno, Wales. The relationship was particularly clear in their data from September 2002, when rainfall was less than half the average precipitation for the month. This indicates that the relationship between soil moisture and water indices may be stronger when a larger range of water contents is included, and our study period was continuously wet as indicated by the SMD values that were negative for almost the entire growing season except a short period in May. It is in this dryer May period that a decrease in water table depth and soil moisture, and also in both water indices, was observed. Future studies assessing the performance of these indices during drought periods in the field would be useful.

There does appear to be a connection between SMD and the two water indices in the field, and between SMD, soil moisture, and WTD. This suggests that the relationships between WTD, SMD, and the wavelengths used in water indices are not straightforward and require further investigation. Future work in this area should consider measuring water indices in the field at higher temporal frequencies to aid comparison with SMD, WTD, and precipitation data, and thereby improve our understanding of these relationships. WTD and moisture content are key indicators of peatland health, and developing our understanding of the connection between water indices and these variables in the field is key to furthering the use of such indices in peatland monitoring.

It is interesting that the field values from the two water indices were mainly in the lower part of the range seen in the laboratory study. This would suggest that the collars measured in

the field were drier than the saturated *Sphagnum* samples, which is probably indicative of the wider mix of vegetation that was present in the collars (i.e. not just *Sphagnum*). This is supported by the *Sphagnum*-dominated collars having higher NDWI values than the other collars. The optimum plant tissue water content for *Sphagnum* mosses is around twenty times their dry weight, but much less for other plants such as shrubs and sedges also present at our field sites (Arroyo-Mora et al., 2018; Hancock et al., 2018).

In the field data, the NDWI appears to have a closer relationship with SMD than the fWBI. Meingast et al. (2014), in contrast, found that the fWBI performed better than the NDWI in the field, although they used a hyperspectral formulation of NDWI rather than the broad-band formulation used in the current study. In the laboratory study, both *Sphagnum* species could be fitted with Gompertz functions, although the fit was better for *S. capillifolium*. We can therefore suggest that the NDWI is at least as useful as the fWBI in both the field and the laboratory experiments completed for this study.

4.4.2. GPP

The three best performing indices, the NDVI, EVI and Clm, are all based on the difference between the red and the NIR reflectance. The PRI has no connection to the red absorption band, and the SIPI only makes slight use of the wavelengths in this region.

The poor performance of the PRI contrasts with Van Gaalen et al.'s (2007) work, which indicated a good relationship between PRI and photosynthesis. However, their experiments were over much shorter timescales (minutes rather than weeks or months); PRI may therefore be effective in providing information about short-term changes in *Sphagnum* carbon flux, but not as useful in longer-term studies such as those involving satellite data. Harris (2008) agrees with the current work in finding that PRI has a poor correlation with photosynthetic efficiency pooled amongst different *Sphagnum* species. Harris (2008) suggested that this might be due to species-specific differences, which is supported by our findings that PRI has a more linear relationship with GPP changes in *S. capillifolium* than in *S. papillosum*. Interestingly, Van Gaalen et al. (2007) and Harris (2008) found most relationships between photosynthesis and PRI to be positive, whereas all significant relationships in this study were negative. This may be due to the time period over which measurements were taken; it is possible that the xanthophyll mechanism is also limited by prolonged drought. Another cause might be changes in the physical structure of the *Sphagnum* affecting light scattering and so disrupting the clarity of the wavelengths measured to calculate the PRI. Sims et al. (2006) found that the PRI relationship with light use efficiency changed dramatically at their Californian heathland study site during a severe drought year in comparison with wetter years. Cole et al. (2014) found that the PRI is very

sensitive to the differences between bryophytes, shrubs and graminoids, particularly in the summer months. This may explain why the field experiment showed little agreement between GPP and PRI on collars containing mixed vegetation, and therefore limits the usefulness of this index for estimating photosynthesis in the field.

Harris (2008) showed results from a laboratory study comparing photosynthetic efficiency (measured using chlorophyll fluorescence, Φ_{PSII}) of water limited *Sphagnum* mosses to spectral indices. In agreement with the current work, Harris' (2008) study found that the NDVI gave a strong positive correlation with the photosynthesis of all samples (0.68 Pearson's correlation). However, Harris (2008) found that SIPI gave a better correlation with pooled photosynthetic efficiency data from all samples (-0.76). In our study, the SIPI gave significant results in both the field and the laboratory, but the agreement with GPP was not as strong as the NDVI, EVI or CIm.

Letendre et al. (2008) also completed a field study comparing chamber carbon fluxes with spectral data from a handheld spectroradiometer but found that NDVI explained only 15% of the variation in GPP, whilst CIm explained 57%. Our study showed similar results for CIm, with GPP explaining 60% of the variance in CIm in the field (and 43% in the lab), but we showed much stronger relationships for NDVI than Letendre et al. (2008), with GPP explaining 49% of the variance in NDVI in the field (and 38% in the lab).

The two indices which make use of the difference between the red and NIR zones (NDVI and EVI), and the CIm that uses the red-edge, show good results for both the lab and field experiments, although the field relationship appeared to vary by time of year. The slope of the relationship between these three indices and GPP in the lab work was closest to the steeper slope seen in March in the field data, compared to the shallower slopes later in the season. The slope of the relationship for *Sphagnum*-dominated collars was also steeper than that of all collars combined, indicating that *Sphagnum* has a steeper slope of relationship between GPP and the red:NIR relationship than other (vascular) bog plants. As *Sphagnum* is a more dominant component of GPP in the field earlier in the year, before vascular plants have greened up/sprouted up, this would explain the steeper slope in March. This agrees with Whiting's, (1994) findings that *Sphagnum* may give unusually high NDVI values compared to other blanket bog vegetation, due to its higher NIR reflectance. There is therefore potential for these indices to be used to give an indication of the proportional presence of *Sphagnum* in certain areas. The difference in slopes at different times of the year could be compensated for in a model that uses NDVI or EVI by adding a seasonal component, or a temperature component, as seen in Lees et al. (in press). This method would allow a linear relationship between GPP and the vegetation index to be assumed, but

would reduce the unrealistically high values of GPP estimated in the colder months over peatland areas where *Sphagnum* is present

4.5. Conclusions

Both the water indices considered in this work had significant relationships with the moisture contents measured in the laboratory. There was a possible link with SMD in the field, but the temporal spread of the available data made the evidence inconclusive. Further studies into the correlation between SMD and water indices at peatland sites would be beneficial.

All vegetation indices tested in this study gave significant relationships with GPP in the laboratory and the field, although the PRI was clearly the least successful. The indices which focused on the difference between the red and NIR zones (NDVI and EVI), and the CIm which uses the red-edge, gave the best agreement with GPP in both the field and the laboratory. The slope of the laboratory indices, using only *Sphagnum,* were steeper than those from the field which include a variety of vegetation.

Overall, this study suggests that broad-band indices such as the NDWI, NDVI and EVI give good agreement with vegetation moisture content and GPP from the Forsinard Flows reserve. Therefore, we conclude that broad-band indices derived from freely available satellite data offer much potential to estimate moisture content and vegetation productivity of peatlands. This approach could be developed, with further testing, to allow cheap, widescale monitoring of peatland condition for biodiversity and climate regulation.

Acknowledgements

Thanks are due to the Forsinard Flows RSPB reserve (particularly Daniela Klein) for site access and access to facilities, and also to Chobham Common NNR for allowing us to collect a few *Sphagnum* samples for methods testing. Thanks to Kevin White and Suvarna Punalekar for spectroradiometer training. Thanks to Alison Wilkinson for making 48 collars for the fieldwork, and to Mike Lees for making 40 collars for the laboratory study.

We are very grateful for the help of our field assistants Ainoa Pravia, Jose van Paassen, Paul Gaffney, Wouter Konings, Elias Costa, Zsofi Csillag, Valeria Mazzola, David and Parissa Lumsden, and Joe Croft.

Funding

Kirsten Lees was part funded by a studentship from The James Hutton Institute, and part funded by the Natural Environment Research Council (NERC) SCENARIO DTP (Grant number: NE/L002566/1). Tristan Quaife was funded by the NERC National Centre for Earth Observation (NCEO). Myroslava Khomik and Rebekka Artz were funded by The Scottish

Government Strategic Research Programme 2016-2021. Ritson is supported by the Engineering and Physical Sciences Research Council Twenty-65 project [Grant number EP/N010124/1]. Much of the restoration work reported in this study was funded by EU LIFE, Peatland Action, HLF, and the RSPB.

5. Remote Sensing data suggests peat bogs undergoing restoration regain full photosynthesis capacity after five to ten years.

Lees KJ, Quaife T, Artz RRE, Khomik M, Sottocornola M, Kiely G, Hambley G, Hill T, Saunders M, Cowie NR , Ritson J & Clark JM

Abstract

Peatlands are an important part of the Earth's carbon cycle, comprising approximately one third of the global terrestrial carbon store. However, peatlands are sensitive to climatic change, atmospheric deposition, and human management, resulting in the degradation of many peatland ecosystems which causes them to act as a net carbon source. Restoration work is being undertaken at many sites around the world, but monitoring the success of these schemes can be difficult and costly using traditional field-based methods. A landscape-scale alternative is to use satellite data in order to assess the condition of peatlands and to estimate gaseous carbon fluxes. In this study we used Moderate Resolution Imaging Spectroradiometer (MODIS) products from 2004 to present, to model Gross Primary Productivity (GPP) over peatland sites at various stages of restoration, in order to develop a cost-effective way to monitor the impact of restoration progress on carbon fluxes. We found that the MOD17A2H GPP product overestimates GPP modelled from data collected by eddy covariance towers situated at two ex-forestry sites undergoing restoration towards blanket bog at the Forsinard Flows RSPB reserve, Scotland, UK (one full year of data), and a near-natural bog site in Glencar, Ireland (ten-year data series). We calibrated a Temperature and Greenness (TG) model for the Forsinard sites and found it to be more accurate than the MODIS GPP product at local scale. We also found that inclusion of a wetness factor using the Normalised Difference Water Index (NDWI) improved inter-annual accuracy of the model. This TGWa (annual Temperature, Greenness and Wetness) model was then applied to six control sites comprising near-natural bog across the reserve, and to six sites on which restoration began between 1998 and 2006. GPP from 2005-2016 was estimated for each site using the model. The resulting modelled trends are positive at all six restored sites, indicating a clear increase in GPP with time since restoration at sites in the Forsinard Flows reserve. The results suggest that the GPP of peatland sites at Forsinard Flows reserve undergoing restoration increases by approximately 5.5 g $C/m^2/yr$ every year since restoration began, and that they reach the carbon assimilation potential of near-natural bog sites between 5 to 10 years after restoration was begun.

5.1. Introduction

Peatlands are one of the most effective terrestrial ecosystems for the long-term sequestration of carbon (C), and as such are a key natural resource in combatting climate

change (Parish et al., 2008). Due to the unique vegetation composition and semi-permanently water-saturated state of pristine and near-natural peatlands, photosynthetic carbon uptake exceeds decomposition losses, and so a small fraction of the carbon taken up through photosynthesis is not lost to the atmosphere, but becomes a new layer of peat which can remain in the ecosystem for thousands of years (Yu, 2012; Rydin and Jeglum, 2013). Many peatlands in the British Isles, however, have experienced large scale degradation through land management schemes such as drainage, peat cutting, and commercial afforestation or agriculture (Holden et al., 2007). This means that landscapes which were once net carbon sinks are now emitting carbon into the atmosphere and water courses (Silvola et al., 1996; Worrall et al., 2011; Fleischer et al., 2016).

Restoration is being explored as a method to reduce carbon losses (in addition to recreation of lost peatland habitat), and ultimately encourage a return to net carbon uptake from once degraded peatlands (Minayeva et al., 2017). Recent studies have shown promising results, where rewetting has reduced carbon emissions from previously drained bog sites, restored vegetation communities, and improved resilience in the face of climatic change (Soini et al., 2009; Strack and Zuback, 2013; Urbanova et al., 2013; Beetz et al., 2013; Hancock et al., 2018; Smith et al., 2014). Because the water-saturated state of peatlands is very important to their function as a carbon store, raising the water table (known as rewetting) is a vital part of restoration (Andersen et al., 2017; Bonn et al., 2016; Minayeva et al., 2017; Parish et al., 2008; Parry et al., 2014). Methods to encourage rewetting include drain-blocking, tree or scrub felling, and in some cases surface landscaping of erosion gullies and re-seeding of bare peat (Parry et al., 2014). Peatland restoration is now being promoted by governments as a means of reaching carbon emission targets set in international agreements, and is included in the land use management section of the 2030 EU climate and energy framework (European Commission, 2018; IUCN, 2016). One of the indicators of successful peatland restoration is the re-establishment of peat-forming vegetation and subsequently an increase in photosynthesis and carbon uptake (known as Gross Primary Productivity, GPP).

Monitoring the effect of restoration on carbon fluxes over time is necessary for meaningful interpretation of the effectiveness of peatland restoration for delivering carbon emissions abatement, but such monitoring is often difficult and expensive (Andersen et al., 2017). Ground-based methods of measuring carbon include flux chambers and eddy-covariance (EC) towers, both of which require expensive equipment and regular monitoring, and only cover limited areas of land (Humphreys et al., 2006; Marushchak et al., 2013). Modelled carbon uptake using satellite data may be a useful means to upscale ground based methods, as satellite-based observations can provide regular data over large areas, and are often freely available (Chasmer et al., 2018; Lees et al., 2018). Eddy covariance data is often

sparsely available, giving estimates of carbon flux which are not replicated across the ecosystem and can only be assumed to represent the immediate area surrounding the tower (the footprint) (Hill et al., 2017). This is particularly challenging in peatlands, where fluxes are small and variable (Hambley et al., 2019). Satellite data could help to fill these gaps and increase the coverage of carbon flux estimates.

Models utilising satellite data have been used to estimate carbon fluxes over many ecosystems (eg. Desai et al., 2011; Quaife et al., 2008; Sims et al., 2008; Wu, 2012; Xiao et al., 2004; Yuan et al., 2010), but there has only been limited work done on peatland landscapes globally (Connolly et al., 2009; Gatis et al., 2017; Harris and Dash, 2011; Kross et al., 2013; Lees et al., 2018; Letendre et al., 2008; Schubert et al., 2010), and especially few studies that we are aware of on restored peatlands (Chasmer et al., 2018). Models known as Temperature and Greenness (TG) models have shown successes in matching GPP across a range of ecosystems (Lees et al., 2018), but have not previously been considered in peatland landscapes. These models use a vegetation index as a measure of greenness, and surface temperature as a modifier on light use efficiency.

This study uses data from the NASA Moderate Resolution Imaging Sensor (MODIS), as it has long archives of freely available data (1999 to present) which allows monitoring across peatlands undergoing restoration over many years. The satellites carrying MODIS also have a frequent return interval (imaging the same area every 1 to 2 days), and the system for processing the data and deriving data products is well established (Heinsch et al., 2006; Huete et al., 2002). MODIS provides data at coarse resolution (250 m to 1 km), which allows landscape scale (or similar to EC scale) monitoring across large areas of ecosystems such as blanket bog (peatland sustained by rainfall, Lindsay, 2010). The current work builds on the TG model developed by Sims et al.(2008), which combines the MODIS MOD13Q1 250 m vegetation indices product and the MOD11A2 1 km Land Surface Temperature (LST) product. This model was developed in a range of North American ecosystems including evergreen and deciduous forest, grassland and shrubland, but has not to our knowledge been tested on wetland or peatland sites. Considering the importance of water-saturation of peatlands in relation to the carbon flux, research is needed to evaluate whether a wetness factor needs to be included in the TG model for peatlands.

The objective of this work was to (a) evaluate the success of the TG model in estimating peat bog carbon uptake and whether an additional wetness factor is needed, and (b) to apply this model and an augmented version to evaluate changes in photosynthesis following restoration. Work is based on EC data collected at two sites undergoing restoration in the Forsinard Flows RSPB nature reserve in Scotland and the near-natural site at Glencar,

Ireland to enable assessment of the TG model's suitability at peatland sites of different condition, and across inter-annual time series.

5.2. Methods

5.2.1. Field sites

5.2.1.1. Forsinard Flows

The Forsinard Flows RSPB reserve, Northern Scotland (approx. 58.3585, -4.0409 to 58.4327, -3.6264, WGS84, see Figure 5.1), is the site of one of the largest scale peatland restoration programmes in the UK (Gaffney et al., 2018; Hambley, 2016; Hambley et al., 2019; Hancock et al., 2018; Hermans, 2018). Significant areas of what is the current reserve were planted with commercial forestry in the 1980s, and are now being felled and restored to rehabilitate the peatland ecosystem and associated hydrological, ecological and biochemical functions. The reserve comprises areas of near-natural bog which form part of the much larger Flow Country EU Natura site, protected under EU nature conservation law (Levy and Gray, 2015), areas of plantation forestry which will soon be felled, sites that were drained but never planted (and where drains were subsequently blocked), and finally forestry areas which have been felled and are undergoing restoration. The earliest fellings at the reserve were completed in the late 1990s (Hancock et al., 2018), and successive sites have been felled and/or had drains blocked in the years since, providing a useful chronosequence of restoration sites spanning 3,000 ha within the 21,000 ha reserve. The chronosequence makes this a unique and valuable location for studying the progress and success of restoration methods whilst minimising inter-annual variability due to meteorological factors.

The landscape was ploughed prior to planting creating distinct microtopographic features of plough throw and ridge with a small section of the 'original' surface still visible. The trees were planted in rows on the ridges created by the plough throw. Felling/restoration practices until the mid-2000s involved leaving most of the trees at the site and placing them in the furrows in an attempt to return nutrients to the soil, and to reduce drainage ('fell to waste', see Figure 5.1). Further restoration measures have been implemented since then, including (additional) brash mulching and furrow blocking, in order to speed up regeneration of the peatland vegetation and hydrological recovery.

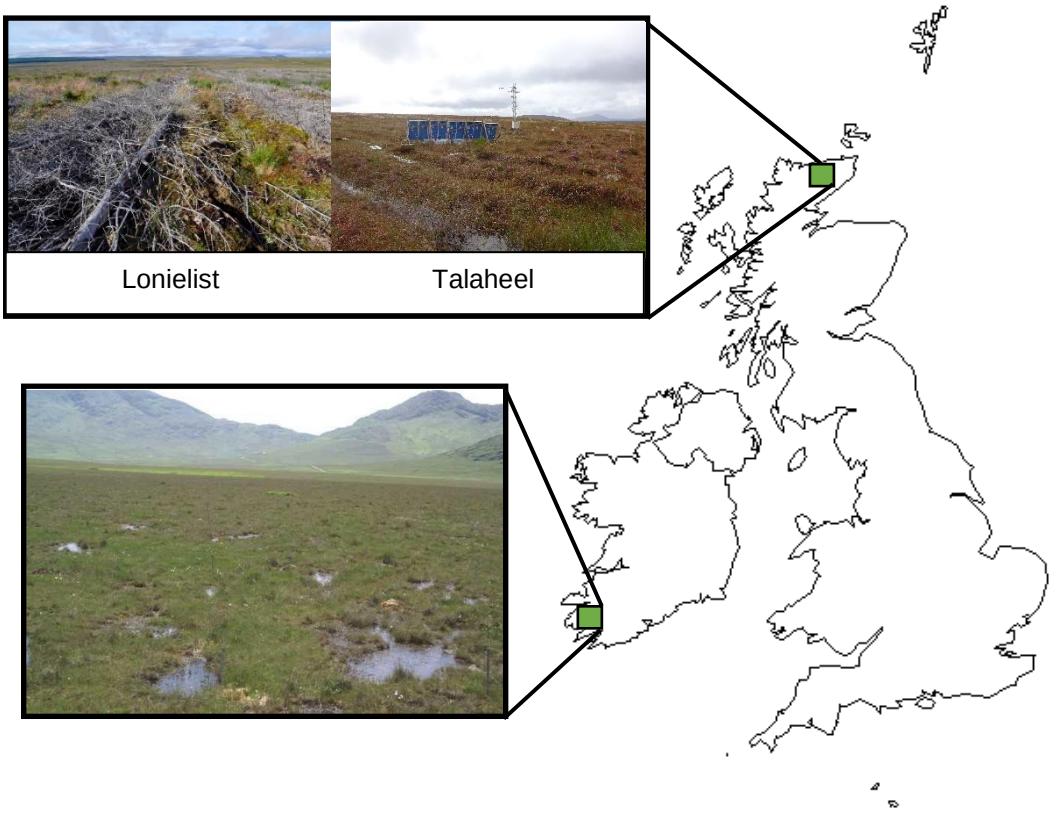

Figure 5.1 – Locations of the Forsinard Flows RSPB Reserve, Scotland, and the Glencar Bog site, Ireland. The Lonielist site image shows felled trees laid in former planting furrows (which acted as drainage ditches). The Talaheel site has had peat dams built in the former planting furrows, and the landscaping and vegetation growth have started to obscure the ridge and furrow topography.

This study uses data from eddy covariance towers at two sites in the Forsinard Flows Reserve which are undergoing restoration, Talaheel and Lonielist.

The Talaheel site is located on an area which was originally planted in 1985 and then felled to waste in 1998 (see Hambley et al., 2019.; Hancock et al., 2018, for further details of this site). The area immediately around the tower has been subject to additional management by furrow blocking in 2015/16. The tower is located at 58.4146, -3.8006 (WGS84), elevation 196 m.

A vegetation survey was completed in June 2017 on sixteen collars, each of 24 cm diameter, laid out in a cross pattern within the footprint of the tower (also see Hancock et al., 2018, for more detailed vegetation information at this site). The dominant species at Talaheel are *Pleurozium schreberi* (red-stemmed feather moss, 23.6%), *Eriophorum angustifolium* (common cotton grass, 17.9%), *Sphagnum capillifolium* (16.7%), and *Cladonia portentosa* (reindeer lichen, 17.6%). There is also significant presence (1 to 5%) of *Calluna vulgaris* (common heather), *Erica tetralix* (cross-leaved heath), *Trichophorum germanicum* (deer

grass), *Molinia caerulea* (purple moor grass), *Polytrichum commune* (haircap moss), and *Dicranum scoparium.*

The Lonielist site was planted 1985-1990 and felled to waste in 2003/04, with no further management within the timelines of this study (-end of 2017). The tower is located at 58.3910, -3.7651 (WGS84), elevation 180 m. A vegetation survey in June 2017 (completed in the same manner as described at Talaheel, above) showed that the dominant species at Lonielist are *Polytrichum commune* (haircap moss, 21.6%), *Sphagnum capillifolium* (19.9%), *Cladonia portentosa* (reindeer lichen, 12.8%), *Pleurozium schreberi* (red-stemmed feather moss, 12.3%) and *Eriophorum angustifolium* (common cotton grass, 10.9%). There are also significant amounts (1 to 10%) of *Calluna vulgaris* (common heather), *Molinia caerulea* (purple moor grass), *Narthecium ossifragum* (Bog asphodel), and *Aulacominum palustre*.

Both sites within the Forsinard Flows RSPB nature reserve are subject to grazing by red deer (*Cervus elephantus*). Talaheel is fenced as part of a larger enclosure including some forestry, although some deer are present inside the fence, whilst Lonielist is entirely open to grazing.

The Altnaharra meteorological station approximately 35 km south-west of the Forsinard Flows reserve has been used to characterise the meteorology of the site. At the Altnaharra station the annual rainfall average is 1196 mm over 196 days, and the average high/low temperature ranges from 17.8/9.7˚C in July to 6.1/-1.3˚C in December (Met Office, 2018).

5.2.1.2. Glencar

Glencar is an area of Atlantic blanket bog in South-West Ireland (see Figure 5.1), where an EC tower recorded carbon dioxide fluxes for a ten year period (2002-2012), one of the longest EC records on peatland (Koehler et al., 2011; Mcveigh et al., 2014). As the climate, proximity to the coast, and peatland type of this blanket bog area are similar to the conditions found at the Forsinard Flows Reserve, it is considered a comparable site. At the Valentia meteorological station approximately 30 km west of Glencar the annual rainfall average is 1430 mm over 239 rain days (Sottocornola and Kiely, 2010a). The average monthly temperature at Valentia ranges from 14.8˚C in August to 6.6˚C in February (Sottocornola and Kiely, 2010a).

This site has been included in the model development phase of this study as it provides a long time series to test the inter-annual accuracy of the TG model. Glencar has been subjected to peat cutting in the past, but only outside the EC footprint area. 25% of the surface near the Glencar EC tower is *Sphagnum* covered, and the most abundant vascular species are *Molinia caerulea, Calluna vulgaris, Erica tetralix* and *Narthecium ossifragum*

(Sottocornola et al., 2009). The EC tower is located at 51.9166, -9.9166 (WGS84), site elevation 150 m.

5.2.2. Ground-based GPP measurements: Eddy Covariance

Net ecosystem CO_2 exchange (NEE) at Lonielist was measured using a LICOR 7200 enclosed CO_2/H_20 (water) gas analyser (LI-COR Biosciences Inc. Lincoln, NE, USA), and a Gill HS-50 3-D sonic anemometer (Gill Instruments, Lymington, UK). The data period at Lonielist is from June 2014 to June 2015.

At Talaheel, NEE was measured using the LICOR 7500A open path CO_2/H_20 gas analyser (LI-COR Biosciences Inc. Lincoln, NE, USA) with a custom enclosure added to the analyser to create an enclosed system (Clement et al., 2009), and a CSAT sonic anemometer (Campbell Scientific, Logan, USA). The data period at Talaheel is from March 2014 to April 2015.

At Lonielist NEE was then partitioned into GPP and ecosystem respiration (Reco) using the EddyPro® (Version 5) (2014 Lincoln, NE. LI-COR Inc.; Infrastructure for Measurements of the European Carbon Cycle consortium). At Talaheel EdiRe software (University of Edinburgh, Edinburgh, UK) was used due to the combination of monitoring systems. Post-processing and gap-filling at Lonielist and Talaheel are explained in Hambley et al. (2019), and the nocturnal partitioning approach was used. The vast majority (90%) of the footprint of the Lonielist and Talaheel towers has been shown to originate from an area within 350m and 380m of the towers respectively (Hambley, 2016).

The tower at Glencar has a LICOR LI-7500 and a sonic anemometer (81000, R.M. Young Company, Minnesota, USA for the first 5 years; then a CSAT3; Campbell Scientific, Utah, USA; (Sottocornola and Kiely, 2010b, 2010a). Sottocornola and Kiely (2010a) calculated that the tower has a typical fetch of 300 m during the day and 750 m at night. The data period at Glencar is from September 2002 to October 2012. Post-processing and gap-filling at Glencar is explained in Mcveigh et al. (2014). Partitioning into GPP and respiration was done using a respiration model based on the relationship to temperature of night-time fluxes (McVeigh et al., 2014).

For comparison with the MOD17A2H product and the TG model, EC GPP data from all sites in umol/m^2/s was averaged over 8-day periods, then converted to g C/m^2/hr and multiplied up to give g C/m^2/day.

5.2.3. Applying the model to the restoration sequence

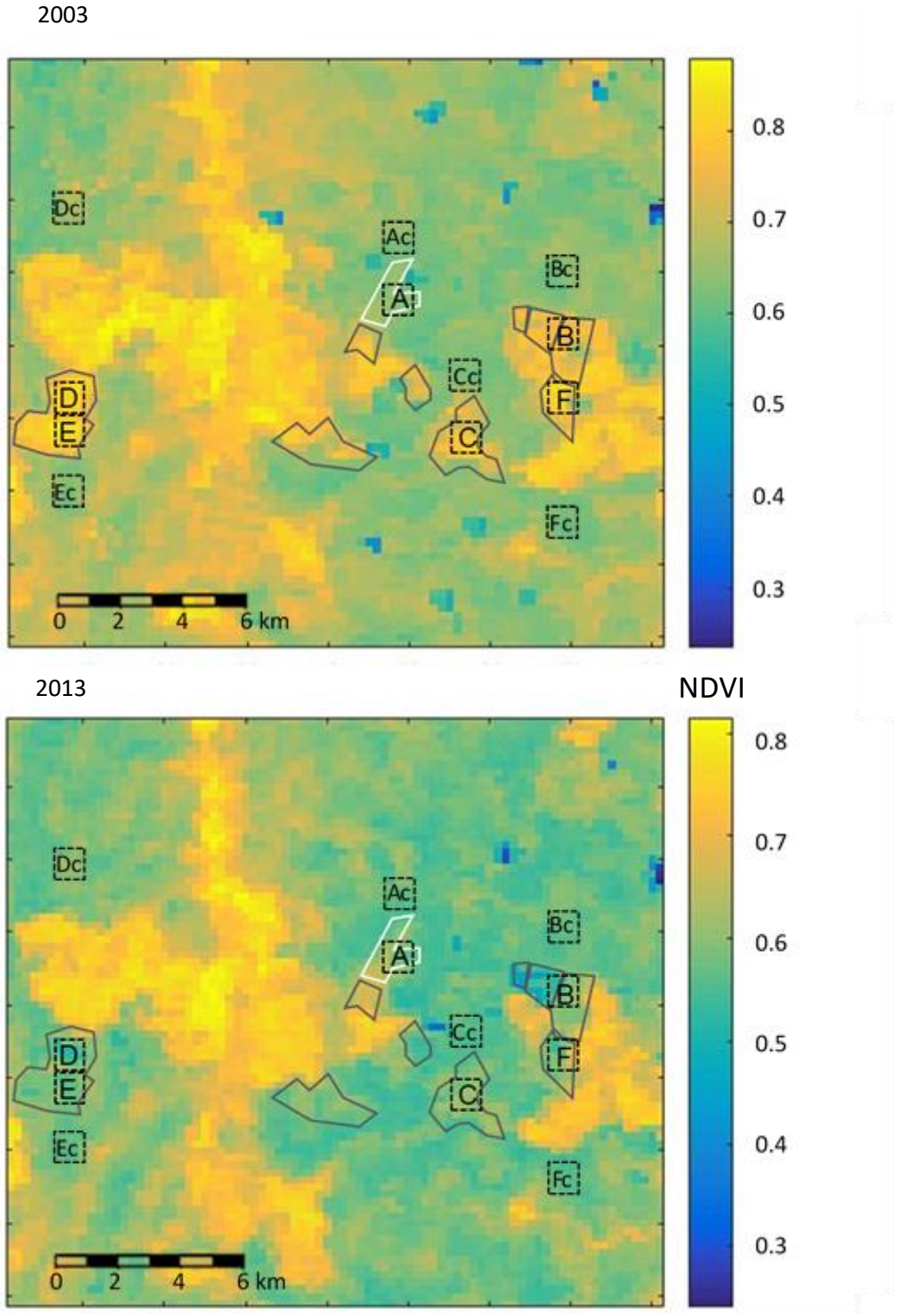

Figure 5.2 – MODIS NDVI images (250 m) of the Forsinard Flows reserve in 2003 (top) and 2013 (bottom). Grey outlines indicate areas which were felled in the period 2003-2013, whilst the white outline indicates the Talaheel area which was felled in 1998. The drop in NDVI after felling is easily visible (very high NDVI areas are largely standing forestry). The black

boxes are equivalent to 1 km MODIS pixels and show the selected sites A to F, and the control sites Ac to Fc.

In order to assess the photosynthetic recovery of the peat bog after felling and restoration, six restored sites were selected across the Forsinard Flows reserve (see Figure 5.2). The selection criteria required that there was an area of at least 1 km (the size and shape of MOD11A2 pixels) of purely restored peatland, with no large areas of near-natural bog or remaining forestry included. The sites selected were labelled A-F (see Table 5.1). The six sites selected for this project were felled and collector drains blocked, in initial efforts to restore peatland habitat, in different years from 1998 to 2006, and most have since undergone further restoration procedures. GPP was estimated using remote sensing data for each of these sites for the years 2005 (for those sites where felling had been completed by that time) to 2016.

Table 5.1 – selected restored sites, the coordinates each site is centred on (one MODIS pixel used at each site), and the period in which felling took place. Years since felling are given including the first full year after felling was completed, up to and including 2016.

Site label	**Coordinates (WGS84) and elevation (m)**	**Felling year(s)**	**Years since felling (to 2016)**
A	58.415, -3.8057, 180	1998	18
B	58.4093, -3.7211, 178	2003-04	12
C	58.3843, -3.7703, 175	2003-05	13
D	58.3918, -3.9586, 163	2004-06	10
E	58.3841, -3.9581, 193	2004-06	10
F	58.3914, -3.7208, 178	2006-07	9

Control pixels were selected from the same longitude as the restored sites (as there is a possibility of an east-west gradient in wetness (Perry and Hollis, 2005) and GPP) and a maximum difference in elevation of 50 m, containing only near-natural peatland. These are given the same codes as the restored sites, but with a small c to indicate control (Ac, Bc, Cc, Dc, Ec, Fc, see Figure 5.2). The control sites Ac, Bc and Fc are unfenced, unlike their corresponding treatment sites. This may mean that they are subject to some additional grazing from red deer, although some deer are also present within the fenced areas (Hancock et al., 2018). The model was applied to each control site for the same years as the sites undergoing restoration.

The annual result from each restored site was subtracted from the corresponding control site result for the same year. This was designed to control for factors other than management affecting GPP, such as weather conditions and atmospheric deposition.

5.3. Model development

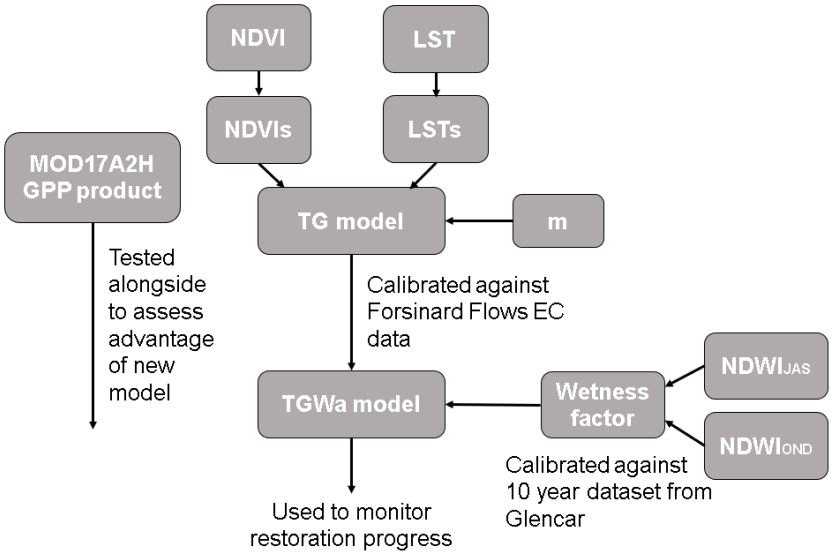

Figure 5.3 - Flow chart showing the process of developing the TGWa model.

5.3.1. Satellite based GPP modelled data: MOD17A2H

The MOD17A2H 500 m GPP product is ready calculated and easily available (Running et al., 2015); it is therefore considered in this study as a standard measure for estimating global GPP (see Figure 5.3). We expect the TG model to be an improvement on estimating photosynthesis at peatland sites over MOD17A2H, in part because of its local calibration. Our research tests the MOD17A2H GPP product by comparing it to EC GPP.

MOD17A2H GPP is calculated using the Light Use Efficiency (LUE) approach developed by Monteith, (1977), which is given as:

$$GPP = \varepsilon \times PAR \times fPAR \qquad (1)$$

Where ε is the LUE term, which gives the conversion efficiency of absorbed energy to fixed carbon in kg C/MJ, PAR is photosynthetically active radiation in W/m^2, and *f*PAR is the fraction of photosynthetically active radiation absorbed by vegetation. In MOD17A2H ε is calculated from a value of εmax, specified for each ecosystem type identified in the MODIS land classification product MOD12Q1, and limited by Vapour Pressure Deficit (VPD, in Pascals) and minimum temperature (˚C), both of which are taken from NASA Global Meteorological Assimilation Office (GMAO) data (Heinsch et al., 2006; Running and Zhao,

2015). PAR data is also taken from NASA/GMAO, and *f*PAR is obtained from the MODIS Leaf Area Index (LAI) product, MOD15 (Running and Zhao, 2015). MOD12Q1 land cover classifications do not include a peatland class, so peatland areas are classified by the algorithm as other land use types. MOD17A2H products are given as 8-day totals of GPP at 500 m resolution.

5.3.2. MODIS data processing

MOD17A2H for the same time periods as the Talaheel, Lonielist and Glencar EC data was downloaded using the AppEEARS service (https://lpdaacsvc.cr.usgs.gov/appeears/). The 250 m MOD13Q1 vegetation indices product (Didan, 2015) and the 1 km MOD11A2 LST product (Wan et al., 2015) were downloaded using the MODIS ORNL web service through Matlab code (see Appendix C) (Santhana Vannan et al., 2009). All MODIS products used were version 6.

Cloud filtering was applied to all MODIS products to remove images extensively affected by cloud cover, whilst letting though data which was affected by clouds but still useable. Each of the MODIS products contains information about the quality of the data in each pixel, and this was used to select which 8-day or 16-day pixels were useable. For the MOD17A2H product, the quality control data was used to remove pixels with significant cloud cover. MOD13Q1 pixel reliability index was used to remove snow/ice or cloud affected values. MOD11A2 quality control data was used to remove periods when data was not produced due to cloud effects or other issues. MOD09A1 surface reflectance state data was used to remove any pixels affected by significant cloud. Gap-filling was then performed across each year using the techniques described by Wang et al. (2012).

5.3.3. Adapting the Sims et al. (2008) TG model to estimate GPP over peatlands

Previous studies have shown that TG models give good results for GPP (when compared with measures of ground-based carbon flux estimation such as EC) across a range of ecosystems (Moore et al., 2013; Sims et al., 2008; Verma et al., 2015). Such models combine a measure of greenness, calculated from a vegetation index, with a measure of temperature. In this study we build on the TG model developed by Sims et al. (2008) which uses MODIS data products to give an estimate of average daily GPP in time steps matching the 16-day MODIS product period.

The TG model used by Sims et al. (2008) can be written as (Moore et al., 2013):

$$GPP = EVIs \times LSTs \times m \quad (2)$$

$$EVIs = EVI - 0.1 \quad (3)$$

$$LSTs = \min[(LST-minLST)/(optLST-minLST), (maxLST-LST)/(maxLST-optLST)] \quad (4)$$

Where EVIs is the scaled Enhanced Vegetation Index and LSTs is the scaled Land Surface Temperature (see Sims et al., 2008). minLST, optLST and maxLST (given in ˚C) are the minimum, optimum and maximum Land Surface Temperature for GPP calculated for an ecosystem from past data. 'm' is a site-optimisation parameter used to fit the model outputs more closely to the units of flux measurement.

Two vegetation indexes which are often used in remote sensing GPP models, and which are available from MODIS product MOD13Q1, are the Normalised Difference Vegetation Index (NDVI) and the EVI. The NDVI is calculated from the difference between reflectance in red wavelengths of light, which plants absorb strongly, and the near-infrared (NIR), which plants reflect much more strongly than the red. The EVI uses the same principle but has generally lower values to compensate for the saturation effect sometimes seen in the NDVI at high LAI values, and includes reflectance at blue wavelengths to minimise the impact of scattering by atmospheric aerosols (Huete et al., 2002; Lees et al., 2018)

MOD13Q1 250 m datasets for NDVI and EVI, and MOD11A2 1 km daytime and night-time Land Surface Temperature (LST) were downloaded and tested in the TG model. Temperature values from MODIS are given in averages for 8-day periods, whilst vegetation indexes are given in 16-day periods. We found that NDVI gave a better relationship than EVI with the GPP data from both sites, and EVI was therefore replaced with NDVI in the model.

As the values given by Sims et al. (2008) and Moore et al. (2013) are likely not applicable to peat bogs, we used the data from Talaheel and Lonielist to calculate the minimum, maximum and optimum LST for GPP (see Figure 5.3). Maximum LST is the temperature above which photosynthesis can no longer occur. As our data did not include extreme heat events, we were unable to calculate the exact value of maxLST, and so we have used 40˚C. The optimum LST is the temperature at which the ecosystem reaches maximum photosynthesis. We have used 25˚C for optLST, as this is the highest temperature and greatest GPP reached at both sites during the period of available EC data (the true optimum may be higher but the data is not available). Minimum LST is the temperature below which photosynthesis no longer occurs. minLST was calculated using the linear regression models for both sets of data, giving Lonielist minLST as -3.22˚C and Talaheel as -1.26˚C (-2.5˚C was therefore used for the work described in Section 5.2.4).

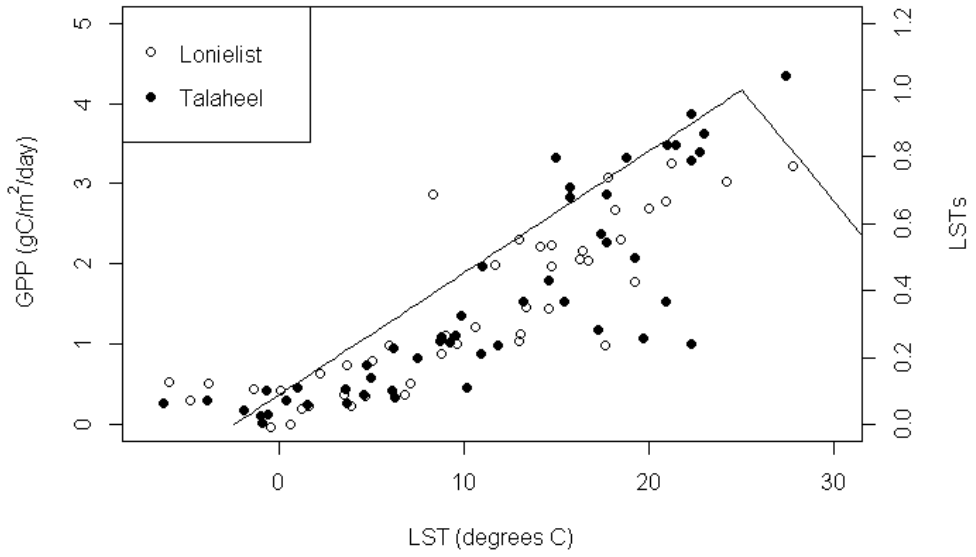

Figure 5.4 –The response of GPP (from EC data) to LST (from MOD11A2) for the Lonielist and Talaheel sites. The black line shows the minimum (-2.5˚C) and optimum (25˚C) following the explanation of the LST scaling algorithm given in Sims et al. (2008).

The original Sims et al. (2008) model gives the calculation for the 'm' parameter using the annual night-time LST (LSTan) with a linear model based on Plant Functional Types (PFT), but only includes deciduous and coniferous forests and not blanket peatlands. Hence, we consider the LSTan with a linear model optimised to Glencar, and also using a single optimised 'm' parameter. Glencar was used for this part of the study rather than the Forisnard sites as it has a multi-year data series. The GRG Nonlinear Solver in Microsoft Office Excel 2013 was used to optimise the 'm' parameter in all cases (this was done separately for the two Forsinard sites and the Glencar site). The results showed an R^2 value of 0.63 for the model using an 'm' parameter calculated from LSTan, compared to a value of 0.68 for the model with a single optimised 'm' parameter. It was therefore decided to use a single optimised 'm' parameter for this study.

The optimum 'm' value was found to be 5.875 at both Lonielist and Talaheel (m = 5.875 was therefore used for the work in Section 5.2.4, see Figure 5.3). The response of GPP to 'm' is linear, so a 10% change in m causes a corresponding 10% change in the GPP value.

The MOD17A2H product and the results from the fitted TG model are compared against the Lonielist and Talaheel EC data in Figure 5.4. It is clear from the graphs in Figure 5.4 that MOD17A2H overestimates GPP, whereas the TG model results have a much better fit with the EC data at both sites. The TG model RMSE (root mean squared error) is 0.50 g

C/m^2/day for Lonielist and 0.54 g C/m^2/day for Talaheel, compared to the MOD17A2 RMSE values of 1.33 g C/m^2/day and 1.10 g C/m^2/day respectively.

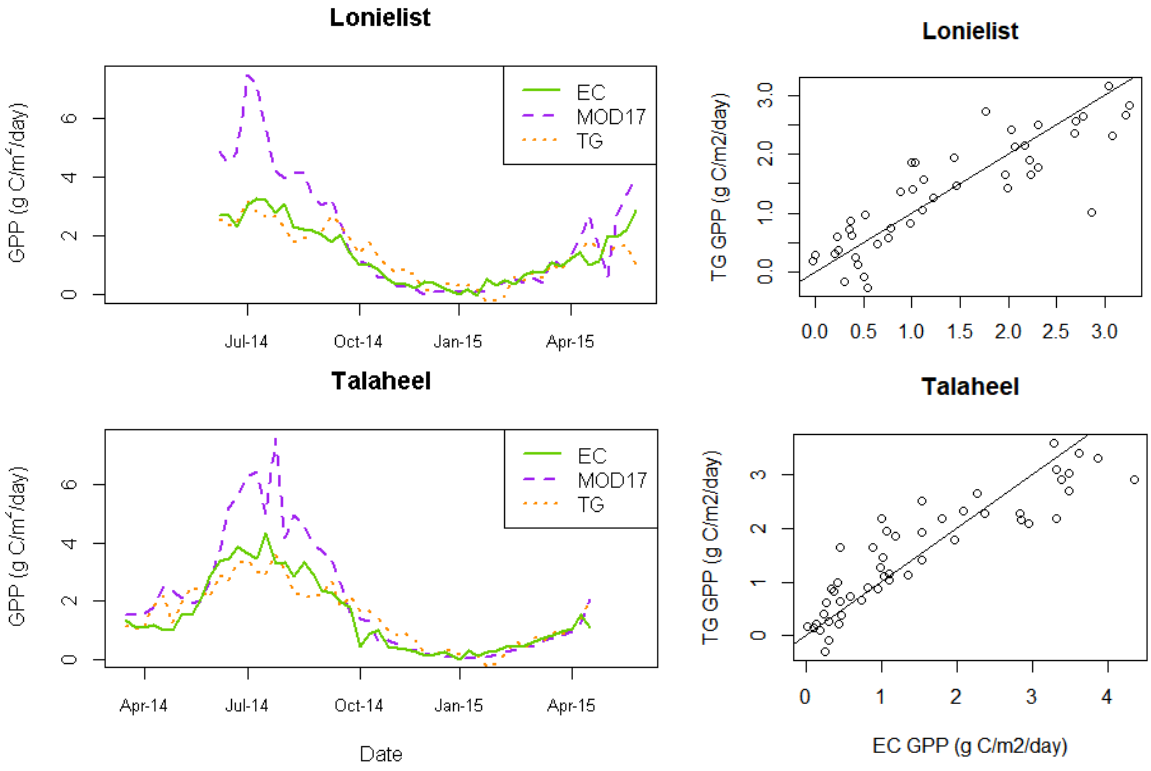

Figure 5.5 – Graphs showing Lonielist (top left) and Talaheel (bottom left) EC GPP plotted against the MOD17A2H product and the results of the TG model optimised to the EC data. Also graphs showing the TG model results plotted directly against the EC data for Lonielist (top right) and Talaheel (bottom right), with a 1:1 line plotted.

5.3.4. Inter-annual accuracy of the model and a water component

Using the Glencar data, 'm' was calibrated to the data from 2011 only, in order to test the inter-annual reliability of the parameter with only one year of data, using the Microsoft Office Excel 2013 GRG Nonlinear Solver, with the resulting optimum 'm' parameter being 3.75. The model with this value for 'm' was then applied to the whole data series from 2002-2012. The total annual GPP for each year was calculated using the summed data from the EC tower and the model estimates.

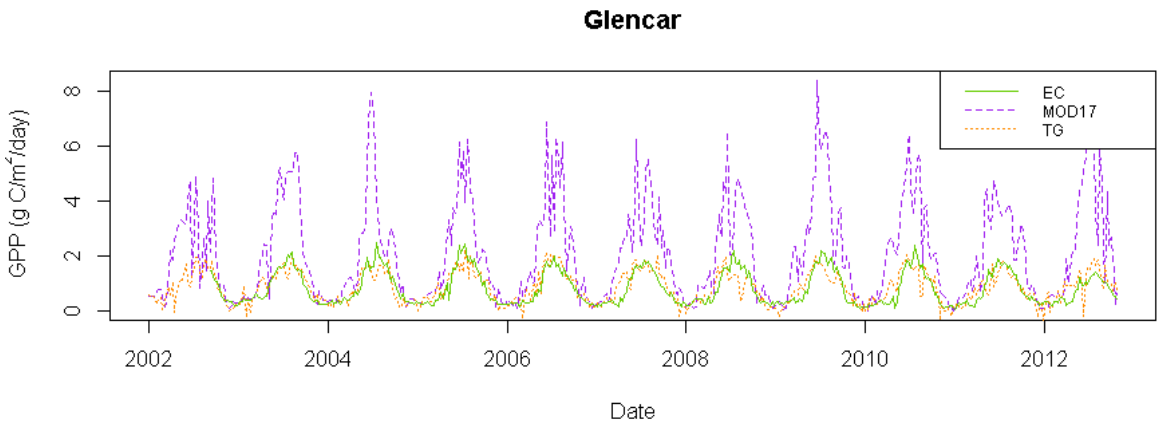

Figure 5.6 – Glencar EC data plotted with MOD17A2H product, and the TG model results with m optimised to the 2011 EC data.

Table 5.2 – The annual EC GPP totals from Glencar compared to the results from the TG model and the MOD17A2H product. All given in g C/m^2/yr.

	EC	**TG**	**MOD17A2H**
2003	316.0	341.3	808.6
2004	321.8	286.5	714.6
2005	326.2	324.4	741.5
2006	279.6	333.8	734.3
2007	287.9	347.6	793.4
2008	295.8	271.6	693.6
2009	301.7	295.9	873.7
2010	273.7	291.5	793.4
2011	288.1	275.4	729.5
Average	299.0	307.6	764.7

The average annual GPP value for Glencar across the ten year period (given by the TG model with m optimised to 2011) is 308 g C/m^2/yr, very close to the average annual GPP from the EC data of 299 g C/m^2/yr (see Table 5.2). The MOD17A2H average by contrast is 765 g C/m^2/yr, more than double the EC value. The MOD17A2H results greatly overestimate EC GPP in every year of the dataset. Overall there was a very good match between the EC GPP and the TG model GPP across the ten year Glencar data series (see Figure 5.5 and Table 5.2).

However, the TG model does not perform as well on inter-annual accuracy as it does on intra-annual accuracy. The average difference between the model annual GPP (parameter m optimised to the 2011 data only) and the EC annual GPP ranges between 1.85 g C/m^2/yr

(in 2005) and 59.69 g C/m^2/yr (in 2006), with an average difference of 26.30 g C/m^2/yr (an 8.8% error). There is very little correlation between the annual GPP values from the EC data and the TG model (0.10, Pearson's correlation).

As this study aims to use the model to assess long term trends, the current model comprising only LST and NDVI does not have a good enough annual correlation with EC data to give reliable results. It was considered that the wetness of the site may have an effect on inter-annual GPP variation, following Kross et al. (2016) who suggest that wetness has more effect on inter-annual variation in peatland ecosystems, compared to NDVI and air temperature which are more important for monthly variation.

In order to test whether wetness might be the missing factor in inter-annual variation, the Normalised Difference Water Index (NDWI) was considered as a proxy for site wetness (Lees et al., 2018; Letendre et al., 2008). The NDWI is calculated from the MOD09A1 500 m band 2 (NIR) and band 6 (Short-Wave Infra-Red, SWIR) (Vermote, 2015) using the formula (Gao, 1996):

NDWI = (NIR - SWIR) / (NIR + SWIR) (5)

A small negative Pearson's correlation (-0.25) between annual EC GPP and average annual NDWI was found at Glencar. However, when NDWI is split seasonally the correlations become more complex. The NDWI values were summed in three-month groups, beginning with January, named $NDWI_{JFM}$, $NDWI_{AMJ}$, $NDWI_{JAS}$, and $NDWI_{OND}$. Using this method there is a negative Pearson's correlation between the previous autumn/winter NDWI and annual GPP (-0.64 with previous $NDWI_{OND}$, -0.48 with $NDWI_{JFM}$ at start of year). Spring and summer NDWI show positive correlations with annual EC GPP (0.51 $NDWI_{AMJ}$ and 0.44 $NDWI_{JAS}$). This may suggest that higher water levels in the colder months of autumn, winter and early spring can impede plant photosynthesis, whereas high water levels in the growing season can encourage it.

In order to apply this knowledge to the TG model, several formulations were tested against the EC data from Glencar. Due to the parameterisation of the model and the annual nature of the NDWI parameters being tested, it was decided to fit the summed annual TG model results (TGa) to the summed annual EC data from Glencar, rather than daily values. The TGa model already includes NDVI and LST data, and the tested model formulations simply add seasonal NDWI as a factor into the annual model.

The equations were tested using leave-one-out cross validation to fit optimising 'a' and 'b' parameters, and the model with the lowest average difference to EC data and highest correlation was selected.

The final annual model had an adjusted R-squared value of 0.5 (p-value 0.02), and average annual difference to the EC data of 12.4 g C/m^2/yr. This can be compared to the TGa model with no NDWI factor (but still optimised with 'a' and 'b' parameters) which had an adjusted r-squared value of -0.13 (p-value 0.8) and an average annual difference of 19.1 g C/m^2/yr.

The final model includes both summer and winter NDWI, and the equation is given as:

$$TGWa = TGa \times (1\text{-}NDWI_{OND}) \times NDWI_{JAS} \times a + b \qquad (6)$$

Where 'a' is 2.34 and 'b' is 212.86. This is referred to as the annual Temperature, Greenness & Wetness (TGWa) model hereafter (see Figure 5.3). Figure 5.6 gives a visual illustration of the improvement on annual fit given by the TGWa model compared to the initial TG model.

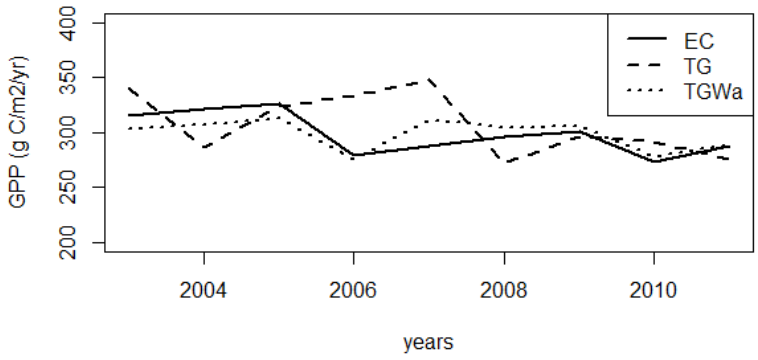

Figure 5.7 – The annual EC GPP values from Glencar, plotted against the summed annual results from the TG model and the TGWa model.

The model applied to the six selected restored sites (and control sites) is therefore the TGWa model, which includes the sum of values from the TG model comprising NDVI, LST, and the 'm' parameter optimised to Lonielist and Talaheel, and the summer and winter NDWI, and the 'a' and 'b' parameters optimised to the multi-year dataset from Glencar.

5.4. Restoration results

The trend in the restored sites (after using the control sites to minimise effects from factors other than management) shows an increase in GPP as restoration progresses, from an average of 270 g C/m^2/yr one year after felling to 337 g C/m^2/yr eight years after felling. Figure 5.7 shows the change in the annual GPP of each of the restored sites over a ten year period (2005-2015), plotted to demonstrate the change against years after felling was completed. The control sites' annual GPP was used as the zero mark.

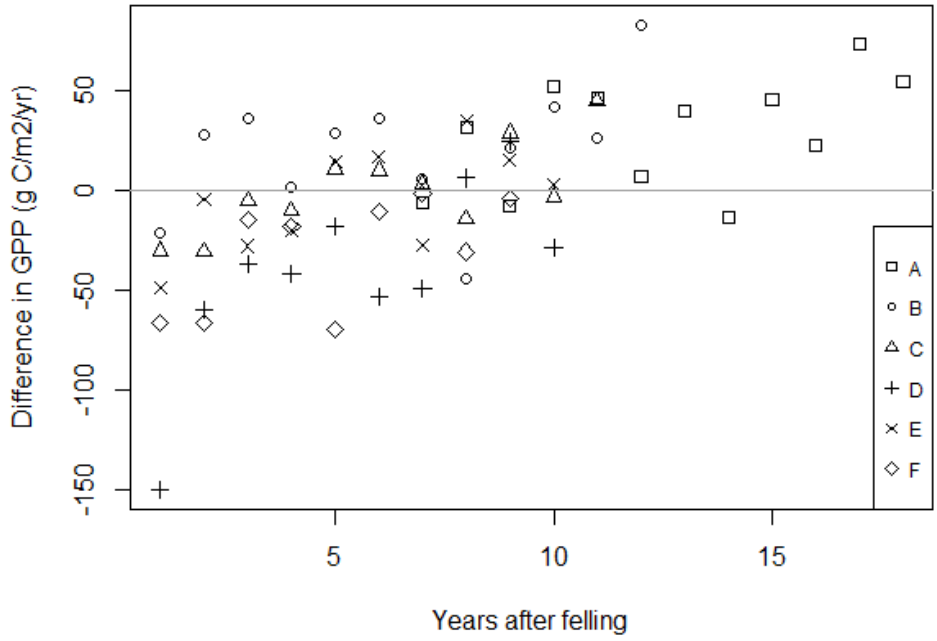

Figure 5.8 – Difference in TGWa model estimates of annual GPP compared to control sites in the years after felling for the six restored sites A to F at Forsinard Flows Reserve. Details of felling dates for each site can be found in Table 5.1. The grey line shows the zero point, ie. the control site GPP.

Table 5.3 shows the equations for the linear regression models of the sites' relationships between time and modelled annual photosynthesis over the 1 to 18 years period. The p-values suggest that sites C, D and E have trends significant at the 95% level. The general linear model for all sites is significant at the 99% level, and crosses the zero line at 7.2 years. Note that the GPP of the oldest sites, site A in particular, appears to increase above the zero line, suggesting that it has a higher GPP than the control sites.

The slope of the linear models gives the estimated year-to-year increase in photosynthesis at each site (Table 5.3), suggesting that the average increase is approximately 5.5 g C/m^2/yr (or 7.3 g C/m^2/yr for the average slope of C to E) every year after felling (within the time frame of this work, which mainly covers the earlier years post restoration).

Table 5.3 – linear models for each of the six selected restored sites. Sites C to E have trends significant at the 95% level. The final column shows the result when the equations are solved for a 'y' value of zero, i.e. the number of years before the site reaches the photosynthesis level of its paired control site. The 'All' row represents a general linear model which was fitted with site as a factor. Interactions were tested but were excluded from the

final model (all interactions were non-significant with the exception of site D which had a barely significant interaction with years p=0.045).

Site	Slope	Intercept	p-value	Adjusted R-squared	Years
A	3.77	-18.15	0.11	0.15	4.8
B	3.58	-2.82	0.2	0.07	0.8
C	5.23	-30.97	0.0076*	0.52	5.9
D	11.21	-102.38	0.018*	0.46	9.1
E	5.44	-34.26	0.049*	0.33	6.3
F	6.5	-63.92	0.069	0.31	9.8
All	5.46	-39.25	<0.001*	0.56	7.2

5.5. Discussion

5.5.1. Model accuracy

It is clear that the MOD17A2H product poorly estimates EC GPP at the peatland sites (see Section 5.3). MOD17A2H overestimates peatland GPP at all sites considered in this study, but especially at Glencar where the MOD17A2H average annual GPP is more than double the average determined from the EC tower. Kross et al. (2013) also found that the MODIS GPP product had poor agreement with EC data over their peatland sites in Canada and Finland, although their results showed underestimation. This poor relationship between the MOD17A2H product and the EC data may be due to the misclassification of land cover type by the MODIS products (Heinsch et al., 2006). MOD12Q1, the land cover product, is used to prescribe εmax (maximum light use efficiency) in the MOD17A2H equation (Running and Zhao, 2015), and a misclassification could cause either a higher or lower emax value than the actual, and therefore give an over- or under-estimation (Tan et al., 2012). Kross et al. (2013) found that MODIS misclassified their peatland sites as evergreen needle forest for two sites, mixed forest for a third, and closed shrubland for the fourth. They would therefore expect an overestimation, but in fact their results showed an underestimation, and they suggest that the MODIS downscaling algorithm is inappropriate for peatlands (Kross et al., 2013). All three sites used as ground validation in this study (Lonielist, Talaheel and Glencar) were classified as closed shrubland in most years by MODIS, although in some years they were classified as open shrubland or mixed forest. The much larger error in the MOD17A2H results for Glencar is therefore unlikely to be caused by the limited land cover classification product, as the two Forsinard Flows reserve sites have the same classification but much smaller errors. Gatis et al. (2017) also found that the MODIS GPP product underestimated chamber flux data at their study site in Exmoor, England, and suggested that this may be due to the assumptions the MODIS GPP algorithm makes about water

availability effects, which are not necessarily applicable to peatlands. A larger study into the differences between MOD17A2H and EC or chamber data over peatland sites would be beneficial in identifying which part of the MODIS algorithm is problematic in peatland landscapes.

The TG and TGWa models give results which have a much better agreement with the EC data, perhaps partially because they do not rely on any land cover classification system or prior assumptions of any values. The TG model's use of a locally calibrated 'm' parameter also explains why the results are closer to the EC data than the MOD17A2H product. Future work is needed to assess the variation in local calibration within such models across a variety of Northern peat bog sites, and test whether calibrating globally would still provide better results than the MOD17A2H product.

It is surprising that model designs using the NDVI performed better than those using the EVI. It may be the case that the generally low LAI of blanket bog, consisting only of a low canopy of bryophytes and some vascular plants, may mean that the saturation limitation effects of the EVI are unnecessary. Schubert et al. (2010) found that NDVI did saturate over peatlands and that EVI gave a better correlation with EC data from their sites in Sweden. However, the vegetation of their sites included dwarf pines (*Pinus sylvestris*) and a high proportion of dwarf shrubs and sedges, which may give a higher LAI in comparison to the sites used in this study (Schubert et al., 2010). It may also be the case, as some authors have suggested (Huete et al., 2002; Rossini et al., 2012) that the EVI is more sensitive to near-infrared (NIR) and is therefore a more structural measure, whereas the NDVI is more a measure of plant greenness and chlorophyll as it is more sensitive to the red bands. Also, it is worth noting that the restored sites at Forsinard have a large amount of dead plant (felling brash/logging slash) matter, due to the fell to waste restoration method used at these earlier restoration sites, which has a strong NIR signal and may therefore distort the EVI results. Chasmer et al. (2018) also found a good relationship between NDVI and GPP over restored peatland sites in Canada, but they did not test EVI.

Adding the NDWI to the model on an annual basis greatly improves the inter-annual fit of the model with the Glencar EC data. Letendre et al. (2008) found that combining a water index with the NDVI gave a better agreement with flux chamber NEE values at their study site than the NDVI alone. Although Letendre et al. (2008) used a different formulation of water index focusing on the absorption trough at 950-970 nm, their work agrees with this study's findings that adding a measure of wetness can improve estimates of carbon uptake over peatlands.

The common understanding is that a high NDWI, indicating plenty of moisture in the vegetation, will correlate with a high GPP (Nijp et al., 2014; Schipperges and Rydin, 1998;

Sottocornola and Kiely, 2010b; Strack and Price, 2009). This is the case with the summer NDWI in this study, during July to September, when peatland vegetation is likely to be limited by water availability and by a lack of nutrients which are mostly gained from rainfall. In contrast, this work found a negative correlation between winter NDWI and annual GPP. This may be partly explained by the fact that in the winter months, high rainfall and low evaporation means that the ecosystem is rarely water limited. Nijp et al. (2015) found that carbon uptake at their site at Degerö Stormyr peatland in Sweden decreased after rain events. They suggest that this is due to the decrease of light availability during rainfall events, and advise that this could cause particularly noticeable decreases in photosynthesis during seasons when light conditions are below the light saturation level of the ecosystem. Therefore the combination of optimal water conditions and light limitation in the winter, and optimal light levels and water limitation in the summer, could perhaps explain the relationships between NDWI and GPP used to build this model. Further work could explore different methods for estimating peatland wetness using remote sensing, for example thermal imaging (Luscombe et al., 2015). The combination of different techniques in the future of this field of study may yield a greater range of information about peatland condition.

It is important to consider that the EC flux tower data used as a validation method in this study may not be entirely accurate, as they are themselves model outputs. Flux partitioning is particularly likely to be a source of uncertainty within the EC data, as it relies on assumed and modelled relationships. Other parts of the processing methodology, such as filtering and gap-filling, may also introduce errors. Finally, it is worth noting that the footprint of the EC towers is not likely to be entirely comparable to the same area as the MODIS data. More work at different scales and using diverse methodologies will help to overcome this concern, such as comparisons between chamber and EC flux data, and between remote sensing from unmanned aerial vehicles (UAVs) and from satellites.

Using Glencar as an inter-annual validation site was greatly beneficial as it has a ten-year data series. Also, using an independent site encourages confidence that the usefulness of the TGWa model is not peculiar to the Forsinard Flows reserve sites. As longer term EC records for peat bog sites undergoing restoration become available it will be interesting to see whether the TGWa model results continue to match the EC data at different stages of restoration.

5.5.2. Model results

The results from the six restored sites A-F show an increasing trend in GPP in the years between felling and 2016. The results from all sites suggest that the average time taken for a site undergoing restoration to reach the GPP of near-natural sites is 7.2 (5 to 10) years. This

fits with previous studies, which suggest the average time for a restored bog to reach the GPP capacity of near natural sites to be from three (Tuittila et al., 1999) to ten years (Soini et al., 2009; Strack and Zuback, 2013; Waddington et al., 2010).

The oldest site in this study (site A, 18 years) shows an increase above the zero line of the control sites. This may simply be due to site A being more productive, or it could be an effect of restoration. One explanation may be that in the early stages of restoration a higher proportion of vascular plants is evident, leading to higher GPP (but also most likely to higher respiration), compared to a near-natural bog site with a higher proportion of non-vascular plants such as *Sphagnum* moss. This agrees with Strack and Zuback (2013) who found that after ten years the restored bog sites at Bois-des-Bel in Canada had a greater CO_2 uptake than the near-natural sites during the growing season. Their study also found that uptake was correlated with vascular plant cover (Strack and Zuback, 2013), as did Strack et al.'s (2016) study covering six restored sites across Canada. A similar result was found in a restored fen in Finland by Soini et al. (2009), who also studied their peatland sites ten years after restoration and found that the restored sites appeared to be greater carbon sinks than the pristine sites, although this result was not statistically significant due to the greater variation amongst the restored sites. Hancock et al. (2018) found that conditions at the Talaheel site were favourable to vegetation species characteristic of heathland environments, which generally have a higher productivity than intact blanket bog vegetation communities.

It is worth mentioning that sites A and B have relatively weak trends. It was not expected that site A would show a significant result, as the earliest modelled GPP in this study is for 2005, which is already seven years after felling was completed at this site. Vegetation is often well established early after felling, and changes little over time leading to a lack of further trend (Hancock et al., 2018). In the case of site B, the shallow slope of the trend is likely due to a high uptake value in the first years after felling. Sites which were felled in the earlier years had smaller trees, and therefore a more open canopy allowing some ground vegetation which would have remained after felling. Site B also includes an area of forestry in the top left corner of the pixel (see Figure 5.1) which was not felled until 2010-2011. This may explain why site B has the highest GPP result in the first year after felling, and therefore the shallowest slope.

At most of the sites the TGWa model shows GPP increases even in the first year after felling. Due to the size of the MODIS data product pixels, an area considered to be under restoration also often includes small areas of near-natural bog, and generally includes a significant proportion of access tracks for machinery into the areas (the former forestry

“rides” which were unplanted areas remaining under peatland vegetation). Many of the blocks were felled in stages rather than all at once, so it is likely that each 1 km MODIS pixel in what is considered the first year of felling actually contained areas which had been felled up to two years previously, as well as immediately prior to the modelling period start. Sites C, D and E had felling periods of 2 to 3 years, which means that in the year counted in this study as the first year after felling would actually have been the second or third year after felling for some areas included within the pixel. Also, as trees were felled to waste rather than removed from the site, it may be that in the first year after felling the satellite is picking up some chlorophyll signal from trees which had been felled but would remain green for several months.

Due to the calibration of the TGWa model with the Glencar data series, the absolute values of GPP for the restored sites A to F may be smaller than the actual values. The annual GPP values of the two restored sites at the Forsinard reserve for which we have EC data, Lonielist and Talaheel, are 501 g C/m^2/yr and 551 g C/m^2/yr respectively. These values are higher than the 337 g C/m^2/yr suggested by the model as the average value reached eight years after restoration. This effect is due to the optimisation of the ‘a’ and ‘b’ parameters using the multi-year dataset from Glencar, which has a lower average annual GPP from the EC data than Lonielist or Talaheel. However, the trends in the model results remain unaffected by this calibration.

Here, we focus on GPP rather than NEE. Data are beginning to emerge which suggest that the largest control over healthy peatland respiration is in fact GPP, both through the direct relationship between GPP and autotrophic respiration, and also a link with heterotrophic respiration through the labile carbon availability (Zhao et al., 2016). This suggests that although respiration estimates are essential to derive NEE and therefore give a complete comparison of atmospheric carbon fluxes at different sites, nevertheless GPP data alone can be a very useful indicator of peatland status. Strack et al.'s (2016) study of six Canadian peatlands found that restoration had little effect on ecosystem respiration, which remained lower than natural sites. Waddington et al. (2010) however found that in the years after restoration work at the Bois-des-Bel peat bog, respiration decreased, possibly due to higher water tables limiting aerobic respiration, whilst GPP increased. Tuittila et al. (1999) found the same effects at a raised bog site in Finland. Both studies suggest that restored peat bog sites can function as a carbon sink, for at least part of the year, just two years after restoration. However, without respiration data (and other carbon fluxes) we cannot say for certain that the sites in this study are carbon sinks, despite an increased GPP. Raising the water tables at bog sites undergoing restoration is a crucial part of the process to keep the bog healthy and to suppress heterotrophic respiration. Further research is needed to explore

how well satellite products can be used to derive modelled estimates of NEE and how these compare to GPP.

It is important to consider that GPP, or even NEE, alone does not give a complete picture of peatland restoration. This model should be used in conjunction with ground data to take into account not only flux measurements (Hambley et al., 2019), but also vegetation communities (Hancock et al., 2018), water table (Gaffney et al., 2018), and other indicators of restoration to a healthy bog. Future work should test how suitable this model is for application on peat bogs which are being restored from peat extraction sites as well as from forestry plantations.

5.6. Conclusions

We have used remote sensing data from MODIS to analyse the response of peatland photosynthesis to restoration. Here, we develop a modified version of the Temperature and Greenness (TG) model, the annual Temperature, Greenness and Wetness model (TGWa) model, which includes additional factors to account for wetness. The TGWa model using temperature, NDVI, and NDWI to estimate annual GPP is more accurate in peatland environments than the more complex MOD17A2H GPP product. The TGWa model has been shown to give good estimates of GPP at three peat bog sites in Scotland and Ireland, where the MOD17A2H product performed poorly. The next step is to attempt to calibrate the TG model across global boreal peat bogs.

The results from the six selected restored sites in the Forsinard Flows reserve (aged between 1 and 7 years at the start of the modelling time window) indicate that restoration improves the uptake of CO_2. Modelled GPP fluxes imply that bog sites that undergo felling and restoration procedures, such as those in this study, appear likely to reach rates of GPP exhibited by near-natural bog after 5 to 10 years. We emphasise that GPP is only one measure of successful peat bog restoration, and consideration should also be made of the changes in respiration, other carbon fluxes, water table, and vegetation communities.

Acknowledgements

Thanks are due to the RSPB for their work on this project, and for site access and access to facilities. Thanks also to the Environmental Research Institute (ERI) for their role in restoration monitoring at the Forsinard Flows RSPB reserve. Thanks to Danni Klein for facilitating this work, Roxane Andersen for site set up and work coordination, and Rebecca McKenzie and Peter Gilbert for site maintenance. Thanks to Mark Hancock and Alessandro Gimona for very helpful comments on this manuscript.

Funding

Kirsten Lees was part funded by a studentship from The James Hutton Institute, and part funded by the Natural Environment Research Council (NERC) SCENARIO DTP (Grant number: NE/L002566/1). Tristan Quaife was funded by the NERC National Centre for Earth Observation (NCEO). Myroslava Khomik and Rebekka Artz were funded by The Scottish Government Strategic Research Programme 2016-2021. Graham Hambley was funded by ScotGov, the RSPB and the University of St Andrews. Much of the restoration work reported in this study was funded by EU LIFE, Peatland Action, HLF, and the RSPB.

6. Assessing the reliability of peatland GPP measurements by remote sensing from plot to landscape scale.

Lees KJ, Khomik M, Quaife T, Clark JM, Hill T, Klein D, Ritson J & Artz RRE

Abstract

Estimates of peatland carbon fluxes based on remote sensing data are a useful addition to monitoring methods in these remote and precious ecosystems. There are, however, questions as to whether such large-scale estimates can be truly accurate given the small-scale heterogeneity of many peatlands. This study considers the reliability of remote sensing for estimating ecosystem photosynthesis at different scales at the Forsinard Flows RSPB reserve in Northern Scotland. Three sites across the reserve were monitored during the growing season of 2017. One site is near-natural blanket bog, and the other two are at different stages of the restoration process (19 and 13 years in) after removal of commercial forestry. At each site we measured small and landscape scale carbon dioxide fluxes (using chamber-based and Eddy Covariance measurement techniques), small scale spectral data using a handheld spectrometer, and obtained corresponding satellite data from MODIS. The variables influencing GPP at small scale, including microforms and dominant vegetation species, were assessed using exploratory factor analysis. A model using land surface temperature and a measure of greenness from remote sensing data was tested as an estimate of GPP, and compared to chamber and eddy covariance CO_2 fluxes. Our results show that the temperature and greenness model gives good results at all scales (correlations of 0.57 to 0.70 at small scale, 0.74 to 0.85 at large scale), although it is dependent on calibration with ground data. Further work is needed to assess how well this methodology performs under more extreme conditions and at other locations. Overall, our results indicate reasonable confidence in estimates of GPP in blanket bog by remote sensing at both small and large scales.

6.1. Introduction

Peatlands are important ecosystems for carbon sequestration, but many areas in the British Isles have experienced degradation through human land use. As an organic-rich, water-saturated substrate, peat is capable of storing huge amounts of carbon relative to land area. For example, in Scotland peatlands store 56% of total soil carbon whilst occupying 24% of the land area (Chapman et al., 2009). Many peatland areas have, however, been subject to management such as draining, grazing, burning and planting for commercial forestry, which have reduced saturation and increased bulk density and subsidence of the peat (JNCC, 2011). Restoration of peatland areas is of interest to policy makers as a carbon emissions abatement scheme (European Commission, 2018; IUCN, 2016). Remote sensing has the

potential to help monitor carbon fluxes in these important, remote and extensive areas that are difficult to access for conventional field-based measurements, yet little testing of methods has been carried out (Lees et al., 2018). The Forsinard Flows RSPB reserve is an ideal study location as it has a chronosequence of areas undergoing restoration from commercial forestry (Hancock et al., 2018), and three similar eddy covariance (EC) towers at different sites.

Upscaling of ecosystem processes is an important research area in ecology, as landscape and regional scale estimates are needed for policy decisions (Fu et al., 2014; Le Clec'h et al., 2018). Models using satellite data to estimate peatland carbon fluxes are being developed to cover large areas (Lees et al., 2018), but it is also important to consider landscape heterogeneity in total flux estimates (Zhang et al., 2007). Blanket bogs (peatland sustained by rainfall, Lindsay, 2010) in particular have small scale heterogeneity in topographic features known as hummocks and hollows, which can vary at scales of less than a metre (Belyeal and Clymo, 2001). This microtopographical variation influences vegetation communities at small-scale, which can have a significant impact on carbon fluxes (Arroyo-Mora et al., 2018; Dinsmore et al., 2009b; Peichl et al., 2018). The existence of satellites with very fine spatial resolution (down to tens of metres) means that studies can now consider variation within a landscape, but the microtopography of blanket bogs is still too small to be detectable from non-commercial satellite data.

Traditional methods of carbon dioxide exchange measurement include flux chambers and Eddy Covariance (EC) towers, both of which are small-scale and expensive to manage and maintain. Practitioners need techniques to assess changes in peatland carbon fluxes at a landscape scale in order to measure the success of restoration processes and detect where to focus their efforts. Satellite data-based models have recently shown successes in estimating carbon fluxes from peatland landscapes (Kross et al., 2016; Lees et al., in press), but there is still uncertainty over whether these models can adequately detect the variation from small-scale peatland heterogeneity (Arroyo-Mora et al., 2018). A Temperature and Greenness (TG) model is specifically considered in this study, as this has previously been shown to give good results over the reserve (Lees et al., in press). This model combines a measure of land surface temperature with a vegetation index, in this case the Normalised Difference Vegetation Index (NDVI), to give an estimate of Gross Primary Productivity (GPP).

The aim of this work is to consider what factors affect GPP in blanket bog, and whether the results from small scale measures of photosynthesis are significantly different to results from large scale models using satellite data. We hypothesise that the TG model will give good

agreement with chamber flux data at the small scale, and with EC data at the larger scale. We also expect that the measurements and estimates at different spatial scales will be correlated and within the standard deviation range of each other.

6.2. Methods

6.2.1. Field sites

This research is based at three field sites within the Forsinard Flows RSPB reserve in Northern Scotland (approx. 58.3585, -4.0409 to 58.4327, -3.6264, WGS84). The reserve is part of the much larger blanket bog Flow Country EU Natura site. Cross Lochs is a near-natural site (see Levy and Gray, 2015), where no drainage has been applied. An EC tower is located at 58.3703, -3.9644 (WGS84), elevation 211 m. Talaheel and Lonielist are both sites undergoing restoration, which were previously planted for commercial forestry in the 1980s.

Talaheel was initially felled, with the trees laid into the planting furrows, in 1998 and has since undergone further landscaping to crush the decomposing conifer brash and to create peat dams in the furrows (2015/16), which has led to raised water levels (see Hancock et al., 2018). The EC tower is located at 58.4146, -3.8006 (WGS84), elevation 196 m.

Lonielist was felled in 2003/2004. At the time of the experiment it retained the distinctive pattern of ridges on which the trees were planted, and drainage ditches infilled with the felled trees. This site has undergone no further management until the end of this project (-end of 2017). The EC tower is located at 58.3910, -3.7651 (WGS84), elevation 180 m.

All three sites are subject to some light grazing by wild red deer (*Cervus elephantus*). Talaheel is fenced as part of a larger enclosure including some forestry, although some deer are present inside the fence, whilst Lonielist and Cross Lochs are entirely open to grazing.

Small scale measurement points were set up in the area within each site's EC tower footprint. The precise distances from the tower and dominant wind directions (Northwest and Southwest) were determined from Hambley (2016). At each site two perpendicular crossing transects were set up, one including five points and extending away from the tower into the dominant wind direction, and one including four points and extending into the secondary wind direction (see Figure 6.1). At each point two PVC collars (24 cm in diameter) were placed: one on higher microforms (ridges in the restored sites, hummocks at Cross Lochs) and one on lower microforms (in the furrows at the restored sites, hollows/lawns at Cross Lochs). The collars included a range of vegetation species commonly found within the tower footprints and across the Forsinard Flows reserve (see Appendix B for species compositions).

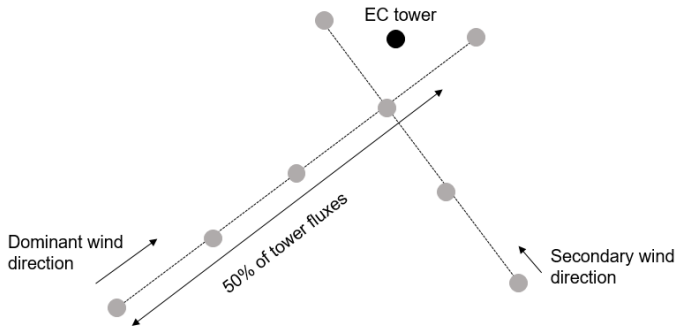

Figure 6.1 – Location of points within the tower footprint. Two collars, one on a higher microform and one in a lower area, were placed at each point.

6.2.2. Chamber fluxes

In situ CO_2 flux measurements were taken using a LICOR-8100 (LICOR Inc., Lincoln, Nebraska, USA) portable infrared gas analyser and custom Perspex chambers of 24 cm diameter and 30 cm height. Small 9V battery-operated fans were installed within the chambers to circulate the air. The two chambers, one clear and one covered with a blackout cloth, were sealed to the collars using rubber mastic (Terostat), and consecutive measurements were taken. Each measurement period was five minutes, with a 20 second pre-measurement stabilisation period.

For comparison with the EC and satellite data, the fluxes from all of the collars at each site were averaged. A weighted average taking into account the proportion of different microfeatures was not used due to the minimal differences found between microform fluxes.

6.2.3. Field spectrometry

Spectral measurements in the field were taken using a handheld SVC HR-1024 (Spectra Vista Corporation) spectroradiometer mounted on a monopod and held approximately 1m from the surface using an 8˚ FOV lens with an on-the-ground footprint within the diameter of the collars. The spectral range of the instrument is from 337 nm to 2521 nm. Three measurements were taken of the vegetation within each collar, at three different angles to minimise structural effects (opposite the position of the sun and at 90˚ to either side). A Spectralon reference panel was also measured between these observations to normalise from radiance to reflectance.

The Normalised Difference Vegetation Index (NDVI) is calculated from the difference between reflectance in red wavelengths of light, which plants absorb strongly, and the near-infrared (NIR), which plants reflect:

$NDVI = (R_{NIR} – R_{red})/ (R_{NIR} + R_{red})$

In this study we calculated the red and NIR bands as the average of the values in wavelengths 630-680 nm and 845-885 nm respectively.

6.2.4. Other factors measured in the field

Soil moisture was measured using a moisture probe with 6 cm prongs (Theta probe ML2x , Eijkelkamp, connected to HH2 moisture meter, Delta-T Devices). At the Lonielist site, dipwells were inserted next to each collar, and the water level was monitored manually at the same time as the spectral measurements were taken. Soil temperature was measured at two different depths, 5 cm and 15 cm, and surface temperature inside the chamber was taken at the start and end of each measurement using a lollipop thermometer (Fisherbrand, accurate to ± 1˚C).

To consider the different vegetation communities of the microforms, the species within the collars were surveyed in June 2017. All species were recorded as percentage cover over the area of the collar, and overlapping canopies sometimes allowed total percentage cover to be over 100%. Six species which were found at all three sites were selected as indicators of microform vegetation communities. These are shown in Table 6.1.

Table 6.1 – species selected which were present at all three sites, which microform they prefer, and their average (and standard deviation) percentage presence in collars at each site.

Common name	**Latin name**	**Hummock or Hollow**	**Lonielist**	**Talaheel**	**Cross Lochs**
Heather	*Calluna vulgaris*	Hummock	7.5 ± 11.7 %	4.7 ± 9.8 %	9.7 ± 9.5 %
Common cotton grass	*Eriophorum angustifolium*	Hollow	10.9 ± 13.6 %	17.9 ± 15 %	9.4 ± 10.5 %
Reindeer lichen	*Cladonia portentosa*	Hummock	12.8 ± 18 %	17.6 ± 26.9 %	11.4 ± 18.2 %
	Sphagnum capillifolium	Hummock	19.9 ± 22.5 %	16.7 ± 30.1 %	27.7 ± 18.1 %
Red-stemmed feather moss	*Pleurozium schreberi*	Hollow	12.3 ± 22.1 %	23.6 ± 27.9 %	3.9 ± 7.2 %
Deer grass	*Trichiophorum germanicum*	Hollow	0.6 ± 2.5 %	4.9 ± 8.3 %	21.8 ± 21.6 %

6.2.5. Eddy Covariance

Net ecosystem exchange of CO_2 (NEE) at Lonielist was measured using a LICOR 7200 enclosed CO_2/H_2O infrared gas analyser (LI-COR Biosciences Inc. Lincoln, NE, USA), and a Gill HS-50 3-D sonic anemometer (Gill Instruments, Lymington, UK). Data was collected at

20Hz frequency and half-hourly values recorded by the LI-7550 Analyzer Interface Unit (LICOR Biosciences, Inc. NE, USA). The instruments were mounted on top of a scaffolding-tower at 2.90 m height, pointing into the predominant wind direction (W-SW, 240˚ North offset).

At Talaheel, NEE was measured using the LICOR 7500A open path CO_2/H_2O gas analyser (LI-COR Biosciences Inc. Lincoln, NE, USA) with a custom enclosure added to the analyser to create an enclosed system (Clement et al., 2009), and a CSAT sonic anemometer (Campbell Scientific, Logan, USA). Data was measured at 10Hz frequency, averaged and stored as half-hourly values by the CR5000 datalogger. Instruments were set-up at 4.3m height on a scaffolding tower.

At Cross Lochs NEE was measured using an open-path infra-red gas analyser that was integrated into a 3D-CSAT anemometer, the IRGASON, controlled by the EC100 electronics control module (Campbell Scientific Ltd. UK). Data was measured at 10Hz and half-hourly averages were recorded on a CR3000 datalogger. The instruments were set up at 2.3m height on a tri-pod tower, pointing 310^o NW.

Raw flux and associated meteorological data were processed using the Eddy Pro software, (version 6.2.1, LI-COR Biosciences, NB, USA) for the Lonielist and Talaheel datasets, to calculate half-hourly NEE fluxes and frictional velocity (u-star) values. For Cross Lochs, EasyFluxPC software was used (version 1.008CS Campbell Scientific, UT, USA) to obtain non-gapfilled half-hourly NEE values and u-star values. The raw NEE was further quality checked using histograms and site-measured global radiation values. The quality screened data from all three sites was then further processed in ReddyProc package in R-software (Wutzler et al., 2018) to obtain gap-filled NEE values and also to partition the fluxes into GPP and Reco. Measurements at Lonielist began in March, so 23% of the data was missing at the start of the 2017 year. 26% (of 13550 hh) of available NEE half hours were gap-filled at Lonielist, 52% at Talaheel (of 17520 hh), and 60% at Cross Lochs (of 17520hh).

For comparison with the chamber and spectrometer data, the EC data covering the same period as the chamber measurements were selected and averaged. For comparison with the TG model using MODIS data, the EC fluxes were averaged across 8-day periods and then multiplied to give daily values, following Lees et al. (in press).

6.2.6. Satellite data

The Moderate Resolution Imaging Spectroradiometer (MODIS) on satellite Terra was used in this study as an example of a coarse resolution broad band satellite, which is widely used in environmental studies. Two MODIS products were used in this study, the 250 m

MOD13Q1 NDVI product (Didan, 2015), and the 1 km MOD11A2 Daytime Land Surface Temperature (LST) product (Wan et al., 2015). The NDVI product is given in 16-day periods, whilst the LST product is given in 8-day periods. The MODIS data products were downloaded using the MODIS ORNL web service through Matlab code (see Appendix C) (Santhana Vannan et al., 2009). Cloud filtering was applied to remove pixels extensively affected by cloud cover, whilst letting though data which was affected by clouds but still useable. Each of the MODIS product contains information about the quality of the data in each pixel, and this was used to select which 8-day or 16-day pixels were useable. MOD13Q1 pixel reliability index was used to remove snow/ice or cloud affected values. MOD11A2 quality control data was used to remove periods when data was not produced due to cloud effects or other issues. Gap-filling was then performed across each year using the techniques described by Wang et al. (2012), before combining the data into the TG model.

6.2.7. The TG model

The Temperature and Greenness (TG) model combines a measure of temperature with a vegetation index to give an estimate of GPP (Sims et al., 2008). The model is formulated, following Moore et al. (2013), but using NDVI following the results of Lees et al. (in press):

$$GPP = NDVIs \times LSTs \times m$$

$$NDVIs = NDVI - 0.1$$

$$LSTs = \min[(LST-minLST)/(optLST-minLST), (maxLST-LST)/(maxLST-optLST)]$$

Where NDVIs is the scaled Normalised Difference Vegetation Index and LSTs is the scaled Land Surface Temperature (see Sims et al., 2008). minLST, optLST and maxLST (given in ˚C) are the minimum, optimum and maximum Land Surface Temperature calculated for an ecosystem from past data. We have used 40˚C, 25˚C and -2.5˚C for maxLST, optLST and minLST respectively, following Lees et al.'s (in press) work on the same study sites.

'm' is a site-optimisation parameter which was given the value of 5.875 in Lees et al. (in press). For this study the GRG Nonlinear Solver in Microsoft Office Excel 2013 was used to optimise the m parameter at both small and large scales. The m parameter for the TG model using spectrometer data was optimised to the chamber data across all months and sites, and was given the value 0.4397. This small-scale version of the TG model gives an estimate of GPP per hour.

The m parameter for the TG model using MODIS data was optimised to the EC data across the whole of 2017 (where EC data was available) and across all three sites. It was given the

value 8.046. This large-scale version of the TG model gives an estimate of GPP per day. The small-scale m parameter was also applied to the large-scale TG model to assess the effect of scale versus methodological error (see Section 6.3.3).

6.2.8. Statistical analysis

An Exploratory Factor Analysis (EFA) was used to simplify the large range of variables measured which could affect GPP on a small scale. EFA is a variable reduction technique designed to draw out the underlying factors affecting the measured variables. In this case the EFA was used because we expect that the variables measured are related to each other by means of underlying constructs, for example, the vegetation species included are likely to be related to each other due to underlying features of their microhabitats.

The variables considered included those explained in Section 6.2.4 (selected vegetation species, PAR, surface temperature, soil temperature at 5 cm and 15 cm, soil moisture, and microforms), and also the NDVI, which is a measure of vegetation greenness and health, and the Normalised Difference Water Index (NDWI) which has been shown to have a relationship with moisture conditions in peatland vegetation (Lees et al., in prep).Repeated measures were accounted for by including the time of year as a variable. In order to create a linear relationship the temporal distance from the midsummer solstice (in days) was used as a measure of season. These variables are referred to in the results by short names given in Table 6.2.

Table 6.2 – short names given to each variable in the EFA.

Short name	**Description**
Feather_moss	The proportion of *Pleurozium schreberi* in the collar (%)
Reindeer_lichen	The proportion of *Cladonia portentosa* in the collar (%)
S_cap	The proportion of *Sphagnum capillifolium* in the collar (%)
Deer grass	The proportion of *Trichiophorum germanicum* in the collar (%)
Cotton grass	The proportion of *Eriophorum angustifolium* in the collar (%)
Heather	The proportion of *Calluna vulgaris* in the collar (%)
NDWI	The calculated NDWI of the collar from the hand-held spectrometer
NDVI	The calculated NDVI of the collar from the hand-held spectrometer
PAR	The average PAR taken across the clear chamber flux measurement period.
Surface_temp	The air temperature at the soil surface (˚C)
Soil_temp_5cm	The soil temperature at 5 cm depth (˚C)
Soil_temp_15cm	The soil temperature at 15 cm depth (˚C)
Solstice_dist	Temporal distance (days) of each measurement from the midsummer solstice
microfeature	Whether the collar was on a high area (hummock/ridge) or low area (hollow/ditch)

The EFA was limited to five factors, and explained the majority of the variance seen in variables at each site. The resulting factor scores were then correlated with the GPP in order to assess which factors and variables were most important in determining peatland GPP at small scales, and whether these could be assessed using remote sensing.

All analysis was done in base R (R Core Team, 2017).

6.3. Results

6.3.1. Factors affecting GPP at small scale

The six vegetation species considered in this analysis show several significant differences between hummock and hollow percentage coverage (see Figure 6.2). At the near-natural Cross Lochs site there is significantly more heather (*Calluna vulgaris*) and *S. capillifolium* on the hummocks, but significantly more deer grass (*Trichiophorum germanicum*) in the hollows. The Lonielist site also has significantly more heather on the hummocks, but significantly more red-stemmed feather moss (*Pleurozium schreberi*) in the hollows. There were no significant differences between hummock and hollow vegetation at the Talaheel site in 2017 (see Appendix D).

There are also differences between the three sites in terms of vegetation cover. Cross Lochs is richer in deer grass than the other two sites, whilst Talaheel is particularly favourable to common cotton grass (*Eriophorum angustifolium*) (see Table 6.1). Cross Lochs also has a greater variety of species, with some present that were not included in our collars at the other two sites such as bog myrtle (*Myrica gale*), bog asphodel (*Narthecium ossifragum*), and sundew (*Drosera rotundifolia*).

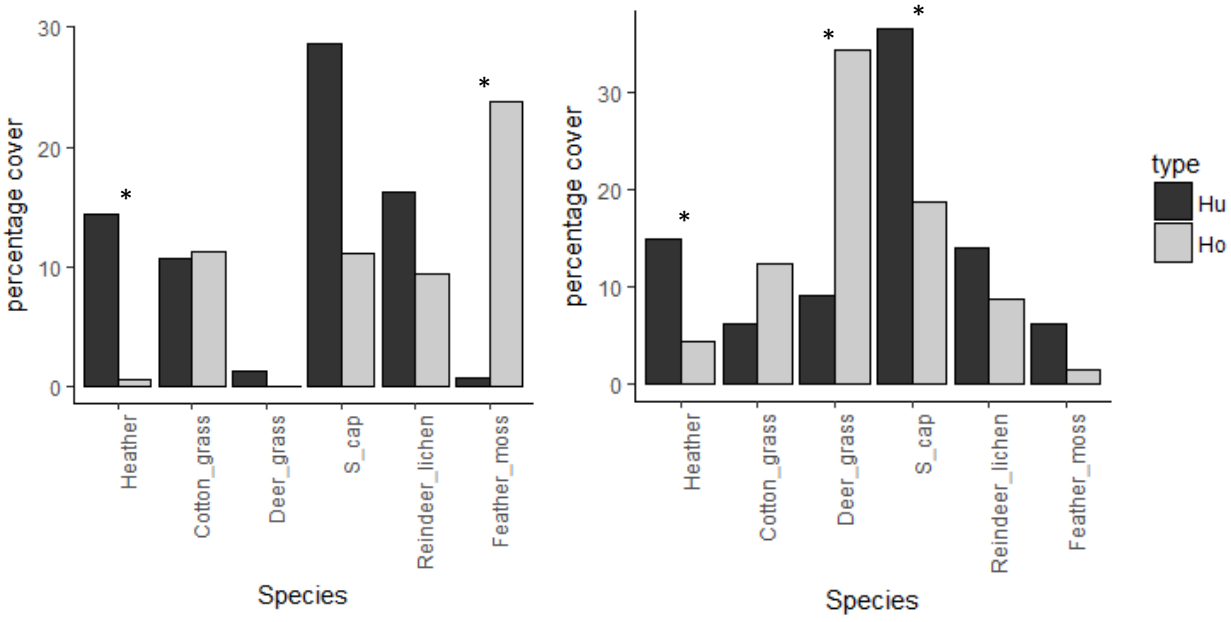

Figure 6.2 – The left graph is the data from Lonielist, whilst the right is from Cross Lochs. There were no significant differences at Talaheel. Stars show a significant difference between hummock and hollow.

These selected vegetation species were also used in the EFA, where they are linked to underlying factors which also affect microtopography (Lonielist and Cross Lochs), the NDWI (Talaheel and Cross Lochs), and soil moisture (Cross Lochs). These factors also correlate with GPP.

The EFA results are shown in Figure 6.3, along with the factor correlations with GPP. At Lonielist the second factor has the highest correlation with GPP (0.68), and is linked with the NDVI and the three temperature variables. The third and fourth factors also show some correlation with GPP (0.21, 0.28) and are connected with the microforms variable and the vegetation species variables.

At Talaheel only the first and third factors show much correlation with GPP (0.46, 0.36). The first factor is connected to the NDVI, NDWI, temperature and temporal distance from solstice variables, whilst the third is linked with the NDWI and NDVI, and percentage cover of cotton grass and deer grass.

At Cross Lochs the first factor is correlated with GPP (0.50) and links with temporal distance from solstice, temperature, NDWI and PAR. The second factor also correlates with GPP (-0.22) and is connected to the microform variable, several plant species, soil moisture and the NDWI. The negative correlation here suggests that the collars classed as hollows have a higher GPP than those classed as hummocks; this is opposite of the result at Lonielist. The third factor correlates positively with GPP (0.36) and is connected to the two soil temperature variables, NDWI and NDVI.

Lonielist

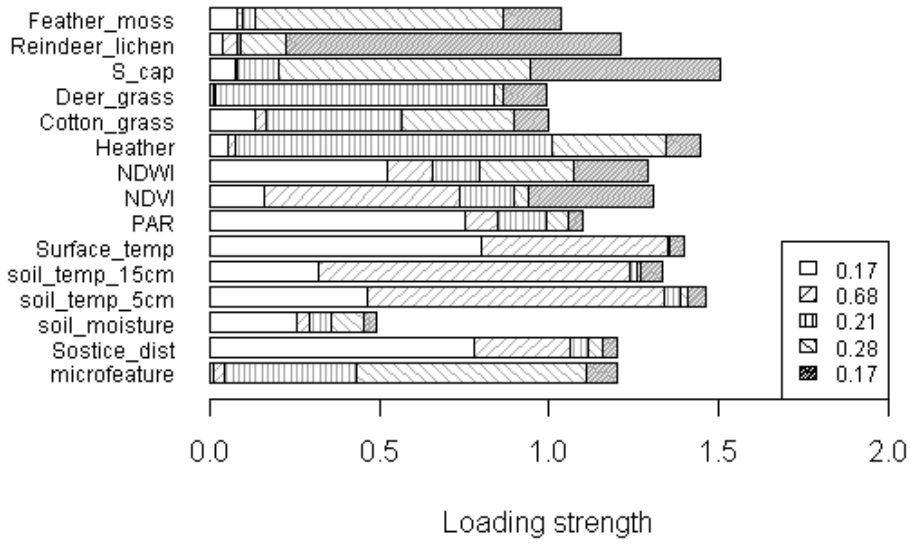

Talaheel

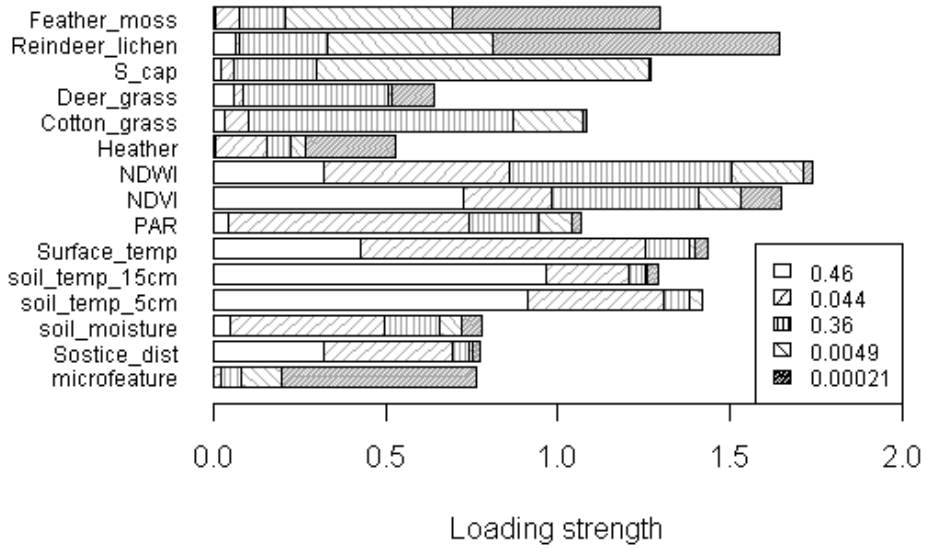

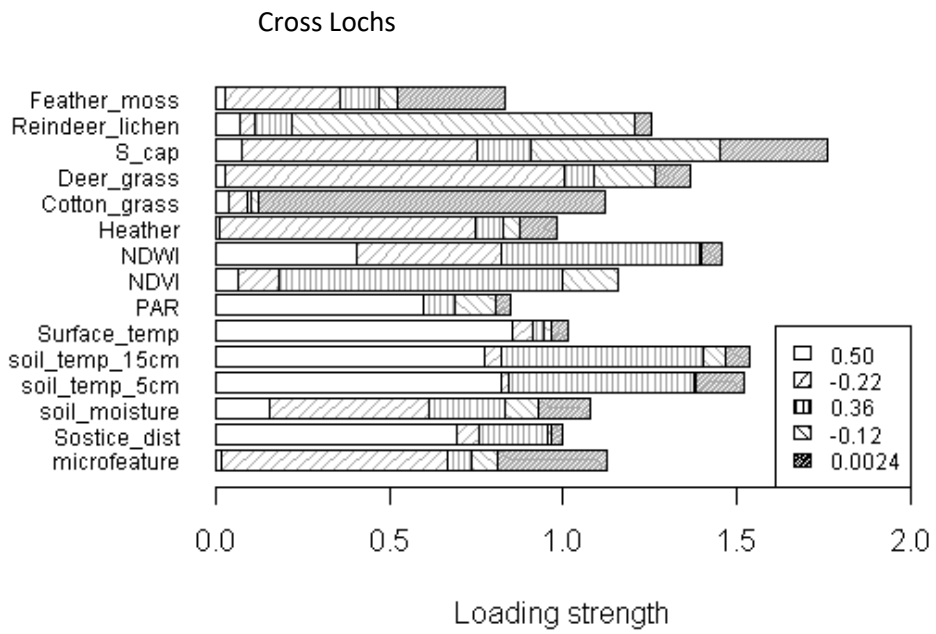

Figure 6.3 – Lonielist, Talaheel and Cross Lochs factors. Each of the five factors is indicated by a different pattern fill. The variables are given on the y axis, and the factors which underly and are connected with each variable have a loading strength shown by the stacked bar lengths. Legends show correlation of the scores for each factor with GPP values. For example, the first factor at Cross Lochs is shown by the unfilled bars, and has high loading strengths associated with PAR, the three temperature variables, and the temporal distance from the solstice. It also has a correlation of 0.50 with GPP. See Appendix D for more information.

6.3.2. Comparison of modelled and measured GPP at small scale

Figure 6.4 shows the TG model using the spectrometer NDVI and the surface temperature applied to each of the sites across the measurement period. The agreement between the model and the chamber data is generally very good temporally, with the boxplots well within error bars across the year. The chamber fluxes have larger ranges than the TG model results at each site throughout the growing season. The TG model tends to underestimate the highest chamber GPP values, as can be seen from the scatter plots in Figure 6.4. It appears that a polynomial model might better describe the relationship than a 1:1 line, particularly at the Cross Lochs site. The possible reasons for this are discussed in Section 6.4.

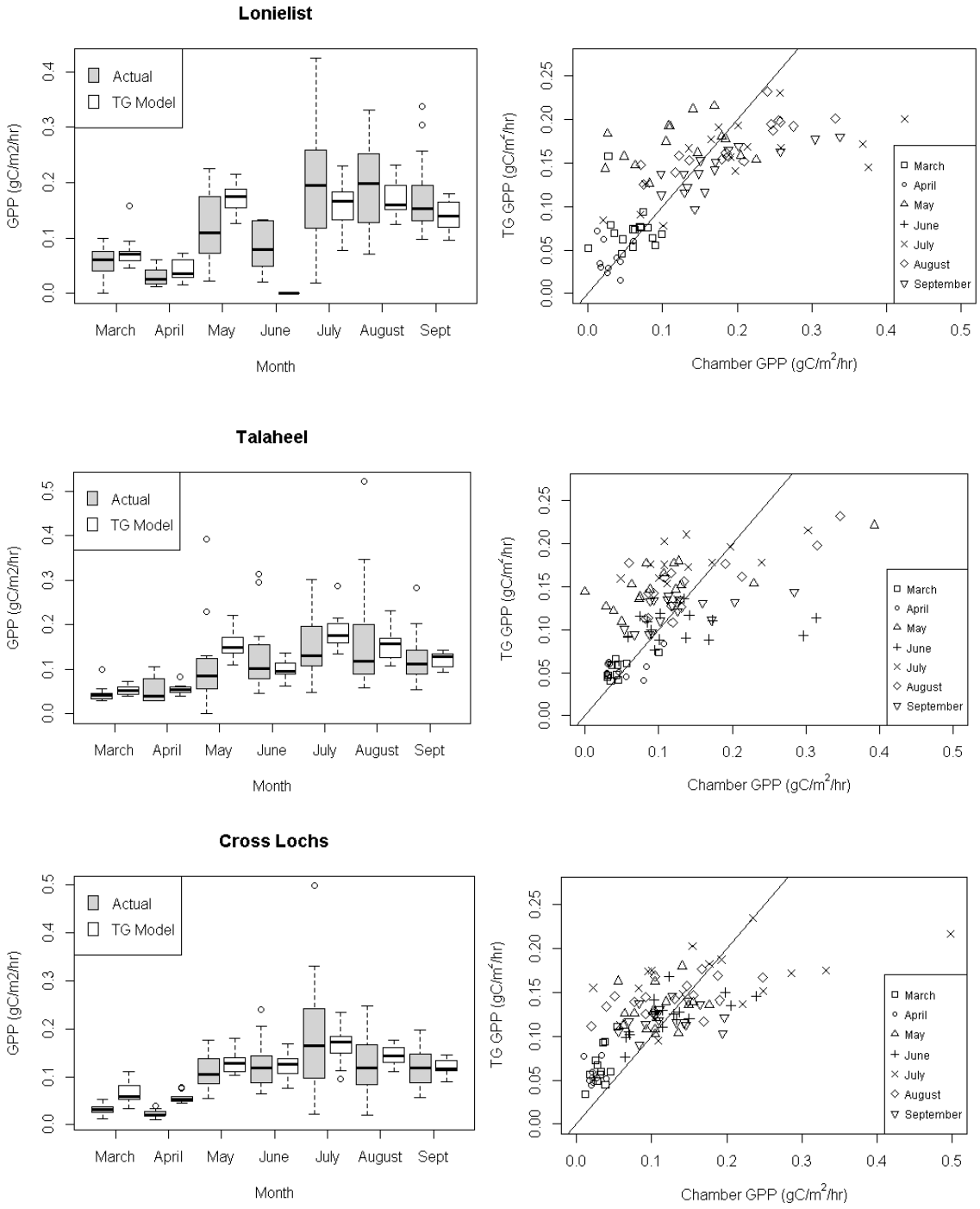

Figure 6.4 - Boxplots and scatterplots (by month) comparing the chamber-measured GPP and GPP calculated from the TG model using hand-held spectrometer data and the surface temperature measurements for each site. There is no TG model result in June at Lonielist due to the poor weather causing lack of spectral measurement. 1:1 lines are plotted on the scatter graphs.

6.3.3. Comparison of small-scale modelled and measured GPP with EC and satellite data

Figure 6.5 shows the average GPP across the experiment period from the chamber data and EC data, and modelled from the spectrometer and MODIS data. The correlations between the chamber fluxes and the spectrometer TG fluxes across all months are 0.57 at Talaheel, 0.68 at Lonielist, and 0.70 at Cross Lochs. The TG model using MODIS data is calibrated on a daily rather than hourly time frame, and so is shown in separate graphs. The correlation between the EC data and the MODIS TG model (DoY 70 to 265) is 0.74 at Lonielist, 0.74 at Cross Lochs, and 0.85 at Talaheel.

The chamber GPP is lower than the EC GPP at all three sites (54.9% lower at Lonielist, 72% at Talaheel, 62% at CrossLochs). The TG model using MODIS data and the 'm' parameter calibrated from small-scale data matches better with hourly chamber fluxes than EC fluxes.

The difference between chamber GPP from hummocks and hollows is greatest at Lonielist and shows higher GPP values from hummocks. The difference is less pronounced at Cross Lochs, but shows the opposite effect, with higher GPP from hollows. Talaheel shows less clear differences between the two types of microform. At all three sites the differences in microtopography shown by the spectrometer TG results are less pronounced than those from the chambers.

Figure 6.6 gives an example image of the TG model applied across part of the Flow Country in July 2017. The forested areas have the highest values in the model, whilst the recently felled areas have the lowest GPP.

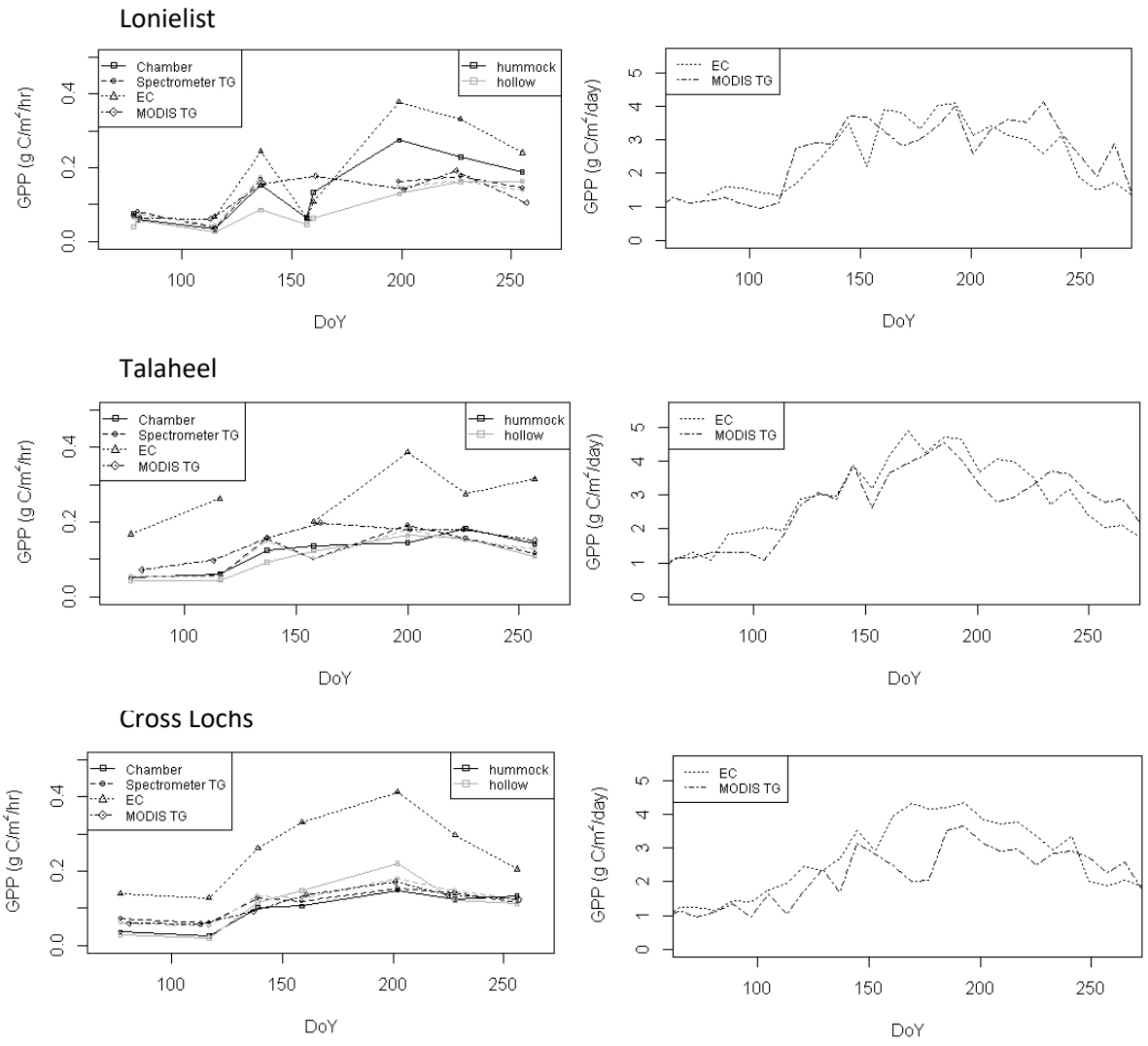

Figure 6.5 – The different estimates of GPP for each site across the growing season. Chamber is the GPP data from the flux chamber measurements, Spectrometer TG is the GPP estimates from the TG model incorporating surface temperature and the NDVI taken in the field, MODIS TG is the TG model using LST and NDVI MODIS data, and EC is the data from the partitioned EC tower data. The small-scale results are split into hummocks (black) and hollows (grey). The data are shown on two separate graphs for each site due to the differing temporal calibrations of the TG model from spectrometer and MODIS data – left-hand graphs are on an hourly timescale, right-hand on daily. EC and MODIS TG are shown on both graphs; the EC data on the left graph are averaged across the half-hourly periods covering the chamber flux measurement period, and on the right graph are averaged over 8-day periods to match the MODIS time period. The MODIS TG is calibrated to the EC data in the right-hand graphs, and using the 'm' parameter calculated for the small-scale TG model in the left graphs.

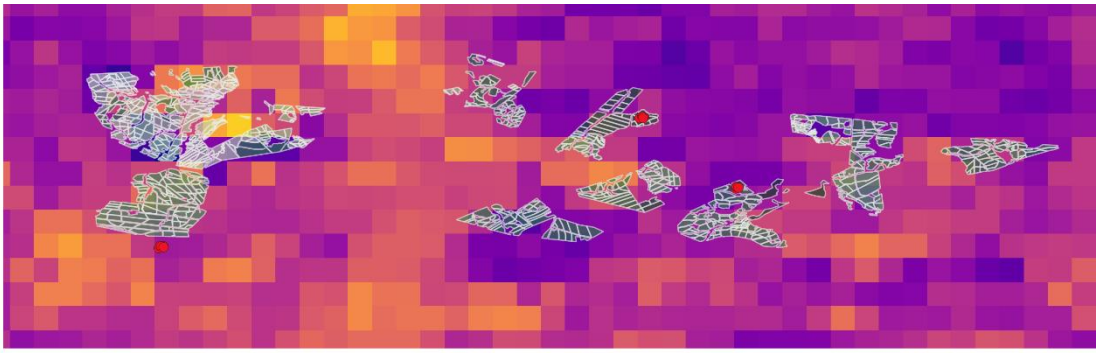

0 1 2 km

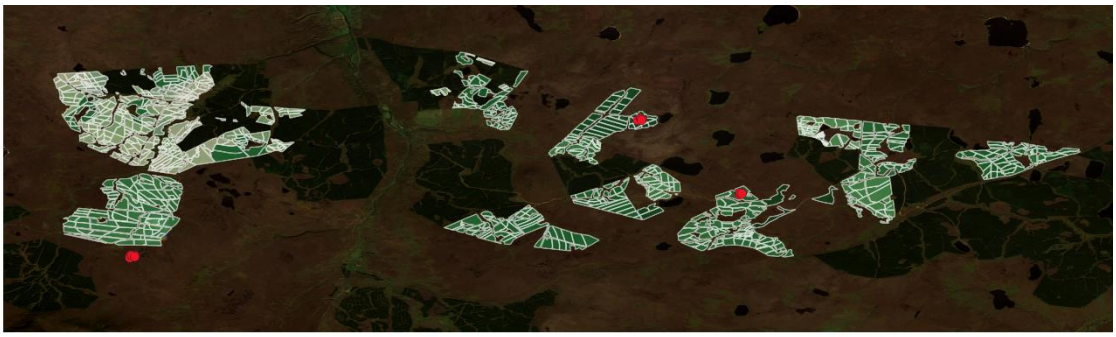

0 1 2 km

Forestry compartments year of felling

- 1994
- 1998
- 2001-2002
- 2002-2003
- 2003-2004
- 2004-2005
- 2005-2006
- 2006-2007
- 2010-2011
- 2011-2012
- 2012-2013
- 2014-2015
- 2015-2016
- 2016-2017

0 500 1000 m

GPP
gC m^{-2} day^{-1}
4.0
3.0
2.0

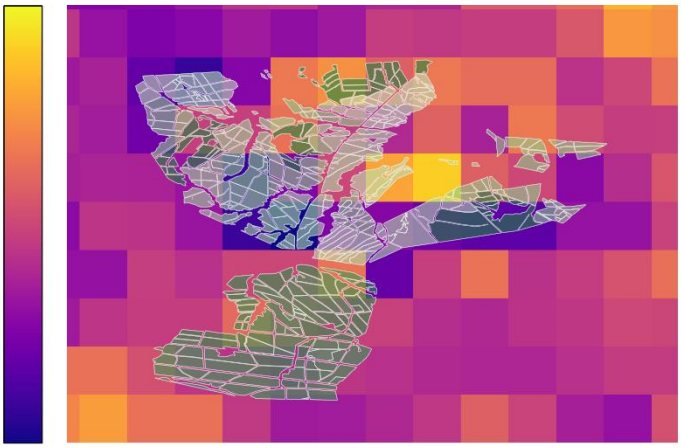

0 500 1000 m

Figure 6.6– Images showing GPP calculated with the TG model using MODIS data from 12th July 2017, and RGB Sentinel-2 imagery from September 2017 (closest clear image) over part of the Flow Country including the Forsinard Flows RSPB reserve. Forestry compartments are overlaid on the images, with darker green showing earlier felling and therefore ecosystems which should be closer to natural bog. Red dots show field chamber measurement points.

6.4. Discussion

The EFA correlations with GPP showed that the NDVI and temperature were dominant in the factors affecting GPP at all sites. This endorses the use of the TG model, which makes use of both these variables. All three temperature variables, at surface, 5 cm and 15 cm, were included as variables, but they are strongly related and only one is necessary in the model. The surface temperature provides much more short-term variation compared to soil temperature, and has a relationship with the incoming radiation available for photosynthesis, as shown by the EFA. The variation which surface temperature adds to the model is therefore more than seasonal change, and can provide information on day-to-day changes in GPP due to weather and radiation, and even changes throughout the day.

Lonielist GPP results at small scale showed the greatest difference between hummocks and hollows, particularly in July when we had clear skies and high temperatures during the measurement period. This difference may be more evident at Lonielist than the other sites due to the relic furrow and ridge system creating more extreme microtopographical features than would otherwise be found in a peat bog. Wu et al. (2011) found that there was no difference in GPP between hummocks and hollows at the Mer Bleue bog in Canada, consistent with our results from Cross Lochs, but did find a significant difference in respiration with hummock ecosystem respiration higher than hollows. They showed that shrubs were the dominant influence on hummock carbon cycling, whilst mosses were the dominant factor in hollows. In contrast, Waddington and Roulet (1996) found that hummocks at their study site in a Swedish peatland had greater CO_2 uptake than hollows during the growing season, similar to our results at Lonielist. It is somewhat surprising that Cross Lochs, the near-natural site, showed a small but opposite difference in fluxes between microforms. Lindsay et al (1988) found that some areas of the Flow Country were dominated by pool and hollow type landforms due to the wet climate, and it may be the case that our classifications of landforms at Cross Lochs were based on the need to distinguish areas of different heights within close range, and did not always satisfy the descriptions of true hummocks and hollows. In general, the differences in GPP fluxes between microforms did not seem to be large or temporally consistent during our study period. The period during

which measurements were taken, however, was mostly quite cold and wet and a stronger difference between fluxes from microforms might have been seen under dryer conditions.

Despite small differences in GPP among the chamber locations, we did observe significant differences in vegetation between the microtopographical features at each site and also in general between the sites. The significant differences in selected vegetation species are consistent with their preferred microhabitats. Both Lonielist and Cross Lochs show a greater proportion of heather (*Calluna vulgaris*) on the higher areas of ground. Cross Lochs has higher percentages of *S. capillifolium*, a *Sphagnum* species well known to be hummock forming (Laine et al., 2009) on the higher areas, and more deer grass (*Trichiophorum germanicum*) in the hollows, whilst Lonielist has significantly more red-stemmed feather moss (*Pleurozium Schreberi*) in the furrows. It is worth noting that there is ecological succession in play as well as microtopographical features when we consider these three sites, as shown in Hancock et al. (2018). The presence of deer grass (*Trichiophorum germanicum*) seems to be associated more with the near-natural site at Cross Lochs. Talaheel has higher relative proportions of common cotton grass (*Eriophorum angustifolium*) which has been found to colonise disturbed areas of ground (Phillips, 1954). Malhotra et al. (2016) found that there was there was a clear relationship between microtopography and species distribution at the Mer Bleue bog in Canada. Their work showed that microtopography in the bog was due to varying rates of decomposition of different vegetation communities, and that fine spatial structures explained up to 40% of species distribution.

The selected vegetation species showed influence on GPP, although these varied between the sites. The two wetter sites, Cross Lochs and Talaheel, show greater connections between GPP and measures of moisture, both NDWI and soil moisture measured using the probe. Both Lonielist and Cross Lochs show some correlations between factors linked with microtopography and GPP, although the relationship is stronger at Lonielist. Malhotra et al. (2016) found that water table depth was a significant factor in maintaining distinct vegetation communities on microtopographical features. Their work was done on the Mer Bleue bog in Canada, which can be described as near-natural, and therefore is most similar to our site at Cross Lochs which also had links between microtopography and soil moisture, as shown by the EFA.

The apparent polynomial relationship between the chamber GPP and spectrometer TG results is possibly a result of the different species dominating the flux at different times of year. As shown in Lees et al. (in prep), NDVI linear model relationships to GPP were steeper in the early months of the growing season (particularly March) and shallower at the peak of the growing season. It was hypothesised that this was due to *Sphagnum* species having a

steeper linear model relationship between NDVI and GPP than vascular plants (Letendre et al., 2008; Whiting, 1994). As *Sphagnum* is a dominant influence on carbon fluxes in the colder months of the year (Glenn et al., 2006) but vascular plants dominate during peak growing season, this could cause the changes seen in the relationship across the months measured. Although the temperature factor in the TG model corrects for this somewhat by reducing the higher NDVI values of the early months and increasing the lower NDVI values of the peak months, it does not completely eliminate these different relationships. Cross Lochs shows this effect very clearly, as this is the site with the most mixed vegetation and the highest proportion of *Sphagnum* (27.7 ± 18.1 % *S. capillifolium*). It may be that in order to develop a TG model which has a linear relationship with measured GPP at small-scale, vascular plants and mosses such as *Sphagnum* need to be considered separately (Huemmrich et al., 2010; Peichl et al., 2018). These differently calibrated models could then be combined in different proportions across the year according to when each type of vegetation is dominant.

There was a clear difference between the GPP values from the chambers and the EC towers, with the EC data giving higher results at all three sites (Figure 6.6). There are many possible reasons for this, including errors from the chamber methodology. The collar insertion method, which involved cutting into the peat and root mass around the collar base, could have damaged the vegetation and so reduced chamber fluxes. Heinemeyer et al. (2011) found that collar insertion prior to using a flux chamber could reduce respiration at peatland sites by up to 30-50%, even several months after insertion. The chamber measurements were also subject to a reduction in PAR, which is likely to result in a reduction in GPP. Background concentrations of CO_2 within the chambers were monitored to ensure they were close to atmospheric levels at the start of each measurement, and as the measurements were only five minutes long CO_2 build-up is unlikely to have affected the results. Some of the chamber data showed noise, suggesting that there were minor leaks where the chamber was not perfectly sealed. The data from these measurements was still useable, but may show slightly lower results than the real flux. It is possible that there were some changes in chamber volume throughout the experimental period due to collar settling and vegetation growth which were not accounted for in the measurements and could have led to slight under or overestimation (Morton and Heinemeyer, 2018).

Factors affecting the EC fluxes may also be responsible for the differences seen. Cross Lochs, which shows a large difference between EC and chamber GPP results, has an open path sensor compared to the other two sites which have closed paths, and this may have led to inaccuracies in the flux measurements (Helbig et al., 2016). Cross Lochs was also dominated during the measurement periods by winds from the South, and some North-

Easterlies, rather than the South-West and North-West directions of the transects, and this may have affected the areas included in the footprint and therefore the overall flux. The ecosystem respiration results are similar from the chambers and the EC tower (not shown), suggesting that the difference is not caused by the partitioning equations used in EC data processing.

Laine et al. (2006) compared NEE from EC and chamber measurements at a blanket bog site in Glencar, Ireland, which is climatically and structurally similar to the Forsinard Flows reserve. They found that there were significant differences between microforms, but that these were linked to soil moisture (Heikkinen et al., 2002, also showed this), corroborating the suggestion that our study period was generally too wet to show much influence on GPP from microforms. Laine et al. (2006) found a correlation of 0.82 between EC and interpolated chamber NEE, even when footprint size and direction variation was not accounted for. They did note, however, that agreement decreased towards the extremes of the temperature range, agreeing with the current work where differences were particularly noticeable in the hot period of July.

Griffis et al. (2000) also compared chamber and EC fluxes, at a subarctic fen in Manitoba. They found that chamber measurements of GPP were 32% lower than EC GPP results, similar to the current work. They also showed that hummocks dominated the CO_2 fluxes, which corresponds with the Lonielist site showing greater agreement between hummock and EC GPP than between hollow and EC GPP. Heikkinen et al. (2002) also found that carbon fluxes from chamber measurements were somewhat lower than those from EC over the same period, at a subarctic fen in Northern Finland.

Application of the TG model with MODIS data and small-scale ‘m’ parameter matched chamber data better than hourly EC data, suggesting that the difference between chamber and EC GPP is not only a result of spatial scale. The TG model is clearly very dependent on calibration to measured data, and therefore the uncertainty of measurements used in the model calibration will form a large part of the uncertainty estimates of the TG model.

Generally, the agreement between the TG model and the measured fluxes is shown to be good at small scale, with correlations of 0.57 to 0.70. The Lonielist and Cross Lochs sites show slightly better agreement than the Talaheel site. Talaheel was also the only site to show almost no connection between microtopography and GPP. This may be due to the recent landscaping of the site to put in peat dams in the remaining planting furrows, which has created large flat areas and deep pools, rather than the more natural small hummocks and hollows. It may be the case that the vegetation species have not had time since the work done in 2015/16 to develop their ecological niches. It is also clear that the water levels

at Talaheel have been increased by the recent drain blocking, and areas which we would consider hollows are often flooded and so unsuitable for taking flux or spectral measurements. This may also be affecting the agreement with the model, as the Talaheel site might be responding to temperature and seasonal changes differently to sites which have had less recent disturbance.

The GPP estimates calculated with the TG model that used data from MODIS were in very good agreement with the GPP derived from EC data (correlations of 0.74 to 0.85). This corroborates the work done on developing the model in Lees et al. (in press). The 'm' parameter calibrated for the TG model against EC data in this study, which uses data from 2017, is higher than that calculated in Lees et al. (in press) which used 2014/15 data. This may be because the growing season of 2017 was particularly wet; this supports the development of the annual Temperature, Greenness and Wetness (TGWa) model in Lees et al. (in press), which associates high summer wetness with increased annual GPP.

The application of the TG model across part of the Flow Country in Figure 6.6 gives an example of how the model could be used to monitor peatland health, and in particular restoration progress. It is evident that areas which have been recently felled have a low GPP, whilst those which were felled a decade ago are shown to have a GPP similar to near-natural blanket bog areas. The size of the MODIS pixels makes the model using this data useful over landscapes where large areas are under consistent management, but less useful over areas of the Forsinard reserve where forestry blocks are small.

Previous studies suggest that finer resolution remote sensing data matches other measurements of GPP better than coarser resolution satellites (Fu et al., 2014; Gonzalez del Castillo et al., 2018; Knox et al., 2017). Fu et al. (2014) found that Landsat-like reflectance at 30 m resolution gave better agreement with Eddy Covariance measurements of GPP than coarser resolution MODIS reflectance across different ecosystems in the USA. Similarly, Gonzalez del Castillo et al. (2018) used proximal measurements of NDVI 10-20 m above the canopy of a tropical dry forest in Mexico to give better agreement with EC data than satellite measurements. Knox et al. (2017) found that a vegetation index calculated using a digital camera at fine spatial resolution gave better agreement with EC GPP than Landsat indices at restored marshland in California. However, all these studies used EC data as a comparison, whereas our study also includes chamber data. We have found that both small-scale spectrometer data and large-scale MODIS data can be used to give good estimates of GPP in peatland landscapes, but the results are dependent on the calibration. Future work should consider aerial remote sensing as an intermediate scale between field spectrometry and satellite data.

6.5. Conclusions

In this study we have used a Temperature and Greenness (TG) model to estimate GPP from remotely sensed data at small-scale and large-scale, and compared this to chamber and EC measures of GPP.

The TG model successfully models the factors which have the greatest relationship with GPP at our study sites, and so produces an estimate of GPP which is comparable at small and large scales. Our results suggest that the differences in GPP caused by peatland small-scale heterogeneity are temporally and spatially inconsistent, and that the TG model provides an average estimate. However, the difference in the NDVI factor of the model between *Sphagnum* and vascular species does appear to have an effect on the relationship between measured and modelled GPP, and it is suggested that future iterations of the TG model for use at small scale should consider the dominant flux influences from different vegetation types across the year.

The EC results for GPP are larger than those from the chambers, possibly due to several reasons including variation within the tower footprint, and the challenges of collar insertion and chamber methodology. Future work should consider taking chamber measurements at higher temporal frequency, possibly using automated chambers, to assess the causes of this discrepancy. The TG model, however, shows good agreement with the chamber data at small-scale and the EC data at large scale, suggesting that the model design is robust at all scales, although dependent on the calibration data used.

Acknowledgements

Thanks are due to the RSPB for their work on this project, and for site access and access to facilities. Thanks also to the Environmental Research Institute (ERI) for their role in restoration monitoring at the Forsinard Flows RSPB reserve. Thanks to Danni Klein for facilitating this work, Graham Hambley, Matthew Saunders, Roxane Andersen and Neil Cowie for site set up and work coordination, and Rebecca McKenzie and Peter Gilbert for site maintenance. Thanks to Kevin White and Suvarna Punalekar for spectroradiometer training. Thanks to Alison Wilkinson for making 48 collars for the fieldwork.

We are very grateful for the help of our field assistants Ainoa Pravia, Jose van Paassen, Paul Gaffney, Wouter Konings, Elias Costa, Zsofi Csillag, Valeria Mazzola, David and Parissa Lumsden, and Joe Croft.

Funding

Kirsten Lees was part funded by a studentship from The James Hutton Institute, and part funded by the Natural Environment Research Council (NERC) SCENARIO DTP (Grant number: NE/L002566/1). Tristan Quaife was funded by the NERC National Centre for Earth Observation (NCEO). Myroslava Khomik and Rebekka Artz were funded by The Scottish Government Strategic Research Programme 2016-2021. Much of the restoration work reported in this study was funded by EU LIFE, Peatland Action, HLF, and the RSPB.

7. Discussion and Conclusions

7.1. Summary of research

Remote sensing data have been used to model carbon fluxes over many different ecosystems, but it is only within the last fifteen years that this has occurred with peatland studies. The literature review showed that there have been very promising results in the use of remote sensing to give information about peatland carbon fluxes (e.g. Connolly et al., 2009; Harris and Dash, 2011; Kross et al., 2016, 2013; Letendre et al., 2008; Schubert et al., 2010; Van Gaalen et al., 2007), but that there are still many challenges for future research. Many of the models discussed in the literature review were developed over forestry, agriculture, or grassland (e.g. Running and Zhao, 2015; Sims et al., 2008; Xiao et al., 2004; Yuan et al., 2007), and it was suggested that the unique features of peatlands, such as water saturation and small-scale heterogeneity, could cause challenges when applying these models to peatland area.

In particular, Chapter 2 highlighted the need for longer-term, larger-scale studies taking into account different study sites around the world. It suggested that future projects which consider the whole carbon cycle, starting with a better understanding of how ecosystem respiration relates to remotely sensed data, will be hugely beneficial. GPP was shown to have reliable correlations with variables which can be measured by remote sensing, such as vegetation indices, whilst other elements of the peatland carbon cycle such as heterotrophic respiration and DOC, are harder to analyse using remote sensing techniques.

The literature review brought out a research gap in the use of remote sensing data at peatland sites undergoing restoration, and the work in this thesis has contributed towards filling that gap. The literature review also suggested that looking into the best spectral indices for use in peatland environments would be helpful to researchers working in this area, as would a better understanding of the issues surrounding microtopography and the upscaling of carbon fluxes across heterogeneous sites. These two issues have both been considered in this thesis, and we are now in a position to suggest answers to some of the questions raised by the literature.

The literature review concludes by suggesting that the most accurate model for peatland GPP using remote sensing data may include a vegetation index such as the NDVI or EVI, a measure of temperature, and a measure of wetness. This has proved to be the case throughout this thesis, and particularly in the development of the TGWa (annual Temperature, Greenness and Wetness) model.

The laboratory study (Chapter 3) into *Sphagnum* drought stress considers the strengths of remote sensing data for detecting changes in photosynthesis of this key peatland genus under extreme conditions. This experiment was designed to consider the effects of different precipitation patterns and long drought periods on *Sphagnum* functioning, as these may become more common as a result of climate change (Hoegh-Guldberg et al., 2018; Jenkins et al., 2010). Recovery after prolonged drought was measured to give more information about *Sphagnum* resilience to desiccation. Spectral reflectance was recorded throughout the experiment, and the areas which showed change were noted, including particularly the red absorption zone. A laboratory study was designed for this part of the project to allow control over the environment and the different inputs of water. The controlled environment also enabled very accurate measures of carbon flux and spectral reflectance to be taken, by minimising background variation.

The work found that there was no significant difference in the carbon function response to drought between the two species, *S. capillifolium* and *S. papillosum*. This was somewhat unexpected, as we had predicted that a hummock-forming species such as *S. capillifolium* would be more resilient to drought than *S. papillosum* which prefers wetter microhabitats. In fact, our results showed that both species were very resilient to drought, and only showed a significant decrease in GPP (compared to the control samples) after approximately 30 days of zero water input. We did find that the optimum water content was different for the two species, and that it was higher for *S. papillosum* as predicted.

The spectral data collected in this study showed a clear decrease in the absorption of red light as the samples were progressively affected by water limitation. This change can be given a numerical value through using the NDVI which considers the difference between the red light wavelengths and the Near Infrared (NIR). The NDVI is easily calculated from satellite bands which are freely available from sources such as MODIS, Landsat and Sentinel-2. There were some limitations to implementing this study in the laboratory rather than under field conditions, for example the removal of *Sphagnum* from its basal stem, the use of deionised water rather than rainwater, and the lack of wind-enhanced drying and drainage from below. If there was the opportunity to study *Sphagnum* GPP and vegetation indices under drought stress in the field, this would improve our understanding of the relationships found here.

Recovery after inundation was assessed as part of this experiment. The samples which had been subjected to uninterrupted drought did not show much sign of carbon function recovery, and still showed no red absorption feature. This suggests that although *Sphagnum* is resilient to drought, once function is affected recovery becomes difficult. This study was

limited, however, by the use of small *Sphagnum* cushion samples with no basal stem contact. It also points to the NDVI as an index which can detect drought damage in *Sphagnum* even after water levels have risen. This chapter concludes by recommending that further work into the recovery of drought-affected *Sphagnum* would aid researchers in determining the likely effects of climate change induced drought periods on blanket bog ecosystems.

Chapter 4 looked at spectral indices in more depth, and aimed to answer some of the questions raised by the literature review concerning which spectral indices give the best information about blanket bog photosynthesis and wetness. It particularly considered the differences in results from broad-band and hyperspectral indices, using data from both the laboratory and the field. The results from this study showed that the NDWI gave the best agreement with laboratory measures of *Sphagnum* wetness. The correlation between NDWI and wetness in the field was less conclusive, and more work needs to be done into the links between water table, which is commonly measured in the field, surface wetness, rainfall, and water indices. Spectral indices which use the difference between the red and near-infrared zones (the EVI, NDVI and the CIm) gave the best agreement with field and lab measures of photosynthesis.

The robust testing of the different indices, in varying conditions in both the field and the laboratory, suggests that these results are reliable. The key outcome of this study is that the use of hyperspectral indices is not necessarily an improvement on broad-band indices, meaning that broad-band satellite sensors such as MODIS can be used with confidence.

In the fifth chapter we validated and adapted the TG (Temperature and Greenness) model for use over blanket bog sites, and then applied it to a chronosequence of restored sites at the Forsinard Flows reserve. The TG model, locally calibrated to each site, was shown to give much better agreement with the EC data than the global MOD17A2H product. In order to improve the inter-annual variation of the model, the wetness factor, based on winter and summer NDWI differences, was added to the TG model, giving the TGWa model introduced in this thesis. This model contains the three elements identified in the literature review as those which would give the best estimate of GPP. This model can be considered a useful addition to peatland monitoring methods, but currently relies on site-specific calibration. Future work should validate the TGWa model against a greater range of peatland sites and assess whether the need for site-specific calibration can be limited.

The developed TGWa model was applied to six different sites across the Forsinard Flows reserve which were felled in different years from 1998 to 2007. The results suggest that photosynthesis increases in the years after felling, and reaches the GPP of near-natural bog

sites after 5 to 10 years. This study is one of the first to use remote sensing data to study peatland restoration progress, and so gives useful information for governments and stakeholders. We suggest that this model is useful as an addition to the range of techniques used to monitor peatland restoration progress, to aid in upscaling point-scale field data to the wider landscape.

One of the concerns raised by the literature review was the difficulty in applying models using coarse resolution satellite data to environments which are so heterogeneous at the microtopographic scale. The upscaling research project in this thesis aimed to further our understanding of the factors affecting peatland GPP at small scales, and whether the TG model can adequately capture the effects of these factors. This chapter also considers the agreement between EC data and the TG model calculated from MODIS data, and whether the results from the satellite data based model and the hand-held spectrometer data based model are comparable.

The results from this study showed that the TG model is scalable as it is based on input variables which affect GPP at both small and large scales. Small-scale heterogeneity of the blanket bog was shown to have minimal effects on the GPP results, although it was noted that 2017 had an unusually cold and wet summer, and microtopography might have been more influential under dryer conditions. The comparison of the TG model results calculated using data from the handheld spectroradiometer with the flux chamber GPP indicated a good performance of the model at small scale. The relationship is not entirely linear, however, and it is suggested that this is an effect of the dominance of different vegetation types across the year. The relationship between the EC data and the MODIS TG model was maintained, although the calibration of the 'm' parameter was different to the results of Chapter 5. Much of the model's goodness of fit is still dependent on calibration methodology, as seen from the difference between EC data and chamber fluxes, which in turn influenced the TG results at different scales. Future work should consider testing the TG model at intermediate scales, perhaps using data from UAVs, and testing a version of the model which includes different calibrations for vascular and non-vascular vegetation.

7.2. Improving conceptualisation of peatland productivity

In order to better visualise the relationships between factors affecting carbon fluxes, and the remote sensing methods we have used in this project to estimate them, a conceptual diagram was created (see Figure 7.1). This diagram is not intended to be the basis of a comprehensive process model, but rather a lens through which to view the progress made in this research project.

Much of the work in this thesis has focused on measuring and estimating GPP, and so this is shown in the central graph of the diagram. The key factors which have been found to control GPP are: PAR, which in turn influences surface temperature; soil and vegetation moisture content, which is linked to rainfall and microtopography (as well as other variables not considered, e.g. wind speed); and vegetation composition and health (which are related to the two previous factors). The vegetation health and composition are detectable using spectral reflectance through indices such as the NDVI.

The laboratory study on drought stress in *Sphagnum* made it clear that water input is a major factor influencing GPP. Chapter 4 on spectral indices shows that the water content of *Sphagnum* samples in the lab was strongly correlated to the water indices tested. The relationship between water input and GPP, and also with the water indices, was also somewhat supported by the fieldwork performed at Forsinard Flows, although as the growing season of 2017 was generally wet throughout the range of moisture contents is minimal. The EFA in chapter 6 indicated that microtopography, moisture levels, and the NDWI were all related to each other, and also have a correlation with GPP.

The two other factors which have an effect on GPP are PAR and surface temperature, which are also related to each other. PAR was shown to have a strong effect on GPP in the laboratory experiment and needed to be corrected for. In the field, surface temperature had a large impact on GPP and was clearly related to incoming solar radiation. Surface temperature functions therefore partly as a proxy for PAR within the TG model, both across the year and across the day.

Vegetation indices using the NIR and red, or red-edge, areas of the spectrum, which were shown to be the most effective for estimating GPP in peatland vegetation, are affected both by the vegetation community and by plant function. The laboratory and field correlations between NDVI and GPP showed different slopes, which we assessed as likely to be related to the difference between *Sphagnum* alone and other peatland vegetation communities. Plant carbon function (ie. the presence and activity of chlorophyll) which is affected by the factors listed above, is largely what determines changes in vegetation indices assuming species is constant. This is seen in both the laboratory and field studies.

The plant species which have the most influence on GPP and red-edge indices vary seasonally. In the winter and early spring months *Sphagnum* is a dominant influence on ecosystem GPP, whilst vascular plants dominate the summer. Because of this, the temperature component of the TG model acts partly as a seasonal modifier on the relationship between NDVI and GPP, minimising the effect of dominant plant species.

Figure 7.1 shows how the TGWa model takes into account the factors we have found to affect GPP. The NDWI is a proxy for surface wetness, the surface temperature is a factor in its own right but also performs as a proxy for PAR, and the vegetation indices take into account both vegetation species and other factors affecting the LUE of plants.

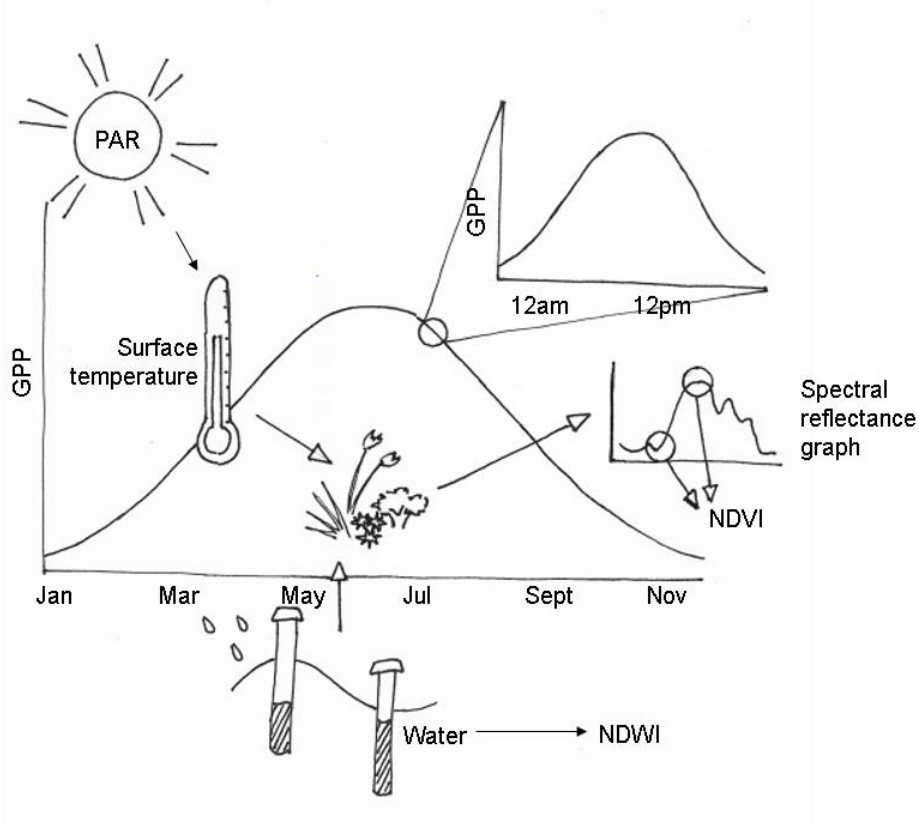

Figure 7.1 – Conceptual diagram of the relationships between key environmental factors and measured variables in this thesis. The central time-series graph represents the annual cycle of GPP, whilst the top right graph shows the daily cycle. The factors which we have found to affect GPP include PAR (represented by the sun), which affects surface temperature (the thermometer) and the relationship between moisture content, microtopography and rainfall (represented in the bottom image by undulating surface topography, water input rainfall, and dipwells). The vegetation health and composition (central image) is affected by both moisture and temperature, resulting in GPP that is detectable by vegetation indices such as the NDVI (represented by the spectral reflectance diagram to the right).

7.3. Wider implications and future work

The success of the TG model across all our study sites and at different scales is a step forward in developing remote sensing methods to study peatland carbon fluxes. Application of this model to restored sites in the Forsinard Flows RSPB reserve is a useful addition to

the growing body of literature which recommends peatland restoration as a carbon emissions reduction technique. We hope that future iterations of this model will be part of the suite of methods used to monitor peatland health and restoration in Great Britain and beyond, and that the estimates it provides will be an asset to groups restoring peatlands under government-funded schemes. Currently we recommend that the model is used in conjunction with other monitoring methods, but we suggest that future work into the site-specific 'm' parameter could increase its usage as a stand-alone measure across large areas. Future work on the TGWa model should include calibrating against more peatland sites around the world, and attempting to discern whether there are other factors related to this calibration which could be added to the model to make it applicable worldwide with less reliance on ground data collection.

Future research from this project could take several different pathways. Work looking at the impact of climate change on peatland ecosystems could continue the research done in Chapter 3 into the damage done to *Sphagnum* moss carbon function by long drought periods, and in particular whether this damage is irreversible. The focus of such work should be on how well vegetation indices such as the NDVI can continue to match photosynthesis measurements during recovery from drought. Water and vegetation indices could then be used to detect peatland areas which are particularly vulnerable to climatic change. The wildfires on English peatlands in the summer of 2018 provide a unique opportunity to use remote sensing for retrospective analysis of the conditions that caused the fire (low moisture content etc.) for future risk modelling.

The understanding of the link between water table depth, water indices, rainfall, moisture content and microtopography could also be improved through further work. To test the link between water indices and field measures, spectral data collected at more frequent intervals across peatlands could be used to assess the relationship to both rainfall, which is commonly measured at meteorological stations, and water table depth, which is often recorded at peatland field sites. Another study on moisture and GPP variation across microtopography could give additional information if completed in a dryer year when the variations are likely to be more pronounced. Such an experiment could be used to suggest whether or not the robustness of the TG model across scales would endure under more extreme conditions.

In addition to this, future work into extending the model to include an estimate of peatland ecosystem respiration would be a good step forward towards being able to model the complete carbon cycle of peatland ecosystems from remote sensing data. Our work in chapter 3 suggests that the correlation between GPP and respiration in *Sphagnum* is strong

and remains constant under drought stress. If this correlation was found to be similar across other peatland vegetation types, modelled GPP could be the starting point for estimating respiration.

Another avenue of potential future work in this area would be to extend the work done on method development in this thesis to a wider range of satellite data sensors, in particular newer satellites with higher spatial resolution such as Sentinel-2. This could be pursued in combination with developing new methods from other available forms of remotely sensed data, for example SAR data from ENVISAT and Sentinel-1.

7.4. Conclusions

Here, the key findings from this project are mapped onto the six research objectives specified in Section 1.2.

Objective 1: To analyse the current state of remote sensing for peatland carbon flux estimation, and to determine the gaps in our knowledge.

It was found that gaps in the literature included an understanding of how peatland microtopography could affect remote sensing based estimates of carbon flux, a thorough consideration of the best indices for estimating peatland carbon fluxes under different conditions, and the use of remote sensing based estimates of carbon flux over peatlands undergoing restoration. These gaps were used as research questions to define the direction of this project. The literature review also found that the best model for estimating peatland GPP was likely to include temperature, a vegetation index, and a measure of wetness.

Objective 2: To assess how peatland vegetation carbon fluxes change under stress, and whether this change is detectable using remote sensing.

The carbon fluxes of *Sphagnum* moss decrease under drought stress, and this change is detectable using remote sensing. The laboratory experiment showed that *Sphagnum* was resilient to drought stress up to approximately 30 days without water. After that period drought damage started to be evident from changes in carbon fluxes, and also changes in the spectral reflectance. The change in the red light area of the reflectance spectrum was particularly interesting, as it did not recover after the samples were rewetted. This suggests that indices such as the NDVI could be useful in detecting long-term *Sphagnum* damage caused by drought.

Objective 3: To compare different spectral indices under a range of conditions and determine which give the most accurate information about peatland environments.

Hyperspectral indices were found to give minimal improvement over broad-band indices on monitoring peatland vegetation health. Using both laboratory and field results, it was evident that the best index for giving information about peatland vegetation moisture content was the NDWI, and the best indices for matching GPP were the NDVI, EVI and the CIm. This shows that broad-band indices, which can easily be calculated from freely available satellite data such as from MODIS, can give useful information about peatland vegetation health.

Objective 4: To develop a model using remote sensing data that can give reliable and accurate estimates of peatland GPP.

The TG model and TGWa model were calibrated and developed for peatland ecosystems and are shown to give good agreement with intra- and inter-annual EC data, respectively, at blanket bog sites. The calibrated TG model gave good agreement with the data available from two restored sites at the Forsinard Flows reserve. The TGWa model incorporates a wetness component on an annual basis which improved the fit with annual values of GPP from EC data at the long-running site at Glencar. This model is suggested as a useful addition to the suite of monitoring methods available for peatland sites undergoing restoration.

Objective 5: To use the developed model to measure restoration progress at a landscape scale.

The TGWa model suggested that peatland restoration at the Forsinard Flows reserve is successful in terms of GPP after five to ten years. This result, drawn from over ten years of applying the TGWa model using satellite data from six sites undergoing restoration across the reserve, is a success story for practitioners. Increasing GPP to near-natural levels is a key aim of peatland restoration, particularly when protecting carbon stores and increasing carbon sequestration is the aim. The work in this study adds to a growing body of evidence that such work is successful over relatively short timescales of less than a decade.

Objective 6: To assess whether the developed model is accurate at both small and large scale, particularly taking into account the small-scale heterogeneity of many peatland landscapes.

The TG model was found to match field measurements of GPP at small and large scales, although the relationship is dependent on model calibration. The TG model results calculated from hand-held spectrometer data matched the flux chamber GPP quite well, and the relationship was maintained for the TG model using MODIS data when the ‘m’ parameter calculated from calibration against the chamber data was applied. When the TG

model using MODIS data was calibrated against EC data the relationship between the model results and the EC values was strong. However, the EC and chamber GPP were different across the growing season, indicating that the success of the TG model is dependent upon the data used for calibration. Heterogeneity had some influence on small-scale GPP, but other factors such as NDVI and temperature were more consistently important.

Overall, the results from the studies included in this project have progressed our understanding of remote sensing for the estimation of peatland carbon uptake. The work described in this thesis has led to a clearer picture of the effects of extreme conditions on carbon flux and spectral reflectance, and has given further evidence that the spectral data available from satellites is useful in monitoring peatland health, even when the available data is at coarse spatial resolutions and produces broad-band indices. The developed TGWa model is proven to be an asset to peatland restoration monitoring, and the application of the model to sites across the Forsinard Flows reserve gave an indication of ongoing restoration success for carbon uptake.

Bibliography

Adkinson, A.C., Humphreys, E.R., 2011. The response of carbon dioxide exchange to manipulations of Sphagnum water content in an ombrotrophic bog. Ecohydrology 4, 733–743. https://doi.org/10.1002/eco.171

Andersen, R., Farrell, C., Graf, M., Muller, F., Calvar, E., Frankard, P., Caporn, S., Anderson, P., 2017. An overview of the progress and challenges of peatland restoration in Western Europe. Restor. Ecol. 25, 271–282. https://doi.org/10.1111/rec.12415

Anderson, K., Bennie, J.J., Milton, E.J., Hughes, P.D.M., Lindsay, R., Meade, R., 2010. Combining LiDAR and IKONOS Data for Eco-Hydrological Classification of an Ombrotrophic Peatland. J. Environ. Qual. 39, 260. https://doi.org/10.2134/jeq2009.0093

Anderson, M.C., Norman, J.M., Kustas, W.P., Houborg, R., Starks, P.J., Agam, N., 2008. A thermal-based remote sensing technique for routine mapping of land-surface carbon, water and energy fluxes from field to regional scales. Remote Sens. Environ. 112, 4227–4241. https://doi.org/10.1016/J.RSE.2008.07.009

Arroyo-Mora, J., Kalacska, M., Soffer, R., Moore, T., Roulet, N., Juutinen, S., Ifimov, G., Leblanc, G., Inamdar, D., Arroyo-Mora, J.P., Kalacska, M., Soffer, R.J., Moore, T.R., Roulet, N.T., Juutinen, S., Ifimov, G., Leblanc, G., Inamdar, D., 2018. Airborne Hyperspectral Evaluation of Maximum Gross Photosynthesis, Gravimetric Water Content, and CO2 Uptake Efficiency of the Mer Bleue Ombrotrophic Peatland. Remote Sens. 10, 565. https://doi.org/10.3390/rs10040565

Backeus, I., 1988. Weather variables as predictors of Sphagnum growth on a bog. Ecography (Cop.). 11, 146–150. https://doi.org/10.1111/j.1600-0587.1988.tb00793.x

Bain, C.G., Bonn, A., Stoneman, R., Chapman, S., Coupar, A., Evans, M., Gearey, B., Howat, M., Keenleyside, C., Lindsay, J., Littlewood, R., Orr, A., Reed, H., Smith, M., Swales, P., Thompson, V., Thompson, D.B.A., 2011. UK Commission of Inquiry on Peatlands. IUCN UK Peatland Programme.

Balzarolo, M., Vicca, S., Nguy-Robertson, A.L., Bonal, D., Elbers, J.A., Fu, Y.H., Grünwald, T., Horemans, J.A., Papale, D., Peñuelas, J., Suyker, A., Veroustraete, F., 2016. Matching the phenology of Net Ecosystem Exchange and vegetation indices estimated with MODIS and FLUXNET in-situ observations. Remote Sens. Environ. 174, 290–300. https://doi.org/10.1016/J.RSE.2015.12.017

Baranoski, G.V.G., Rokne, J.G., 2005. A practical approach for estimating the red edge position of plant leaf reflectance. Int. J. Remote Sens. 26, 503–521.

https://doi.org/10.1080/01431160512331314029

Basiliko, N., Blodau, C., Roehm, C., Bengtson, P., Moore, T.R., 2007. Regulation of Decomposition and Methane Dynamics across Natural, Commercially Mined, and Restored Northern Peatlands. Ecosystems 10, 1148–1165. https://doi.org/10.1007/s10021-007-9083-2

Beetz, S., Liebersbach, H., Glatzel, S., Jurasinski, G., Buczko, U., Höper, H., 2013. Effects of land use intensity on the full greenhouse gas balance in an Atlantic peat bog. Biogeosciences 10, 1067–1082. https://doi.org/10.5194/bg-10-1067-2013

Belyeal, L.R., Clymo2, R.S., 2001. Feedback control of the rate of peat formation 268, 1315–1321. https://doi.org/10.1098/rspb.2001.1665

Bonn, A., Allott, T., Evans, M., Joosten, H., Stoneman, R., 2016. Peatland restoration and ecosystem services: science, policy and practice. Peatl. Restor. Ecosyst. Serv. Sci. policy Pract.

Bonnet, S., Ross, S., Linstead, C., Maltby, E., 2009. A review of techniques for monitoring the success of peatland restoration.

Bortoluzzi, E., Epron, D., Siegenthaler, A., Gilbert, D., Buttler, A., 2006. Carbon balance of a European mountain bog at contrasting stages of regeneration. New Phytol. 172, 708–718. https://doi.org/10.1111/j.1469-8137.2006.01859.x

Bragazza, L., 2008. A climatic threshold triggers the die-off of peat mosses during an extreme heat wave. Glob. Chang. Biol. 14, 2688–2695. https://doi.org/10.1111/j.1365-2486.2008.01699.x

British Geological Survey, 2007. Geology of Britain.

Bryant, R.G., Baird, A.J., 2003. The spectral behaviour of *Sphagnum* canopies under varying hydrological conditions. Geophys. Res. Lett. 30, 1134. https://doi.org/10.1029/2002GL016053

Bubier, J.L., Bhatia, G., Moore, T.R., Roulet, N.T., Lafleur, P.M., 2003. Spatial and Temporal Variability in Growing-Season Net Ecosystem Carbon Dioxide Exchange at a Large Peatland in Ontario, Canada. https://doi.org/10.1007/s10021-003-0125-0

Bubier, J.L., Rock, B.N., Crill, P.M., 1997. Spectral reflectance measurements of boreal wetland and forest mosses. J. Geophys. Res. Atmos. 102, 29483–29494. https://doi.org/10.1029/97JD02316

Bussel, J., Jones, D., Healey, J., Pullin, A., 2010. How do draining and re-wetting affect

carbon stores and greenhouse gas fluxes in peatland soils? CEE review 08-012 (SR49).

Chapman, S.J., Bell, J., Donnelly, D., Lilly, A., 2009. Carbon stocks in Scottish peatlands. Soil Use Manag. 25, 105–112. https://doi.org/10.1111/j.1475-2743.2009.00219.x

Chasmer, L., Baker, T., Carey, S.K., Straker, J., Strilesky, S., Petrone, R., 2018. Monitoring ecosystem reclamation recovery using optical remote sensing: Comparison with field measurements and eddy covariance. Sci. Total Environ. 642, 436–446. https://doi.org/10.1016/j.scitotenv.2018.06.039

Chong, M., Humphreys, E., Moore, T.R., 2012. Microclimatic response to increasing shrub cover and its effect on *Sphagnum* CO_2 exchange in a bog. Écoscience 19, 89–97. https://doi.org/10.2980/19-1-3489

Christian, B., Joshi, N., Saini, M., Mehta, N., Goroshi, S., Nidamanuri, R.R., Thenkabail, P., Desai, A.R., Krishnayya, N.S.R., 2015. Seasonal variations in phenology and productivity of a tropical dry deciduous forest from MODIS and Hyperion. Agric. For. Meteorol. 214–215, 91–105. https://doi.org/10.1016/J.AGRFORMET.2015.08.246

Cigna, F., Sowter, A., 2017. The relationship between intermittent coherence and precision of ISBAS InSAR ground motion velocities: ERS-1/2 case studies in the UK. Remote Sens. Environ. 202, 177–198. https://doi.org/10.1016/J.RSE.2017.05.016

Clark, J., Gallego-Sala, A., Allott, T., Chapman, S., Farewell, T., Freeman, C., House, J., Orr, H., Prentice, I., Smith, P., 2010. Assessing the vulnerability of blanket peat to climate change using an ensemble of statistical bioclimatic envelope models. Clim. Res. 45, 131–150. https://doi.org/10.3354/cr00929

Clark, J.M., Chapman, P.J., Heathwaite, A.L., Adamson, J.K., 2006. Suppression of dissolved organic carbon by sulfate induced acidification during simulated droughts. Environ. Sci. Technol. 40, 1776–83.

Clark, J.M., Heinemeyer, A., Martin, P., Bottrell, S.H., 2012. Processes controlling DOC in pore water during simulated drought cycles in six different UK peats. Biogeochemistry 109, 253–270. https://doi.org/10.1007/s10533-011-9624-9

Clement, R.J., Burba, G.G., Grelle, A., Anderson, D.J., Moncrieff, J.B., 2009. Improved trace gas flux estimation through IRGA sampling optimization. Agric. For. Meteorol. 149, 623–638. https://doi.org/10.1016/J.AGRFORMET.2008.10.008

Clymo, R.S., 1973. The growth of *Sphagnum*: some effects of environment., Source: Journal

of Ecology.

Cole, B., McMorrow, J., Evans, M., 2014. Spectral monitoring of moorland plant phenology to identify a temporal window for hyperspectral remote sensing of peatland. ISPRS J. Photogramm. Remote Sens. 90, 49–58. https://doi.org/10.1016/J.ISPRSJPRS.2014.01.010

Connolly, J., Roulet, N.T., Seaquist, J.W., Holden, N.M., Lafleur, P.M., Humphreys, E.R., Heumann, B.W., Ward, S.M., 2009. Using MODIS derived PAR with ground based flux tower measurements to derive the light use efficiency for two Canadian peatlands. Biogeosciences 6, 225–234. https://doi.org/10.5194/bg-6-225-2009

Couwenberg, J., Thiele, A., Tanneberger, F., Augustin, J., Bärisch, S., Dubovik, D., Liashchynskaya, N., Michaelis, D., Minke, M., Skuratovich, A., Joosten, H., 2011. Assessing greenhouse gas emissions from peatlands using vegetation as a proxy. Hydrobiologia 674, 67–89. https://doi.org/10.1007/s10750-011-0729-x

Crichton, K.A., Anderson, K., Bennie, J.J., Milton, E.J., 2015. Characterizing peatland carbon balance estimates using freely available Landsat ETM+ data. Ecohydrology 8, 493–503. https://doi.org/10.1002/eco.1519

Dash, J., Curran, P.J., 2004. The MERIS terrestrial chlorophyll index. Int. J. Remote Sens. 25, 5403–5413. https://doi.org/10.1080/0143116042000274015

Desai, A.R., Moore, D.J.P., Ahue, W.K.M., Wilkes, P.T. V., De Wekker, S.F.J., Brooks, B.G., Campos, T.L., Stephens, B.B., Monson, R.K., Burns, S.P., Quaife, T., Aulenbach, S.M., Schimel, D.S., 2011. Seasonal pattern of regional carbon balance in the central Rocky Mountains from surface and airborne measurements. J. Geophys. Res. 116, G04009. https://doi.org/10.1029/2011JG001655

Didan, K., 2015. MOD13Q1 V006 | LP DAAC :: NASA Land Data Products and Services. https://doi.org/10.5067/MODIS/MOD13Q1.006

Didan, K., Barreto Munoz, A., Solano, R., Huete, A., 2015. MODIS Vegetation Index User's Guide (MOD13 Series).

DigitalGlobe, 2016. About our constellation [WWW Document]. URL https://www.digitalglobe.com/about/our-constellation (accessed 10.28.16).

Dinsmore, K.J., Skiba, U.M., Billett, M.F., Rees, R.M., 2009a. Effect of water table on greenhouse gas emissions from peatland mesocosms. Plant Soil 318, 229–242. https://doi.org/10.1007/s11104-008-9832-9

Dinsmore, K.J., Skiba, U.M., Billett, M.F., Rees, R.M., Drewer, J., 2009b. Spatial and temporal variability in CH4 and N2O fluxes from a Scottish ombrotrophic peatland: Implications for modelling and up-scaling. Soil Biol. Biochem. 41, 1315–1323. https://doi.org/10.1016/j.soilbio.2009.03.022

Dong, J., Xiao, X., Wagle, P., Zhang, G., Zhou, Y., Jinwei Dong, A., Jin, C., Torn, M.S., Meyers, T.P., Suyker, A.E., Wang, J., Yan, H., Biradar, C., Moore III, B., 2015. Comparison of four EVI-based models for estimating gross primary production of maize and soybean croplands and tallgrass prairie under severe drought. Pap. Nat. Resour. Nat. Resour. 2015. https://doi.org/10.1016/j.rse.2015.02.022

Drolet, G.G., Huemmrich, K.F., Hall, F.G., Middleton, E.M., Black, T.A., Barr, A.G., Margolis, H.A., 2005. A MODIS-derived photochemical reflectance index to detect inter-annual variations in the photosynthetic light-use efficiency of a boreal deciduous forest. Remote Sens. Environ. 98, 212–224. https://doi.org/10.1016/J.RSE.2005.07.006

EnMAP, 2016. EnMAP - hyperspectral imager [WWW Document]. URL http://www.enmap.org/ (accessed 10.28.16).

ESA, 2017. MERIS [WWW Document]. URL https://earth.esa.int/web/guest/missions/esa-operational-eo-missions/envisat/instruments/meris (accessed 4.4.17).

ESA, 2016. ESA EO missions [WWW Document]. URL https://earth.esa.int/web/guest/missions/esa-eo-missions (accessed 10.28.16).

ESA, 2015. No 42–2015: FLEX mission to be next ESA Earth Explorer. [WWW Document]. URL http://www.esa.int/For_Media/Press_Releases/FLEX_mission_to_be_next_ESA_Earth_Explorer (accessed 10.28.16).

European Commission, 2018. Regulation on land use, land use change and forestry in 2030 climate and energy framework adopted | Climate Action [WWW Document]. URL https://ec.europa.eu/clima/news/regulation-land-use-land-use-change-and-forestry-2030-climate-and-energy-framework-adopted_en (accessed 7.9.18).

European environment agency, 2017. Nationally designated areas (CDDA).

Feng Gao, Masek, J., Schwaller, M., Hall, F., 2006. On the blending of the Landsat and MODIS surface reflectance: predicting daily Landsat surface reflectance. IEEE Trans. Geosci. Remote Sens. 44, 2207–2218. https://doi.org/10.1109/TGRS.2006.872081

Fleischer, E., Khashimov, I., Hölzel, N., Klemm, O., 2016. Carbon exchange fluxes over

peatlands in Western Siberia: Possible feedback between land-use change and climate change. Sci. Total Environ. 545–546, 424–433. https://doi.org/10.1016/J.SCITOTENV.2015.12.073

Forbrich, I., Kutzbach, L., Wille, C., Becker, T., Wu, J., Wilmking, M., 2011. Cross-evaluation of measurements of peatland methane emissions on microform and ecosystem scales using high-resolution landcover classification and source weight modelling. Agric. For. Meteorol. 151, 864–874. https://doi.org/10.1016/J.AGRFORMET.2011.02.006

Frankenberg, C., O'Dell, C., Berry, J., Guanter, L., Joiner, J., Köhler, P., Pollock, R., Taylor, T.E., 2014. Prospects for chlorophyll fluorescence remote sensing from the Orbiting Carbon Observatory-2. Remote Sens. Environ. 147, 1–12. https://doi.org/10.1016/J.RSE.2014.02.007

Frolking, S.E., Bubier, J.L., Moore, T.R., Ball, T., Bellisario, L.M., Bhardwaj, A., Carroll, P., Crill, P.M., Lafleur, P.M., McCaughey, J.H., Roulet, N.T., Suyker, A.E., Verma, S.B., Waddington, J.M., Whiting, G.J., 1998. Relationship between ecosystem productivity and photosynthetically active radiation for northern peatlands. Global Biogeochem. Cycles 12, 115–126. https://doi.org/10.1029/97GB03367

Fu, D., Chen, B., Zhang, H., Wang, J., Black, T.A., Amiro, B.D., Bohrer, G., Bolstad, P., Coulter, R., Rahman, A.F., Dunn, A., McCaughey, J.H., Meyers, T., Verma, S., 2014. Estimating landscape net ecosystem exchange at high spatial–temporal resolution based on Landsat data, an improved upscaling model framework, and eddy covariance flux measurements. Remote Sens. Environ. 141, 90–104. https://doi.org/10.1016/J.RSE.2013.10.029

Gaffney, P.P.J., Hancock, M.H., Taggart, M.A., Andersen, R., 2018. Measuring restoration progress using pore- and surface-water chemistry across a chronosequence of formerly afforested blanket bogs. J. Environ. Manage. 219, 239–251. https://doi.org/10.1016/j.jenvman.2018.04.106

Gamon, J.A., Peñuelas, J., Field, C.B., 1992. A narrow-waveband spectral index that tracks diurnal changes in photosynthetic efficiency. Remote Sens. Environ. 41, 35–44. https://doi.org/10.1016/0034-4257(92)90059-S

Gao, B., 1996. NDWI—A normalized difference water index for remote sensing of vegetation liquid water from space. Remote Sens. Environ. 58, 257–266. https://doi.org/10.1016/S0034-4257(96)00067-3

Gao, Y., Yu, G., Li, S., Yan, H., Zhu, X., Wang, Q., Shi, P., Zhao, L., Li, Y., Zhang, F., Wang,

Y., Zhang, J., 2015. A remote sensing model to estimate ecosystem respiration in Northern China and the Tibetan Plateau. Ecol. Modell. 304, 34–43. https://doi.org/10.1016/J.ECOLMODEL.2015.03.001

Garbulsky, M.F., Peñuelas, J., Gamon, J., Inoue, Y., Filella, I., 2011. The photochemical reflectance index (PRI) and the remote sensing of leaf, canopy and ecosystem radiation use efficiencies: A review and meta-analysis. Remote Sens. Environ. 115, 281–297. https://doi.org/10.1016/J.RSE.2010.08.023

Garrigues, S., Lacaze, R., Baret, F., Morisette, J.T., Weiss, M., Nickeson, J.E., Fernandes, R., Plummer, S., Shabanov, N. V., Myneni, R.B., Knyazikhin, Y., Yang, W., 2008. Validation and intercomparison of global Leaf Area Index products derived from remote sensing data. J. Geophys. Res. Biogeosciences 113, n/a-n/a. https://doi.org/10.1029/2007JG000635

Gatis, N., Anderson, K., Grand-Clement, E., Luscombe, D.J., Hartley, I.P., Smith, D., Brazier, R.E., 2017. Evaluating MODIS vegetation products using digital images for quantifying local peatland CO_2 gas fluxes. Remote Sens. Ecol. Conserv. 3, 217–231. https://doi.org/10.1002/rse2.45

Geophysical and Environmental Research corp., 1999. GER 3700 User Manual Release 2.1. Milbrook, New York.

Gitelson, A.A., Peng, Y., Masek, J.G., Rundquist, D.C., Verma, S., Suyker, A., Baker, J.M., Hatfield, J.L., Meyers, T., 2012. Remote estimation of crop gross primary production with Landsat data. Remote Sens. Environ. 121, 404–414. https://doi.org/10.1016/J.RSE.2012.02.017

Glenn, A.J., Syed, K.H., Carlson, P.J., 2006. Comparison of net ecosystem CO2 exchange in two peatlands in western Canada with contrasting dominant vegetation, Sphagnum and Carex. Agric. For. Meteorol. 140, 115–135. https://doi.org/10.1016/J.AGRFORMET.2006.03.020

Goerner, A., Reichstein, M., Tomelleri, E., Hanan, N., Rambal, S., Papale, D., Dragoni, D., Schmullius, C., 2011. Remote sensing of ecosystem light use efficiency with MODIS-based PRI. Biogeosciences 8, 189–202. https://doi.org/10.5194/bg-8-189-2011

Gonzalez del Castillo, E., Sanchez-Azofeifa, A., Paw U, K.T., Gamon, J.A., Quesada, M., 2018. Integrating proximal broad-band vegetation indices and carbon fluxes to model gross primary productivity in a tropical dry forest. Environ. Res. Lett. 13, 065017. https://doi.org/10.1088/1748-9326/aac3f0

Gorham, E., 1991. Northern Peatlands: Role in the Carbon Cycle and Probable Responses to Climatic Warming. Ecol. Appl. 1, 182–195. https://doi.org/10.2307/1941811

Grace, J., Nichol, C., Disney, M., Lewis, P., Quaife, T., Bowyer, P., 2007. Can we measure terrestrial photosynthesis from space directly, using spectral reflectance and fluorescence? Glob. Chang. Biol. 13, 1484–1497. https://doi.org/10.1111/j.1365-2486.2007.01352.x

Griffis, T.J., Rouse, W.R., Waddington, J.M., 2000. Scaling net ecosystem CO2 exchange from the community to landscape-level at a subarctic fen. Glob. Chang. Biol. 6, 459–473. https://doi.org/10.1046/j.1365-2486.2000.00330.x

Guanter, L., Alonso, L., Gómez-Chova, L., Amorós-López, J., Vila, J., Moreno, J., 2007. Estimation of solar-induced vegetation fluorescence from space measurements. Geophys. Res. Lett. 34. https://doi.org/10.1029/2007GL029289

Gunnarsson, U., 2005. Global patterns of Sphagnum productivity. J. Bryol. 27, 269–279. https://doi.org/10.1179/174328205X70029

Hambley, G., 2016. The effect of forest-to-bog restoration on net ecosystem exchange in The Flow Country peatlands. University of St Andrews.

Hambley, G., Andersen, R., Levy, P., Saunders, M., Cowie, N.R., Teh, Y.A., Hill, T.C., 2019. Net ecosystem exchange from two formerly afforested peatlands undergoing restoration in the Flow Country of Northern Scotland. Mires Peat 23, 1–14.

Hancock, M.H., Klein, D., Andersen, R., Cowie, N.R., 2018. Vegetation response to restoration management of a blanket bog damaged by drainage and afforestation. Appl. Veg. Sci. 21, 167–178. https://doi.org/10.1111/avsc.12367

Harris, A., 2008. Spectral reflectance and photosynthetic properties of Sphagnum mosses exposed to progressive drought. Ecohydrology 1, 35–42. https://doi.org/10.1002/eco.5

Harris, A., Bryant, R., Baird, A., 2005. Detecting near-surface moisture stress in spp. Remote Sens. Environ. 97, 371–381. https://doi.org/10.1016/j.rse.2005.05.001

Harris, A., Bryant, R.G., 2009. A multi-scale remote sensing approach for monitoring northern peatland hydrology: Present possibilities and future challenges. J. Environ. Manage. 90, 2178–2188. https://doi.org/10.1016/j.jenvman.2007.06.025

Harris, A., Bryant, R.G., Baird, A.J., 2006. Mapping the effects of water stress on Sphagnum: Preliminary observations using airborne remote sensing. Remote Sens. Environ. 100, 363–378. https://doi.org/10.1016/J.RSE.2005.10.024

Harris, A., Dash, J., 2011. A new approach for estimating northern peatland gross primary productivity using a satellite-sensor-derived chlorophyll index. J. Geophys. Res. 116, G04002. https://doi.org/10.1029/2011JG001662

Harris, A., Gamon, J.A., Pastorello, G.Z., Wong, C.Y.S., 2014. Retrieval of the photochemical reflectance index for assessing xanthophyll cycle activity: a comparison of near-surface optical sensors. Biogeosciences 11, 6277–6292. https://doi.org/10.5194/bg-11-6277-2014

Hayward, P.M., Clymo, R.S., 1983. The Growth of Sphagnum: Experiments on, and Simulation of, Some Effects of Light Flux and Water-Table Depth. J. Ecol. 71, 845. https://doi.org/10.2307/2259597

Hayward, P.M., Clymo, R.S., 1982. Profiles of Water Content and Pore Size in Sphagnum and Peat, and their Relation to Peat Bog Ecology. Proc. R. Soc. B Biol. Sci. 215, 299–325. https://doi.org/10.1098/rspb.1982.0044

Heikkinen, J.E.P., Maljanen, M., Aurela, M., Hargreaves, K.J., Martikainen, P.J., 2002. Carbon dioxide and methane dynamics in a sub-Arctic peatland in northern Finland. Polar Res. 21, 49–62. https://doi.org/10.3402/polar.v21i1.6473

Heinemeyer, A., Di Bene, C., Lloyd, A.R., Tortorella, D., Baxter, R., Huntley, B., Gelsomino, A., Ineson, P., 2011. Soil respiration: implications of the plant-soil continuum and respiration chamber collar-insertion depth on measurement and modelling of soil CO2 efflux rates in three ecosystems. Eur. J. Soil Sci. 62, 82–94. https://doi.org/10.1111/j.1365-2389.2010.01331.x

Heinemeyer, A., Gornall, J., Baxter, R., Huntley, B., Ineson, P., 2013. Evaluating the carbon balance estimate from an automated ground-level flux chamber system in artificial grass mesocosms. Ecol. Evol. 3, 4998–5010. https://doi.org/10.1002/ece3.879

Heinsch, F.A., Maosheng Zhao, Running, S.W., Kimball, J.S., Nemani, R.R., Davis, K.J., Bolstad, P.V., Cook, B.D., Desai, A.R., Ricciuto, D.M., Law, B.E., Oechel, W.C., Hyojung Kwon, Hongyan Luo, Wofsy, S.C., Dunn, A.L., Munger, J.W., Baldocchi, D.D., Liukang Xu, Hollinger, D.Y., Richardson, A.D., Stoy, P.C., Siqueira, M.B.S., Monson, R.K., Burns, S.P., Flanagan, L.B., 2006. Evaluation of remote sensing based terrestrial productivity from MODIS using regional tower eddy flux network observations. IEEE Trans. Geosci. Remote Sens. 44, 1908–1925. https://doi.org/10.1109/TGRS.2005.853936

Helbig, M., Wischnewski, K., Gosselin, G.H., Biraud, S.C., Bogoev, I., Chan, W.S.,

Euskirchen, E.S., Glenn, A.J., Marsh, P.M., Quinton, W.L., Sonnentag, O., 2016. Addressing a systematic bias in carbon dioxide flux measurements with the EC150 and the IRGASON open-path gas analyzers. Agric. For. Meteorol. 228–229, 349–359. https://doi.org/10.1016/J.AGRFORMET.2016.07.018

Helfter, C., Campbell, C., Dinsmore, K.J., Drewer, J., Coyle, M., Anderson, M., Skiba, U., Nemitz, E., Billett, M.F., Sutton, M.A., 2015. Drivers of long-term variability in CO₂ net ecosystem exchange in a temperate peatland. Biogeosciences 12, 1799–1811. https://doi.org/10.5194/bg-12-1799-2015

Hermans, R.E.M., 2018, Impact of forest-to-bog restoration on greenhouse gas fluxes. University of Stirling.

Hilker, T., Coops, N.C., Wulder, M.A., Black, T.A., Guy, R.D., 2008. The use of remote sensing in light use efficiency based models of gross primary production: A review of current status and future requirements. Sci. Total Environ. 404, 411–423. https://doi.org/10.1016/J.SCITOTENV.2007.11.007

Hill, T., Chocholek, M., Clement, R., 2017. The case for increasing the statistical power of eddy covariance ecosystem studies: why, where and how? Glob. Chang. Biol. 23, 2154–2165. https://doi.org/10.1111/gcb.13547

Hill, T.C., Quaife, T., Williams, M., 2011. A data assimilation method for using low-resolution Earth observation data in heterogeneous ecosystems. J. Geophys. Res. 116, D08117. https://doi.org/10.1029/2010JD015268

Hiraishi, T., Krug, T., Tanabe, K., Srivastava, N., Jamsranjav, B., Fukuda, M., Troxler, T., 2014. Revised Supplementary Methods and Good Practice Guidance Arising from the Kyoto Protocol.

Hoegh-Guldberg, O., Jacob, D., Taylor, M., 2018. Chapter 3: Impacts of 1.5^{o}C global warming on natural and human systems.

Holden, J., Shotbolt, L., Bonn, A., Burt, T.P., Chapman, P.J., Dougill, A.J., Fraser, E.D.G., Hubacek, K., Irvine, B., Kirkby, M.J., Reed, M.S., Prell, C., Stagl, S., Stringer, L.C., Turner, A., Worrall, F., 2007. Environmental change in moorland landscapes. Earth-Science Rev. 82, 75–100. https://doi.org/10.1016/J.EARSCIREV.2007.01.003

Huemmrich, K.., Gamon, J.A., Tweedie, C.E., Oberbauer, S.F., Kinoshita, G., Houston, S., Kuchy, A., Hollister, R.D., Kwon, H., Mano, M., Harazono, Y., Webber, P.J., Oechel, W.C., 2010. Remote sensing of tundra gross ecosystem productivity and light use

efficiency under varying temperature and moisture conditions. Remote Sens. Environ. 114, 481–489. https://doi.org/10.1016/J.RSE.2009.10.003

Huete, A., Didan, K., Miura, T., Rodriguez, E.., Gao, X., Ferreira, L.., 2002. Overview of the radiometric and biophysical performance of the MODIS vegetation indices. Remote Sens. Environ. 83, 195–213. https://doi.org/10.1016/S0034-4257(02)00096-2

Humphreys, E.R., Lafleur, P.M., Flanagan, L.B., Hedstrom, N., Syed, K.H., Glenn, A.J., Granger, R., 2006. Summer carbon dioxide and water vapor fluxes across a range of northern peatlands. J. Geophys. Res. Biogeosciences 111. https://doi.org/10.1029/2005JG000111

Irving, W., Zhou, L., 2013, Review Editors Overview 2013 Revised Supplementary Methods and Good Practice Guidance Arising from the Kyoto Protocol.

IUCN, 2016. A Secure Peatland Future A vision and strategy for the protection, restoration and sustainable management of UK peatlands [WWW Document]. URL http://www.iucn-uk-peatlandprogramme.org/sites/www.iucn-uk-peatlandprogramme.org/files/CONSULTATION DRAFT A Secure Peatland Future_WEB.pdf (accessed 7.9.18).

Jägermeyr, J., Gerten, D., Lucht, W., Hostert, P., Migliavacca, M., Nemani, R., 2014. A high-resolution approach to estimating ecosystem respiration at continental scales using operational satellite data. Glob. Chang. Biol. 20, 1191–1210. https://doi.org/10.1111/gcb.12443

Jenkins, G., Murphy, J., Sexton, D., Lowe, J., Jones, P., Watson, R., Scientific Advisor, C., 2010. UK Climate Projections: Briefing report Foreword from Professor.

JNCC, 2011. Towards an assessment of the state of UK peatlands.

Kasischke, E.S., Bourgeau-Chavez, L.L., Rober, A.R., Wyatt, K.H., Waddington, J.M., Turetsky, M.R., 2009. Effects of soil moisture and water depth on ERS SAR backscatter measurements from an Alaskan wetland complex. Remote Sens. Environ. 113 1868-1873 113, 1868–1873.

Ketcheson, S.J., Price, J.S., 2014. Characterization of the fluxes and stores of water within newly formed *Sphagnum* moss cushions and their environment. Ecohydrology 7, 771–782. https://doi.org/10.1002/eco.1399

Knox, S.H., Dronova, I., Sturtevant, C., Oikawa, P.Y., Matthes, J.H., Verfaillie, J., Baldocchi, D., 2017. Using digital camera and Landsat imagery with eddy covariance data to

model gross primary production in restored wetlands. Agric. For. Meteorol. 237–238, 233–245. https://doi.org/10.1016/J.AGRFORMET.2017.02.020

Koehler, A.-K., Sottocornola, M., Kiely, G., 2011. How strong is the current carbon sequestration of an Atlantic blanket bog? Glob. Chang. Biol. 17, 309–319. https://doi.org/10.1111/j.1365-2486.2010.02180.x

Kraft, S., Bello, U. Del, Drusch, M., Gabriele, A., 2014. FLORIS: The Fluorescence Imaging Spectrometer of the Earth Explorer Mission Candidate FLEX.

Kross, A., Seaquist, J.W., Roulet, N.T., 2016. Light use efficiency of peatlands: Variability and suitability for modeling ecosystem production. Remote Sens. Environ. 183, 239–249. https://doi.org/10.1016/J.RSE.2016.05.004

Kross, A., Seaquist, J.W., Roulet, N.T., Fernandes, R., Sonnentag, O., 2013. Estimating carbon dioxide exchange rates at contrasting northern peatlands using MODIS satellite data. Remote Sens. Environ. 137, 234–243. https://doi.org/10.1016/J.RSE.2013.06.014

Lafleur, P.M., Roulet, N.T., Bubier, J.L., Frolking, S., Moore, T.R., 2003. Interannual variability in the peatland-atmosphere carbon dioxide exchange at an ombrotrophic bog. Global Biogeochem. Cycles 17, n/a-n/a. https://doi.org/10.1029/2002GB001983

Laine, A., Sottocornola, M., Kiely, G., Byrne, K.A., Wilson, D., Tuittila, E.-S., 2006. Estimating net ecosystem exchange in a patterned ecosystem: Example from blanket bog. Agric. For. Meteorol. 138, 231–243. https://doi.org/10.1016/J.AGRFORMET.2006.05.005

Laine, J., Helsingin yliopisto. Metsäekologian laitos., 2009. The intricate beauty of Sphagnum mosses : a Finnish guide for identification. Department of Forest Ecology, University of Helsinki.

Landsberg, J.J., Waring, R.H., 1997. A generalised model of forest productivity using simplified concepts of radiation-use efficiency, carbon balance and partitioning. For. Ecol. Manage. 95, 209–228. https://doi.org/10.1016/S0378-1127(97)00026-1

Le Clec'h, S., Sloan, S., Gond, V., Cornu, G., Decaens, T., Dufour, S., Grimaldi, M., Oszwald, J., 2018. Mapping ecosystem services at the regional scale: the validity of an upscaling approach. Int. J. Geogr. Inf. Sci. 32, 1593–1610. https://doi.org/10.1080/13658816.2018.1445256

Lees, K.J., Artz, R.R.E., Khomik, M., Clark, J., Ritson, J., Quaife, T., in prep. Broad-band indices perform as well as hyperspectral indices in estimating peatland photosynthesis

and water content. IEEE Trans. Geosci. Remote Sens.

Lees, K.J., Clark, J.M., Quaife, T., Khomik, M., Artz, R.R.E., in review. Changes in carbon flux and spectral reflectance of Sphagnum mosses as a result of simulated drought. J. Ecol.

Lees, K.J., Quaife, T., Artz, R.R.E., Khomik, M., Clark, J.M., 2018. Potential for using remote sensing to estimate carbon fluxes across northern peatlands – A review. Sci. Total Environ. 615, 857–874. https://doi.org/10.1016/J.SCITOTENV.2017.09.103

Lees, K.J., Quaife, T., Artz, R.R.E., Khomik, M., Sottocornola, M., Kiely, G., Hambley, G., Hill, T.C., Saunders, M., Cowie, N.R., Ritson, J., Clark, J.M., in press. A model of gross primary productivity based on satellite data suggests formerly afforested peatlands undergoing restoration regain full photosynthesis capacity after five to ten years. J. Environ. Manage.

Letendre, J., Poulin, M., Rochefort, L., 2008. Sensitivity of spectral indices to CO_2 fluxes for several plant communities in a *Sphagnum* -dominated peatland. Can. J. Remote Sens. 34, S414–S425. https://doi.org/10.5589/m08-053

Levy, P.E., Gray, A., 2015. Greenhouse gas balance of a semi-natural peatbog in northern Scotland. Environ. Res. Lett. 10, 094019. https://doi.org/10.1088/1748-9326/10/9/094019

Limpens, J., Berendse, F., Blodau, C., Canadell, J.G., Freeman, C., Holden, J., Roulet, N., Rydin, H., Schaepman-Strub, G., 2008. Peatlands and the carbon cycle: from local processes to global implications – a synthesis. Biogeosciences 5, 1475–1491. https://doi.org/10.5194/bg-5-1475-2008

Lindsay, R., 2010. Peatbogs and Carbon: A critical synthesis.

Lindsay, R., Rigall, J., Burd, F., 1985. The use of small-scale surface patterns in the classification of British Peatlands.

Lindsay, R.A., Charman, J., Everingham, F., O'reilly, R.M., Palmer, M.A., Rowell, T.A., Stroud, D.A., Ratcliffe, D.A., Oswald, P.H., 1988. The Flow Country - The peatlands of Caithness and Sutherland.

Littlewood, N., Anderson, P., Artz, R., Bragg, O., Lunt, P., Marrs, R., 2010. Peatland Biodiversity.

Lloyd, J., Taylor, J.A., 1994. On the Temperature Dependence of Soil Respiration. Funct. Ecol. 8, 315. https://doi.org/10.2307/2389824

Lund, M., Christensen, T.R., Lindroth, A., Schubert, P., 2012. Effects of drought conditions on the carbon dioxide dynamics in a temperate peatland. Environ. Res. Lett. 7, 045704. https://doi.org/10.1088/1748-9326/7/4/045704

Lund, M., Lafleur, P.M., Roulet, N.T., Lindroth, A., Christensen, T.R., Aurela, M., Chojnicki, B.H., Flanagan, L.B., Humphreys, E.R., Laurila, T., Oechel, W.C., Olejnik, J., Rinne, J., Schubert, P., Nilsson, M.B., 2009. Variability in exchange of CO2 across 12 northern peatland and tundra sites. Glob. Chang. Biol. 16, no-no. https://doi.org/10.1111/j.1365-2486.2009.02104.x

Luscombe, D.J., Anderson, K., Gatis, N., Grand-Clement, E., Brazier, R.E., 2015. Using airborne thermal imaging data to measure near-surface hydrology in upland ecosystems. Hydrol. Process. 29, 1656–1668. https://doi.org/10.1002/hyp.10285

Malenovský, Z., Turnbull, J.D., Lucieer, A., Robinson, S.A., 2015. Antarctic moss stress assessment based on chlorophyll content and leaf density retrieved from imaging spectroscopy data. New Phytol. 208, 608–624. https://doi.org/10.1111/nph.13524

Malhotra, A., Roulet, N.T., Wilson, P., Giroux-Bougard, X., Harris, L.I., 2016. Ecohydrological feedbacks in peatlands: an empirical test of the relationship among vegetation, microtopography and water table. Ecohydrology 9, 1346–1357. https://doi.org/10.1002/eco.1731

Marushchak, M.E., Kiepe, I., Biasi, C., Elsakov, V., Friborg, T., Johansson, T., Soegaard, H., Virtanen, T., Martikainen, P.J., 2013. Carbon dioxide balance of subarctic tundra from plot to regional scales. Biogeosciences 10, 437–452. https://doi.org/10.5194/bg-10-437-2013

Mcmorrow, J.M., Cutler, M.E.J., Evans, M.G., Al-Roichdi, A., 2004. Hyperspectral indices for characterizing upland peat composition. Int. J. Remote Sens. 25, 313–325. https://doi.org/10.1080/0143116031000117065

McNeil, P., Waddington, J.M., 2003. Moisture controls on Sphagnum growth and CO 2 exchange on a cutover bog. J. Appl. Ecol. 40, 354–367.

Mcveigh, P., Sottocornola, M., Foley, N., Leahy, P., Kiely, G., 2014. Meteorological and functional response partitioning to explain interannual variability of CO 2 exchange at an Irish Atlantic blanket bog. Agric. For. Meteorol. 194, 8–19. https://doi.org/10.1016/j.agrformet.2014.01.017

Meingast, K.M., Falkowski, M.J., Kane, E.S., Potvin, L.R., Benscoter, B.W., Smith, A.M.S., Bourgeau-Chavez, L.L., Miller, M.E., 2014. Spectral detection of near-surface moisture

content and water-table position in northern peatland ecosystems. Remote Sens. Environ. 152, 536–546. https://doi.org/10.1016/J.RSE.2014.07.014

Meroni, M., Rossini, M., Guanter, L., Alonso, L., Rascher, U., Colombo, R., Moreno, J., 2009. Remote sensing of solar-induced chlorophyll fluorescence: Review of methods and applications. Remote Sens. Environ. 113, 2037–2051. https://doi.org/10.1016/J.RSE.2009.05.003

Met Office, 2018. Altnaharra SAWS climate information - Met Office [WWW Document]. URL https://www.metoffice.gov.uk/public/weather/climate/gfkgdgj2j (accessed 7.9.18).

Met Office, 2012. Met Office Integrated Data Archive System (MIDAS) Land and Marine Surface Stations Data (1853-current).

Millard, S.P., 2013. EnvStats : an R package for environmental statistics.

Min, Q., 2005. Impacts of aerosols and clouds on forest-atmosphere carbon exchange. J. Geophys. Res. Atmos. 110, n/a-n/a. https://doi.org/10.1029/2004JD004858

Minayeva, T.Y., Bragg, O.M., Sirin, A.A., 2017. Towards ecosystem-based restoration of peatland biodiversity 19. https://doi.org/10.19189/MaP.2013.OMB.150

Monteith, J.L., Moss, C.J., 1977. Climate and the Efficiency of Crop Production in Britain [and Discussion]. Philos. Trans. R. Soc. B Biol. Sci. 281, 277–294. https://doi.org/10.1098/rstb.1977.0140

Moore, D.J.P., Trahan, N.A., Wilkes, P., Quaife, T., Stephens, B.B., Elder, K., Desai, A.R., Negron, J., Monson, R.K., 2013. Persistent reduced ecosystem respiration after insect disturbance in high elevation forests. Ecol. Lett. 16, 731–737. https://doi.org/10.1111/ele.12097

Moore, P.A., Waddington, J.M., 2015. Modelling *Sphagnum* moisture stress in response to projected 21st-century climate change. Hydrol. Process. 29, 3966–3982. https://doi.org/10.1002/hyp.10484

Morton, P.A., Heinemeyer, A., 2018. Vegetation matters: Correcting chamber carbon flux measurements using plant volumes. Sci. Total Environ. 639, 769–772. https://doi.org/10.1016/J.SCITOTENV.2018.05.192

NASA, 2016a. MODIS - Moderate Resolution Imaging Spectroradiometer [WWW Document]. URL https://modis.gsfc.nasa.gov/ (accessed 10.28.16).

NASA, 2016b. Orbiting Carbon Observatory 2 [WWW Document]. URL http://www.nasa.gov/mission_pages/oco2/index.html (accessed 10.28.16).

NASA, 2016c. HyspIRI mission study [WWW Document]. URL https://hyspiri.jpl.nasa.gov/ (accessed 10.28.16).

NASA, 2010. Artist's rendering of Aqua [WWW Document]. URL https://earthobservatory.nasa.gov/Features/Water/page4.php (accessed 9.7.17).

NBN Atlas Partnership, 2017. No Title [WWW Document]. NBN Atlas. URL https://nbnatlas.org/

NERC, 2016. Airborne research and survey facility [WWW Document].

NIES, 2016. GOSAT project - Greenhouse Gases Observing Satellite [WWW Document]. URL http://www.gosat.nies.go.jp/en/ (accessed 10.28.16).

Nijp, J.J., Limpens, J., Metselaar, K., Peichl, M., Nilsson, M.B., van der Zee, S.E.A.T.M., Berendse, F., 2015. Rain events decrease boreal peatland net CO_2 uptake through reduced light availability. Glob. Chang. Biol. 21, 2309–2320. https://doi.org/10.1111/gcb.12864

Nijp, J.J., Limpens, J., Metselaar, K., van der Zee, S.E.A.T.M., Berendse, F., Robroek, B.J.M., 2014. Can frequent precipitation moderate the impact of drought on peatmoss carbon uptake in northern peatlands? New Phytol. 203, 70–80. https://doi.org/10.1111/nph.12792

Nilsson, M., Sagerfors, J., Buffam, I., Laudon, H., Eriksson, T., Gelle, A., Klemedtsson, L., Weslien, P., Lindroth, A., 2008. Contemporary carbon accumulation in a boreal oligotrophic minerogenic mire - a significant sink after accounting for all C-fluxes. Glob. Chang. Biol. 14, 2317–2332. https://doi.org/10.1111/j.1365-2486.2008.01654.x

Olofsson, P., Lagergren, F., Lindroth, A., Lindström, J., Klemedtsson, L., Kutsch, W., Eklundh, L., 2008. Towards operational remote sensing of forest carbon balance across Northern Europe. Biogeosciences 5, 817–832. https://doi.org/10.5194/bg-5-817-2008

Parish, R., Sirin, F., Charman, A., Joosten, D., Minayeva, H., Silvius, T., Stringer, M., 2008. Supported By United Nations Environment Programme/Global Environment Facility (UNEP/GEF) with assistance from the Asia Pacific Network for Global Change Research (APN) Design by. Assess. Peatlands, Biodivers. Clim. Chang. Main Report. Glob. Environ. Centre, Kuala Lumpur Wetl. Int.

Parry, L.E., Chapman, P.J., Palmer, S.M., Wallage, Z.E., Wynne, H., Holden, J., 2015. The influence of slope and peatland vegetation type on riverine dissolved organic carbon and water colour at different scales. Sci. Total Environ. 527–528, 530–539.

https://doi.org/10.1016/J.SCITOTENV.2015.03.036

Parry, L.E., Holden, J., Chapman, P.J., 2014. Restoration of blanket peatlands. J. Environ. Manage. 133, 193–205. https://doi.org/10.1016/J.JENVMAN.2013.11.033

Peichl, M., Gažovič, M., Vermeij, I., de Goede, E., Sonnentag, O., Limpens, J., Nilsson, M.B., 2018. Peatland vegetation composition and phenology drive the seasonal trajectory of maximum gross primary production. Sci. Rep. 8, 8012. https://doi.org/10.1038/s41598-018-26147-4

Penuelas, J., Fillella, I., Gamon, J.A., 1995. Assessment of photosynthetic radiation-use efficiency with spectral reflectance. New Phytol. 131, 291–296. https://doi.org/10.1111/j.1469-8137.1995.tb03064.x

Peñuelas, J., Garbulsky, M.F., Filella, I., 2011. Photochemical reflectance index (PRI) and remote sensing of plant CO2 uptake. New Phytol. 191, 596–599. https://doi.org/10.1111/j.1469-8137.2011.03791.x

Penuelas, J., Pinol, J., Ogaya, R., Filella, I., 1997. Estimation of plant water concentration by the reflectance Water Index WI (R900/R970). Int. J. Remote Sens. 18, 2869–2875. https://doi.org/10.1080/014311697217396

Perry, M., Hollis, D., 2005. The development of a new set of long-term climate averages for the UK. Int. J. Climatol. Int. J. Clim. 25, 1023–1039. https://doi.org/10.1002/joc.1160

Pfeifer, M., Disney, M., Quaife, T., Marchant, R., 2012. Terrestrial ecosystems from space: a review of earth observation products for macroecology applications. Glob. Ecol. Biogeogr. 21, 603–624. https://doi.org/10.1111/j.1466-8238.2011.00712.x

Phillips, M.E., 1954. Eriophorum Angustifolium Roth. J. Ecol. 42, 612. https://doi.org/10.2307/2256893

Pohlert, T., 2018, PMCMRplus: Calculate Pairwise Multiple Comparisons of Mean Rank Sums Extended. R package version 1.2.0.

Potter, C.S., Randerson, J.T., Field, C.B., Matson, P.A., Vitousek, P.M., Mooney, H.A., Klooster, S.A., 1993. Terrestrial ecosystem production: A process model based on global satellite and surface data. Global Biogeochem. Cycles 7, 811–841. https://doi.org/10.1029/93GB02725

Prince, S.D., Goward, S.N., 1995. Global Primary Production: A Remote Sensing Approach. J. Biogeogr. 22, 815. https://doi.org/10.2307/2845983

Quaife, T., Lewis, P., De Kauwe, M., Williams, M., Law, B.E., Disney, M., Bowyer, P., 2008.

Assimilating canopy reflectance data into an ecosystem model with an Ensemble Kalman Filter. Remote Sens. Environ. 112, 1347–1364. https://doi.org/10.1016/J.RSE.2007.05.020

R Core Team, 2017. R: A language and environment for statistical computing.

Rahman, A.F., Sims, D.A., Cordova, V.D., El-Masri, B.Z., 2005. Potential of MODIS EVI and surface temperature for directly estimating per-pixel ecosystem C fluxes. Geophys. Res. Lett. 32, n/a-n/a. https://doi.org/10.1029/2005GL024127

Reichstein, M., Rey, A., Freibauer, A., Tenhunen, J., Valentini, R., Banza, J., Casals, P., Cheng, Y., Grünzweig, J.M., Irvine, J., Joffre, R., Law, B.E., Loustau, D., Miglietta, F., Oechel, W., Ourcival, J.-M., Pereira, J.S., Peressotti, A., Ponti, F., Qi, Y., Rambal, S., Rayment, M., Romanya, J., Rossi, F., Tedeschi, V., Tirone, G., Xu, M., Yakir, D., 2003. Modeling temporal and large-scale spatial variability of soil respiration from soil water availability, temperature and vegetation productivity indices. Global Biogeochem. Cycles 17, n/a-n/a. https://doi.org/10.1029/2003GB002035

Robroek, B.J.M., Limpens, J., Breeuwer, A., Ruijven, J. van, Schouten, M.G.C., 2007. Precipitation determines the persistence of hollow Sphagnum species on hummocks. Wetlands 27, 979. https://doi.org/10.1672/0277-5212(2007)27[979:pdtpoh]2.0.co;2

Robroek, B.J.M., Schouten, M.G.C., Limpens, J., Berendse, F., Poorter, H., 2009. Interactive effects of water table and precipitation on net CO_2 assimilation of three co-occurring *Sphagnum* mosses differing in distribution above the water table. Glob. Chang. Biol. 15, 680–691. https://doi.org/10.1111/j.1365-2486.2008.01724.x

Rochefort, L., Campeau, S., Bugnon, J.-L., 2002. Does prolonged flooding prevent or enhance regeneration and growth of Sphagnum? Aquat. Bot. 74, 327–341. https://doi.org/10.1016/S0304-3770(02)00147-X

Rossini, M., Cogliati, S., Meroni, M., Migliavacca, M., Galvagno, M., Busetto, L., Cremonese, E., Julitta, T., Siniscalco, C., Morra Di Cella, U., Colombo, R., 2012. Remote sensing-based estimation of gross primary production in a subalpine grassland. Biogeosciences 9, 2565–2584. https://doi.org/10.5194/bg-9-2565-2012

Roulet, N.T., Lafleur, P.M., Richard, P.J.H., Moore, T.R., Humphreys, E.R., Bubier, J., 2007. Contemporary carbon balance and late Holocene carbon accumulation in a northern peatland. Glob. Chang. Biol. 13, 397–411. https://doi.org/10.1111/j.1365-2486.2006.01292.x

Rouse, J.W.. J., Haas, R.H., Schell, J.A., Deering, D.W., 1974. Monitoring vegetation

systems in the Great Plains with ERTS.

Running, S., Mu, Q., Zhao, M., 2015. MOD17A2H MODIS/Terra Gross Primary Productivity 8-Day L4 Global 500m SIN Grid V006. https://doi.org/10.5067/MODIS/MOD17A2H.006

Running, S., Zhao, M., 2015. User's Guide - Daily GPP and Annual NPP (MOD17A2A2/A3) Products - NASA Earth Observing System MODIS Land Algorithm.

Running, S.W., Nemani, R.R., Heinsch, F.A., Zhao, M., Reeves, M., Hashimoto, H., 2004. A Continuous Satellite-Derived Measure of Global Terrestrial Primary Production. Bioscience 54, 547–560. https://doi.org/10.1641/0006-3568(2004)054[0547:acsmog]2.0.co;2

Rydin, H., Jeglum, J.K., 2013. The Biology of Peatlands. Oxford University Press. https://doi.org/10.1093/acprof:osobl/9780199602995.001.0001

Salisbury, J.W., 1998. Spectral measurements field guide.

Santhana Vannan, S.K., Cook, R.B., Holladay, S.K., Olsen, L.M., Dadi, U., Wilson, B.E., 2009. A Web-Based Subsetting Service for Regional Scale MODIS Land Products. IEEE J. Sel. Top. Appl. Earth Obs. Remote Sens. 2, 319–328. https://doi.org/10.1109/JSTARS.2009.2036585

Schipperges, B. B., Rydin, H, 1998. Response of photosynthesis of Sphagnum species from contrasting microhabitats to tissue water content and repeated desiccation. New Phytol 140, 677–684.

Schubert, P., Eklundh, L., Lund, M., Nilsson, M., 2010. Estimating northern peatland CO2 exchange from MODIS time series data. Remote Sens. Environ. 114, 1178–1189. https://doi.org/10.1016/J.RSE.2010.01.005

Shurpali, N.J., Verma, S.B., Kim, J., Arkebauer, T.J., 1995. Carbon dioxide exchange in a peatland ecosystem. J. Geophys. Res. 100, 14319. https://doi.org/10.1029/95JD01227

Silvola, J., Alm, J., Ahlholm, U., Nykanen, H., Martikainen, P.J., 1996. CO 2 Fluxes from Peat in Boreal Mires under Varying Temperature and Moisture Conditions. J. Ecol. 84, 219. https://doi.org/10.2307/2261357

Sims, D.A., Gamon, J.A., 2002. Relationships between leaf pigment content and spectral reflectance across a wide range of species, leaf structures and developmental stages. Remote Sens. Environ. 81, 337–354. https://doi.org/10.1016/S0034-4257(02)00010-X

Sims, D.A., Luo, H., Hastings, S., Oechel, W.C., Rahman, A.F., 2006. Parallel adjustments in vegetation greenness and ecosystem CO2 exchange in response to drought in a

Southern California chaparral ecosystem. Remote Sens. Environ. 103, 289–303. https://doi.org/10.1016/J.RSE.2005.01.020

Sims, D.A., Rahman, A.F., Cordova, V.D., El-Masri, B.Z., Baldocchi, D.D., Bolstad, P. V., Flanagan, L.B., Goldstein, A.H., Hollinger, D.Y., Misson, L., Monson, R.K., Oechel, W.C., Schmid, H.P., Wofsy, S.C., Xu, L., 2008. A new model of gross primary productivity for North American ecosystems based solely on the enhanced vegetation index and land surface temperature from MODIS. Remote Sens. Environ. 112, 1633–1646. https://doi.org/10.1016/J.RSE.2007.08.004

Smith, D.M., Barrowclough, C., Glendinning, A.D., Hand, A., 2014. Exmoor Mires Project: Initial analyses of post restoration vegetation monitoring data, in: In the Bog Conference 2014.

Soini, P., Riutta, T., Yli-Petäys, M., Vasander, H., 2009. Comparison of Vegetation and CO 2 Dynamics Between a Restored Cut-Away Peatland and a Pristine Fen: Evaluation of the Restoration Success. https://doi.org/10.1111/j.1526-100X.2009.00520.x

Sottocornola, M., Kiely, G., 2010a. Hydro-meteorological controls on the CO 2 exchange variation in an Irish blanket bog. Agric. For. Meteorol. 287–297. https://doi.org/10.1016/j.agrformet.2009.11.013

Sottocornola, M., Kiely, G., 2010b. Energy fluxes and evaporation mechanisms in an Atlantic blanket bog in southwestern Ireland. Water Resour. Res. 46. https://doi.org/10.1029/2010WR009078

Sottocornola, M., Laine, A., Kiely, G., Byrne, K.A., Tuittila, E.-S., 2009. Vegetation and environmental variation in an Atlantic blanket bog in South-western Ireland. Plant Ecol. 203, 69–81. https://doi.org/10.1007/s11258-008-9510-2

Stoy, P.C., Quaife, T., 2015. Probabilistic Downscaling of Remote Sensing Data with Applications for Multi-Scale Biogeochemical Flux Modeling. PLoS One 10, e0128935. https://doi.org/10.1371/journal.pone.0128935

Strachan, I.B., Pattey, E., Boisvert, J.B., 2002. Impact of nitrogen and environmental conditions on corn as detected by hyperspectral reflectance. Remote Sens. Environ. 80, 213–224. https://doi.org/10.1016/S0034-4257(01)00299-1

Strachan, I.B., Pelletier, L., Bonneville, M.-C., 2016. Inter-annual variability in water table depth controls net ecosystem carbon dioxide exchange in a boreal bog. Biogeochemistry 127, 99–111. https://doi.org/10.1007/s10533-015-0170-8

Strack, M., Cagampan, J., Fard, G.H., Keith, A.M., Nugent, K., Rankin, T., Robinson, C., Strachan, I.B., Waddington, J.M., Xu, B., 2016. Controls on plot-scale growing season CO2 and CH4 fluxes in restored peatlands: Do they differ from unrestored and natural sites? 17, 1–18. https://doi.org/10.19189/MaP.2015.OMB.216

Strack, M., Price, J.S., 2009. Moisture controls on carbon dioxide dynamics of peat-*Sphagnum* monoliths. Ecohydrology 2, 34–41. https://doi.org/10.1002/eco.36

Strack, M., Zuback, Y.C.A., 2013. Annual carbon balance of a peatland 10 yr following restoration. Biogeosciences 10, 2885–2896. https://doi.org/10.5194/bg-10-2885-2013

Sturtevant, C.S., Oechel, W.C., 2013. Spatial variation in landscape-level CO_2 and CH_4 fluxes from arctic coastal tundra: influence from vegetation, wetness, and the thaw lake cycle. Glob. Chang. Biol. 19, 2853–2866. https://doi.org/10.1111/gcb.12247

Tagesson, T., Mastepanov, M., Mölder, M., Tamstorf, M.P., Eklundh, L., Smith, B., Sigsgaard, C., Lund, M., Ekberg, A., Falk, J.M., Friborg, T., Christensen, T.R., Ström, L., 2013. Modelling of growing season methane fluxes in a high-Arctic wet tundra ecosystem 1997–2010 using in situ and high-resolution satellite data. Tellus B Chem. Phys. Meteorol. 65, 19722. https://doi.org/10.3402/tellusb.v65i0.19722

Tan, K.P., Kanniah, K.D., Cracknell, A.P., 2012. A review of remote sensing based productivity models and their suitability for studying oil palm productivity in tropical regions. Prog. Phys. Geogr. 36, 655–679. https://doi.org/10.1177/0309133312452187

Thomas, V., Treitz, P., Jelinski, D., Miller, J., Lafleur, P., McCaughey, J.H., 2003. Image classification of a northern peatland complex using spectral and plant community data. Remote Sens. Environ. 84, 83–99. https://doi.org/10.1016/S0034-4257(02)00099-8

Titus, J.E., Wagner, D.J., 1984. Carbon Balance for Two Sphagnum Mosses: Water Balance Resolves a Physiological Paradox. Ecology 65, 1765–1774. https://doi.org/10.2307/1937772

Titus, J.E., Wagner, D.J., Stephens, M.D., 1983. Contrasting Water Relations of Photosynthesis for Two Sphagnum Mosses. Ecology 64, 1109–1115. https://doi.org/10.2307/1937821

Tuittila, E.-S., Komulainen, V.-M., Vasander, H., Laine, J., 1999. Restored cut-away peatland as a sink for atmospheric CO 2. Oecologia 120, 563–574. https://doi.org/10.1007/s004420050891

Turner, D.P., Ritts, W.D., Styles, J.M., Yang, Z., Cohen, W.B., Law, B.E., Thornton, P.E.,

2006. A diagnostic carbon flux model to monitor the effects of disturbance and interannual variation in climate on regional NEP. Tellus B Chem. Phys. Meteorol. 58, 476–490. https://doi.org/10.1111/j.1600-0889.2006.00221.x

Turner, T.E., Billett, M.F., Baird, A.J., Chapman, P.J., Dinsmore, K.J., Holden, J., 2016. Regional variation in the biogeochemical and physical characteristics of natural peatland pools. Sci. Total Environ. 545–546, 84–94. https://doi.org/10.1016/J.SCITOTENV.2015.12.101

Turunen, J., Tomppo, E., Tolonen, K., Reinikainen, A., 2002. Estimating carbon accumulation rates of undrained mires in Finland–application to boreal and subarctic regions. The Holocene 12, 69–80. https://doi.org/10.1191/0959683602hl522rp

Urbanova, Z., Picek, T., Tuittila, E.-S., Tuittila, E.-S., Tuittila, E.-S., Tuittila, E.-S., Tuittila, E.-S., Tuittila, E.-S., 2013. Sensitivity of carbon gas fluxes to weather variability on pristine, drained and rewetted temperate bogs. Mires Peat 11.

USGS, 2016. Landsat missions [WWW Document]. URL http://landsat.usgs.gov/ (accessed 10.28.16).

USGS, 2011. Hyperion [WWW Document]. URL https://eo1.usgs.gov/sensors/hyperion (accessed 10.28.16).

Van Gaalen, K.E., Flanagan, L.B., Peddle, D.R., 2007. Photosynthesis, chlorophyll fluorescence and spectral reflectance in Sphagnum moss at varying water contents. Oecologia 153, 19–28. https://doi.org/10.1007/s00442-007-0718-y

Van Wittenberghe, S., Alonso, L., Verrelst, J., Moreno, J., Samson, R., 2015. Bidirectional sun-induced chlorophyll fluorescence emission is influenced by leaf structure and light scattering properties — A bottom-up approach. Remote Sens. Environ. 158, 169–179. https://doi.org/10.1016/j.rse.2014.11.012

Verma, M., Friedl, M.A., Law, B.E., Bonal, D., Kiely, G., Black, T.A., Wohlfahrt, G., Moors, E.J., Montagnani, L., Marcolla, B., Toscano, P., Varlagin, A., Roupsard, O., Cescatti, A., Arain, M.A., D'Odorico, P., 2015. Improving the performance of remote sensing models for capturing intra- and inter-annual variations in daily GPP: An analysis using global FLUXNET tower data. Agric. For. Meteorol. 214–215, 416–429. https://doi.org/10.1016/j.agrformet.2015.09.005

Vermote, E., 2015. MOD09A1 MODIS/Terra Surface Reflectance 8-Day L3 Global 500m SIN Grid V006. https://doi.org/10.5067/MODIS/MOD09A1.006

Vermote, E.F., Tanre, D., Deuze, J.L., Herman, M., Morcette, J.-J., 1997. Second Simulation of the Satellite Signal in the Solar Spectrum, 6S: an overview. IEEE Trans. Geosci. Remote Sens. 35, 675–686. https://doi.org/10.1109/36.581987

Vieira, S., Hoffmann, R., 1977. Comparison of the Logistic and the Gompertz Growth Functions Considering Additive and Multiplicative Error Terms. Appl. Stat. 26, 143. https://doi.org/10.2307/2347021

Vogelmann, J.E., Moss, D.M., 1993. Spectral reflectance measurements in the genus Sphagnum. Remote Sens. Environ. 45, 273–279. https://doi.org/10.1016/0034-4257(93)90110-J

Vourlitis, G.L., Verfaillie, J., Oechel, W.C., Hope, A., Stow, D., Engstrom, R., 2003. Spatial variation in regional CO2 exchange for the Kuparuk River Basin, Alaska over the summer growing season. Glob. Chang. Biol. 9, 930–941. https://doi.org/10.1046/j.1365-2486.2003.00639.x

Waddington, J.M., Price, J.S., 2000. Effect of peatland drainage, harvesting, and restoration on atmospheric water and carbon exchange. Phys. Geogr. 21, 433–451. https://doi.org/10.1080/02723646.2000.10642719

Waddington, J.M., Roulet, N.T., 1996. Atmosphere-wetland carbon exchanges: Scale dependency of CO_2 and CH_4 exchange on the developmental topography of a peatland. Global Biogeochem. Cycles 10, 233–245. https://doi.org/10.1029/95GB03871

Waddington, J.M., Strack, M., Greenwood, M.J., 2010. Toward restoring the net carbon sink function of degraded peatlands: Short-term response in CO_2 exchange to ecosystem-scale restoration. J. Geophys. Res. 115, G01008. https://doi.org/10.1029/2009JG001090

Wagner, D.J., Titus, J.E., 1984. Comparative desiccation tolerance of two Sphagnum mosses. Oecologia 62, 182–187. https://doi.org/10.1007/BF00379011

Walker, J.J., de Beurs, K.M., Wynne, R.H., 2014. Dryland vegetation phenology across an elevation gradient in Arizona, USA, investigated with fused MODIS and Landsat data. Remote Sens. Environ. 144, 85–97. https://doi.org/10.1016/J.RSE.2014.01.007

Walker, T.N., Garnett, M.H., Ward, S.E., Oakley, S., Bardgett, R.D., Ostle, N.J., 2016. Vascular plants promote ancient peatland carbon loss with climate warming. Glob. Chang. Biol. 22, 1880–1889. https://doi.org/10.1111/gcb.13213

Wan, Z., Hook, S., Hulley, G., 2015. MOD11A2 MODIS/Terra Land Surface

Temperature/Emissivity 8-Day L3 Global 1km SIN Grid V006. https://doi.org/10.5067/MODIS/MOD11A2.006

Wang, G., Garcia, D., Liu, Y., de Jeu, R., Johannes Dolman, A., 2012. A three-dimensional gap filling method for large geophysical datasets: Application to global satellite soil moisture observations. Environ. Model. Softw. 30, 139–142. https://doi.org/10.1016/J.ENVSOFT.2011.10.015

Watts, J.D., Kimball, J.S., Parmentier, F.J.W., Sachs, T., Rinne, J., Zona, D., Oechel, W., Tagesson, T., Jackowicz-Korczyński, M., Aurela, M., 2014. A satellite data driven biophysical modeling approach for estimating northern peatland and tundra CO2 and CH4 fluxes. Biogeosciences 11, 1961–1980. https://doi.org/10.5194/bg-11-1961-2014

Weber, T.K.D., Iden, S.C., Durner, W., 2017. Unsaturated hydraulic properties of *Sphagnum* moss and peat reveal trimodal pore-size distributions. Water Resour. Res. 53, 415–434. https://doi.org/10.1002/2016WR019707

Weston, D.J., Timm, C.M., Walker, A.P., Gu, L., Muchero, W., Schmutz, J., Shaw, A.J., Tuskan, G.A., Warren, J.M., Wullschleger, S.D., 2015. *Sphagnum* physiology in the context of changing climate: emergent influences of genomics, modelling and host-microbiome interactions on understanding ecosystem function. Plant. Cell Environ. 38, 1737–1751. https://doi.org/10.1111/pce.12458

Whiting, G.J., 1994. CO_2 exchange in the Hudson Bay lowlands: Community characteristics and multispectral reflectance properties. J. Geophys. Res. 99, 1519. https://doi.org/10.1029/93JD01833

Wickham, H., 2016. ggplot2: Elegant Graphics for Data Analysis.

Worrall, F., Chapman, P., Artz, R., Smith, P., Grayson, &, 2011. A review of current evidence on carbon fluxes and greenhouse gas emissions from UK peatlands.

Wu, C., 2012. Use of a vegetation index model to estimate gross primary production in open grassland. J. Appl. Remote Sens. 6, 063532. https://doi.org/10.1117/1.JRS.6.063532

Wu, C., Gaumont-Guay, D., Andrew Black, T., Jassal, R.S., Xu, S., Chen, J.M., Gonsamo, A., 2014. Soil respiration mapped by exclusively use of MODIS data for forest landscapes of Saskatchewan, Canada. ISPRS J. Photogramm. Remote Sens. 94, 80–90. https://doi.org/10.1016/J.ISPRSJPRS.2014.04.018

Wu, J., Roulet, N.T., Moore, T.R., Lafleur, P., Humphreys, E., 2011. Dealing with microtopography of an ombrotrophic bog for simulating ecosystem-level CO2

exchanges. Ecol. Modell. 222, 1038–1047. https://doi.org/10.1016/J.ECOLMODEL.2010.07.015

Wutzler, T., Lucas-Moffat, A., Migliavacca, M., Knauer, J., Sickel, K., Šigut, L., Menzer, O., Reichstein, M., 2018. Basic and extensible post-processing of eddy covariance flux data with REddyProc. Biogeosciences 15, 5015–5030. https://doi.org/10.5194/bg-15-5015-2018

Xiao, X., Zhang, Q., Braswell, B., Urbanski, S., Boles, S., Wofsy, S., Moore, B., Ojima, D., 2004. Modeling gross primary production of temperate deciduous broadleaf forest using satellite images and climate data. Remote Sens. Environ. 91, 256–270. https://doi.org/10.1016/J.RSE.2004.03.010

Yu, Q., Wang, S., Mickler, R., Huang, K., Zhou, L., Yan, H., Chen, D., Han, S., Yu, Q., Wang, S., Mickler, R.A., Huang, K., Zhou, L., Yan, H., Chen, D., Han, S., 2014. Narrowband Bio-Indicator Monitoring of Temperate Forest Carbon Fluxes in Northeastern China. Remote Sens. 6, 8986–9013. https://doi.org/10.3390/rs6098986

Yu, Z.C., 2012. Northern peatland carbon stocks and dynamics: a review. Biogeosciences 9, 4071–4085. https://doi.org/10.5194/bg-9-4071-2012

Yuan, W., Liu, S., Dong, W., Liang, S., Zhao, S., Chen, J., Xu, W., Li, X., Barr, A., Andrew Black, T., Yan, W., Goulden, M.L., Kulmala, L., Lindroth, A., Margolis, H.A., Matsuura, Y., Moors, E., van der Molen, M., Ohta, T., Pilegaard, K., Varlagin, A., Vesala, T., 2014. Differentiating moss from higher plants is critical in studying the carbon cycle of the boreal biome. Nat. Commun. 5, 4270. https://doi.org/10.1038/ncomms5270

Yuan, W., Liu, S., Yu, G., Bonnefond, J.-M., Chen, J., Davis, K., Desai, A.R., Goldstein, A.H., Gianelle, D., Rossi, F., Suyker, A.E., Verma, S.B., 2010. Global estimates of evapotranspiration and gross primary production based on MODIS and global meteorology data. Remote Sens. Environ. 114, 1416–1431. https://doi.org/10.1016/J.RSE.2010.01.022

Yuan, W., Liu, S., Zhou, G., Zhou, G., Tieszen, L.L., Baldocchi, D., Bernhofer, C., Gholz, H., Goldstein, A.H., Goulden, M.L., Hollinger, D.Y., Hu, Y., Law, B.E., Stoy, P.C., Vesala, T., Wofsy, S.C., 2007. Deriving a light use efficiency model from eddy covariance flux data for predicting daily gross primary production across biomes. Agric. For. Meteorol. 143, 189–207. https://doi.org/10.1016/J.AGRFORMET.2006.12.001

Zeileis, A., Hothorn, T., 2002. Diagnostic Checking in Regression Relationships.

Zhang, N., Yu, Z., Yu, G., Wu, J., 2007. Scaling up ecosystem productivity from patch to

landscape: a case study of Changbai Mountain Nature Reserve, China. Landsc. Ecol. 22, 303–315. https://doi.org/10.1007/s10980-006-9027-9

Zhang, Y., Song, C., Sun, G., Band, L.E., Noormets, A., Zhang, Q., 2015. Understanding moisture stress on light use efficiency across terrestrial ecosystems based on global flux and remote-sensing data. J. Geophys. Res. Biogeosciences 120, 2053–2066. https://doi.org/10.1002/2015JG003023

Zhao, J., Peichl, M., Öquist, M., Nilsson, M.B., 2016. Gross primary production controls the subsequent winter CO_2 exchange in a boreal peatland. Glob. Chang. Biol. 22, 4028–4037. https://doi.org/10.1111/gcb.13308

Zotarelli, L., Dukes, M.D., Romero, C.C., Migliaccio, K.W., Morgan, K.T., n.d. Step by Step Calculation of the Penman-Monteith Evapotranspiration (FAO-56 Method) 1.

Appendix A – Correcting for background light effects

When it became apparent that background light levels were affecting the carbon flux results, a PAR sensor was added to the Licor-8100, and PAR measurements were recorded for each net carbon flux measurement (NEE). Sample CapA1 (a sample of *S. capillifolium* from control group A) was selected as a control, and 11 measurements of NEE and PAR were taken across the course of a morning, approximately every 25 minutes from 8.30am to 12 noon. This was repeated with eight other randomly selected samples (covering both species and different stages of dryness) in the next few weeks of the experiment. The results are shown in Figure A1 and Table A1. It can be seen that for all the samples tested, the GPP was increasing with PAR.

It is likely that each sample would have a different response curve to PAR, and that this might change with water content. Unfortunately time constraints meant that we could not create an individual response line for each sample on each day, so we compromised by using an averaged response line.

A PAR to GPP regression is normally a response curve but the low light levels in this experiment meant that the saturation point was not reached and so a linear regression is appropriate. The intercept value is unimportant as it will be applied equally across all samples. The slope value is the focus here. The average slope value is 0.0204, so the regression equation used is:

$$GPPr = 0.0204 \times PAR$$

The correction applied to the GPP measurements is then:

$$GPP = GPPm - GPPr + 1.4$$

Where GPPm is the measured GPP from the chamber fluxes, and GPPr is the estimated GPP from the regression line.

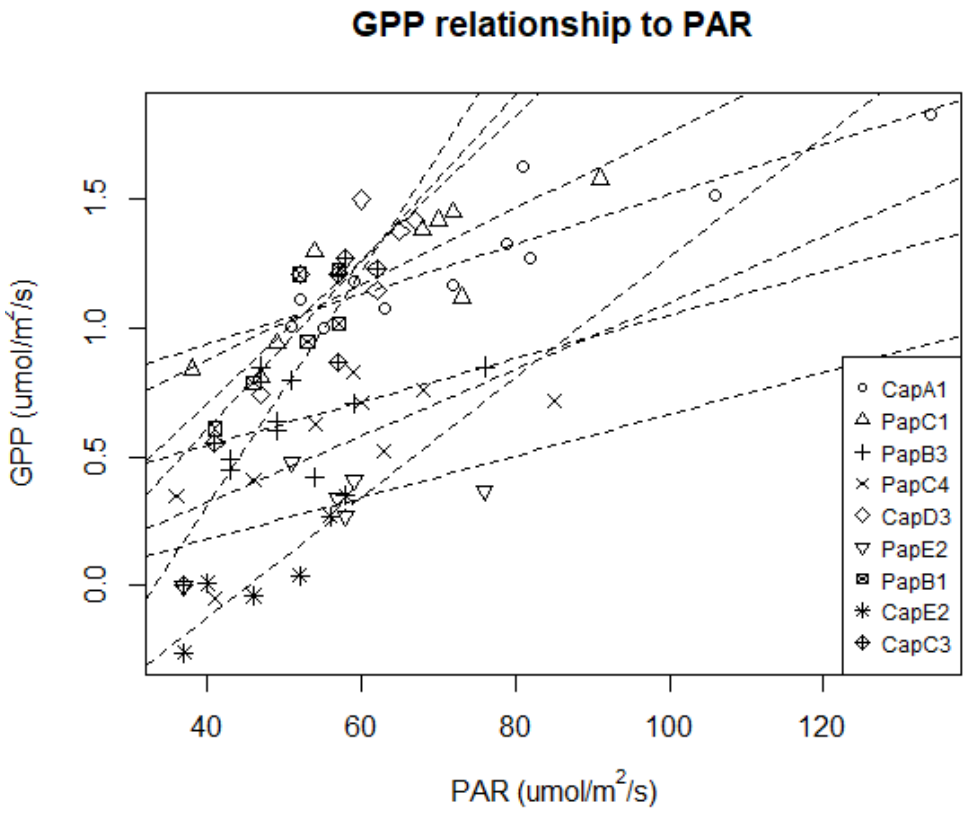

Figure A1 –GPP related to PAR for nine different Sphagnum samples.

Table A1 –Each sample tested for PAR:GPP relationship, as shown in Figure A1. This table gives the slope of the regression line for each sample, the correlation between the PAR and GPP values, and the number of measurements taken.

Sample	slope	correlation	no. of measurements
PapC1	0.00148	0.86	9
CapC3	0.00455	0.96	6
PapB1	0.003247	0.86	6
PapC4	0.001292	0.7	9
PapB3	0.000844	0.51	9
PapE2	0.000811	0.61	6
CapE2	0.002336	0.91	6
CapA1	0.000967	0.91	11
CapD3	0.002798	0.79	6

As the first four weeks of the experiment did not have attached PAR data, it was necessary to find a proxy correction method. The timing of the NEE measurements was considered a proxy for PAR, because the main changes in background light were seen across the mornings as the sun rose. Cloud cover changes had some effect on PAR, but these were

minimal in comparison with the increasing PAR across the mornings. Figure A2 and Table A2 show the models used.

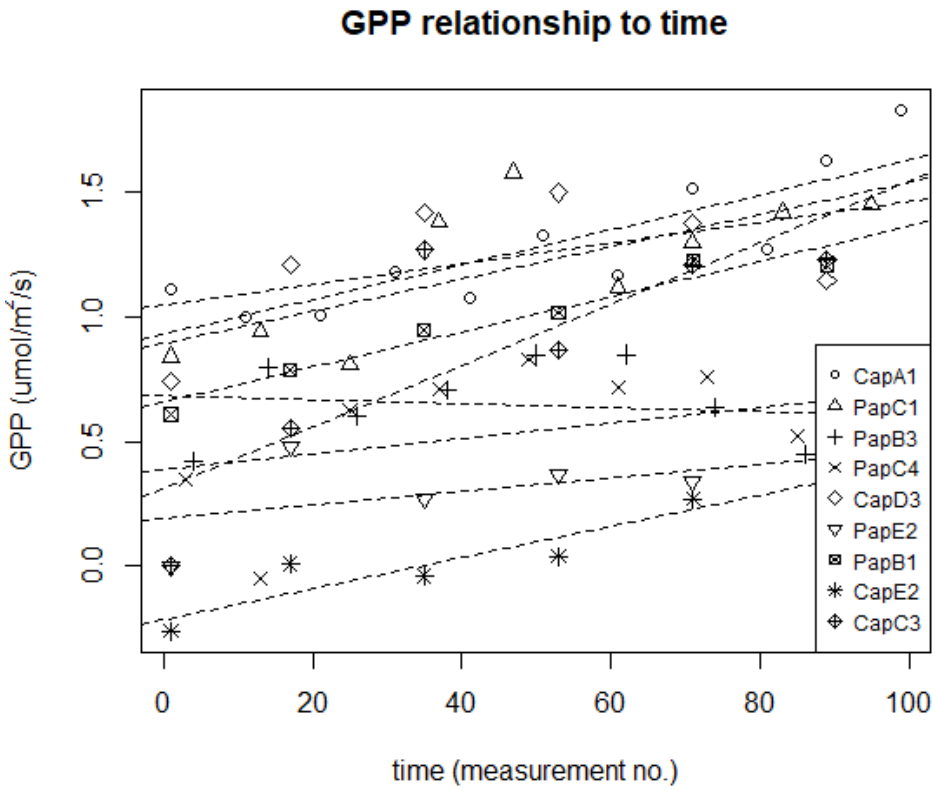

Figure A2 – GPP as a function of time for nine different Sphagnum samples. Measurement no. is used to indicate time, as measurements started at the same time each morning, and each sample took five minutes to complete measurements.

Table A2 –Each sample tested for PAR-time relationship, as shown in Figure A2. This table gives the slope of the regression line for each sample, the correlation between the PAR and GPP values, and the number of measurements taken.

Sample	slope	correlation	no. of measurements
PapC1	0.0065	0.73	9
CapC3	0.0123	0.81	6
PapB1	0.0071	0.97	6
PapC4	0.0031	0.37	9
PapB3	-0.0008	-0.16	9
PapE2	0.0027	0.54	6
CapE2	0.0063	0.94	6
CapA1	0.007	0.85	11
CapD3	0.0041	0.5	6

The average slope value is 0.0054, so the equation used is:

GPPr = 0.0054 × measurement number

GPP = GPPm – GPPr + 0.2

1.4 is added to the PAR correction, and 0.2 to the time correction, in order to match the midpoint of GPP results across the dataset. Figure A3 compares the results from the time correction and the PAR correction for the nine samples used to compute the corrections.

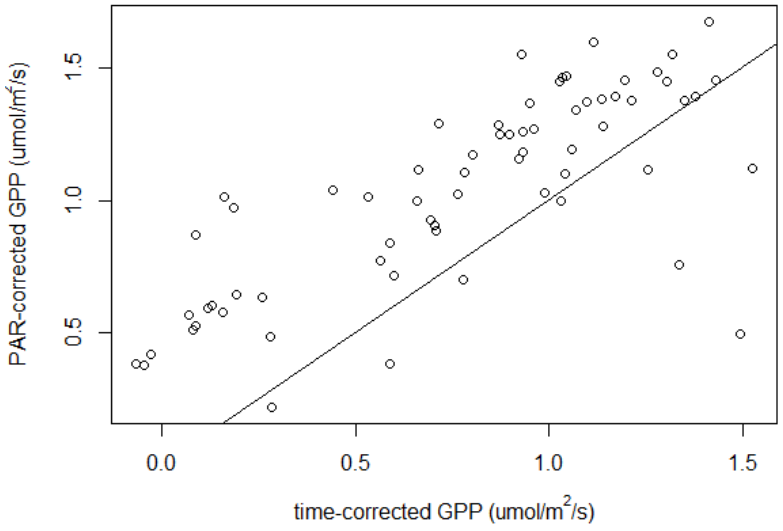

Figure A3 – PAR-corrected GPP plotted against time-corrected GPP for the nine tested samples. A 1:1 line is drawn.

Note that the order of samples on each day was randomised, and all significant trends are considered with respect to the control A, and the same correction is applied to all samples.

Appendix B – Field collars species composition

Collar	L1a	L1b	L2a	L2b	L3a	L3b	L4a	L4b	L5a	L5b	L6a	L6b	L7a	L7b	L8a	L8b
Calluna_vulgaris	10		5		20				40		20	5			20	
Erica_tetralix			5											10		
Eriophorum_angustifolium	40	10	20	40		20	15	5		15	10					
Eriophorum_vaginatum																
Trichiophorum_germanicum									10							
Molinia_caerulea												30	10	15		20
Sphagnum_capillifolium	50			40	60	30	60		20		9		30			19
Sphagnum_papillosum																
Cladonia_portentosa		40	25			5	5		5	25	60		5		30	5
Woody_debris		35	4	5			5					5				5
Polytrichum_commune		5	40	10	5	40		35	5	50		30	50	5	50	20
Pleurozium_schreber		10						60	5	10	1	10		70		30
Narthecium_ossifragum			1		15		15		10							
Cladonia_chlorophate																1
Aulacominum_palustre				5								15				
Lichenomphalia_umbellifera						1										
Dicranum_scoparium																
Camplyopos_introflexus																
Drosera																
Myrica_gale																
Menyanthes_trifoliata																

Marchantiophyta																
bare																
dung						4			5			5	5			

Collar	T1a	T1b	T2a	T2b	T3a	T3b	T4a	T4b	T5a	T5b	T6a	T6b	T7a	T7b	T8a	T8b
Calluna_vulgaris	2.5						8			20		10			35	
Erica_tetralix	2.5	5		3		3	7	2	10	5		1	5	10	2	
Eriophorum_angustifolium	60	15	20	15	35	30	5	25	9	20	15			5	13	20
Eriophorum_vaginatum																
Trichiophorum_germanicum		14							5	20		15	24			
Molinia_caerulea											15	20				
Sphagnum_capillifolium		65				2	80				70	50				
Sphagnum_papillosum																
Cladonia_portentosa		1	60	1	25	40			70	15			70			
Woody_debris				5										5	10	
Polytrichum_commune								2				1				70
Pleurozium_schreber	25		20	75	20	20		70	5	10		2	1	80	40	10
Narthecium_ossifragum																
Cladonia_chlorophate				1				1				1				
Aulacominum_palustre																
Lichenomphalia_umbellifera																
Dicranum_scoparium	10				20											
Camplyopos_introflexus									1							

Drosera																
Myrica_gale																
Menyanthes_trifoliata																
Marchantiophyta																
bare						5				10						
dung																

Collar	C1a	C1b	C2a	C2b	C3a	C3b	C4a	C4b	C5a	C5b	C6a	C6b	C7a	C7b	C8a	C8b
Calluna_vulgaris	5		20	15	10	1	1		20		18	15	30	5	15	
Erica_tetralix	5	10	5		10	1.5		15	10	15		5	7		2	2
Eriophorum_angustifolium	5	20	2.5	20			10	15				10	33	25		10
Eriophorum_vaginatum															15	
Trichiophorum_germanicum	15	60		5	3	40	30	30	10	60	15	30				50
Molinia_caerulea																
Sphagnum_capillifolium			65	15	45	30	35	30	55	10	40	20	30	30	23	15
Sphagnum_papillosum														40		
Cladonia_portentosa	65	5		40	2	10		5	5	5	10				30	5
Woody_debris																
Polytrichum_commune																
Pleurozium_schreber				5	25	7.5	10								15	
Narthecium_ossifragum																
Cladonia_chlorophate																

Aulacominum_palustre	5															
Lichenomphalia_umbellifera																
Dicranum_scoparium						7.5	5									10
Camplyopos_introflexus																
Drosera			7.5				4			5	2					2
Myrica_gale											15					
Menyanthes_trifoliata					5	2.5	5									
Marchantiophyta		5						5		5		20				6
bare																
dung																



Photos taken in June, collars L5b, T1b, C6a, showing the variety of species present.

Appendix C – Matlab code for MODIS data extraction, and MODIS datasets

All MODIS data used in this project (unless specified otherwise) were downloaded using a version of the MODIS ORNL web service (Santhana Vannan et al., 2009) through the Matlab code 'modisClient' written by Tristan Quaife. The ORNL web service has since changed its API and consequently the version of the modisClient code in this thesis no longer works.

This example shows the Matlab code to retrieve, cloud-filter, and gap-fill the daytime LST, NDVI, and bands needed to calculate the NDWI, at a site located at 45.4094, -75.5185 (WGS84) in the year 2015.

```
lat = 45.4094;
lon = -75.5185;
filename = 'data.xls';
date1 = 2015000;
date2 = 2015365;
modisClient();
addpath( [pwd '/utils'] );
addpath( [pwd '/utils/inpaintn'] );
d2=modisClient ('MOD11A2', 'LST_Day_1km', lat, lon, date1, date2,3,3);
d2=modisClientGetQC (d2, 'QC_Day');
dmask2= modisMaskQC(d2, [[0:4:2^8],[0:4:2^8]+1]);
dtirp2=modisDCT_interp( dmask2 );
newdata2=squeeze(dtirp2.data(4,4,:));
xlswrite(filename,newdata2,'Sheet3');
d3 = modisClient ('MOD13Q1', '250m_16_days_NDVI', lat, lon, date1,
date2,1,1);
d3=modisClientGetQC (d3, '250m_16_days_pixel_reliability');
dmask3= modisMaskQC(d3, [0,1]);
ditrp3=modisDCT_interp( dmask3 );
newdata3=squeeze(ditrp3.data(5,5,:));
plot(newdata3);
u=repelem(newdata3,2);
xlswrite(filename,u,'Sheet4');
```

This example shows the Matlab code to retrieve, cloud-filter, and gap-fill the bands needed to calculate the NDWI in summer (JAS) and previous winter (OND), at a site located at 45.4094, -75.5185 (WGS84) in the year 2015.

```
lat = 45.4094;
lon = -75.5185;
filename = 'data.xls';
date1 = 2015177;
date2 = 2015265;
date3 = 2014273;
date4 = 2014361;
modisClient();
addpath( [pwd '/utils'] );
addpath( [pwd '/utils/inpaintn'] );
d = modisClient ('MOD09A1', 'sur_refl_b02', lat, lon, date1, date2,1,1);
d=modisClientGetQC (d, 'sur_refl_state_500m');
dmask= modisMaskQC_special(d);
ditrp=modisDCT_interp( dmask );
newdata=squeeze(ditrp.data(3,3,:));
plot(newdata);
d2 = modisClient ('MOD09A1','sur_refl_b06', lat, lon, date1, date2,1,1);
d2=modisClientGetQC (d2, 'sur_refl_state_500m');
dmask2= modisMaskQC_special(d2);
ditrp2=modisDCT_interp( dmask2 );
newdata2=squeeze(ditrp2.data(3,3,:));
```

```
plot(newdata2);

C = newdata - newdata2;
D = newdata + newdata2;
NDWI = C./D;
NDWI_JAS = mean(NDWI);
d = modisClient ('MOD09A1', 'sur_refl_b02', lat, lon, date3, date4,1,1);
d=modisClientGetQC (d, 'sur_refl_state_500m');
dmask= modisMaskQC_special(d);
ditrp=modisDCT_interp( dmask );
newdata=squeeze(ditrp.data(3,3,:));
plot(newdata);
d2 = modisClient ('MOD09A1','sur_refl_b06', lat, lon, date3, date4,1,1);
d2=modisClientGetQC (d2, 'sur_refl_state_500m');
dmask2= modisMaskQC_special(d2);
ditrp2=modisDCT_interp( dmask2 );
newdata2=squeeze(ditrp2.data(3,3,:));
plot(newdata2);
C = newdata - newdata2;
D = newdata + newdata2;
NDWI = C./D;
NDWI_OND = mean(NDWI);
NDWI_JAS;
NDWI_OND
```

Product code	Spatial resolution	Temporal resolution	Date range
MOD17A2H GPP	500 m	8-day	Talaheel: June 2014 – June 2015 Lonielist: March 2014 – April 2015 Glencar: Jan 2002 – Dec 2012
MOD13Q1 NDVI	250m	16-day	Talaheel: June 2014 – June 2015 Lonielist: March 2014 – April 2015 Glencar: Jan 2002 – Dec 2012 Restoration and Control sites: Jan 2005 – Dec 2016
MOD11A2 daytime LST	1 km	8-day	Talaheel: June 2014 – June 2015 Lonielist: March 2014 – April 2015 Glencar: Jan 2002 – Dec 2012 Restoration and Control sites: Jan 2005 – Dec 2016
MOD09A1 bands 2 and 6	500 m	8-day	Glencar: Jan 2002-Dec 2011 Restoration and Control sites: 2005 – 2016, day 177-265 and 273-361

Appendix D – Supplementary material from Chapter 6

The raw results from the EFA, and the correlations of each factor with GPP, for each site are shown here.

Lonielist

```
Loadings:
               Factor1 Factor2 Factor3 Factor4 Factor5
Sostice_dist    -0.78
Surface_temp     0.80    0.55
PAR              0.75
NDWI            -0.52
soil_temp_5cm    0.46    0.88
soil_temp_15cm   0.32    0.92
NDVI                     0.57                    0.37
Heather                          0.93    0.34
Deer_grass                       0.82
microfeature                     0.39    0.68
S_cap                                    0.74    0.56
Feather_moss                            -0.73
Reindeer_lichen                                 -0.99
soil_moisture
Cotton_grass                    -0.40    0.33

               Factor1 Factor2 Factor3 Factor4 Factor5
SS loadings       2.53    2.35    1.94    1.88    1.56
Proportion Var    0.17    0.16    0.13    0.13    0.10
Cumulative Var    0.17    0.33    0.45    0.58    0.68

Test of the hypothesis that 5 factors are sufficient.
The chi square statistic is 133.59 on 40 degrees of freedom.
The p-value is 5.23e-12
```

Factor	1	2	3	4	5
GPP	0.17	0.68	0.21	0.28	0.17

Talaheel

```
Loadings:
               Factor1 Factor2 Factor3 Factor4 Factor5
soil_temp_5cm    0.91    0.40
soil_temp_15cm   0.96
NDVI             0.73            0.42
Surface_temp     0.43    0.83
PAR                      0.70
NDWI             0.32   -0.54    0.64
Cotton_grass                    -0.77
S_cap                                    0.97
microfeature                                    0.57
Reindeer_lichen                         -0.48    0.83
Feather_moss                            -0.48   -0.60
Sostice_dist    -0.32   -0.37
soil_moisture           -0.45
Heather
Deer_grass                       0.42

               Factor1 Factor2 Factor3 Factor4 Factor5
SS loadings       2.69    2.12    1.59    1.53    1.49
```

```
Proportion Var    0.18    0.14    0.11    0.10    0.10
Cumulative Var    0.18    0.32    0.43    0.53    0.63

Test of the hypothesis that 5 factors are sufficient.
The chi square statistic is 205.54 on 40 degrees of freedom.
The p-value is 3.95e-24
```

Factor	1	2	3	4	5
GPP	0.46	0.044	0.36	0.0049	0.00021

Cross Lochs

```
Loadings:
               Factor1 Factor2 Factor3 Factor4 Factor5
Sostice_dist    -0.69
soil_temp_5cm    0.82            0.53
soil_temp_15cm   0.77            0.58
Surface_temp     0.85
PAR              0.60
microfeature             0.65                    -0.31
Heather                  0.73
Deer_grass              -0.97
S_cap                    0.68           -0.55    -0.31
NDVI                             0.81
NDWI            -0.41    0.42    0.57
Reindeer_lichen                           0.99
Cotton_grass                                       1.00
soil_moisture           -0.46
Feather_moss             0.33                    -0.31

               Factor1 Factor2 Factor3 Factor4 Factor5
SS loadings       3.05    2.89    1.77    1.37    1.36
Proportion Var    0.20    0.19    0.12    0.09    0.09
Cumulative Var    0.20    0.40    0.51    0.60    0.70

Test of the hypothesis that 5 factors are sufficient.
The chi square statistic is 233.18 on 40 degrees of freedom.
The p-value is 4.2e-29
```

Factor	1	2	3	4	5
GPP	0.50	-0.22	0.36	-0.12	0.0024

Tables C1 to C4 show the results from Mann-Whitney tests to determine whether any of the variables considered in this study have significant differences between hummocks and hollows across the months and sites studied.

Table C1 – P-values for Mann-Whitney tests for key vegetation species at each site. If the value is significant the microtopographical feature with the higher proportions of that species is given in brackets.

Species	Cross Lochs	Talaheel	Lonielist
Calluna vulgaris	0.017* (Hu)	0.75	0.011* (Hu)
Eriophorum angustifolium	0.18	0.87	0.87
Cladonia portentosa	0.91	0.47	0.38
Sphagnum capillifolium	0.039* (Hu)	0.95	0.12
Pleurozium schreberi	0.41	0.37	0.016* (Ho)
Trichiophorum germanicum	0.034* (Ho)	0.65	0.38

Table C2 – P-values for Mann-Whitney tests showing whether the difference between hummocks and hollows was significant or not for each factor at Lonielist. If the value is significant the microtopographical feature with the higher proportions of that species is given in brackets.

Lonielist	March	April	May	June	July	August	September
Moisture	0.27	0.095	0.96	0.81	0.67	0.23	0.63
WTD	0.23	0.84	0.82	0.62	0.96	0.80	0.60
Surface temp	1	0.68	0.96	0.17	1	0.63	0.71
5 cm temp	0.63	0.25	0.15	0.62	0.56	0.19	0.59
15 cm temp	1	0.23	0.56	0.46	0.039* (Hu)	0.015* (Hu)	0.019* (Hu)
GPP	0.38	0.69	0.054 (Hu)	0.11	0.0074** (Hu)	0.038* (Hu)	0.28
Respiration	0.28	0.42	0.015* (Hu)	0.019* (Hu)	0.0070** (Hu)	0.23	0.46
NDVI	0.71	0.69	0.91	N/A	0.10	0.28	0.51
CIm	0.33	0.84	0.54	N/A	0.0499* (Hu)	0.10	0.13
NDWI	0.065	0.69	0.61	NA	0.01* (Ho)	0.083	0.28
PAR	0.19	0.84	0.15	0.29	0.60	0.83	0.79

Table C3 – P-values for Mann-Whitney tests showing whether the difference between hummocks and hollows was significant or not for each factor at Talaheel. If the value is significant the microtopographical feature with the higher proportions of that species is given in brackets.

Talaheel	March	April	May	June	July	August	September
Moisture	0.53	0.53	0.33	0.87	0.90	0.56	0.92
Surface temp	1	0.53	0.37	0.92	0.80	0.87	0.27
5 cm temp	0.83	0.53	0.53	0.92	0.95	0.63	0.92
15 cm temp	0.52	0.75	0.83	0.19	0.52	1	0.83
GPP	0.84	1	0.65	0.88	0.54	0.44	0.88
Respiration	1	0.53	0.72	0.88	0.16	0.83	0.96
NDVI	1	1	1	0.80	0.71	0.96	0.65
CIm	0.31	0.69	0.19	0.51	0.90	0.44	0.96
NDWI	0.55	0.22	0.88	0.51	0.097	0.88	0.88
PAR	0.92	1	0.16	0.80	0.89	0.63	0.0030* (Hu)

Table C4 – P-values for Mann-Whitney tests showing whether the difference between hummocks and hollows was significant or not for each factor at Cross Lochs. If the value is significant the microtopographical feature with the higher proportions of that species is given in brackets.

Cross Lochs	March	April	May	June	July	August	September
Moisture	0.74	0.20	0.16	0.015 * (Ho)	0.043* (Ho)	0.0040** (Ho)	0.026* (Ho)
Surface temp	0.87	0.62	0.37	0.75	0.96	0.65	0.60
5 cm temp	0.42	0.62	0.64	0.40	0.29	0.36	0.31
15 cm temp	0.51	0.71	0.046* (Ho)	0.016 * (Ho)	0.039* (Ho)	0.31	0.014* (Hu)
GPP	0.34	0.54	0.33	0.38	0.28	0.65	0.96
Respiration	0.13	0.11	0.96	0.27	0.28	0.92	0.0018** (Hu)
NDVI	0.75	0.41	0.32	0.083	0.083	0.44	0.19
CIm	0.39	0.11	0.57	0.083	0.23	0.57	0.88
NDWI	0.31	0.56	0.23	0.96	0.57	0.33	0.065
PAR	0.39	0.90	0.83	0.75	0.96	0.23	0.56

Data storage information

Dataset	Description	Chapters used in	Location/contact
KJL_README	Information file for all data	3,4, 5, 6	https://doi.org/10.5285/ab9f47f9-9faf-4403-a57e-25e31f581ed0
KJL_spectrometry_lab	Raw spectral measurements from the lab, in the format KL_DD_MM	3,4	The James Hutton Institute
KJL_data_lab	All laboratory measurements including fluxes and vegetation indices	3,4	https://doi.org/10.5285/ab9f47f9-9faf-4403-a57e-25e31f581ed0
KJL_corrections_lab	Data used for PAR corrections	3,4, Appendix A	https://doi.org/10.5285/ab9f47f9-9faf-4403-a57e-25e31f581ed0
KJL_spectrometry_field	Raw spectral measurements from the field, in the format KJL_site_month	4,6	The James Hutton Institute
KJL_LICOR_field	Raw LICOR data files from the field, in the format KJL_site_month	4,6	The James Hutton Institute
KJL_data_field	All field measurements including fluxes and vegetation indices	4,6, Appendix C	https://doi.org/10.5285/ab9f47f9-9faf-4403-a57e-25e31f581ed0
KJL_species_field	Percentage of species in each collar, surveyed in June	4,6, Appendix B, C	https://doi.org/10.5285/ab9f47f9-9faf-4403-a57e-25e31f581ed0
KJL_TGdevelopment_MODIS	Processed and gap-filled MODIS data used to develop the TG model (Lonielist, Talaheel)	5	https://doi.org/10.5285/ab9f47f9-9faf-4403-a57e-25e31f581ed0
KJL_TGWa_development_MODIS	Processed and gap-filled MODIS data used to develop the TGWa model (Glencar)	5	https://doi.org/10.5285/ab9f47f9-9faf-4403-a57e-25e31f581ed0
KJL_restoration_MODIS	Processed and gap-filled MODIS data for the six sites undergoing restoration	5	https://doi.org/10.5285/ab9f47f9-9faf-4403-a57e-25e31f581ed0
KJL_data_MODIS	Processed and gap-filled MODIS data for the field sites (Lonielist, Talaheel and Cross Lochs)	6	https://doi.org/10.5285/ab9f47f9-9faf-4403-a57e-25e31f581ed0